Dissecting the Genetic Basis of Parkinson Disease, Dystonia and Chorea

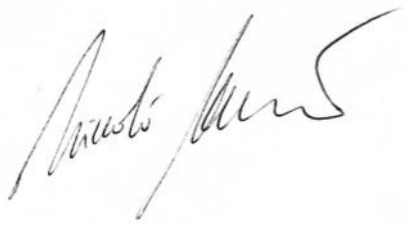A thesis submitted to the University College London for the degree of Doctor of Philosophy

June 2016

by

Dr Niccolò Emanuele Mencacci

Declaration of Authorship

I, Niccolò Emanuele Mencacci, confirm that the work presented in this thesis is my own. Where information has been derived from other sources, I confirm that this has been indicated in the thesis.

Incontenibile andare, di monte in monte, inquieti dietro un mistero che sempre ti seduce, da un'altra valle

Abstract

In this thesis I used of a range of genetic methodologies and strategies to unravel the genetic bases of Parkinson disease (PD), myoclonus-dystonia (M-D), and chorea.

First, I detail the work I performed in PD, including (1) the screening of *GBA* in a cohort of early-onset PD cases, which led to the identification of the allele E326K (p.Glu365Lys) as the single most frequent, clinically relevant, risk variant for PD; (2) a detailed genetic analysis in a large cohort of PD cases who underwent deep-brain stimulation treatment and a longitudinal comparison of the phenotypic features of carriers of mutations in different genes; (3) the observation that rare *GCH1* coding variants, known to be responsible for the childhood-onset disorder DOPA-responsive dystonia, are a novel risk factor for PD.

Then, I describe the work I performed to identify novel causes of M-D, including (1) the discovery of the missense p.Arg145His mutation in *KCTD17* as a novel cause of autosomal dominant M-D; (2) the identification of tyrosine hydroxylase deficiency as a novel treatable cause of recessive M-D; and (3) the conclusive disproof of the pathogenic role of the p.Arg1389His variant in *CACNA1B* as a cause of M-D.

Finally, I detail my work in the field of choreic syndromes, including (1) the genetic screening of *NKX2-1* in the Queen Square cohort of benign hereditary chorea (BHC) cases; (2) the identification of *ADCY5* mutations, the gene thought to be responsible for the condition familial dyskinesias with facial myokymia, as an important cause of BHC; and (3) the identification of *de novo* mutations in *PDE10A* as a novel genetic cause of chorea.

These findings are discussed in light of the recent literature. Following my analysis, I suggest future directions for the identification of novel genetic causes of movement disorders, in light of my recent findings and ongoing research.

Table of Contents

List of Figures

List of Tables

Peer-Reviewed Publications

Publications Relating to the Work Contained Within This Thesis

Mencacci NE, Kamsteeg EJ, Nakashima K, R'Bibo R, Lynch DS, Balint B, Willemsen M, Adams M, Wiethoff S, Ng J, et al. De novo mutations in *PDE10A* cause childhood-onset chorea with bilateral striatal lesions. *American Journal of Human Genetics*. 2016;98:763-71.

Mencacci NE, R'Bibo L, Bandres-Ciga S, Carecchio M, Zorzi G, Nardocci N, Garavaglia B, Batla A, Bhatia KP, Pittman AM, et al. The *CACNA1B* R1389H variant is not associated with myoclonus-dystonia in a large European multicentric cohort. *Human Molecular Genetics*. 2015;24(18):5326-9.

Mencacci NE, Erro R, Wiethoff S, Hersheson J, Ryten M, Balint B, Ganos C, Stamelou M, Quinn N, Houlden H, Wood NW, Bhatia KP. *ADCY5* mutations, another cause of benign hereditary chorea. *Neurology*. 2015 ;85(1):80-8.

Mencacci NE, Rubio-Agusti I, Zdebik A, Asmus F, Ludtmann MHR, Ryten M, Plagnol V, Hauser AK, Bandres Ciga S, Bettencourt C, et al. A missense mutation in *KCTD17* causes autosomal dominant myoclonus-dystonia. *American Journal of Human Genetics*. 2015;96(6):938-47.

Mencacci NE, Isaias IU, Reich MM, Ganos C, Plagnol V, Polke JM, Bras J, Hersheson J, Stamelou M, Pittman AM, et al. Parkinson's disease in GTP cyclohydrolase 1 mutation carriers. *Brain*. 2014;137(Pt 9):2480-92.

Angeli A, **Mencacci NE**, Duran R, Aviles-Olmos I, Kefalopoulou Z, Candelario J, Rusbridge S, Foley J, Pradhan P, Jahanshahi M, et al. Genotype and phenotype in Parkinson's disease: lessons in heterogeneity from deep brain stimulation. *Movement Disorders*. 2013;28(10):1370-5.

Duran R, **Mencacci NE** (joint first authors), Angeli AV, Shoai M, Deas E, Houlden H, Mehta A, Hughes D, Cox TM, Deegan P, et al. The glucocerobrosidase E326K variant predisposes to Parkinson's disease, but does not cause Gaucher's disease. Mov Disord. 2013;28(2):232-6.

Stamelou M, **Mencacci NE,** (joint first authors), Cordivari C, Batla A, Wood NW, Houlden H, Hardy J, Bhatia KP. Myoclonus-dystonia syndrome due to tyrosine

hydroxylase deficiency. *Neurology*. 2012;79(5):435-41.

Other Significant Contribution During Thesis Period

Mencacci NE, Carecchio M**.** Recent advances in the genetics of chorea. *Current Opinion in Neurology*. In press.

Mencacci NE. The endless expansion of the disease spectrum of *ATP1A3* mutations: a true diagnostic challenge. *Movement Disorders Clinical Practice.* DOI: 10.1002/mdc3.12358.

Bandrés-Ciga S, **Mencacci NE**, Durán R, Barrero FJ, Escamilla-Sevilla F, Morgan S, Hehir J, Vives F, Hardy J, Pittman AM. Analysis of the genetic variability in Parkinson's disease from Southern Spain. *Neurobiol Aging*. 2016;37:210.e1-5.

Noyce AJ, **Mencacci NE** (joint first authors), Schrag A, Bestwick JP, Giovannoni G, Lees AJ, Hardy J. Web-based assessment of Parkinson's prodromal markers identifies *GBA* variants. *Movement Disorders*. 2015;30(7):1002-3..

Macerollo A, **Mencacci NE** (joint first authors), Erro R, Cordivari C, Edwards MJ, Wood NW, Bhatia KP. Screening of mutations in NOL3 in a myoclonic syndromes series. *Journal of Neurology*. 2014;261(9):1830-1.

Ganos G, **Mencacci NE** (joint first authors), Gardiner A, Erro R, Batla A, Houlden H, Bhatia KP. Paroxysmal Kinesigenic Dyskinesia May Be Misdiagnosed in Co-occurring Gilles de la Tourette Syndrome. *Movement Disorders Clinical Practice*. 2014; 1(1):84-6.

Hersheson J, **Mencacci NE**, Davis M, MacDonald N, Trabzuni D, Ryten M, Pittman A, Paudel R, Kara E, Fawcett K, et al. Mutations in the autoregulatory domain of β-tubulin 4a cause hereditary dystonia. *Annals of Neurology*. 2013;73(4):546-53.

Other Peer-Reviewed Publications During Thesis Period

Brugger F, Kägi, G, Pandolfo M, **Mencacci NE**, Batla A, Wiethoff S, Bhatia KP. Neurodegeneration with brain iron accumulation (NBIA) syndromes presenting with late-onset craniocervical dystonia – an illustrative case series. Movement Disorders Clinical Practice. *In press.*

Mok KY, Sheerin U, Simón-Sánchez J, Salaka A, Chester L, Escott-Price V, Mantripragada K, Doherty KM, Noyce AJ, **Mencacci NE**, et al. Deletions at 22q11.2 in

idiopathic Parkinson's disease: a combined analysis of genome-wide association data. *Lancet Neurology*. 2016. pii: S1474-4422(16)00071-5.

Mencacci NE, Erro R, Bhatia KP. Reply: ADCY5 mutations are another cause of benign hereditary chorea. Letter to the editor. Neurology. 2016 Mar 8;86(10):978-9.

Antelmi E, Erro R, Pisani A, **Mencacci NE**, Bhatia KP. Persistent chorea due to anticholinergic therapy in DYT6. *Parkinsonism & Related Disorders*. 2015. 21(10):1282-3

Mencacci NE, Pittman AM, Isaias IU, Hardy J, Klebe S, Bhatia KP, Wood NW. Reply: Parkinson's disease in GTP cyclohydrolase 1 mutation carriers. Letter to the editor. *Brain*. 2015;138(Pt 5):e352.

Praschberger R, Balint B, **Mencacci NE**, Hersheson J, Rubio-Agusti I, Kullmann DM, Bettencourt C, Bhatia K, Houlden H. Expanding the phenotype and genetic defects associated with the GOSR2 gene. *Movement Disorders Clinical Practice*. 2015. doi: 10.1002/mdc3.12190

Erro R, Hersheson J, Ganos C, **Mencacci NE**, Stamelou M, Batla A, Thust SC, Bras JM, Guerreiro RJ, Hardy J, Quinn NP, Houlden H, Bhatia KP. H-ABC syndrome and DYT4: Variable expressivity or pleiotropy of TUBB4 mutations? *Movement Disorders* 2015;30(6):828-33.

Sadnicka A, Teo JT, Kojovic M, Pareés I, Saifee TA, Kassavetis P, Schwingenschuh P, Katschnig-Winter P, Stamelou M, **Mencacci NE**, Rothwell JC, Edwards MJ, Bhatia KP. All in the blink of an eye: new insight into cerebellar and brainstem function in DYT1 and DYT6 dystonia. *European Journal of Neurology*. 2015;22(5):762-7.

Batla A, Adams ME, Erro R, Ganos C, Balint B, **Mencacci NE**, Bhatia KP. Cortical pencil lining in neuroferritinopathy: A diagnostic clue. *Neurology*. 2015;84(17):1816-8.

Kefalopoulou Z, Politis M, Piccini P, **Mencacci NE**, Bhatia K, Jahanshahi M, Widner H, Rehncrona S, Brundin P, Björklund A, et al. Long-term clinical outcome of fetal cell transplantation for Parkinson disease: two case reports. *JAMA Neurology*. 2014;71(1):83-7.

McNeill A, Wu RM, Tzen KY, Aguiar PC, Arbelo JM, Barone P, Bhatia K, Barsottini O,

Bonifati V, Bostantjopoulou S, Bressan R, Cossu G, Cortelli P, Felicio A, Ferraz HB, Herrera J, Houlden H, Hoexter M, Isla C, Lees A, Lorenzo-Betancor O, **Mencacci NE**, Pastor P, Pappata S, Pellecchia MT, Silveria-Moriyama L, Varrone A, Foltynie T, Schapira AH. Dopaminergic neuronal imaging in genetic Parkinson's disease: insights into pathogenesis. *PLoS One*. 2013 23;8(7):e69190.

Batla A, Stamelou M, **Mencacci NE**, Schapira AH, Bhatia KP. Ropinirole monotherapy induced severe reversible dyskinesias in Parkinson's disease. *Movement Disorders*. 2013;28(8):1159-60.

Doherty KM, Silveira-Moriyama L, Parkkinen L, Healy DG, Farrell M, **Mencacci NE**, Ahmed Z, Brett FM, Hardy J, et al. Parkin disease: a clinicopathologic entity? *JAMA Neurology*. 2013;70(5):571-9.

Winder-Rhodes SE, Evans JR, Ban M, Mason SL, Williams-Gray CH, Foltynie T, Duran R, **Mencacci NE**, Sawcer SJ, Barker RA. Glucocerebrosidase mutations influence the natural history of Parkinson's disease in a community-based incident cohort. *Brain*. 2013;136(Pt 2):392-9.

Acknowledgements

This thesis is dedicated to the loving memory of my godmother Franca. Her words and teaching shaped my mind and soul and will always guide me throughout my life.

I am deeply grateful to the many persons that made the years of my PhD one the most enjoyable and rewarding experiences of my life.

First, I would like to express my most sincere gratitude to my primary supervisor Professor Nicholas Wood for his support, mentorship, advice and encouragement throughout the course of my work at the Institute of Neurology. I am also grateful for the unlimited freedom he granted me, which allowed me to freely direct my research efforts.

I could not have made it through without the help of my secondary supervisor Dr Alan Pittman, who, since day one in the lab, patiently and carefully guided me into the fascinating world of genetics and taught me almost everything I know.

I am also immensely indebted to Professor John Hardy, who first gave me the opportunity to work in his lab as a visitor and then offered me to stay and pursue a PhD. I feel blessed to have had the chance to work close to a person who, thanks to his enlightening, enthusiastic and charismatic attitude, has made the history of genetics of neurological disorders and will always represents a source of inspiration.

Thanks also to Prof. Vincenzo Silani, who, with his open and longsighted views on education of young neurologists, gave me the opportunity to work in the laboratory of Prof John Hardy, while I was still completing my neurology training.

A special thank you goes to Professor Kailash Bhatia, for passionately teaching me the art of diagnosing movement disorders and for his great help in identifying most of the families and cases on which I have worked during my PhD. Thanks also to Prof. Tom Foltynie for the fantastic collaboration we had on the genetic characterisation of the DBS-PD cohort.

The list of people I have come across during my time at the Institute of Neurology, who helped and greatly contributed to the pleasantness of my time during the PhD, is long and I hope not to forget anyone. Big thanks certainly go to Arianna Tucci, Anna Sailer, Lucia Schottlander, Raquel Duran, Sarah Wiethoff, Sara Bandres-Ciga, Lea R'Bibo,

Chapter 1. General Introduction

1.1 Thesis Aim

Movement disorders comprise a large group of clinically and genetically heterogeneous conditions, which may be subdivided into various clinical entities, including Parkinson disease (PD), tremor, dystonia, myoclonus and chorea. Mendelian disorders are disorders in which inheritance of one (dominant) or two (recessive) mutations in a single gene leads to the development of a disease phenotype.

Many movement disorders, such as Huntington's disease (HD) or spinocerebellar ataxias (SCAs), are transmitted as Mendelian diseases. Furthermore, a small but significant percentage of patients with diseases traditionally considered sporadic (e.g. PD or dystonia) are inherited as Mendelian traits. Despite their rarity, Mendelian diseases provide fertile ground for understanding a large number of essential biological processes that are critically involved in the pathogenesis of these complex disorders and represent fitting targets for the development of future treatments.

Although, overall, monogenic causes are rare, more than 200 genes are known to cause either an isolated movement disorder or a syndromic form of movement disorder when mutated (Klein, 2014, Spatola and Wider, 2014, Gardiner *et al.*, 2015). However, in total, mutations in these genes only explain a small proportion of cases, suggesting that mutations in more genes await discovery.

The introduction and diffusion of 'next generation' sequencing (NGS) technologies, in particular whole-exome sequencing (WES) and micro-array based genotyping, has made the time and cost-effective generation of vast amounts of sequencing data increasingly easy, allowing an exponential increase in the understanding of the genetic bases of human diseases.

In the work outlined in this thesis, I used a combination of various genetic techniques and strategies to try and identify novel disease-causing genes or risk factors for familial and sporadic forms of PD, dystonia and chorea. The results of this work represent an example of how genetics can both guide the clinical practice and facilitate the understanding of the cellular pathways implicated in the pathogenesis of these diseases, paving the way for the development of future treatments.

1.2 Summary of Relevant Techniques in Genetics

What follows is a summary of the genetic techniques that I used for the work detailed in this thesis.

1.2.1 Dideoxynucleotide Sequencing

Dideoxynucleotide sequencing, commonly referred to as Sanger sequencing, named after Frederick Sanger who pioneered this technique in 1977, has been the most widely used sequencing method for the last three decades (Sanger *et al.*, 1977).

Sanger sequencing still represents the most reliable and accurate method for variant detection and relevant NGS results are regularly validated by Sanger sequencing for the exclusion of artefacts (Pittman and Hardy, 2013).

The method relies on the principle of random inhibition of the DNA polymerase, creating newly synthesised DNA strands of different lengths that can be subsequently separated by capillary electrophoresis depending on the size. The DNA chain elongation is randomly inhibited by the inclusion in the reaction mix of a small quantity of dideoxynucleotides (ddNTPs). These differ from the normal deoxyribonucleotide (dNTP) as they lack the hydroxyl group at the 2' and 3' carbon positions. This feature prevents the formation of a phosphodiester bond with the subsequent dNTP, stopping DNA from extending the chain elongation any further.

The input DNA sample for Sanger sequencing is a population of identical molecules of DNA obtained by polymerase chain reaction (PCR) amplification. PCR primers are designed to target and amplify individually the portions of the genome of interest, such as the coding exons and the exon-intron boundaries.

Each of the fragments produced during the sequencing reaction will have a common 5' end (determined by the sequencing primer) but a different 3' end (depending on the insertion of the appropriate ddNTP into any one of the different positions that will match that base). As the different ddNTPs are combined with fluorescent dyes with different emission wavelengths, automated DNA sequencing machines, which use laser excitation during electrophoresis, are able to construct the DNA sequence from the intensity profiles of the four different fluorophores.

1.2.2 Next Generation Sequencing

In the last 5-10 years NGS technologies have completely transformed the hunt for Mendelian disease genes due to a dramatic reduction in cost and commensurate increase in the speed of DNA sequencing (Bras *et al.*, 2012).

NGS is applied to three main techniques: whole-genome sequencing (WGS; for sequencing all coding and non-coding portions of the genome), WES (for sequencing only the coding portions of the genome) and targeted gene sequencing (for capturing and sequencing of a more limited set of genes or specific genomic regions).

Although WGS certainly represents the most comprehensive approach, so far its use has been limited by some important factors, including the cost and the capacity required to store the data. Furthermore, interpreting variants in the non-protein-coding portion of the genome is extremely challenging.

Protein-coding genes, which constitute approximately 1-2% of the human genome (the 'exome'), harbor the majority of disease-causing mutations. For this reason WES has become the most widely used NGS technique for the identification of genes underlying Mendelian disorders.

Differently from Sanger sequencing, which is based on conventional capillary-based sequencing, NGS relies on massively parallel sequencing of DNA molecules, which are spatially separated in a flow cell. This enables the automated processing of millions of sequence reads and hundreds of gigabases of nucleotide-sequence output in parallel in a time and cost-effective manner. Different NGS chemistries, technologies and platforms-differing in specific technical details with respect to cost, accuracy, read length and multiplexing capability- are currently available (Metzker, 2010), but the details of this are beyond the scope of this chapter.

The main technical steps of the NGS process are summarised in Figure 1-1. In brief, genomic DNA is first broken up into small fragments. Then, sequence adaptors, which are platform-specific and allow each fragment to be hybridized to the flowcell where the sequencing occurs, are added to both ends of each fragment. WES protocols proceed with the hybridization of the fragments to probes that are complimentary to all the known exons in the genome, which are then captured while the remaining DNA is washed away, leaving a pool of fragments containing exons. WGS requires no extra steps following the addition of adaptors and the library is ready to be sequenced at that

point. The raw sequencing data is subsequently analysed through a bioinformatic pipeline, composed of a series of software tools, which allow the production of the sequence reads, quality score assessment of the reads, alignment of the reads to the reference genome, variant calling and annotation of the called variants.
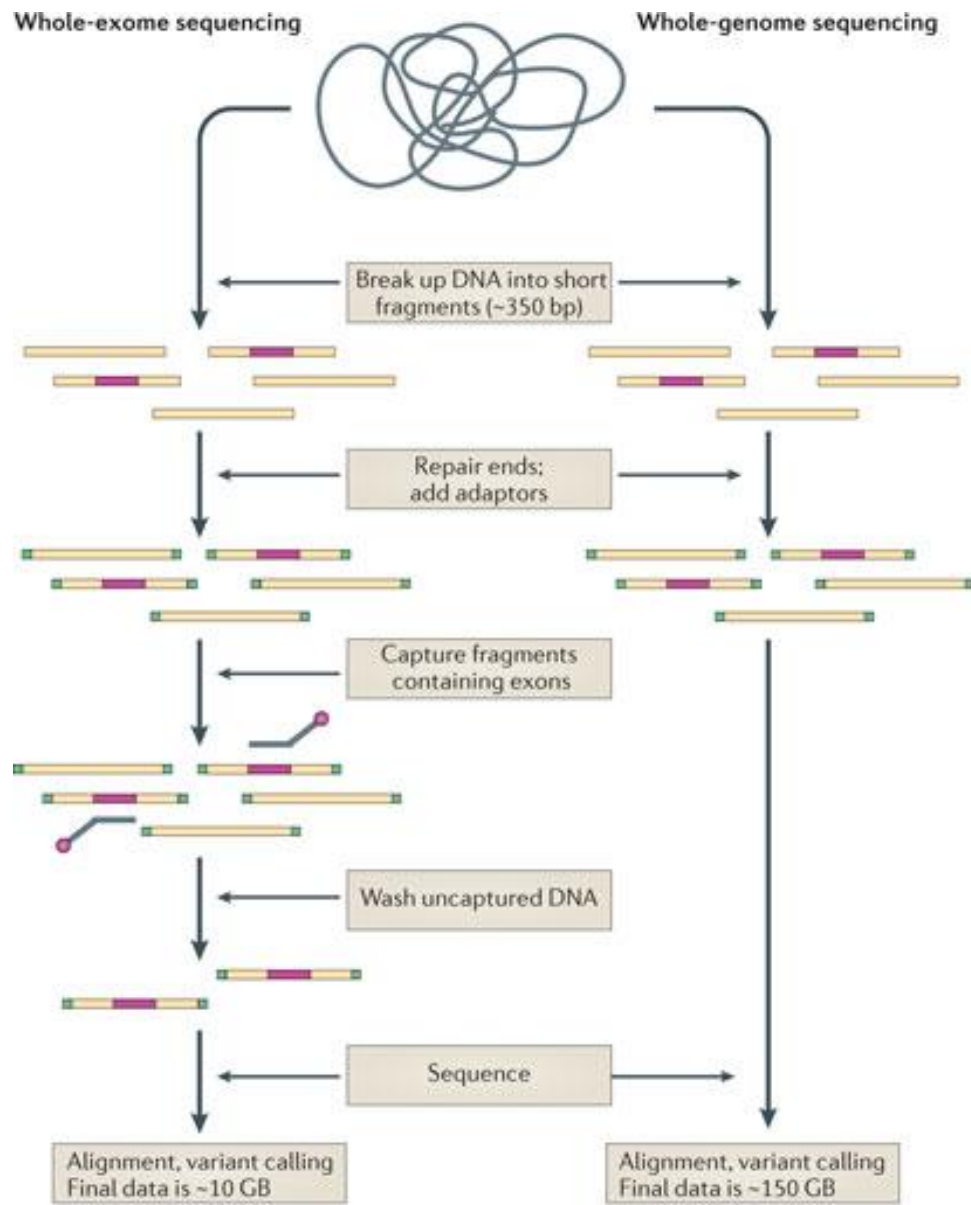
Figure 1-1 Schematic representation of the main technical steps of NGS
Reproduced from (Bras et al., 2012)

One of the first steps and most important aspects for understanding and interpreting the results of WES is the definition of the 'exome'. Indeed, considerable uncertainty still exists regarding which portions of the human genome truly encode for proteins. Initially, exome-capture kits used the CCDS (Consensus Coding Sequence Project) definition (Pruitt et al., 2009), which is subset of genes determined to be coding with high confidence. Currently, most of the available commercial kits target all of the genes contained in Refseq (Pruitt et al., 2014) and an increasingly large number of intronic promoter regions, hypothetical proteins and non-coding RNAs. This aspect is particularly important as mutations may be missed if they are located in portions of the genome not targeted by the used exome-capture kit.

1.2.3 Linkage Analysis

As I will discuss in the next sections of this chapter, even in the age of NGS, linkage analysis, which enables the identification of areas of the genome where the causal variants are more likely to lie, remains of invaluable importance to narrow down the number of possible candidate variants under consideration.

Briefly, genetic linkage analysis is a statistical method that is used to associate a phenotype and the chromosomal location of the causative mutation (Dawn Teare and Barrett, 2005). Linkage analysis relies on the principle that genes or genetic markers, which are located proximal to each other on a chromosome, tend to be inherited together during meiosis. The greater the frequency of recombination between two genetic markers, the further apart they are likely to be. Conversely, the lower the frequency of recombination of two markers, the closer they are. Therefore the position of a disease gene can be inferred by finding markers that tend not to recombine in all affected individuals.

The markers generally assessed in linkage analysis are, on the one hand, the detectable phenotypes of interest, and, on the other, DNA markers evenly spread throughout the genome.

In the past microsatellites, tracts of repetitive DNA in which certain DNA motifs (ranging in length from 2–5 base pairs) are repeated, used to be the most widely adopted genetic markers for linkage analysis. However, sizing of hundreds of microsatellites is a time-consuming and laborious process. Consequently, the use genome-wide arrays, which enable the simultaneous detection of thousand of single-nucleotide

polymorphisms in an automated way, has become the most popular way to generate genetic markers for linkage analysis.

Linkage analysis may be either parametric (if the pattern of transmission of the trait of interest is known) or non-parametric. Parametric linkage analysis is the traditional approach in the study of pedigree with Mendelian diseases.

The proportion of offspring in which two parental alleles are separated by recombination is the recombination fraction (θ). The recombination fraction varies from 0 (for adjacent loci) to 0.5 (for distant loci) and may serve as a measure of the distance between the loci. The probability that a causative gene is linked to a genetic marker is assessed through the LOD score (logarithm -base 10- of odds), which is a function of θ. The LOD score is a value that results from comparing the likelihood of obtaining the data if the two loci are indeed linked, to the likelihood of observing the same data by chance. In order to calculate the LOD score, a model for disease must be specified, which includes the frequency of the disease allele and mode of inheritance (dominant versus recessive), marker allele frequencies, and a full marker map for each chromosome.

Large positive scores are evidence for linkage, and negative scores are evidence against it. By convention, a LOD score greater than 3.0 (equivalent to p=0·001) is considered significant evidence for linkage. On the other hand, a LOD score < -2.0, indicating a probability against linkage of 100 to 1, is considered enough evidence to exclude linkage.

A monogenic mode of inheritance established by segregation analysis and a correct phenotypic designation of affected and unaffected status are the two essential requirements for successful genetic mapping using linkage analysis.

1.3 Models and Strategies to Study the Genetic Architecture of Diseases

Three main models are thought to describe the genetic basis of human diseases and, depending on the postulated underlying model, different sets of genetic tools and strategies are necessary to unravel the architecture of a disease (Singleton *et al.*, 2010).
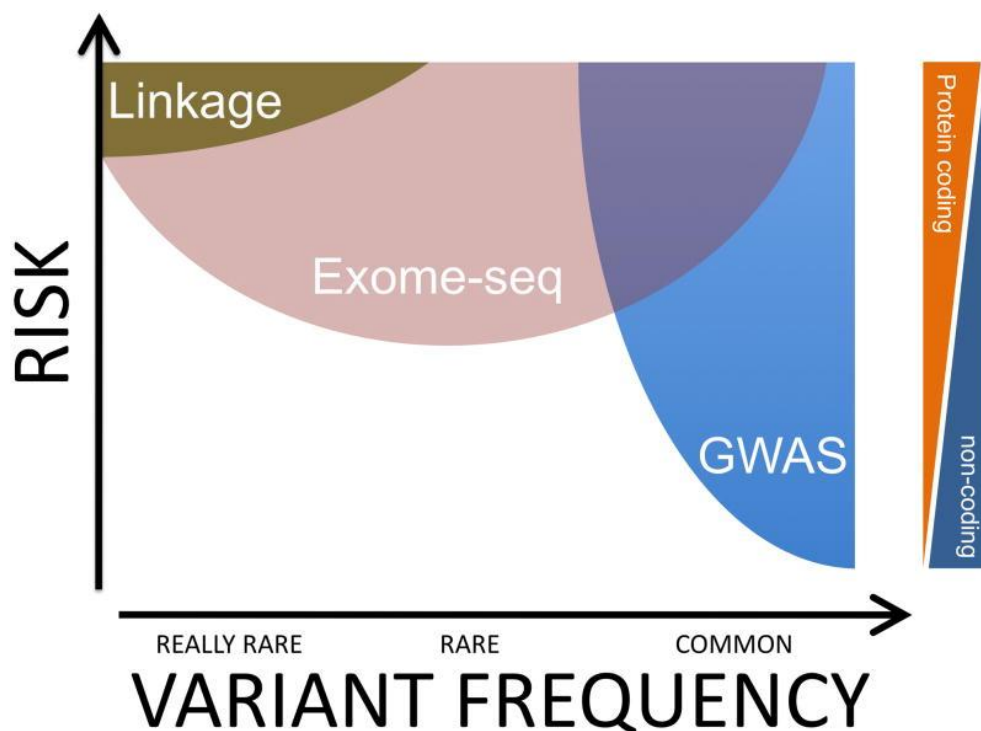
Figure 1-2 Scheme illustrating the necessary methods for gene discovery depending on the hypothesised underlying architecture of disease.
Image reproduced from (Singleton *et al.*, 2010)

Mendelian Disease Model

Mendelian diseases are caused by very rare and highly penetrant variants (minor allele frequency [MAF] far below 1%) that often, but not always (i.e. sporadic cases with recessive or *de novo* mutations) affect multiple individuals in a family. The most effective way of identifying these types of mutations is based on mapping strategies (e.g. linkage analysis or homozygosity mapping). However, as I will discuss more in the next section, WES has revolutionised this field, introducing a series of potential new approaches.

Common Disease-Common Variant Model

Genetically complex diseases may be influenced by single variants or by a combination

of variants that are common in the general population (MAF > than 5%), but exert only a small role in increasing the disease risk. Genome-wide association studies (GWAS) have been shown to be an excellent resource for identifying these types of variants.

Common Disease-Rare Variant Model

Genetically complex diseases may also be caused or influenced by rare variants that exert a moderate effect on disease risk.

Detection of these types of variants is notoriously difficult because they do not have a strong enough effect to be transmitted as Mendelian traits and therefore elude mapping strategies, such as linkage analysis. Furthermore, multiple variants at the same locus may contribute to disease risk in a cumulative way and individual variants tend not be frequent enough to be detected through GWAS and association strategies. For these reasons, rare variants with intermediate effect represent a major challenge for genetic studies currently and in the near future.

Currently, there are two main approaches for the detection of these types of variants:

1) A candidate gene approach, whereby researchers assess the role of variants in genes that are plausibly involved in the biology of a disease. Interestingly, most of the genes identified to date through this approach had initially been suspected thanks to astute clinical observations (e.g. *GBA* mutations in PD or *TREM2* variants in Alzheimer disease) (Sidransky and Lopez, 2012, Guerreiro *et al.*, 2013).

(2) A hypothesis-free exome (or genome)-wide approach, based on the comparison of NGS data obtained from large cohorts of cases and controls. This approach requires the assembly of very large cohorts of cases and controls and, to date, no novel risk genes for movement disorders have been identified. However, this approach has recently led to the identification of *TUBA4A* and *TBK1* mutations in amyotrophic lateral sclerosis/fronto-temporal dementia (Smith *et al.*, 2014, Cirulli *et al.*, 2015).

The architecture of complex diseases, such as PD, may be composed of a combination of various types of causative variants, and some genes may contain multiple types of variants contributing to the disease risk (pleomorphic gene loci).

For the purposes of this thesis, I have elected to focus only on the discovery of rare Mendelian variants and rare variants with intermediate effect.

1.4 Strategies for Gene Identification in Mendelian Diseases

When attempting to identify pathogenic variants, researchers should select the correct technological and analytical approach based on the most likely genetic architecture of the disease of interest, the suspected type of variants, the frequency of the disease of interest, the inheritance pattern, and the penetrance of the mutations. The strategies for gene identification in the NGS era are schematically summarised in Figure 1-3.
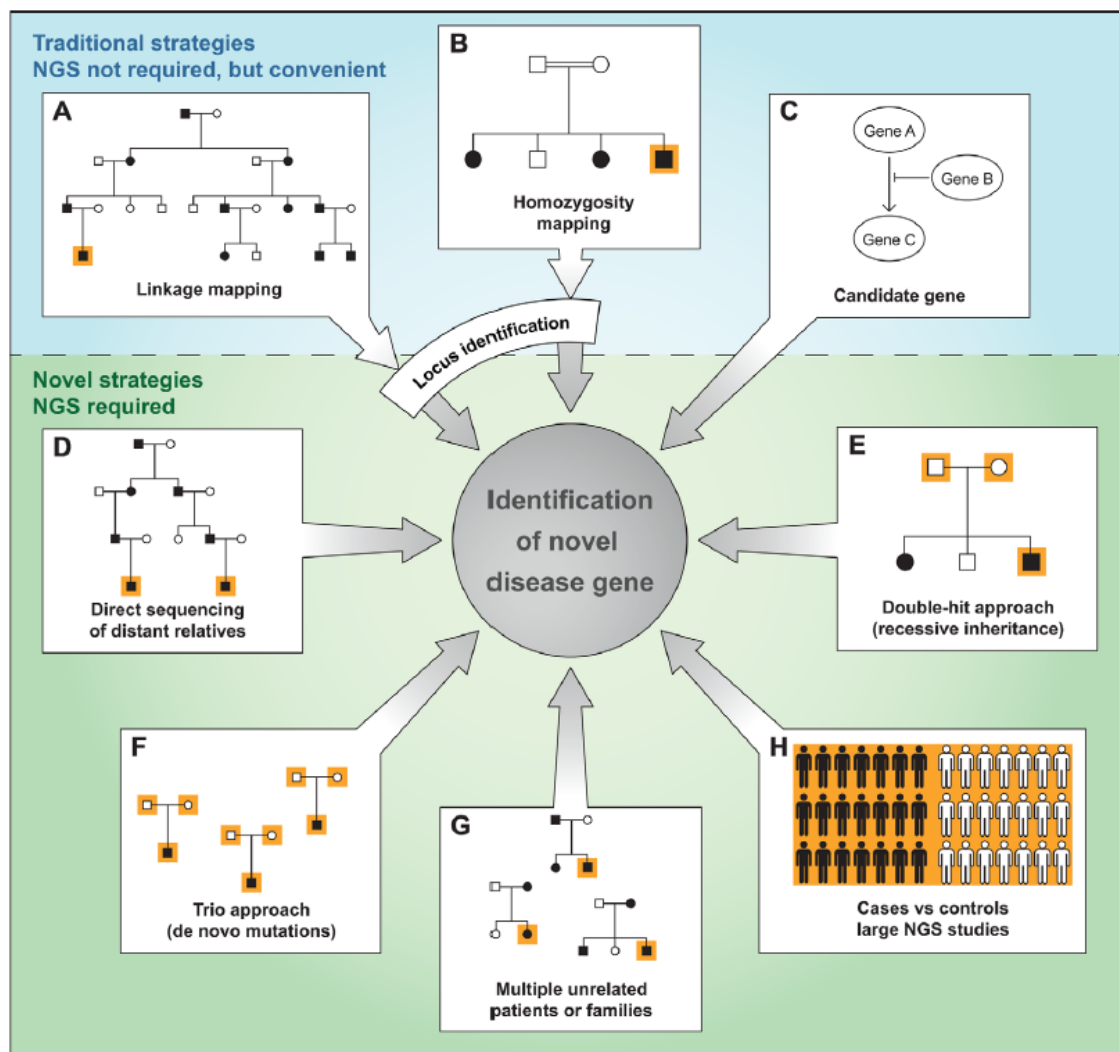
Figure 1-3 NGS strategies for gene identification
Reproduced from (Olgiati *et al.*, 2016).

The identification of mutations causing Mendelian diseases has traditionally relied on the use of mapping strategies (e.g. linkage analysis or homozygosity mapping), followed by gene identification through positional cloning or candidate gene approach (i.e. prioritising genes for Sanger sequencing within the mapped genomic region, based

on the biological plausibility or possible relevance to the disease of interest).

While in theory the power of NGS would not be absolutely necessary for this approach, NGS has made gene discovery tremendously easier when used in combination with traditional mapping strategies. When informative families with several affected individuals from the same family are available, the disease locus can be narrowed down significantly and then NGS can be used to interrogate all the coding exons and splicing regions of the genes contained within the locus for the presence of the causative mutations.

For dominant traits, linkage analysis (discussed in detail in section 1.2.3) represents the gold standard for genetic mapping (Figure 1-3A). However, families that are genetically informative enough for linkage analysis are exceedingly rare. Thus, application of this approach for gene discovery is becoming harder by the day, as there are not many families left which may be suitable for this analysis.

For the study of recessive disorders where a homozygous variant is suspected (e.g. study of consanguineous families), NGS can be complemented by the use of homozygosity mapping (Figure 1-3B), which relies on the identification of regions that are identical by descent in affected individuals only (Alkuraya, 2013).

As discussed previously, NGS can be also used to rapidly screen candidate disease-causing or predisposing genes, selected based on their biological plausibility or on grounds of clinical observations hinting towards a possible genetic association (Figure 1-3C).

As discussed in more detail in the next chapter, applications of these traditional strategies in combination with NGS has been already successfully used in multiple occasions for the discovery of novel genes causing movement disorders.

Besides facilitating traditional mapping strategies, NGS has also offered the opportunity to identify novel disease-causing gene mutations in ways that simply were not possible before the advent of NGS (Olgiati *et al.*, 2016).

For the study of dominant families that are too small for the application of linkage analysis, one novel approach is sequencing the exomes (or genomes) of several distant affected individuals belonging to the same family (Figure 1-3D) and look for shared

variants after applying filtering criteria to prioritise the likely pathogenic variants (see next section for details of prioritisation strategies). Depending on the number of family members available for sequencing and their distance in the pedigree, this approach can result in the identification of relatively small lists of candidate variants that can be then used for replication studies in additional families or cohorts of similarly affected subjects.

For the study of recessive families where homozygosity mapping is not applicable (e.g. non-consanguineous pedigrees), the double hit strategy (Figure 1-3E) may be applied to look for compound heterozygous mutations. Here, the exomes of siblings affected by the same condition are interrogated for the presence of at least two separate, likely pathogenic, mutations in the same gene. With this strategy, when the number of affected individuals is small (i.e. only two affected siblings), it is useful to sequence also the DNA of the healthy parents, as this makes it possible to exclude genes carrying multiple mutations inherited from the same parent (and therefore located on the same allele), a mode of inheritance not compatible with a recessive disease.

Another important novel approach is the study of family trios by NGS, looking for the presence of *de novo* mutations (Figure 1-3F). These are mutations present in the DNA of the affected subject, but not in the DNA of the parents. This type of approach is generally used for individuals without a family history with severe neurological phenotypes that reduce the fitness to procreate. To date, this approach has been incredibly successful for the study of autism-spectrum disorders, schizophrenia and intellectual disability (Rauch *et al.*, 2012, Xu *et al.*, 2012, Gulsuner *et al.*, 2013, Genome of the Netherlands Consortium, 2014, Iossifov *et al.*, 2014).

Finally, NGS can also be used to study a cohort of unrelated patients, looking for the presence of causative mutations in the same gene (Figure 1-3G). This strategy is more likely to be effective for identifying the disease-causing gene when the disease of interest is rare and highly specific (e.g. presence of radiological hallmarks), as this would significantly reduce the possibility of genetic heterogeneity (i.e. multiple genes responsible for the same phenotype). This approach has been proven to be successful even with relatively small cohort of carefully characterised patients (Haack *et al.*, 2012, Simons *et al.*, 2013).

1.5 Identifying Causal Alleles: How to Prioritise Variants?

The key challenge in NGS is the interpretation of the large number of variants that are routinely detected. An average 'exome' would reveal the presence of ~24,000 coding and splice-site variants in individuals of African origin and ~20,000 variants in individuals of European origin (Bamshad *et al.*, 2011). Of these, on average, ~ 98% are known benign polymorphisms, and about ~50-60% are synonymous variants, meaning that they not lead to an amino acid change. However, hundreds of novel non-synonymous variants are found in the exome of each individual. Among these, only one (in case of dominant disease) or two (in recessive diseases) variants will be causative in most families with a Mendelian disease. Therefore, the crucial and more challenging step in the search of THE disease-causing mutation is recognising and differentiating the true disease-related alleles among the myriad of benign common and rare/novel variants and sequencing artefacts.

I will describe in the next section the strategies that are commonly used to filter and reduce the number of possible pathogenic variants, schematically summarised in Figure 1-4.
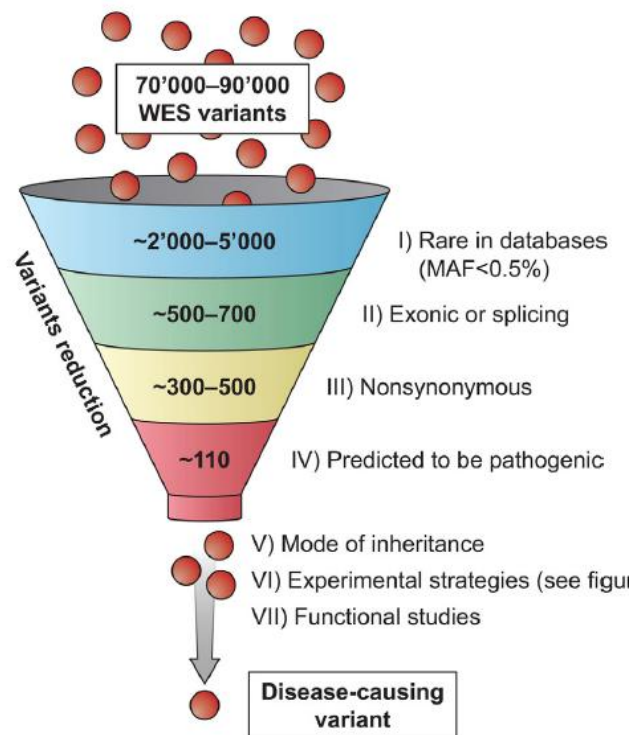
Figure 1-4 Prioritization of NGS candidate variants.
Image reproduced from (Olgiati *et al.*, 2016)

1.5.1 Filtering Based on the Inheritance Mode and Pedigree Information

In the case of Mendelian disorders, a correct understanding of the mode of inheritance can effectively reduce the search space for candidate pathogenic changes. As previously explained, the pattern of inheritance of a monogenic disorder will greatly influence both the experimental design (e.g. the number of cases to sequence and the most informative cases to select for sequencing) and the analytical approach.

Generally, family studies will examine variants that are shared between multiple affected relatives and consequently, it is preferable to select for sequencing subjects that are as distantly related as possible, as they will share a smaller number of genes. Where a dominant mode of inheritance is suspected, only shared heterozygous variants are considered, unless there is the suspicion that recessive mutations are transmitted in a pseudo-dominant way due to multiple loops of consanguinity in the pedigree. When a recessive inheritance is suspected, homozygous or compound heterozygous variants should be considered. Recessive inheritance or *de novo* dominant mutations should be suspected in sporadic cases. However, an increasing number of reports indicate that *de novo* mutations can also be inherited by multiple individuals in the same family due to germinal mosaicism in one of the unaffected parents, leading to pseudo-recessive presentations (Kancheva *et al.*, 2015).

Segregation of candidate variants, usually by Sanger sequencing, in other affected family members can further refine the list of variants. Unaffected individuals can be also of great help in reducing the number of candidate variants, as variants carried by these subjects are less likely to be responsible for the phenotype. However, two caveats should be kept in mind when using unaffected subjects to filter out variants: (i) pathogenic variants may be associated with incomplete penetrance (meaning that carriers of the variants may not manifest the disease); (ii) carriers of pathogenic variants may be too young at the time of the genetic study to firmly exclude that they will not develop the disease.

Importantly, segregation analysis alone in a single family cannot definitively implicate a variant as disease-causing, as there is the possibility that a separate, unobserved pathogenic mutation may lie on the same haplotype as the candidate variant.

Finally, it is important to mention that phenocopies, cases with the familial phenotype or

closely mimicking it but not carrying the causative variant, may be present in pedigree, greatly complicating the correct interpretation of the pedigree structure.

In summary, a substantial number of benign variants can be excluded from the list of disease-causing candidates using as filters the pedigree structure and the assumed mode of inheritance of the disease.

1.5.2 Filtering Based on Rarity

Filtering the list of variants against a variety of publicly available datasets, which contain NGS data from thousands of individuals originating from different human populations, is essential to removing common benign variations and narrowing the fraction of candidate variants down to a workable number.

The list of the most widely used datasets of genetic variations includes the Exome Aggregation Consortium (ExAC; http://exac.broadinstitute.org/), dbSNP version 129 and 137 (www.ncbi.nlm.nih.gov/projects/SNP), 1000 Genomes project (1kGP; www.1000genomes.org), NHLBI Exome Variant Server (EVS; evs.gs.washington.edu) and Complete Genomics 69 (www.completegenomics.com/public-data/69-Genomes).

Furthermore, variants should also be filtered against data from large cohorts of individuals sequenced in-house. This step is particularly important for excluding sequencing artifacts and false positive calls, which tend to be specific for the sequencing chemistry and the pipeline used in the analysis of the NGS data.

The population frequency of a variant is particularly important as it would be expected that Mendelian disease causing alleles are extremely rare, if not absent, in the general population. For dominant disorders, it is sensible to consider only novel or extremely rare variants. Alleles causative for recessive diseases are usually present in the population at MAF of < 0.01. However, it is essential to remember that these are largely arbitrary cut-offs. The frequency filter should be set depending on the frequency of the disease of interest in the general population, the clinical presentation (i.e. early onset/aggressive versus late onset/indolent phenotype), and the expected penetrance of the putatively disease-causing variants.

There are other two important issues that should be considered during this crucial step. First, the frequency of both benign and pathogenic variants can vary substantially among different ethnicities and certain variants are found exclusively in certain specific

populations. This means that variants that are completely absent in one population could be much more frequent in another. Therefore, it is essential to filter the WES results against data derived from ethnicity-matched populations.

Secondly, it is important to consider that well-established pathogenic mutations (e.g. the *LRRK2* mutations p.Gly2019Ser causing autosomal dominant PD) may be present in population variant databases, although at low frequencies. Being too strict with filtering based on MAF may therefore sometimes result in the exclusion of pathogenic alleles from the analysis. This is particularly true for diseases such as PD, which tend to manifest later in life and thus non-manifesting carriers of pathogenic alleles may be present in large control populations.

1.5.3 Filtering Based on Deleteriousness and Conservation

Further stratification of variants can be undertaken based on predictions of their deleteriousness. Synonymous variants are generally excluded from the analysis, as it is expected that causative alleles for Mendelian diseases will be missense, nonsense, frameshift or splice site variants. Importantly, although in rare instances, synonymous variants can potentially affect splice sites and therefore result in loss-of-function alleles (Korvatska *et al.*, 2013). In addition, variants located in deep intronic and in other non-coding genomic regions are generally removed from the list of candidates under the assumption that disease causing-mutations would affect the coding region of the genome. However, one should be aware that this assumption is based on the fact that, as a matter of feasibility, in the Sanger sequencing era only the coding portion of the genes were screened. It is hence plausible that a significant proportion of the missing variability responsible for Mendelian diseases is located in the intronic region.

Greater importance may be given to loss-of-function variants (i.e. frameshift, stop codons and variants disrupting canonical splice sites), than to missense variants.

Additional strategies can be used to further prioritize the remaining candidate variants, especially if they are missense. A powerful approach uses the quantitative estimates of mammalian evolution at the nucleotide level. This approach relies on the principle that deleterious mutations generally present high sequence conservation as a result of purifying selection. Therefore, highly conserved nucleotides and amino acids are likely to be very relevant for the function of the gene and the encoded protein. Examples of tools used in this thesis for assessment and quantification of evolutionary conservation

are PhiloP (Pollard *et al.*, 2010) and GERP++ (Davydov *et al.*, 2010).

The predicted deleteriousness of amino acid substitutions can also be assessed using *in silico* tools such as SIFT (http://sift.jcvi.org/) (Kumar *et al.*, 2009), PolyPhen2 (http://genetics.bwh.harvard.edu/pph2/) (Adzhubei *et al.*, 2010), Provean (http://provean.jcvi.org/) (Choi *et al.*, 2012), MutationTaster (http://www.mutationtaster.org/) (Schwarz *et al.*, 2014) and CADD (http://cadd.gs.washington.edu/home) (Kircher *et al.*, 2014).

Some of these tools (e.g. SIFT or Provean) rely on specific biological aspects of deleterious mutations (often conservation) to classify variants in discrete classes of pathogenicity (first-principles approaches). Another group (e.g. Polyphen-2 or MutationTaster) consists of classifiers that are trained to distinguish between a set of known deleterious mutations against a set of benign polymorphisms (trained classifiers).

Importantly, these methods are particularly useful when assessing the pathogenicity of putatively loss-of-function variants, either causing recessive diseases or causing dominant diseases through haplo-insufficiency or dominant negative effects. However, the *in silico* tools are less reliable for the assessment of dominant variants that are pathogenic through a gain-of-function mechanism.

1.6 Limitations of Next-Generation Sequencing

Despite many successful reports of disease-associated novel genes identified by WES, it is not precisely known how often this approach fails, as negative results are not reported most of the times. The experience in our department teaches that failure in the analysis of kindreds with suspected Mendelian diseases is unfortunately not uncommon.

NGS bears a number of important limitations, which have to be kept in mind when the causative variant is not identified.

1. Current NGS technologies easily detect single nucleotide variants or small deletions are, but there remain significant issues with the identification of large deletions and copy number variants (CNVs).

2. The currently used short read libraries (~250bp) lead to particular problems with the detection of repeat expansions, which not uncommonly are the responsible cause for neurodegenerative diseases, such as the dominant SCAs or HD.

3. Variable coverage of the targeted regions, as mutations may be missed if they are located in poorly covered areas.

4. The causative gene is not in the exome capture kit target definition (for instance, it is not a known gene, or there is a failure in the design)

Finally, even once a single or few promising candidate variant are found in a given pedigree, the significant genetic heterogeneity that exists for many inherited neurological conditions, can hamper the confirmation of the finding, which generally relies on the identification of other mutations in the same gene in unrelated pedigrees.

Chapter 2. Overview on Genetics of Selected Movement Disorders

2.1 The Genetics of Parkinson disease

2.1.1 Introduction

PD is the second most common neurodegenerative disease after Alzheimer disease, affecting >2% of those over 75 years (Mayeux *et al.*, 1995).

The main clinical features of PD and clinical diagnostic criteria include bradykinesia and at least one other sign amongst muscular rigidity, rest tremor, or postural instability (Figure 2-1). A progressive course, unilateral presentation with asymmetrical signs, a classic pill rolling tremor, good sustained response to levodopa (L-DOPA) and a number of non-motor symptoms accompanying or preceding the motor onset (eg. hyposmia, constipation, genito-urinary symptoms, REM-behavioural sleep disorders) generally support the diagnosis (Lees *et al.*, 2009, Noyce *et al.*, 2016).

Figure 2-1 Typical appearance of a patient with Parkinson disease.
Reproduced from (Lees *et al.*, 2009)

The pathological signature of PD is a selective loss of pigmented dopaminergic neurons from the pars compacta of the substantia nigra (Figure 2-2A). Nigral neuron degeneration and consequent decrease in dopaminergic striatal innervation result in classic PD motor symptoms. This nerve cell loss is accompanied by three distinctive intraneuronal inclusions: Lewy bodies (LBs; Figure 2-2B), the pale body, and the Lewy neurite.

α-synuclein (α-syn) is the main component of LBs (Spillantini *et al.*, 1997). According to the model proposed by Braak and colleagues, α-syn pathology may spread ascending from the dorsal motor nucleus of the vagus and involving progressively, the lower brainstem, the olfactory bulb, the midbrain and finally the cortex (Braak *et al.*, 2003).
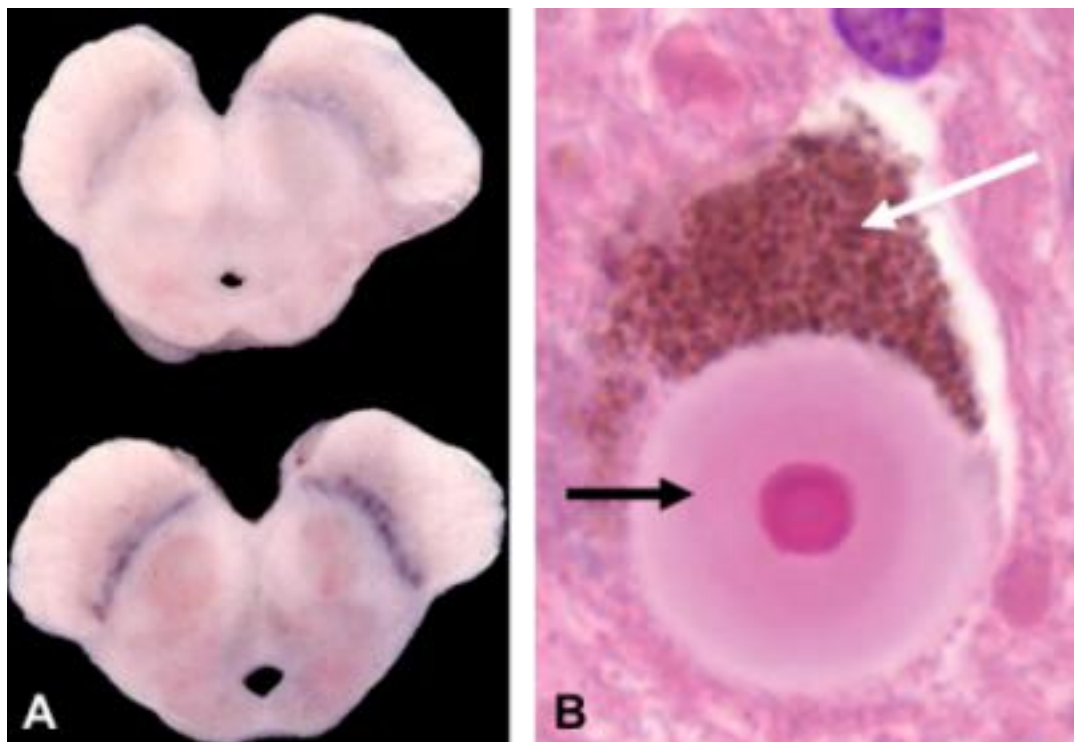
Figure 2-2 Pathological features of Parkinson disease
(A) Cross section of the midbrain showing the pigmented substantia nigra in a normal brain (bottom) and depigmented nigra in a brain with PD (upper). (B) Microscopic section of a substantia nigra pigmented neuron containing neuromelanin (white arrow) and a Lewy body (black arrow) within the cytoplasm of the neuron. The Lewy body has a dense core and a lighter halo.

The aetiology of PD is poorly understood and, similarly to other neurodegenerative conditions, age is the major risk factor. However, 10% of people with the disease are younger than 45 years of age (early-onset PD).

PD was long thought to be a sporadic disorder without genetic causation with most of the research interest focused on the identification of environmental risk factors (reviewed in (Noyce *et al.*, 2012).

Several studies estimating the genetic contribution to PD pathogenesis using twins have shown low concordance rates in monozygotic and dizygotic twins (Duvoisin *et al.*, 1981, Ward *et al.*, 1983, Marttila *et al.*, 1988). However, in studies based on PET scan data, rather than simple cross-sectional observance of the phenotype, the concordance rate was significantly higher for monozygotic twins, than for dizygotic twins (55% versus 18%), suggesting a substantial genetic contribution to the PD pathogenesis (Piccini *et al.*, 1999). It is estimated that approximately 5-10% of people with PD have a positive family history in a first degree-relative.

Over the last 25 years, since the identification of the a-synuclein (*SNCA*) locus, the views on the aetiology of PD have profoundly changed. Mutations in a growing list of genes have been incontrovertibly linked to monogenic forms of PD (recently reviewed in (Hernandez *et al.*, 2016). Furthermore, genome-wide-association studies (GWAS) have succeeded in identifying many common, low risk variants that are likely to play a direct role in the aetiology of the common sporadic disease as well (Nalls *et al.*, 2014). In addition, rare variants with intermediate-effect have been identified as important risk factors (e.g. *GBA*). A schematic overview of the frequency and penetrance of the genes linked to PD is shown in Figure 2-3.
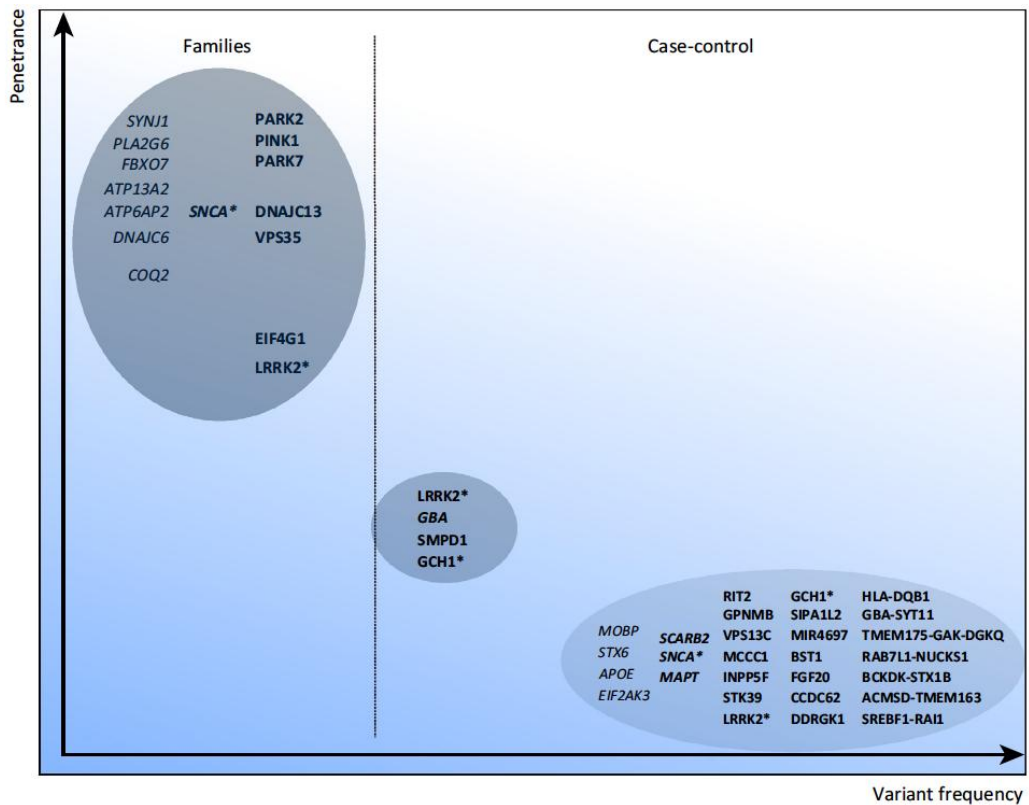
Figure 2-3. Schematic representation of the frequency and penetrance of the Parkinson disease genes
*Pleiotropic loci. Figure adapted from (Verstraeten *et al.*, 2015)

2.1.2 Monogenic Causes of Parkinson Disease

The genes associated with monogenic forms of PD are listed in Table 2-1.

Mendelian forms of PD are overall rare and generally have an earlier disease manifestation than sporadic PD. Mutations in genes identified as causing Mendelian forms of PD explain 30% of familial PD and only 3%-5% of patients with sporadic disease occurrences (Kumar *et al.*, 2011). In the next section I will describe the main clinical and biological features of the most relevant Mendelian genes that have been shown to cause PD.

Table 2-1 Monogenic causes of Parkinson disease

Locus	Gene	Features	Inheritance	Mutational spectrum	Pathology
PARK1/PARK4	*SNCA*	Early and late-onset, fast progression, severe dementia,	AD	Missense and gene dosage	Synucleinopathy
PARK2	*Parkin*	Juvenile- or young-onset parkinsonism, slow progression	AR	Missense, truncating and gene dosage	Synucleinopathy (occasionally)
PARK6	*PINK1*	Early-onset parkinsonism, slow progression	AR	Missense, truncating and gene dosage	Synucleinopathy (occasionally)
PARK7	*DJ-1*	Early-onset parkinsonism, psychiatric features, slow progression	AR	Missense, truncating and gene dosage	Synucleinopathy
PARK8	*LRRK2*	Late onset parkinsonism, slow progression	AD	Missense	Synucleinopathy, tauopathy
PARK9	*ATP13A2*	Juvenile and early onset, atypical, fast progression	AR	Missense, truncating	Not known
PARK14	*PLA2G6*	Juvenile and early onset, atypical, fast progression	AR	Missense, truncating	Synucleinopathy
PARK15	*FBX07*	Juvenile and early onset, atypical, fast progression	AR	Missense, truncating	Not known
PARK17	*VPS35*	Late onset parkinsonism, slow progression	AD	Missense	Not known
PARK17	*DNAJC6*	Juvenile and early onset, atypical, fast progression	AR	Missense, truncating	Not known
PARK20	*SYNJ1*	Juvenile and early onset, atypical, fast progression	AR	Missense, truncating	Tauopathy
NA	*DNAJC13*	Late-onset, typical, slow progression	AD	Missense	Synucleinopathy
NA	*RAB39B*	Early onset, intellectual disability	X-linked	Missense, truncating and gene dosage	Synucleinopathy
NA	*CHCHD2*	Late onset parkinsonism, slow progression	AD	Missense	Synucleinopathy?
NA	*VPS13C*	Early onset, fast progression	AR	Truncating	Synucleinopathy

<u>*SNCA*</u> (PARK1, PARK4)

The identification in 1997 of the p.Ala53Thr missense mutation in *SNCA* as a cause of autosomal dominant PD in families of Greek and Southern Italian origin was the first proof for a genetic aetiology in a subset of PD cases (Polymeropoulos *et al.*, 1997). Furthermore soon after the identification of SNCA mutations in familial PD cases it was discovered that α-Syn is the major component of LBs, the pathological hallmark of PD, therefore linking familial to sporadic PD (Spillantini *et al.*, 1997).

Subsequently, whole-locus duplication and triplication of *SNCA* were identified, proving that not only structurally altered α-synuclein, but also simple overexpression of the wild-type protein is pathogenic (Singleton *et al.*, 2003, Kara *et al.*, 2014). The p.Ala30Pro and p.Glu46Lys mutations have been detected in a single family of German and Spanish ancestry, respectively (Kruger *et al.*, 1998, Zarranz *et al.*, 2004). Only recently, three additional *SNCA* point mutations (p.His50Gln, p.Gly51Asp and Ala53Glu) have been discovered (Kiely *et al.*, 2013, Proukakis *et al.*, 2013, Pasanen *et al.*, 2014).

The missense mutations are pathogenic through a toxic gain of function, whereby they increase the tendency of α-Syn to form β-pleated sheets, which, in turn, are thought to predispose α-Syn to form the aggregates that are localised in LBs (Devine *et al.*, 2011).

Patients with *SNCA* missense mutations usually have EOPD with initial good response to L-DOPA. The disease tends to be aggressive, with dementia often complicating early on the clinical picture.

A dose relationship between α-Syn levels and severity of the clinical phenotype is observed. In *SNCA* multiplications families, duplications (three copies of *SNCA*) are not fully penetrant and lead to late-onset dopa-responsive PD, as seen in typical sporadic PD (Ibanez *et al.*, 2009); triplications (four copies of *SNCA*) are conversely fully-penetrant and cause a much more aggressive phenotype with earlier onset and severe rapidly progression, almost inevitably complicated by early dementia and additional features such as dysautonomia (Farrer *et al.*, 2004, Fuchs *et al.*, 2007).

Brain pathology in patients with *SNCA* mutations is characterized by abundant α-Syn-

positive neuronal inclusions.

LRRK2 Mutations (PARK8)

The PARK8 locus was first mapped on chromosome 12p11.23-q13.11 in a large Japanese family with autosomal dominant PD (Funayama *et al.*, 2002). A few years later two independent groups identified the causative mutations underlying the PARK8 locus in the *LRRK2* gene (Paisan-Ruiz *et al.*, 2004, Zimprich *et al.*, 2004).

Mutations in *LRRK2* have been since then recognized as the most common Mendelian cause of PD. A large number of variants have then been described in PD cases. However, based on segregation with disease in families and frequency in population controls, only few of these variants are firmly considered pathogenic: p.Arg1441Gly, p.Arg1441Cys, p.Arg1441His, p.Tyr1699Cys, p.Gly2019Ser and p.Ile2020Thr (Di Fonzo *et al.*, 2005, Gilks *et al.*, 2005, Zabetian *et al.*, 2005).

The most frequent mutation is by far the c.6055G>A; p.Gly2019Ser which is found in up to 40% of cases of PD in North African populations (Lesage *et al.*, 2006), in about 20% of Ashkenazi Jewish patients (Ozelius *et al.*, 2006) and 1-7% of PD patients of European origin (Di Fonzo *et al.*, 2005, Clark *et al.*, 2006, Zabetian *et al.*, 2006).

The p.Arg1441Cys is the second most common mutation and has been identified worldwide (Nuytemans *et al.*, 2008). Conversely the p.Arg1441Gly and the p.Ile2020Thr are very rare and population-specific, being the first mainly found in the Basques (Simon-Sanchez *et al.*, 2006) and the second in the Japanese population (Tomiyama *et al.*, 2006).

The penetrance of the *LRRK2* p.Gly2019Ser mutation has been established to be ~28% in subjects younger than 60 years of age, but increases up to 74% at 79 years of age (Healy *et al.*, 2008). Of note, there has been a recent report of two monozygotic twins in their 70s with the p.Gly2019Ser but discordant for the presence of PD, suggesting that the variability in onset and penetrance between *LRRK2*, maybe largely non-genetic in origin (e.g. stochastic; environmental) (Xiromerisiou *et al.*, 2012). Furthermore, a recent report suggested that the penetrance in the Ashkenazi Jewish population could be as low as 25% by the age of 80, a figure much lower than in other ethnic background, suggesting the existence of genetic or environmental factors which affect the penetrance of the p.Gly2019Ser mutation in this population (Marder *et al.*, 2015).

The majority of patients with *LRRK2* mutations presents with late-onset asymmetric L-DOPA responsive tremor-predominant PD, clinically indistinguishable from PD (Healy *et al.*, 2008). Neuropathological findings showed pleiomorphic pathologies overlapping with other neurodegenerative diseases, including LBs, tau- and ubiquitin-containing inclusions and pure nigral degeneration without LBs (Zimprich *et al.*, 2004, Giasson *et al.*, 2006).

LRRK2 is a large gene that consists of 51 exons and encodes the 2527-amino acid protein leucine-rich repeat kinase 2. The physiological and pathological functions of LRRK2 have not yet been fully characterized. Several pathogenic *LRRK2* mutations cluster in functionally important domains and impair their function: p.Arg1441Cys, p.Arg1441Gly, and p.Arg1441His reduce protein GTPase activity, whereas the p.Gly2019Ser and p.Ile2020Thr mutations in the kinase domain have been shown to increase its activity (Simon-Sanchez *et al.*, 2006).

VPS35 (PARK17)

A single missense mutation in *VPS35,* p.Asp620Asn, has been identified by two groups through WES as an important cause of autosomal-dominant PD (Vilarino-Guell *et al.*, 2011, Zimprich *et al.*, 2011). Several other studies in which the sequencing of the entire *VPS35* coding region was performed has disclosed a handful of other missense mutations (p.Gly51Ser, p.Met57Ile, p.Thr82Arg, p.Ile241Met, p.Pro316Ser, p.Arg524Trp, and p.Leu774Met). However, none of these additional mutations have been proven to be pathogenically relevant (Lesage *et al.*, 2012, Sharma *et al.*, 2012, Nuytemans *et al.*, 2013). Overall, *VPS35* the p.Asp620Asn mutation is a rare cause of PD accounting for only about 1% of familial parkinsonism and 0.2% of sporadic PD. *VPS35* encodes a highly-conserved component of the retromer, a complex that mediates reterograde transport of transmembrane cargo from endosomes back to the trans-Golgi network (Seaman, 2005, Bonifacino and Rojas, 2006). Clinically *VPS35*-related PD appears to be similar to idiopathic PD (Sheerin *et al.*, 2012).

DNAJC13

WES and linkage analysis identified the missense mutation p.Asn855Ser in *DNAJC13* in a Saskatchewan autosomal-dominant family affected by multi-generational PD with evidence LB pathology. Subsequent genotyping in 2928 patients and 2676 control subjects from Canada, Norway, Taiwan, Tunisia, and the USA identified four additional

patients carrying the same mutation, of which two had familial parkinsonism, but none in controls (Vilarino-Guell *et al.*, 2014). *DNAJC13* regulates the dynamics of clathrin coats on early endosomes. Cellular analysis shows that the mutation confers a toxic gain-of-function and impairs endosomal transport. Subsequent studies have shown that the *DNAJC13* p.Asn855Ser substitution is not a common cause of PD among Caucasian populations (Gustavsson *et al.*, 2015, Lorenzo-Betancor *et al.*, 2015).

<u>CHCHD2</u>

Funayama and colleagues used linkage analysis and WES to successfully identify in a Japanese dominant PD family a missense variant in the *CHCHD2* gene, encoding the mitochondrial protein coiled-coil-helix-coiled-coil-helix domain-containing 2 (Funayama *et al.*, 2015). Screening of a further 340 index patients with autosomal dominant PD identified three additional pathogenic missense and splice-site mutations, p.Thr61Ile, p.Arg145Gln, and c.300+5G>A. Subsequently, other independent groups have confirmed that coding mutations in *CHCHD2* represent a rare genetic cause of autosomal dominant PD and may also represent a risk factor for sporadic PD and other synucleinopathies (Jansen *et al.*, 2015, Ogaki *et al.*, 2015, Koschmidder *et al.*, 2016, Shi *et al.*, 2016, Zhang *et al.*, 2016).

Autosomal Recessive Parkinson Disease
<u>PARK2</u>

Mutations in *PARK2*, firstly identified by positional cloning in Japanese families (Matsumine *et al.*, 1997, Kitada *et al.*, 1998), are the most common cause of autosomal recessive, EOPD. *PARK2* mutations are detected in up to ~50% of cases with recessive familial EOPD (Lucking *et al.*, 2000), as well as ~10% of sporadic cases with onset before the age of 45 (Klein and Lohmann-Hedrich, 2007). A range of loss-of-function variants are detected, including missense, truncating mutations and whole-exon deletions or duplications, most commonly in the compound heterozygous state.

Whether heterozygous mutations in *PARK2* represent a risk factor for PD is still a matter of debate (Klein *et al.*, 2007) and circumstantial evidence suggests that copy-number variants may increase the disease risk (Huttenlocher *et al.*, 2015), but not point mutations (Kay *et al.*, 2007, Kay *et al.*, 2010).

PARK2-related disease usually shows a slowly progressive course with a dramatic

response to dopaminergic treatment. No specific features differentiate *PARK2* mutation carriers from other EOPD forms; however, symmetrical onset, dystonia at onset, hyperreflexia, slower progression of the disease, a tendency toward a better response to L-DOPA, and preservation of olfaction might be more frequent among patients with *PARK2* mutations (Khan *et al.*, 2003, Alcalay *et al.*, 2011).

Post-mortem examination of *PARK2*-mutated cases shows a more restricted distribution of the pathology than in classic sporadic PD, with severe but selective ventral nigral degeneration and absent or scarce LB pathology (Doherty *et al.*, 2013).

PARK2 encodes parkin, a protein that functions as an E3 ubiquitin ligase in the process of ubiquitination, a form of post-translational modification that conjugates ubiquitin proteins to lysine residues of target proteins, in order to address them towards proteosomal degradation. Most *PARK2* mutations lead to loss of its E3 ligase function. Disturbed elimination of damaged mitochondria, which is an important cellular process called mitophagy, appears to be one of the most important mechanisms for neuronal death in parkin deficiency (Deas *et al.*, 2011).

PINK1 (PARK6)

Mutations in phosphatase and tensin homolog-induced putative kinase 1 (*PINK1*) are the second-most common cause of autosomal recessive EOPD, accounting for ~1% to 8% of recessive familial EOPD and ~1% of sporadic EOPD cases (Healy *et al.*, 2004, Rogaeva *et al.*, 2004, Valente *et al.*, 2004, Bonifati *et al.*, 2005). Mutations are found across different populations and one mutation with a founder effect is particularly frequent in the Philippines (Bonifati *et al.*, 2005).

PINK1 is a 581 amino acid ubiquitously expressed protein kinase. It consists of an amino-terminal mitochondrial targeting motif, a conserved serine-theonine kinase domain, and a carboxy-terminal autoregulatory domain. Two-thirds of the reported pathogenic mutations determine a loss-of-function of the PINK1 kinase domain, supporting the relevance of PINK1 enzymatic activity in the pathogenesis of PD. More than 90% of the reported mutations in *PINK1* are missense mutations, whereas the remaining are copy number mutations or truncating mutations. Similarly to *PARKIN*, the role of heterozygous *PINK1* mutations is debated (Abou-Sleiman *et al.*, 2006).

Clinically, *PINK1* mutation carriers present with early-onset, slowly progressive L-

DOPA-responsive parkinsonism, initial gait impairment and often psychiatric symptoms, such as depression and anxiety. Cognitive involvement is rare. Differently from *PARK2* mutated cases, olfactory dysfunction is common in *PINK1* (Ferraris *et al.*, 2009).

The first post-mortem analysis in a case with *PINK1*-linked PD showed neuronal loss in the substantia nigra and the presence of LBs (Samaranch *et al.*, 2010). However, a more recent report showed absence of LB pathology (Takanashi *et al.*, 2016).

PINK1 and Parkin function in a common pathway for detecting mitochondrial damage and selectively eliminating corrupted mitochondria. PINK1 is stabilized on mitochondria with lower membrane potential and recruits Parkin from the cytosol. Once recruited to mitochondria, Parkin becomes enzymatically active and initiates the autophagic clearance of mitochondria by lysosomes (i.e., mitophagy) (Youle and Narendra, 2011).

DJ-1 (PARK7)

Bonifati and colleagues identified mutations in *DJ-1* as an additional cause of EOPD (Bonifati *et al.*, 2003). *DJ-1* mutations are more rare than *PARK2* and *PINK1*, being found in only ~1% of EOPD cases (Abou-Sleiman *et al.*, 2003, Pankratz *et al.*, 2006). The clinical phenotype is similar to that of *PARK2-* and *PINK1*-related EOPD (Abou-Sleiman *et al.*, 2003). Dementia and features of motorneuron disease have been described in individual cases with bi-allelic *DJ-1* mutations (Annesi *et al.*, 2005, Hanagasi *et al.*, 2016).

DJ-1 encodes for a protein working as a cellular sensor of oxidative stress (Canet-Aviles *et al.*, 2004, Junn *et al.*, 2005). Recently, the first neuropathological assessment of a *DJ-1* mutated case has been reported, indicating that *DJ-1* mutations are associated with α-syn aggregation and deposition (Taipa *et al.*, 2016).

RAB39B

Genetic analysis of an Australian and of an American family with a combination of EOPD and intellectual disability with an X-linked pattern of inheritance identified a large deletion and a missense mutation (p.Thr168Lys) in the *RAB39B* gene (Wilson *et al.*, 2014). All affected cases initially presented in childhood with various degrees of intellectual disability, including developmental delay, cognitive impairment,

macroencephaly, and, seizures. EOPD appeared later on, with tremor as the first symptom. Post-mortem studies show that *RAB39B* mutations causes extensive nigral dopaminergic neuronal loss with widespread LB pathology.

Other groups have subsequently replicated this finding and found *RAB39B* mutations in individuals affected by classic EOPD, in absence of the atypical signs observed in the families where the gene was first identified (Lesage *et al.*, 2015, Mata *et al.*, 2015).

Interestingly, previous work had identified *RAB39B* as a cause of X-linked intellectual disability in absence of parkinsonian signs (Giannandrea *et al.*, 2010), indicating that *RAB39B* mutations cause a spectrum of overlapping syndromes. Furthermore, this suggests that shared pathogenic mechanisms may exist linking PD to developmental disorders. Rab proteins are small molecular weight guanosine triphosphatases involved in the regulation of vesicular trafficking (Cheng *et al.*, 2002).

VPS13C

Very recently, *VPS13C* loss of function variants have been recognised as a novel cause of autosomal-recessive EOPD (Lesage *et al.*, 2016). Homozygous or compound heterozygous truncating mutations were detected in three isolated PD subjects. The phenotype associated with *VPS13C* mutations is characterised by rapid and severe disease progression and early cognitive decline. Neuropathological assessment showed evidence of diffuse LB pathology. Functional work demonstrated that VPS13C knock-down leads to a severe mitochondrial pathology and exacerbation of PINK1/Parkin-dependent mitophagy.

Complex Forms of Autosomal Recessive Parkinsonism

Mutations in the genes described in this section are generally associated with more rare and aggressive forms of recessive parkinsonism, characterised by very early-onset (<30 years) and usually additional, atypical features (pyramidal, dystonic, ocular movement, and cognitive disturbances). However, in spite of the different phenotypic presentation, several biological evidences link the pathogenic mechanisms of these conditions to that of PD. Furthermore, several recent observations indicate that mutations in most of these genes can lead to more typical forms of autosomal recessive EOPD.

ATP13A2 (PARK9)

Recessive loss-of-function of *ATP13A2* cause Kufor-Rakeb syndrome, a rare, juvenile-

onset disorder characterized by severe parkinsonism, dementia, pyramidal signs and supranuclear gaze palsy (Ramirez *et al.*, 2006). Subsequently, *ATP13A2* recessive mutations have been detected in cases with a broader phenotype, including isolated juvenile-parkinsonism (Di Fonzo *et al.*, 2007, Martino *et al.*, 2015), parkinsonism with brain iron accumulation (Schneider *et al.*, 2010) and, more recently, also neuronal ceroidal lipofuscinosis (a severe infantile neurodegenerative disorder) (Bras *et al.*, 2012).

ATP13A2 is a large gene encoding for a protein normally located in the lysosomal membrane (Ramirez *et al.*, 2006). Loss of ATP13A2 leads to lysosomal dysfunction and subsequent α-Syn accumulation (Tsunemi and Krainc, 2014).

PLA2G6 Mutations (PARK14)

A broad range of truncating recessive mutations in the phospholipase A2 group VI (*PLA2G6*) gene, encoding for a phospholipase involved in metabolism of phospholipids to free fatty acids, were first described as the cause of infantile neuroaxonal dystrophy and neurodegeneration associated with brain iron accumulation (Kurian *et al.*, 2008).

PLA2G6 mutations were subsequently detected also in subjects with a different presentation, featuring L-DOPA-responsive dystonia-parkinsonism, pyramidal signs and cognitive/psychiatric features, with onset in early adulthood, without evidence of iron accumulation (Paisan-Ruiz *et al.*, 2009). More recently, bi-allelic missense mutations, more likely to have a milder effect on protein function, have also been identified in cases with uncomplicated EOPD (Xie *et al.*, 2015, Giri *et al.*, 2016).

LBs have been described in association with *PLA2G6* mutations (Paisan-Ruiz *et al.*, 2012). Functional work performed in a Drosophila model of *PLA2G6* deficiency shows that loss of normal gene activity leads to lipid peroxidation and mitochondrial dysfunction (Kinghorn *et al.*, 2015).

FBOX7 (PARK15)

FBXO7 mutations were first described in a Persian family and then in an Italian family with severe juvenile-onset parkinsonism associated with spasticity and prominent pyramidal signs (Najim al-Din *et al.*, 1994, Di Fonzo *et al.*, 2009). More recently a homozygous *FBXO7* missense mutation was described also in a family with more classic EOPD (Lohmann *et al.*, 2015). *FBXO7*, like Parkin, is part of an E3 ubiquitin

ligase complex necessary for the correct initiation of the mitophagy process (Laman, 2006, Burchell *et al.*, 2013).

SYNJ1

The same homozygous mutation in *SYNJ1* (p.Arg258Gln) was identified by WES, in two unrelated consanguineous kindred's, as a cause of a complex autosomal recessive parkinsonian syndrome (Krebs *et al.*, 2013, Quadri *et al.*, 2013). The phenotype includes aggressive parkinsonism with severe levodopa-induced dystonia. Additional features are generalized seizures, cognitive decline, dysarthria, eyelid apraxia and supranuclear gaze palsy.

SYNJ1 encodes synaptojanin 1, a phosphoinositide phosphatase protein involved in clathrin-mediated endocytosis in the adult brain (Drouet and Lesage, 2014). A recent report showed that bi-allelic loss of synaptojanin 1 cause severe infantile epileptic encephalopathy with brain accumulation of tau protein (Dyment *et al.*, 2015, Dyment *et al.*, 2015).

DNAJC6

Recessive truncating mutations in *DNAJC6* cause juvenile onset parkinsonism with rapid progression. Associated features include dysarthria, generalised seizures and brain atrophy on MRI (Edvardson *et al.*, 2012, Koroglu *et al.*, 2013). The group of Bonifati recently described *DNAJC6* mutations in cases with a milder presentation, consistent with classic EOPD (Olgiati *et al.*, 2016). *DNAJC6* encodes the protein auxilin, which is a clathrin-associated protein enriched in nerve terminals and may play a role in synaptic vesicle recycling (Ahle and Ungewickell, 1990).

2.1.3 Rare Variants Predisposing to PD

GBA

Homozygous or compound heterozygous loss-of-function mutations in *GBA* are the genetic abnormality underlying Gaucher's disease (GD), the most common lysosomal storage disorder. GD has a prevalence of 1/40,000 to 1/50,000 in all ethnicities and is particularly frequent in the Ashkenazi Jewish population, where it affects 1/800 to 1/1,000 live births (Cox, 2001, Grabowski, 2008).

GD is an autosomal recessive disorder and more than 300 different causative *GBA*

mutations spanning the entire coding region have been described (Figure 2-4), including insertions, deletions, point mutations and complex alleles resulting from recombination events with the neighbouring pseudogene *GBAP* (Hruska *et al.*, 2008).
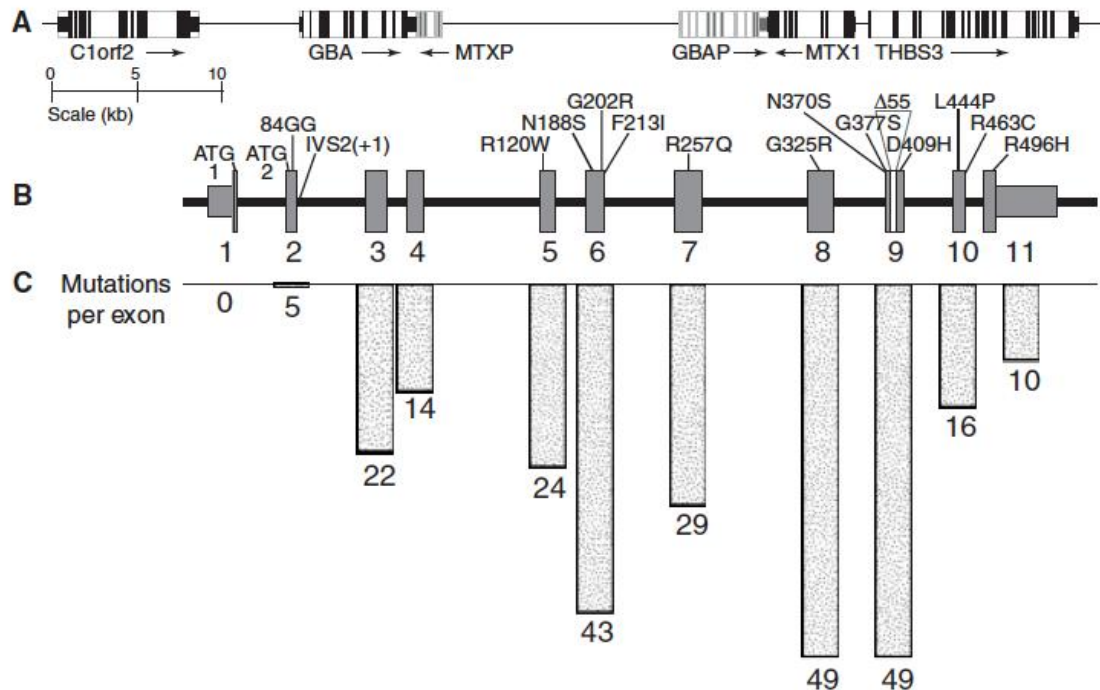
Figure 2-4 *GBA* gene structure and distribution of pathogenic mutations across the coding exons
Image reproduced from (Hruska *et al.*, 2008)

GD is caused by an insufficient activity of glucocerebrosidase (GCase), the lysosomal enzyme coded by *GBA*. Pathogenic mutations affect the enzyme's catalytic function, cellular stability and/or subcellular trafficking, resulting in intracellular build-up of GCase's main substrate, glucosylceramide. mainly in the cells of the reticuloendothelial system of the spleen, liver and bone marrow, and often resulting in organomegaly (Grabowski, 2008).

Clinically, GD presents with a spectrum of manifestations, the severity of which partially depend on the deleteriousness of the mutation on GCase activity: type 1 GD, the non-neuronopathic, most common and mildest form of GD; type 2 (GD2) the acute neuronopathic, most severe form associated with a complete deficiency in GCase activity and short life-expectancy; and type 3 (GD3) the chronically neuronopathic form which has a later onset and longer life-expectancy than GD2.

The main clinical features of GD are summarised in the panel below taken from (Sidransky and Lopez, 2012).

The three types of Gaucher's disease

Type 1: non-neuronopathic

- Panethnic disorder, although more common in Ashkenazi Jews
- Associated with clinical heterogeneity
- Wide range of symptom severity
- Hepatosplenomegaly, anaemia, and thrombocytopenia are common
- Bone disease is a frequent cause of morbidity
- Treated with enzyme replacement therapy

Type 2: acute neuronopathic

- Rare, panethnic disorder
- Can present prenatally, at birth, or in the first year of life
- Rapidly progressive neurological deterioration
- Enzyme replacement therapy does not reverse or halt neurological progression
- Early death within days to years

Type 3: chronic neuronopathic

- Includes several different phenotypes with variable longevity
- Accompanied by a specific disorder of horizontal saccadic eye movements
- Some patients develop myoclonic epilepsy
- A subgroup of patients develop cardiac calcification, hydrocephalus, and other abnormalities
- Associated with distinct learning disabilities in some patients

In the past decade a previously unexpected link between GD and PD has been recognised. The first findings were based on isolated clinic observations of GD cases presenting a parkinsonian picture with clinical features very similar to those classically seen in patients with sporadic PD (Neudorfer et al., 1996, Tayebi et al., 2001, Tayebi et al., 2003). These observations were subsequently extended to the GD first-degree relatives, obligate carriers of *GBA* heterozygous mutations (Goker-Alpan et al., 2004).

Then, many independent case-control studies, performed in PD cases from different ethnical backgrounds (reviewed in (Sidransky and Lopez, 2012), have then consistently observed a higher frequency of *GBA* mutations in PD patients (Figure 2-5), indicating a causal relationship between GD and PD.

GBA mutations are now considered the most relevant genetic risk factors for PD (Neumann *et al.*, 2009, Sidransky *et al.*, 2009). Among Ashkenazi Jewish subjects, *GBA* mutation are found in ~15% of patients and among non-Ashkenazi Jewish subjects mutations are identified in ~7%, with an odds ratio for any *GBA* mutation in patients versus controls of ~5.

Neuropathological analysis of brains from parkinsonian patients with GD or carriers of heterozygous *GBA* mutations revealed the presence of abundant α-syn positive LBs (Bembi *et al.*, 2003, Neumann *et al.*, 2009).

Clinically, patients with PD and *GBA* mutations (both homozygous and heterozygous carriers) present with a classic clinical picture, indistinguishable from that of sporadic PD. Patients are characterized by asymmetric resting tremor, rigidity and bradykinesia and a good response to L-DOPA treatment. Most series of patients with *GBA* mutations report a lower mean age at onset and a higher incidence of cognitive and behavioural symptoms, such as dementia and visual hallucinations, compared to wild type cases (Alcalay *et al.*, 2012, Winder-Rhodes *et al.*, 2013).

Importantly, the replacement therapy used to treat GD cases does not modify the risk of PD. It is not clear though whether the drug simply does not cross the blood-brain barrier or whether enzyme replacement is not targeting the pathogenic mechanisms critical for PD (Rosenbloom *et al.*, 2011).
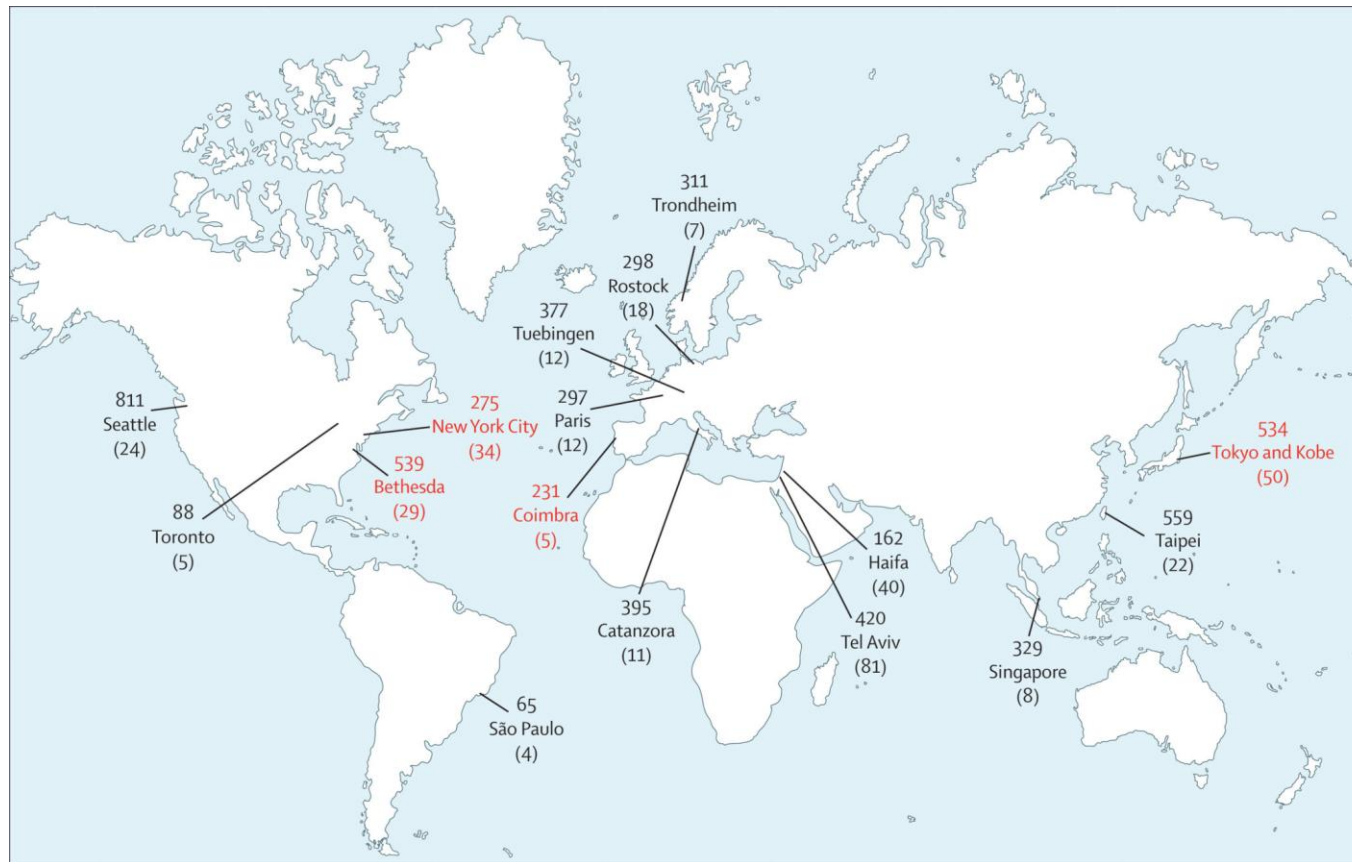
Figure 2-5 Map showing the countries where the frequency of GBA mutations in Parkinson disease patients was assessed
Image taken from (Sidransky and Lopez, 2012)

Despite the numerous investigations that followed from the discovery of this association, the molecular nature of the link between *GBA* mutations, PD and α-syn aggregation remains largely unexplained. Furthermore there exists a deepening debate as to whether the mutant *GBA* protein acts by a loss- or toxic-gain-of-function mechanism (Goldin, 2010).

As previously mentioned, GD is caused by a drastic reduction in the activity of the encoded lysosomal enzyme β-glucocerebrosidase (GCase) and a consequent accumulation of substrates, mainly glucosylceramide and glucosysphingosine, in the tissues where GD is associated with lysosomal storage dysfunction.

However, while it would seem likely that GCase loss of enzymatic activity contribute to the risk of PD, many elements argue against this view, suggesting the mutant *GBA* could instead increase the risk of PD through other mechanisms.

Most patients with *GBA* mutations and PD are heterozygous carriers, which implies that at least 50% of residual enzymatic activity is conserved. This is largely sufficient to avoid the pathogenic build up of substrates, as enzymatic activity needs to be reduced by at least 70-90% before substrate accumulation occurs. However, it is possible that *GBA* has other distinct unidentified regulatory functions of lysosomal activity the loss of which could favour α-syn aggregation and neuronal cell death. Furthermore, studies assessing age-specific penetrance and estimated life cumulative risk for PD in GD patients and heterozygous carriers have demonstrated that the risk is similar in the two groups (from 9 to 12% by the age of 80), thus arguing against the presence of a gene dosage effect, which is a typical of pure loss-of-function-mutations (Rosenbloom *et al.*, 2011, McNeill *et al.*, 2012, Rana *et al.*, 2013, Alcalay *et al.*, 2014).

On the other hand, there is growing evidence of a direct relationship between the severity of the mutation, in terms of GCase activity reduction, and PD risk. For instance, Gan-Or et al. found that carriers of severe mutations had a considerably higher disease risk and reduced age at onset compared to carriers of mild mutations (Gan-Or *et al.*, 2008, Gan-Or *et al.*, 2015). Moreover, Lesage et al. found that the PD onset tended to occur earlier in carriers of severe *GBA* mutations (Lesage *et al.*, 2011). Finally, recent work by Barrett and colleagues determined in a cohort of relatives of GD1 patients that non-N370S mutations (severe or null mutations) conferred a higher risk for PD compared to the mild N370S mutation (Barrett *et al.*, 2013).

Different investigations carried out in cell and animal models of GD and synucleinopathies support the idea that both mechanisms, toxic gain of function due to misfolded mutant proteins and loss of enzymatic activity, are likely to equally contribute to the complex lysosomal dysfunction that leads to aberrant α-syn aggregation and ultimately to nigral neuronal death (Cullen *et al.*, 2011, Mazzulli *et al.*, 2011, Sardi *et al.*, 2011).

SPMD1

SMPD1 encodes sphingomyelin phosphodiesterase 1, a lysosomal enzyme that cleaves the phosphocholine head group of sphingomyelin to generate ceramide. Bi-allelic mutations in the gene are the cause of Niemann-Pick type A, another multi-systemic lysosomal disorder, particularly frequent in the Ashkenazi Jewish population (Schuchman, 2007).

Gan-Or and colleagues recently suggested that a heterozygous missense mutation in this gene, p.Leu230Pro, could be a risk factor for the development of PD in the Ashkenazi Jewish population, with an odds ratio of ~9 (Gan-Or *et al.*, 2013). Importantly, other groups have subsequently replicated this finding in populations of different ethnical background (Foo *et al.*, 2013, Wu *et al.*, 2014), strongly supporting the view that dysfunctional lysosomal activity is critical to α-syn accumulation and PD pathogenesis.

2.1.4 Common Low-Risk Variants Predisposing to PD

Candidate gene association studies have been used in the past to try and identify common loci that increase the risk for PD. Through this approach common variability at the *SNCA* locus (Kruger et al., 1999) and at the *MAPT* locus were shown to contribute to the risk of disease (Golbe et al., 2001).

However, it is mainly thanks to unbiased GWAS that in recent years a growing number of susceptibility genes and risk loci have been undoubtedly associated with increased risk of PD. These studies rely on the common-disease-common variant hypothesis, according to which common genetic variants of small effect size can increase the risk of diseases, such as PD, that are frequent in the general population. GWAS have been made possible by the development of platforms that allow the assessment of genetic variability (usually single-nucleotide polymorphisms; SNPs) across the genome with the disease on the order of 500,000 to 1 million variants (Hardy and Singleton, 2009).

While the first GWAS in PD were underpowered and therefore yielded negative results (Fung *et al.*, 2006), larger GWAS identified that common variability in several loci, including *SNCA*, *MAPT, LRRK2, PARK16, BST1, HLA-DRB5,* and *GAK,* increase PD risk in independent populations (Pankratz *et al.*, 2009, Satake *et al.*, 2009, Simon-Sanchez *et al.*, 2009, Edwards *et al.*, 2010, Saad *et al.*, 2011, Spencer *et al.*, 2011, Sharma *et al.*, 2012)

Subsequently, thanks to imputation of variants and a meta-analysis of different GWAS datasets, additional genes were identified, including *ACMSD, STK39, MCCC1/LAMP3, SYT11,* and *CCDC62/HIP1R* (Nalls *et al.*, 2011).

The largest and most recent meta-analysis of all existing GWAS, which includes a total of ~13,000 PD cases and ~95,000 controls, showed that 24 risk loci containing 28 independent risk variants are associated with an increased risk of PD (Nalls *et al.*, 2014). The Manhattan plot showing the results of this meta-analysis is represented in Figure 2-6.

Importantly, most of the SNPs associated with increased PD risk are non-coding and the functional role of the vast majority of them is far from being understood. Furthermore, the effect size of the individual risk variants is low, although initial evidence suggests that the risk conferred by the combination of multiple risk variants may be more substantial.

It is of interest to note that some of the most robustly associated SNPs are located in close proximity of genes that also contain high penetrant mutations causing Mendelian forms of familial PD, such as *SNCA*, *LRRK2* and *VPS13C*. Importantly, this suggests that there could be a substantial overlap in the pathogenic mechanisms underlying rare Mendelian forms of PD and the more common sporadic forms, reinforcing the crucial importance of dissecting the bases of PD with Mendelian transmission.
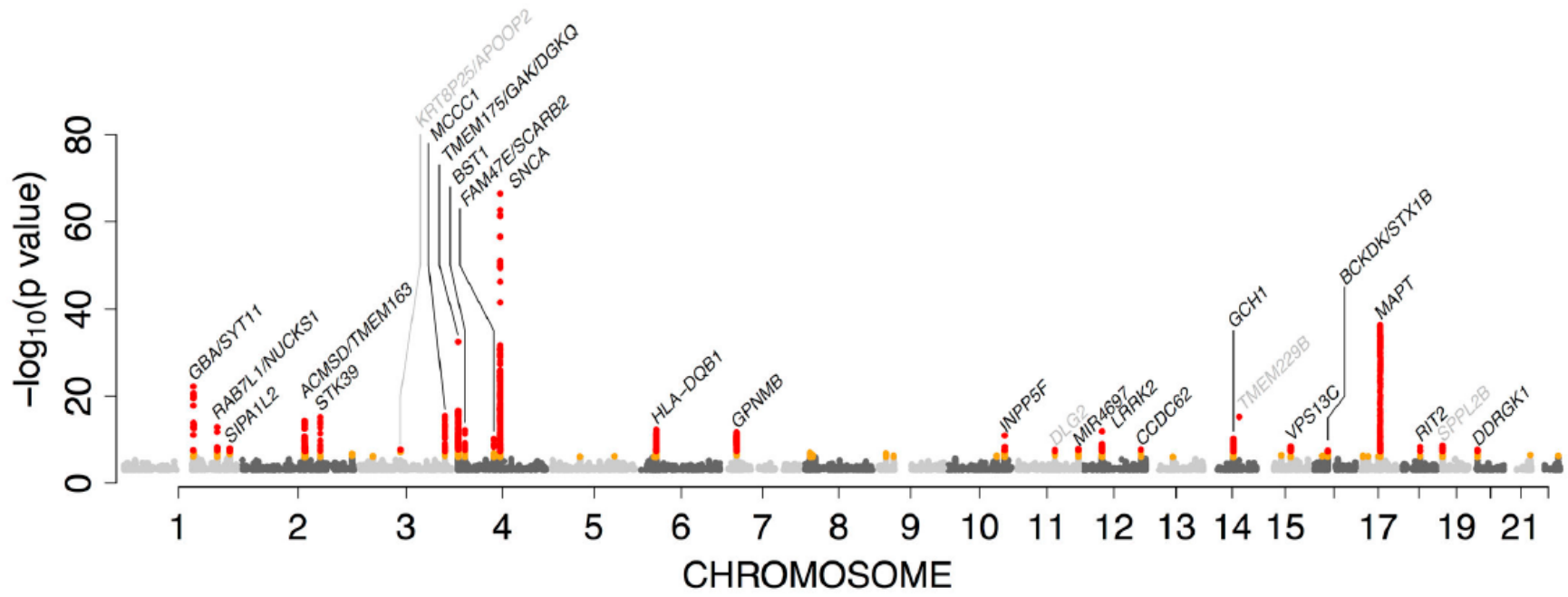
Figure 2-6 Manhattan plot from the latest GWAS meta-analysis for Parkinson disease
Image reproduced from (Nalls *et al.*, 2014)

2.2 Overview on the Genetics of Dystonia

2.2.1 Introduction

The dystonias are a clinically and genetically heterogeneous group of movement disorders. In 2013, an international panel of experts provided a consensus update on definition, phenomenology and classification of dystonia (Albanese *et al.*, 2013). Dystonia was defined as a "*movement disorder characterized by sustained or intermittent muscle contractions causing abnormal, often repetitive, movements, postures, or both. Dystonic movements are typically patterned, twisting, and may be tremulous. Dystonia is often initiated or worsened by voluntary action and associated with overflow muscle activation*".

Dystonia is the third most common movement disorder worldwide and approximately 70,000 people are affected by dystonia in the UK alone (Paudel *et al.*, 2012).

Dystonia has been traditionally classified based on the four main features (Table 2-2): (1) age of onset (early onset vs. adult onset), (2) distribution of affected body parts (focal, segmental or generalised), (3) aetiology (primary vs secondary dystonia) (4) special clinical features (paroxysmal, exercise-induced, task-specific or dopa-responsive)(Albanese et al., 2011). Given the existence of several problems and confusion with this system, a new classification has been recently proposed, which uses two axes to define dystonia. (Albanese *et al.*, 2013).

Axis I describes the clinical features of dystonia and includes age at onset, body distribution, temporal pattern, coexistence of other movement disorders and other neurological manifestations.

Axis II focuses on the presumed aetiology; the two classifying criteria are the presence of nervous system pathology (evidence of degeneration vs structural lesions vs absence of any pathology) and a differentiation among inherited dystonia (when a precise genetic cause is recognized) and acquired dystonia (e.g. perinatal brain injury, infections, drugs among others) or idiopathic dystonia. The old and the new classification are shown and compared in the figure Figure 2-7.

Table 2-2 Traditional clinical classification of dystonia

A) Aetiology	
1. Primary dystonia	No underlying structural, pharmacological or metabolic cause can be identified
1.1) Primary isolated dystonia	Dystonia is the only clinical sign (apart from tremor) and there is no identifiable exogenous cause or other inherited or degenerative disease
1.2) Primary plus dystonia	Dystonia is a prominent sign but is associated with another movement disorder, e.g. myoclonus or parkinsonism.
1.3) Primary paroxysmal dystonia	Torsion dystonia occurs in brief episodes with normalcy in between.
2. Heredodegenerative dystonia	Dystonia is a feature, among other neurological signs, of a genetically determined neurodegenerative disorder
3. Secondary dystonia	Dystonia is a symptom of an identified neurological condition, e.g. a focal brain lesion, exposure to drugs or chemicals
B) By age at onset	
1. Early onset (<30 years of age)	Usually starts in a leg or arm and frequently progresses to involve other limbs and the trunk
2. Late onset	Usually starts in the neck (including the larynx), the cranial muscles or one arm. Tends to remain localized with restricted progression to adjacent muscles
C) By distribution of affected body parts	
1. Focal	Single body region (e.g. writer's cramp, blepharospasm)
2. Segmental	Contiguous body regions (e.g. cranial and cervical, cervical and upper limb)
3. Multifocal	Non-contiguous body regions (e.g. upper and lower limb, cranial and upper limb)
4. Generalised	Both legs and at least one other body region (usually one or both arms)
5. Hemidystonia	Half of the body (usually secondary to a lesion in the contralateral basal ganglia)
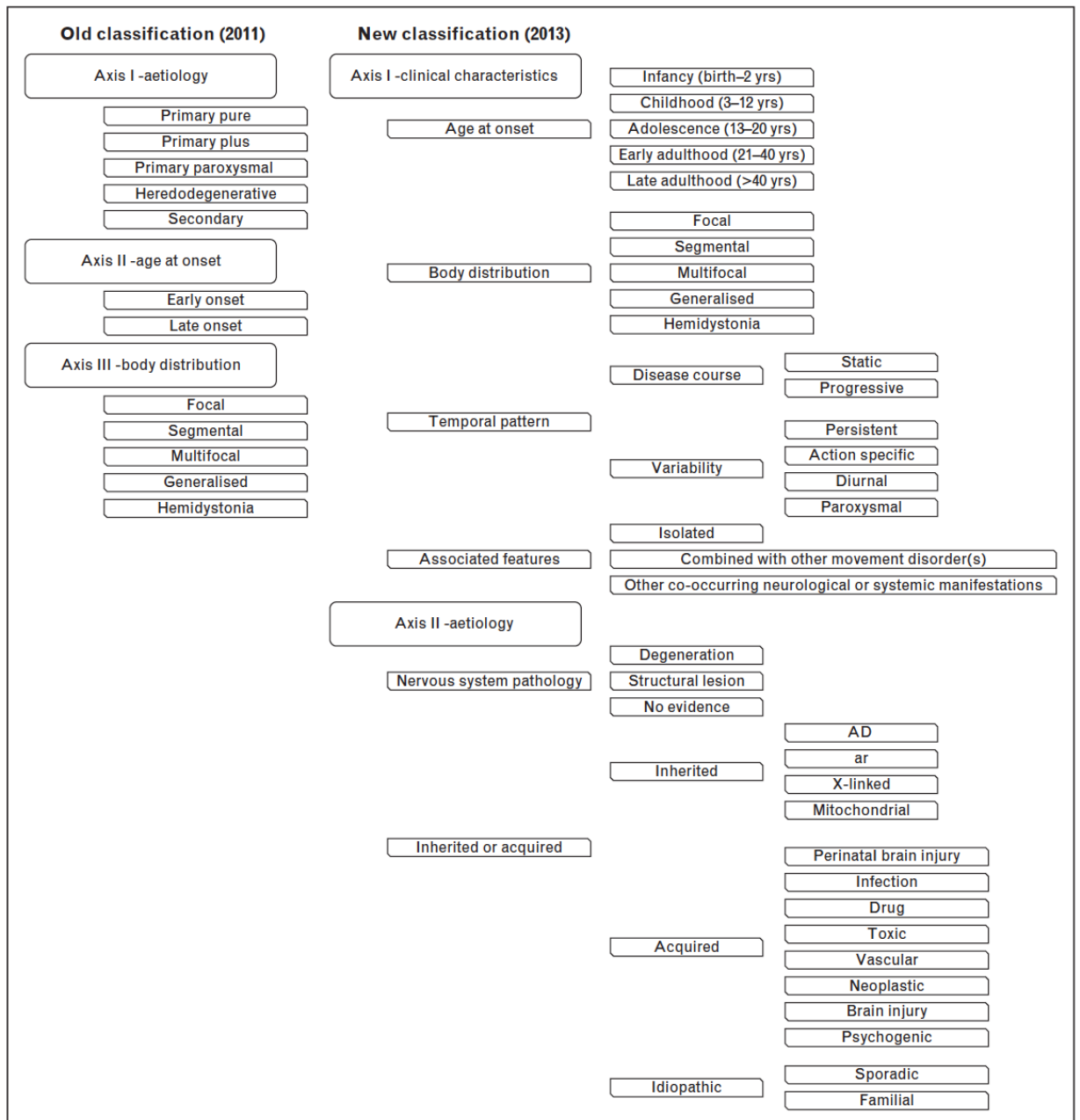
Figure 2-7 Schematic comparison of the old and the new classification system of dystonia
Table reproduced form (Balint and Bhatia, 2014).

The pathophysiology basis of dystonia is poorly understood. It has been proposed that dystonia may derive from a functional impairment of the neural circuits underlying the control and coordination of voluntary movements (Figure 2-8). These include the basal ganglia, the cerebellum, the sensorimotor cortex, and the interactions between these regions of the brain (Neychev *et al.*, 2011). The impairment of these circuits may occur as a consequence of structural lesions of these brain areas (either focal lesions or degeneration), as a consequence of a pharmacological treatment altering the activity of the neurons constituting these pathways (e.g L-DOPA treatment in PD patients or antipsychotic treatments blocking the dopamine receptors), or, most frequently, in absence of any overt brain pathology, which defines the primary dystonias. This last group of conditions is thought to derive from anatomically preserved, but functionally abnormal, basal ganglia and cerebellar circuits.
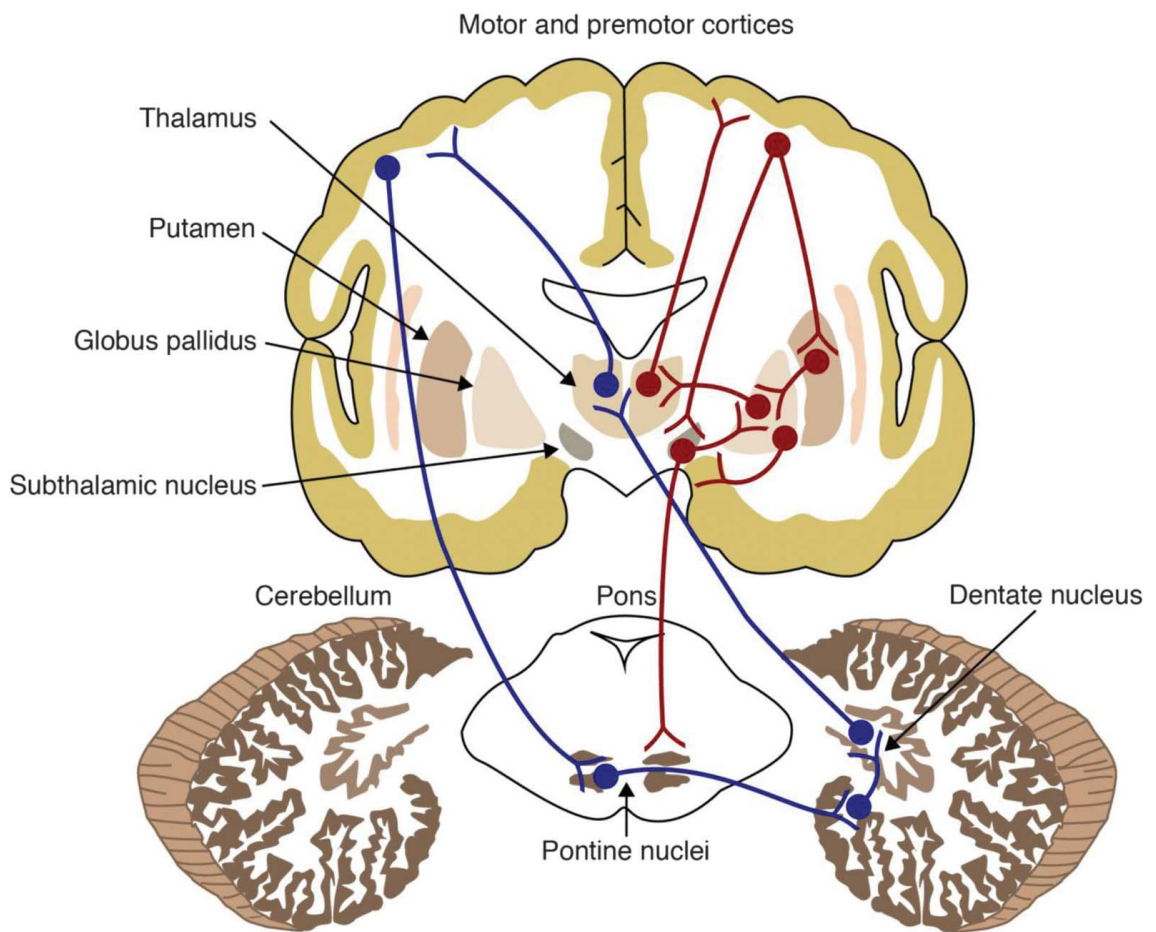
Figure 2-8 The circuits of dystonia
Reproduced from (Berman and Jinnah, 2015)

2.2.2 Overview of Monogenic Forms of Dystonia

Genetic factors largely contribute to the pathogenesis of dystonia. A positive family history in first-degree family members is reported in a very high proportion of patients with primary dystonia, ranging from 18 to 50% of cases (Rubio-Agusti *et al.*, 2013). Moreover, in a small but defined subset of families, dystonia can be transmitted across generations as a clear Mendelian trait.

Mutations in a growing number of genes are responsible for the Mendelian forms of dystonia. Importantly, the identification of these genes has allowed the initial recognition of different cellular pathways that could be involved in the molecular pathogenesis of primary dystonia, including perturbed synaptic transmission and plasticity (in particular of the dopamine system), abnormal transcription and cell-cycle regulation and endoplasmic reticulum (ER) dysfunction (Ledoux *et al.*, 2013).

The genes that have been associated with dystonia are summarised in Table 2-3.

This overview will only focus on genes that cause primary dystonia.

The Primary Isolated Dystonias

This term defines a group of syndromes in which dystonia is the only clinical feature (except for tremor of the arms or head and neck), without any evidence of neurodegeneration or any obvious secondary cause.

TOR1A Mutations (DYT1-related Dystonia)

In 1997 an in-frame 3 base pairs (CAG) deletion in exon 5 of the *TOR1A* gene, was identified as the genetic abnormality underlying the DYT1 locus (Ozelius *et al.*, 1997). This mutation is responsible for approximately 50% of cases with early onset generalized dystonia across different ethnicities (Kramer *et al.*, 1994). Due to a founder mutation, the DYT1 mutation is particularly frequent among Ashkenazi Jewish population, where it accounts for 80% of early onset dystonia.

Clinically, *TOR1A*-related dystonia would present in childhood with dystonic posturing of lower limbs and subsequent generalisation. Dystonia can nevertheless begin in any part of the body, with usual sparing of the neck and face. Late onset forms and atypical presentation of the disorder are not infrequently recognised (Jamora *et al.*, 2006, Stamelou *et al.*, 2013). Most cases would report a family history consistent with

autosomal dominant inheritance. However, the penetrance of the mutation is markedly reduced (~30%), which explains the frequent observation of pseudo-sporadic cases (Hjermind *et al.*, 2002). A small number of other variants have been described in sporadic cases with various forms of dystonia, but none of them has been convincingly shown to be pathogenic due to lack of clear segregation in other family members (Leung *et al.*, 2001, Kabakci *et al.*, 2004, Vulinovic *et al.*, 2014).

TorsinA is a member of the AAA+ superfamily (ATPases associated with different cellular activities) with multiple functions in the cell. *TOR1A* is exclusively expressed in neurons and the protein localizes in the endoplasmic reticulum (ER). Cellular models have demonstrated that mutant torsinA is displaced from the ER to the nuclear envelope (Goodchild and Dauer, 2004). The abnormal localisation may result in dysfunction of the secretory pathway and synaptic vesicle machinery (e.g. transportation of dopamine vesicles and/or dopamine receptors to the pre- and post-synaptic membrane, respectively) (Warner *et al.*, 2010).

Recently the first mouse model of DYT1-dystonia, exhibiting a motor phenotype closely resembling the human disease, has been described (Liang *et al.*, 2014).

Table 2-3 Monogenic causes of dystonia

Locus	Gene locus	Features	Inheritance	Mutational spectrum
DYT1	*TOR1A*	Early-onset primary torsion dystonia	AD with reduced penetrance	Only an in-frame 3 base pairs (CAG) deletion in exon 5 is pathogenic
DYT2	*HPCA*	Early-onset primary dystonia with prominent cranio-cervical involvement	AR	Missense
DYT4	*TUBB4A*	Whispering dystonia (adult onset spasmodic dysphonia) with generalisation and 'hobby horse' gait. Hypomyelination of basal ganglia and cerebellum (H-ABC). Spastic paraparesis	AD/De novo	Missense
DYT5a	*GCH1*	Dopa-responsive dystonia	AD/AR	Missense, truncating and large deletions or duplications
DYT5b	*TH*	Dopa-responsive dystonia	AR	Missense and truncating
NA	*SPR*	Dopa-responsive dystonia	AR	Missense and truncating
DYT6	*THAP1*	Adult-onset torsion dystonia with prominent cranio-cervical and laryngeal involvement	AD with reduced penetrance	Missense and truncating
DYT8	*MR1*	Paroxysmal non-kinesigenic dyskinesia	AD	Missense

DYT10	*PRRT2*	Paroxysmal kinesigenic dyskinesia	AD	Mainly truncating and large deletions
DYT11	*SGCE*	Myoclonic dystonia (often with alcohol responsiveness)	AD	Mainly truncating and large deletions
DYT12	*ATP1A3*	Rapid onset dystonia parkinsonism and alternating hemiplegia of childhood	AD/de novo	Missense
DYT16	*PRKRA*	Early-onset dystonia-parkinsonism	AR	Missense
DYT18	*SLC2A1*	Paroxysmal exercise-induced dyskinesia +/- epilepsy	AD	Missense and truncating
DYT23	*CIZ1*	Adult onset cervical dystonia	AD	Missense
DYT24	*ANO3*	Tremulous cranio-cervical dystonia +/- upper limb tremor	AD	Missense
DYT25	*GNAL*	Adult onset cervical dystonia	AD with reduced penetrance /de novo	Missense and truncating

THAP1 mutations (DYT6)

In 2009 mutations in the _THAP1_ gene, coding for the thanatos-associated protein domain-containing apoptosis-associated protein 1, were identified in two Mennonite families as the genetic abnormality responsible for the DYT6 locus (Almasy _et al._, 1997, Fuchs _et al._, 2009). A range of missense, nonsense and frameshift mutations spread throughout the coding portion of the gene are associated with disease in several genetically diverse populations. The inheritance of DYT6-related dystonia is autosomal dominant with a penetrance of ~60% (Saunders-Pullman _et al._, 2007, Fuchs _et al._, 2009, Houlden _et al._, 2010).

Clinically, mutation carriers tend to develop symptoms later than DYT1-positive patients, with an onset in adolescence or adulthood. DYT6-positive patients usually present with a predominant involvement of the upper body, in particular severe oromandibular, cranio-cervical, laryngeal or upper limbs involvement, and subsequent generalisation (Xiromerisiou _et al._, 2012).

THAP1 is an atypical zinc finger protein with DNA binding properties, involved in the regulation of gene transcription (Roussigne _et al._, 2003). One hypothetical mechanism whereby THAP1 substitutions could lead to dystonia is by dysregulated transcription of strategic genes. Mutations in _THAP1_ have been shown to disrupt binding to the _TOR1A_ promoter and result in decreased _TOR1A_ gene expression, suggesting that under normal conditions _TOR1A_ is negatively regulated by THAP1 (Kaiser _et al._, 2010).

TUBB4A (DYT4-related Dystonia)

The DYT4 family is a large kindred of British origin characterised by onset in the third decade of a severe form of dominantly inherited generalized dystonia (Parker, 1985). Several affected family members spread across five generations have been described. Affected members would present with a laryngeal dysphonia which progresses to a generalized dystonia. Some patients displayed a unique 'hobby horse' gait (Wilcox _et al._, 2011). To date, no other pedigree with similar clinical features has been published.

Through a combination of linkage analysis and exome sequencing, the missense mutation p.Arg2Gly in the _TUBB4A_ gene was independently identified as causal in the DYT4 kindred by our and Klein's group (Hersheson _et al._, 2012, Lohmann _et al._, 2012).

TUBB4A encodes β-tubulin-4a, a constituent of axonal microtubules. The mutation lies in the highly conserved autoregulatory MREI (Methionine–Arginine–Glutamic acid–Isoleucine) domain of the protein. The MREI tetrapeptide sequence at the start of the N-terminal domain is known to be necessary for the autoregulation of the β-tubulin mRNA levels and *in vitro* studies using site-directed mutagenesis have previously shown that mutations in this domain abrogate the autoregulatory ability (Yen *et al.*, 1988, Yen *et al.*, 1988).

Screening of the gene in a cohort of 394 unrelated dystonia patients revealed one further possibly pathogenic variant (p.Ala271Thr) in an individual who exhibited autosomal dominant spasmodic dysphonia (Lohmann *et al.*, 2012). We could not detect other mutation carriers in a cohort of ~200 dystonia cases with prominent laryngeal involvement (Hersheson *et al.*, 2013). A more recent study investigating 575 subjects with primary laryngeal, segmental or generalized dystonia failed to detect any further *TUBB4A* mutations (Vemula *et al.*, 2014), indicating overall that *TUBB4A* mutations are an exceptionally rare cause of dystonia.

Importantly, it was subsequently recognised that *de novo* mutations in *TUBB4A* are also the cause of hypomyelination with atrophy of the basal ganglia and cerebellum (H-ABC syndrome) (Simons *et al.*, 2013, Hamilton *et al.*, 2014). H-ABC is a rare neurodegenerative disorder with onset in infancy and childhood, characterised by the specific combination of hypomyelination, cerebellar atrophy, and absence or disappearance of the putamen (van der Knaap *et al.*, 2002). Clinically, H-ABC cases show a combination of severe dystonia, cerebellar ataxia, and variable degrees of intellectual disability. There is ongoing debate about whether DYT4-dystonia and H-ABC are distinct allelic conditions (brain imaging of members of the DTY4 kindred does not show the classic H-ABC findings) or whether the DYT4-phenotype simply represents a milder clinical presentation of the same disease, possibly questioning *TUBB4A* as a primary dystonia gene (Erro *et al.*, 2015).

CIZ1 mutations (DYT23)

Linkage analysis and WES were recently used to identify a missense mutation in *CIZ1* (c.790A>G p.Ser264Gly) as the possible causal variant in a large Caucasian kindred with adult-onset autosomal dominant cervical dystonia (Xiao *et al.*, 2012). Screening of other unrelated cases with adult-onset dystonia identified 2 additional missense

mutations in 3 individuals (p.Pro47Ser and p.Arg672Met; segregation not confirmed for any of these mutations), but also a similar number of novel variants in matched controls. Two subsequent studies have failed to identify additional mutations in *CIZ1* (Ma *et al.*, 2013, Dufke *et al.*, 2015). This finding is still awaiting independent confirmation and several concerns have been raised questioning the real contribution of *CIZ1* mutations to the pathogenesis of dystonia (Klein *et al.*, 2012).

CIZ1 encodes Cip1-inderacting zinc finger protein 1 and is a p21$^{Cip1/Waf1}$-interacting zinc finger protein, expressed in brain and involved in DNA synthesis and cell-cycle control. The work detailing the features of a *CIZ1* knock-out mouse model has been recently published (Xiao *et al.*, 2016). *Ciz1* showed the highest expression in the cerebellum and *Ciz1*-/- mice did not display features of dystonia, but exhibited mild motoric abnormalities on balance, open-field activity, and gait. Whole-genome gene expression analysis based on RNA extracted from cerebellum suggests that *CIZ1* may be involved in the post-mitotic differentiation of neurons in response to external signals (Xiao *et al.*, 2016).

ANO3 mutations (DYT24)

Our group identified a segregating missense mutation in *ANO3* in a three-generation British family with autosomal dominant cranio-cervical dystonia (Charlesworth *et al.*, 2012). Five further novel variants were detected by a subsequent screening of the gene in 188 probands with dystonia (Charlesworth *et al.*, 2012).

Clinically, patients with *ANO3* mutations exhibit focal or segmental tremulous dystonia, variably affecting the cranio-cervical, laryngeal and brachial regions. Some individuals showed isolated upper limb tremor and had been misclassified as essential tremor. Furthermore two patients exhibited myoclonic jerks of the head or the arms (Stamelou *et al.*, 2014).

A recent screening in a large German cohort of sporadic cases with cervical dystonia identified two novel mutations in cases, but also a similar number of novel variants in controls, indicating that caution should be posed when assigning pathogenicity of individual variants (Zech *et al.*, 2014). However, a screening conducted in the Chinese population identified two additional dominant families with cranio-cervical dystonia that carried a segregating *ANO3* mutation (Ma *et al.*, 2015), confirming the contribution

of *ANO3* to dystonia pathogenesis.

ANO3 is very high and selectively expressed in the striatum, a key brain region in dystonia pathogenesis. *ANO3* encodes a protein called anoctamin 3 and belongs to a family of closely related genes (*ANO1-10*) with different tissue expression patterns. *ANO1* and *ANO2* encode for Ca^{2+}-activated chloride channels. Hence, it is postulated that *ANO3* may function in the same way and regulate striatal neurons excitability (Caputo *et al.*, 2008).

<u>*GNAL* mutations (DYT25-related dystonia)</u>

In 2012 heterozygous mutations in *GNAL* were identified in two unrelated dominant families as a novel cause of familial adult-onset cervical dystonia (Fuchs *et al.*, 2013). Screening of further 39 families revealed 6 additional segregating novel mutations, suggesting that *GNAL* mutations could be a relatively common cause for familial dystonia.

However, a number of subsequent mutational screening have shown a much lower mutational yield with a reported frequency across different populations of around 0.5-1%. Several loss-of-function mutations have been described, including missense and truncating mutations, (Dobricic *et al.*, 2014, Dufke *et al.*, 2014, Kumar *et al.*, 2014, Zech *et al.*, 2014). *GNAL* mutations are most frequently transmitted as a dominant trait, although de novo mutations have been found in sporadic cases (Dobricic *et al.*, 2014, Kumar *et al.*, 2014, Ziegan *et al.*, 2014, Carecchio *et al.*, 2016). More recently a family with severe childhood-onset dystonia harboring a recessive homozygous *GNAL* mutation has also been reported (Masuho *et al.*, 2016).

Clinically, most *GNAL* mutation carriers present the first symptoms in the cervical region. Progression to other body segments is observed in ~50% of cases, although a frank generalisation of dystonia is rare (Fuchs *et al.*, 2013).

GNAL encodes $G\alpha_{olf}$, the alpha subunit of triheteromeric G protein G_{olf}, a striatal protein involved in dopamine (D1) signalling. $G\alpha_{olf}$ is responsible for coupling D1 receptors to adenylyl cyclase 5 in striatal neurons and $G\alpha_{olf}$ is required for D1-mediated behaviour and biochemical effects (Herve *et al.*, 1993, Zhuang *et al.*, 2000, Corvol *et al.*, 2001).

HPCA-related dystonia (DYT2)

Our group has recently identified homozygous and compound heterozygous *HPCA* mutations in two pedigrees with autosomal recessive generalised dystonia. *HPCA* were initially identified through homozygosity mapping and WES in a pedigree with three affected subjects, product of a consanguineous marriage (parents are first cousins), presenting with early-onset generalised dystonia (Charlesworth *et al.*, 2015). Subsequently, compound-heterozygous mutations in *HPCA* were also identified in a second independent kindred affected by AR isolated dystonia.

HPCA are likely to represent an extremely rare cause of dystonia, as a recent study assessing *HPCA* mutation frequency in large cohort of primary dystonia cases, failed to identify any additional mutation (Dobricic *et al.*, 2016).

HPCA encodes hippocalcin, a neuronal calcium sensor protein present almost exclusively in the brain and expressed at particularly high levels in the striatum (Charlesworth *et al.*, 2015).

Primary Dystonia-plus

The dystonia-plus syndromes (also known as combined dystonias, according to the most recent nomenclature system) represent a heterogeneous group of non-neurodegenerative diseases, where additional neurological features (non-epileptic myoclonus or parkinsonism) accompany dystonia (Asmus and Gasser, 2010).

DOPA-responsive dystonia (DYT5)

The term DOPA-responsive dystonia (DRD) defines a group of rare conditions, which share the clinic characteristic of a dramatic improvement in symptoms in response to treatment with oral L-dopa (Kurian *et al.*, 2011). Mutations in three genes have incontrovertibly been shown to cause DRD: *GCH1* (GTP Cyclohydrolase 1), *TH* (Tyrosine Hydroxylase) and *SPR* (Sepiapterin Reductase) (Ichinose *et al.*, 1994, Brautigam *et al.*, 1998, Bonafe *et al.*, 2001). All three genes encode enzymes that are critically involved in the biosynthesis of dopamine in nigrostriatal cells and pathogenic mutations result in a dramatic decrease in dopamine synthesis (Figure 2-9).
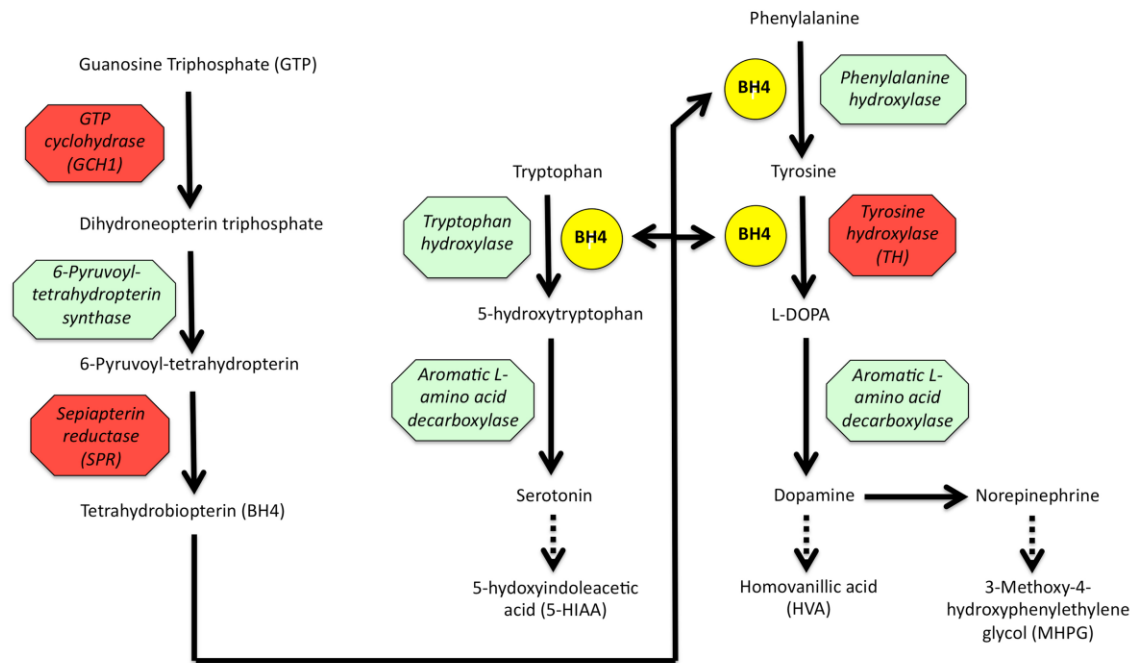
Figure 2-9 Schematic illustration of the cellular pathway involved in dopamine synthesis in nigral neurons
Reproduced from (Charlesworth *et al.*, 2013).

Heterozygous *GCH1* mutations are by far the most common cause of DRD, accounting for 60-80% of autosomal dominant DRD pedigrees (Furukawa, 2004). Penetrance is incomplete being lower for males (~40-50%) than females (~80%) (Wider *et al.*, 2008).

Clinical presentation is typically with lower limb dystonia and gait disturbance, with a variable degree of generalisation over time (Nygaard *et al.*, 1990). The response even to low doses of L-DOPA is excellent, sustained and not generally associated with dyskinesias that often follow chronic use of L-DOPA in PD (Clot *et al.*, 2009). As I will discuss in more detail in chapter 4.4, parkinsonism may occur in the later stages of the disease.

TH and SPR mutations are associated with autosomal recessive DRD (Ludecke *et al.*, 1996, Blau *et al.*, 2001). Typically, patients with mutations in these two genes present with a severe combination of dystonia, parkinsonism, ptosis, seizures and truncal hypotonia in infancy. The clinical picture is overall more severe than in *GCH1*-related DRD and response to L-DOPA treatment is often less satisfactory.

Recently mutations in *ATM*, the gene usually mutated in ataxia- telangiectasia, have

been identified in an Indian pedigree with recessive DOPA-responsive cervical dystonia (Charlesworth *et al.*, 2013). The mechanisms whereby *ATM* mutations may lead to this phenotype are unknown.

<ins>*SGCE*-related Myoclonus-Dystonia (DYT11)</ins>

M-D clinical and genetic aspects will be discussed in detail in chapter 5.2.

<ins>*ATP1A3* Mutations (DYT12)</ins>

Mutations in *ATP1A3* were initially reported as the cause of rapid-onset dystonia-parkinsonism (RDP), a rare autosomal dominant condition characterized by abrupt onset in adolescents or young adults of fixed dystonic and parkinsonian symptoms (de Carvalho Aguiar *et al.*, 2004, Brashear *et al.*, 2007).

It was subsequently recognized that de novo *ATP1A3* mutations are also responsible for alternating hemiplegia of childhood (AHC) (Heinzen *et al.*, 2012, Rosewich *et al.*, 2012). AHC is an infantile disorder characterized by a fluctuating course and recurrent, and alternating, hemiplegic or hemidystonic episodes, followed in most cases by the development of permanent neurological symptoms (i.e. epilepsy, neurodevelopmental delay with intellectual disability, chorea, dystonia, parkinsonism, bulbar symptoms and cerebellar ataxia) (Heinzen *et al.*, 2014).

More recently, a single missense mutation was shown to cause another distinct autosomal dominant condition, featuring progressive cerebellar atrophy with relapsing episodes of cerebellar ataxia, areflexia, pes cavus, optic atrophy, and sensori-neural deafness (CAPOS) (Demos *et al.*, 2014).

Importantly, a growing number of cases with overlapping RDP/AHC (Roubergue *et al.*, 2013, Rosewich *et al.*, 2014, Rosewich *et al.*, 2014, Panagiotakaki *et al.*, 2015, Termsarasab *et al.*, 2015) and CAPOS/AHC (Rosewich *et al.*, 2014) have been reported in the literature.

ATP1A3 encodes the catalytic unit of the sodium pump that uses ATP hydrolysis to exchange Na+ and K+ across the cell membrane to maintain ionic gradients.

PRKRA Mutations (DYT16)

Mutations in *PRKRA* a rare cause of autosomal recessive dystonia-parkinsonism, were initially identified in two apparently unrelated consanguineous Brazilian families featuring young onset generalised dystonia with additional parkinsonian features (Camargos *et al.*, 2008). Autozygosity mapping and subsequent mutational screening revealed the *PRKRA* homozygous missense mutation p.Pro222Leu in both families (Camargos *et al.*, 2008). Only recently three more families with bi-allelic *PRKRA* mutation have been reported (Zech *et al.*, 2014, de Carvalho Aguiar *et al.*, 2015, Quadri *et al.*, 2016), confirming the contributory role of *PRKRA* to dystonia pathogenesis. Two European families (one Italian and one Polish) carried the same homozygous missense change, while the third family carried two novel mutations, p.Cys77Ser and p.Cys213Ph, in the compound heterozygous state.

PRKRA encodes protein kinase, interferon-inducible double-stranded RNA-dependent activator, a protein involved in signal transduction, cell differentiation, cell proliferation, antiviral response and apoptosis (Patel *et al.*, 2000).

The Primary Paroxysmal Dystonias

The paroxysmal dystonias are a clinically and genetically heterogenous group of movement disorders characterized by temporally defined dyskinetic episodes with interictal neurological normality. Paroxysmal dyskinesia can be subdivided into three main clinical syndromes: paroxysmal kinesigenic dyskinesias (PKD), paroxysmal exercise-induced dyskinesias (PED), and paroxysmal non-kinesigenic dyskinesias (PNKD) (Erro *et al.*, 2014).

Paroxysmal kinesigenic dyskinesias

Mutations in *PRRT2,* encoding for the synaptic protein proline-rich transmembrane protein 2, were identified as the cause of PKD in 2011 (Chen *et al.*, 2011, Wang *et al.*, 2011).

Affected individuals have frequent (up to 100 times per day) and short (seconds to minutes) dyskinetic attacks, triggered by sudden movements. PKD attacks respond dramatically to anticonvulsant therapy with carbamazepine.

PRRT2 mutations have also been described as the cause of benign familial infantile

epilepsy and of other childhood-onset movement disorders (i.e. episodic ataxia, paroxysmal torticollis of childhood), headache disorders, and intellectual disability (Ebrahimi-Fakhari *et al.*, 2015).

Most *PRRT2* pathogenic mutations are truncating and by far the most common mutation is the recurrent frameshift c.649dupC, which is present in ~80-90% of the cases described to date (Cao *et al.*, 2012, Friedman *et al.*, 2012, Hedera *et al.*, 2012, Steinlein *et al.*, 2012).

The PRRT2 protein is highly expressed in the developing nervous system and localised to the synapse (Lee *et al.*, 2012). Truncating mutations result in a protein lacking the transmembrane domain, leading to altered subcellular localization. The subsequent reduction of PRRT2 protein may lead to altered synaptic neurotransmitter release and dysregulated neuronal excitability (Chen *et al.*, 2011).

More recently, a single missense mutation (p.Glu1483Lys) in *SCN8A*, encoding a voltage gated Na-channel subunit widely expressed in the CNS, has recently been linked to paroxysmal kinesigenic dyskinesia and benign familial infantile seizures (Gardella *et al.*, 2016). This observation expands the phenotypic spectrum associated with mutations in this gene, which also includes severe epileptic encephalopathy and a neurodevelopmental disorder (Larsen *et al.*, 2015).

Paroxysmal non-kinesigenic dyskinesia

Paroxysmal non-kinesigenic dyskinesia (PNKD) symptoms classically starts in the first two decades of life, featuring attacks of dystonic and choreatic dyskinesias, often triggered by stress or alcohol and/or caffeine consumption (Bruno *et al.*, 2007). PNKD episodes usually last from minutes to hours and occur with a frequency that can vary between 20 attacks per day to only few attacks per year.

PNKD is caused by heterozygous mutations in the *myofribillogenesis regulator* (*MR-1*) gene and mutations are inherited as an autosomal dominant trait. Only three mutations have been described to date, all clustered in the N-terminus of the protein: p.Ala7Val, p.Ala9Val and p.Ala33Pro (Lee *et al.*, 2004, Rainier *et al.*, 2004, Chen *et al.*, 2005, Djarmati *et al.*, 2005, Hempelmann *et al.*, 2006, Ghezzi *et al.*, 2009).

PRRT2 mutations have been found in small number of patients with a *PNKD*

presentation (Gardiner *et al.*, 2015).

Paroxysmal exercise-induced dyskinesia

Mutations in the *SLC2A1* gene, which codes for the glucose transporter GLUT1, cause paroxysmal exercise-induced dyskinesia (PED). PED is characterized by attacks of combined chorea, athetosis, and dystonia, which tend to last from a few minutes to an hour (Bruno *et al.*, 2004). GLUT1 is the main glucose transporter in the brain and PED may be caused by reduced glucose transport into the brain, particularly when energy demand is high after prolonged exercise.

2.3 Genetics of Choreas

2.3.1 Introduction

Chorea (from the Greek word χορεία =dance) is a hyperkinetic movement disorder characterized by continuous and brief involuntary movements. Chorea can affect any body segment, including limbs, trunk, neck, face, and mouth. Typically choreic movements flow from one body part to another and are unpredictable in terms of timing, speed and direction. Different from dystonia, choreic movements are not repetitive or patterned. Chorea is usually worsened by anxiety and execution of voluntary movements, and it is absent during sleep. When chorea is accompanied by athetosis, a term defining slower and continuous writhing involuntary movements, it is referred to as choreo-athetosis. Chorea is commonly observed in combination with other hyperkinesias, such as dystonia (Donaldson *et al.*, 2012).

Focal lesions of the striatum and degeneration and/or functional dysregulation of medium spiny neurons (MSNs), which constitute ~95% of the striatal cells and form the striatal output projections, are considered to underlie the pathophysiology of choreic movements [2].

Chorea is a major feature of several neurological disorders that can be either genetically inherited or acquired.

There are many non-inherited causes of chorea. These include focal lesions of the striatum (e.g. strokes, occupying-space lesions), infection/immune-related conditions (e.g. Sydenham's chorea, systemic lupus erythematosus or anti-phospholipid syndrome), use of drugs such as L-DOPA, neuroleptics, antiemetics and oral contraception, and several metabolic, haematological, or endocrinological disorders (e.g. polycythaemia rubra vera, hyperthyroidism, hypo/hyperparathyroidism and hypo/hyperglycemia) (Wild and Tabrizi, 2007). Acquired causes of chorea will not be further discussed in this chapter.

Clinically, inherited choreas may be classified according to the age at onset of symptoms, as mutations in different genes tend to cause disease with onset either in childhood/juvenile years (< 20 years) or in adulthood. A further important distinction can be made between progressive (i.e. neurodegenerative) and non-progressive causes of inherited chorea.

From a clinical point of view, it is also important to establish whether chorea is the only or the predominant neurological feature or whether other accompanying features are present. This is essential for guiding genetic diagnostic testing. Other neurological features that should be looked for in patients with chorea are cognitive impairment, ataxia, epilepsy, myoclonus, dystonia, peripheral neuropathy, spasticity, and eye movement disorders.

Of relevance, a number of childhood-onset metabolic (e.g. Lesch-Nyhan Syndrome, glutaric aciduria, propionic acidemia) or mitochondrial disorders (e.g. Leigh syndrome, MELAS) can present with a movement disorder (most frequently dystonia, followed by chorea), though typically in the context of a complex multi-systemic neurologic presentation (Hermann and Walker, 2015).

The genes that have been associated with choreic syndromes are summarized in Table 2-4. Mitochondrial diseases and inborn errors of metabolism associated with a choreic presentation are not listed in the table.

Table 2-4 Monogenic causes of chorea

Gene	Main associated phenotype	Gene product	Inheritance	Age of onset	Diagnostic clues
HTT	Huntington disease	Huntingtin	AD (CAG expansion)	Childhood to late adulthood	Cognitive decline, psychiatric disturbances Progressive course MRI: caudate nucleus head atrophy
PRNP	HDL1/ Prion disease	Prion protein	AD (octapeptide coding repeat expansion)	Adulthood	Dementia, seizures and psychiatric features Possible parkinsonism at onset and longer survival than HD
JPH3	HDL2	Junctophilin 3	AD (CAG/CTG expansion)	Adulthood	Parkinsonism may be first manifestation High frequency in people with black African ancestry
TBP	HDL4/ Spinocerebellar ataxia type 17	TATA box-binding protein	AD (CAG expansion)	Childhood to adulthood	Ataxia, epilepsy and cognitive decline Frequent parkinsonism MRI: cerebellar atrophy
ATN1	Dentato-rubral-pallido-luysian atrophy	Atrophin-1	AD (CAG expansion)	Childhood to adulthood	Seizures, myoclonus and cognitive decline MRI: Cerebellar and brainstem atrophy (especially pons) High frequency in Japan
C9orf72	FTD/MND	Chromosome 9 Open Reading Frame 72	AD (GGGGCC expansion)	Childhood to adulthood	Prominent cognitive and psychiatric features Pyramidal signs MRI: diffuse cerebral atrophy
FTL	Neuroferritinopathy	Ferritin light chain	AD	Teenage to late adulthood	Action-specific facial dystonia Reduced ferritin plasma levels MRI: iron deposition in basal ganglia and cortical pencil lining
VPS13A	Chorea-acanthocytosis	Chorein	AR	Early adulthood	Severe oromandibular dystonia with lip and tongue biting Head drops Peripheral axonal neuropathy Elevated serum CK MRI: caudate nucleus head atrophy
XK	Macleod syndrome	Kell blood group protein	X-linked recessive	Adulthood	Peripheral sensorimotor neuropathy Cardiomyopathy Elevated serum CK

ATM	Ataxia-telangiectasia	Ataxia-telangiectasia mutated gene	AR	Childhood to adulthood	Oculocutaneous telangiectases Sensorimotor neuropathy Elevated serum alpha-fetoprotein Predisposition to malignancy MRI: cerebellar atrophy
APTX *SETX*	Ataxia with oculomotor apraxia (AOA) type 1, 2	Aprataxin Senataxin	AR	Childhood to adulthood	Sensorimotor neuropathy Hypoalbuminemia in AOA1 Hypercholesterolemia in AOA1 Elevated alpha-fetoprotein in AOA2 MRI: cerebellar atrophy
FRDA	Friedreich's ataxia	Frataxin	AR	Childhood to adulthood	Cardiac involvement, diabetes, skeletal deformities Pyramidal signs
RNF216	Gordon-Holmes syndrome	Ring finger protein 216	AR	Adulthood	Behavioural problems, and severe dementia Hypogonadism MRI: white matter lesions and cerebellar atrophy
NKX2-1	*NKX2-1*-related chorea (Benign Hereditary Chorea)	Thyroid transcription factor 1	AD/De novo	Infancy	Non-progressive course Hypotonia and early falls Learning difficulties Frequent pulmonary and thyroid involvement

AD: autosomal dominant; **AR**: autosomal recessive; **BFIS**: Benign familial infantile seizures; **HDL**: Huntington's disease-like.

2.3.2 Huntington's disease

HD is by far the most common cause of chorea and represents the archetype of progressive forms of chorea.

HD is a fatal neurodegenerative disorder inherited as an autosomal dominant trait and is caused by heterozygous expansion of a CAG trinucleotide repeat in the *HTT* gene (encoding the huntingtin protein). In healthy individuals the CAG repeat ranges between 10 and 29 copies on normal chromosomes, whereas is expanded to 36–121 in HD patients. CAG repeats equal or above 40 are fully penetrant, whereas expansion between 36 and 39 are associated with reduced penetrance.

Clinically, HD features a triad of relentlessly progressive motor, cognitive and psychiatric symptoms, generally with onset in adult years, and inevitably leading to death after ~15-20 years of disease (Ross and Tabrizi, 2011). Onset of disease is typically in adult years, with less than 10% of patients presenting at an age below 20 (Koutsis *et al.*, 2013). Juvenile HD (Westphal variant) tends to be associated with little choreic movements, while rigidity, parkinsonism, dystonic features, myoclonus and cognitive impairment would dominate the phenotype (Quinn and Schrag, 1998).

Most of the current research efforts in HD genetics are aimed at identifying disease modifiers, which may influence the disease progression and determine the age at onset (AAO) of motor symptoms (Gusella *et al.*, 2014). The length of the CAG expansion is well known to be the most relevant determinant of the age at onset, with longer repeats associated with an earlier onset (Andrew *et al.*, 1993). However, the CAG repeat size accounts for only ~50% of the variation in age at onset (Langbehn *et al.*, 2004) and a substantial portion of the remaining variance in age at onset is highly heritable, strongly indicating the existence of other critical genetic determining factors (Gusella *et al.*, 2014). Neither the size of the non-expanded *HTT* allele, nor the presence of a second smaller CAG pathological expansion, is able to significantly influence age at onset (Lee *et al.*, 2012). A recent study showed that a variant (rs13102260; G>A) in the *HTT* promoter, located in the site that regulates binding of the transcription factor NF-*κB*, exerts a bidirectional effect on HD age at onset (Becanovic *et al.*, 2015). The authors showed *in vitro* and *in vivo* that the presence of the A allele determined a lower NF-κB-mediated *HTT* transcriptional activity, resulting in delayed age at onset when inherited on the same allele of the pathological expansion (reduced expression of the pathological

allele). On the contrary, the A allele was associated with an earlier age at onset when located on the non-expanded allele (reduced expression of the normal *HTT*). An important corollary of these results is that therapeutic strategies aimed at lowering the expression of the pathological CAG expansion should take into account that non allele-specific silencing of *HTT* could bear undesired effects by decreasing the expression of the normal allele. The most relevant advance toward the discovery of HD genetic modifiers is the recent publication of GWAS performed by the Genetic Modifiers of Huntington Disease (GeM—HD) Consortium (Lee *et al.*, 2015). The authors identified two GWAS-significant loci, one on chromosome 15 and one on chromosome 8 that significantly modified the age at onset of motor symptoms as predicted solely by the CAG expansion length. Other suggestive associations, though not passing the stringent GWAS-significance threshold, were observed on chromosomes 3, 5 and 21. Genes located on chromosome 15 locus are *MTMR10* and *FAN1* and on the chromosome 8 locus are *RRM2B* and *UBR5*. Pathway analysis of the GWAS results indicates that HD modifiers may be involved in control of DNA handling and repair mechanisms. Supporting this view, the chromosome 3 locus centred on *MLH1*, a gene previously identified in a HD mouse model as a modifier of somatic instability of the CAG repeats (Pinto *et al.*, 2013).

2.3.3 Huntington's disease-like syndromes

~1% of families with a HD-like clinical presentation do not carry pathogenic expansion in the HD gene and are therefore labelled as HD phenocopies or HD-lookalike (HDL) disorders (Schneider *et al.*, 2007).

Importantly, HD phenocopies are clinically and genetically heterogeneous and a conclusive genetic diagnosis is currently possible in only a small minority of cases. In the Queen Square series, a genetic diagnosis could be achieved in only 8/285 HDL cases (2.8%) (Wild *et al.*, 2008). Other studies report even lower diagnostic yields (Stevanin *et al.*, 2003, Keckarevic *et al.*, 2005, Costa Mdo *et al.*, 2006, Koutsis *et al.*, 2012).

HDL1

HDL1 is an exceptionally rare autosomal dominant neurodegenerative disorder, caused by an 8-octapeptide repeats expansion in the prion protein (PrP) gene (*PRNP*) (Moore *et al.*, 2001).

The clinical features of carriers of the *PRNP* octapeptide repeats are indistinguishable from classic HD and include chorea, personality changes, psychiatric symptoms and cognitive decline. Moreover, few members of a very large British pedigree with a *PRNP* 6-octapeptide repeats expansion presented with a combination of chorea and cognitive decline, mimicking HD (Mead *et al.*, 2006). In the Queen Square series only one HDL case was found to carry a *PRNP* mutation, and was subsequently recognized to be a member of the large family previously reported by Mead and colleagues (Wild *et al.*, 2008).

HDL2

HDL2 is caused by a CTG-CAG triplet repeat expansion in the junctophilin 3 (*JPH3*) gene (Holmes *et al.*, 2001). The expansion is virtually absent in Caucasian population (Margolis *et al.*, 2004), but is common in patients of black South Africans of sub-Saharan descent, where the expansion is responsible for up to ~50% of patients with a HDL presentation (Stevanin *et al.*, 2003, Krause *et al.*, 2015). Abnormally expanded repeat expansions range from 40 to 59 triplets and the penetrance of the expansion is high (Govert and Schneider, 2013). Most HDL2 patients are clinically indistinguishable from HD cases (Margolis *et al.*, 2001). However, Schneider and colleagues reported a large African-American kindred carrying a *JPH3* expansion and presenting with a progressive akinetic-rigid syndrome and severe dementia but very little chorea. This indicates that *JPH3* should be considered in the differential diagnosis of early-onset dementia and hypokinetic-rigid syndromes in individuals of African descent (Schneider *et al.*, 2012)

HDL3

The HDL3 locus was mapped to 4p15.3 in a single consanguineous pedigree from Saudi Arabia with a recessive HDL presentation (Kambouris *et al.*, 2000). However no other pedigrees mapping to this locus have been subsequently identified and the causative gene has not been reported as yet.

HDL4

HDL4 is caused by heterozygous CAG triplet repeat expansions in the TATA box-binding protein (TBP) gene located on chromosome 6q27 (Stevanin and Brice, 2008). The same triplet expansion is also responsible for SCA type 17 (SCA17) (Stevanin *et al.*, 2003). SCA17 expansions account for approximately 1% of the HDL cases, which

makes it one of the most important genetic mutations found in HDL Caucasian subjects (Wild and Tabrizi, 2007). However, chorea is present only in 20% of SCA17 patients, with ataxia, seizures, dementia and parkinsonism being the most frequently detected features (Zuhlke and Burk, 2007). Interestingly, within given SCA17 positive pedigrees, homogenous HDL presentation can be observed in multiple individuals, suggesting that other co-inherited genetic factors may influence he presentation (HDL vs ataxic) (Schneider *et al.*, 2006).

Global cortical atrophy, putaminal enhancement or cerebellar atrophy can be inconsistently found in SCA17-associated HDL. Importantly, other SCA expansions, in particular those associated with SCA1, SCA2, and SCA3, can cause hyperkinetic movement disorders that can sometimes include chorea (Schols *et al.*, 2000, van Gaalen *et al.*, 2011).

Dentato-rubral-pallido-luysian atrophy

Dentato-rubral-pallido-luysian atrophy (DRPLA) is an autosomal dominant neurodegenerative disease. DRPLA is caused by CAG triplet repeat expansions in the gene encoding atrophin-1 (Nagafuchi *et al.*, 1994). DRPLA is particularly frequent in Japan, where it is almost as frequent as HD, but is exceptionally rare in other ethnicities. Clinically, DRPLA presents with a variable combination of chorea, ataxia, cognitive decline, and, especially in young individuals with larger expansions, progressive myoclonic epilepsy (Becher *et al.*, 1997).

C9orf72-Related HDL

A hexanucleotide repeat expansion in a non-coding portion of the *C9orf72* gene was recently shown to be the most important cause of familial and sporadic frontotemporal lobar degeneration and amyotrophic lateral sclerosis (DeJesus-Hernandez *et al.*, 2011, Renton *et al.*, 2011). Hensman Moss and colleagues recently screened a cohort of 514 HDL patients for the presence of the *C9orf72* expansion and 10 subjects (1.95%) carrying the expansion, making this mutation the most common identified cause of HDL syndromes in a UK cohort (Hensman Moss *et al.*, 2014). Not surprisingly, a movement disorder was a prominent feature in these cases, with 3 exhibiting chorea, 4 dystonia, 4 myoclonus, and 3 tremor. Furthermore, 6 cases had rigidity and 5 bradykinesia. Although, none of the cases had been formally diagnosed with fronto-temporal dementia, behavioural, psychiatric and cognitive difficulties were observed in most of

the carriers. Upper motorneuron signs were present in 4 of the 10 subjects, while lower motorneuron signs were not detected.

Other groups have been subsequently confirmed *C9orf72* expansions to be a relevant cause of HDL in other populations (Kostic *et al.*, 2014, Koutsis *et al.*, 2015).

Chorea-Acanthocytosis

Bi-allelic mutations in *VPS13A,* coding for the large protein chorein, are responsible for the neurodegenerative condition chorea-acanthocytosis (CA) (Rampoldi *et al.*, 2001). CA is mainly characterized by orofacial and cervical dyskinesias (chorea, dystonia and tics) combined with abnormal erythrocyte morphology (acanthocytosis) that can be detected with blood film microscopic examination. Highly classical neurological signs are tongue protrusion, biting of the tongue and lips and neck and trunk flexion drops and extension spasms (Schneider *et al.*, 2010). Progressive cognitive decline and psychiatric features are often prominent as in HD. Seizures, ataxia, and a peripheral neuropathy with distal amyotrophy and increased serum creatine kinase are also common features that should prompt a diagnosis of CA (Schneider *et al.*, 2007).

Macleod Syndrome

Macleod syndrome is a recessive X-linked neuro-acanthocytosis syndrome caused by mutations in XK encoding Kell antigen (Wiethoff *et al.*, 2014). Clinical presentation is similar to CA, though often with a later onset and milder and longer course. Dystonia tends to be less pronounced than in CA and cardiomyopathy and haemolytic anaemia may be relevant distinctive features (Walker *et al.*, 2007).

Neurodegeneration with Brain Iron Accumulation

Neurodegeneration with brain iron accumulation (NBIA) is a group of inherited neurological disorders in which iron accumulates in the basal ganglia, which classically present with movement disorders and cognitive decline (Kara *et al.*, 2013). Brain magnetic resonance imaging (MRI) usually shows the presence of iron deposition in the basal ganglia allowing the diagnosis. Most of the NBIA syndromes are recessive and start early in life and therefore are easily distinguishable from HD.

However, mutations in the *FTL1* gene, encoding ferritin light chain, are an exception to this rule as they cause a late-onset dominant disease, called neuroferritinopathy, which may be often misdiagnosed as HD (Curtis *et al.*, 2001). So far, only a small number of

FTL1 mutations have been reported and the frameshift insertion c.460InsA by far the most common in UK cohorts.

Neuroferritinopathy typically presents with chorea and/or dystonia. Other clinical features are variably reported, including parkinsonism, cerebellar signs, dysarthria, frontal lobe syndrome and dementia. An action-specific facial dystonia is reported in ~65% of the patients (Chinnery *et al.*, 2007). Our group has recently shown that *cortical pencil lining,* which reflecting excessive cortical iron deposition, is a useful radiological sign of neuroferritinopathy (Batla *et al.*, 2015).

Other recessive NBIAs (in particular aceruloplasminemia) should be considered too, although chorea alone is rarely a sole prominent feature of these conditions (Walker, 2016).

Chorea in Patients with Mutations in Cerebellar Ataxia-Related Genes

Hyperkinetic movement disorders, including both chorea and dystonia, are frequently observed in a range of genetic neurodegenerative disorders usually presenting with predominant cerebellar ataxia (other than the aforementioned SCA17 and DRPLA).

Ataxia-telangiectasia (A-T) is an autosomal recessive multi-system disorder caused by mutation in the ataxia-telangiectasia mutated gene (*ATM*). A-T is usually characterized by progressive cerebellar ataxia, oculocutaneous telangiectasia, oculomotor apraxia, immunodeficiency with recurrent lung infections, and increased risk for cancer. Patients with bi-allelic *ATM* mutations, the cause of ataxia-telangiectasia (A-T), may present with a broad spectrum of movement disorders, including chorea (Klein *et al.*, 1996, Hardy and Singleton, 2009, Worth *et al.*, 2013), isolated dystonia (Saunders-Pullman *et al.*, 2012, Claes *et al.*, 2013), DOPA-responsive dystonia (Charlesworth *et al.*, 2013), and myoclonus-dystonia (Cheng *et al.*, 2002, Cummins *et al.*, 2013, Termsarasab *et al.*, 2015). Meneret and colleagues recently reported a total of 14 consecutive adults with variant A-T and compared them to patients with typical A-T (Meneret *et al.*, 2014). Patients with variant A-T have milder mutations, which allow a degree of residual protein activity (Gilad *et al.*, 1998), and clinically present with a later age at onset, a milder disease course and longer survival. Dystonia and subcortical myoclonus were the most common movement disorders observed (84%), followed by tremor (48%) (Meneret *et al.*, 2014). Of relevance, patients with *ATM*-related chorea and dystonia may completely lack the classic clinical features of A-T (Kuhm *et al.*, 2015).

Friedrich ataxia (FA) is the most common form of recessively inherited ataxia. FA is caused by mutations in the frataxin gene; 98% of cases have homozygous expansions of a GAA trinucleotide in intron 1 of the frataxin gene (Parkinson *et al.*, 2013). Rarely, chorea can be observed in bi-allelic carriers of frataxin mutations, sometimes preceding the onset of frank cerebellar symptoms (Hanna *et al.*, 1998, Zhu *et al.*, 2002, Wild *et al.*, 2008). Chorea has been rarely described also in cases with ataxia with oculomotor apraxia type 1 and 2, caused respectively by mutation in the genes encoding aprataxin and senataxin (Salvatore *et al.*, 2008, Anheim *et al.*, 2009)

Recessive mutations in *RNF216* have recently been found in families with hypogonadotropic hypogonadism and cerebellar ataxia (Margolin *et al.*, 2013). Expanding the phenotype of *RNF216* mutations-associated diseases, Santens and colleagues identified bi-allelic mutations in the *RNF216* in 2 recessive pedigrees with a HDL presentation, including chorea, behavioural problems, and severe dementia. In the affected cases rain imaging showed white matter lesions and subclinical evidence of hypogonadotropic hypogonadism was detected (Santens *et al.*, 2015).

2.3.4 Benign Hereditary Chorea

Clinical and genetic aspects of benign hereditary chorea will be discussed in detail in chapter 6.2.

Chapter 3. Materials and Methods

3.1 DNA Extraction

3.1.1 Extraction from Whole Blood

Genomic DNA was extracted from whole blood (taken in ethylenediaminetetraacetic acid bottles) in the Diagnostic Genetics Laboratory in the UCL Institute of Neurology using a FlexiGene© kit (Qiagen), according to manufacturer instructions.

In brief, 300μl of whole blood is mixed with 750μl of buffer (FG1), which lyses the cells. The sample is centrifuged for 20 seconds at 10,000xg and then the supernatant was discarded. 150μl of Buffer (FG2 – which contains a protease) is added to the pellet and the tube vortexed until the pellet was homogenized. The sample is subsequently centrifuged for 5 seconds and then placed for 5 minutes in a heating block at 65°C. 150μl of isopropanolol (100%) is then added and the tube inverted several times, allowing the DNA to precipitate. The sample is centrifuged for 3 minutes at 10,000xg and then the supernatant was discarded. 150μl of 70% ethanol is added and the sample vortexed for 5 seconds and centrifuged for 3 minutes at 10,000xg. The supernatant is discarded and the pellet air dried. 200μl of Buffer (FG3) is added and the sample vortexed at 5 seconds. The DNA is then dissolved by heating the sample at 65°C in a heating block.

3.1.2 Extraction from Saliva

Genomic DNA was extracted from saliva samples using the Oragene© DNA kit according to the manufacturers' instructions.

Briefly, the saliva sample and Oragene solution are incubated at 50°C in an air incubator for 2 hours. Then, 500μl of the solution is transferred to a 1.5mL microcentrifuge tube and 20μl of Oragene DNA purifier is added and then vortexed for a few seconds. The sample is then incubated on ice for 10 minutes and subsequently centrifuged at room temperature for 15 minutes at 13,000 rpm. The clear supernatant is transferred into a fresh microcentrifuge tube and the pellet containing impurities discarded. 500μl of 100% ethanol is added to the solution and inverted 10 times. The sample is then left at room temperature for 10 minutes allowing the DNA to precipitate. The sample was then

centrifuged at room temperature for 2 minutes at 13,000 rpm and the supernatant is removed and discarded. 250μl of 70% ethanol was added. The sample is allowed to stand at room temperature for 1 minute. The ethanol is then removed, taking care not to disturb the pellet. 100μl of DNA buffer was then added to dissolve the DNA pellet.

After extraction, the concentration of DNA samples was then measured using the Nanodrop (Thermo Scientific).

3.2 Polymerase-Chain Reaction

PCR primers were designed using Primer3 (http://primer3.ut.ee/). The nucleotide sequence form each exon, along with flanking ~200 down and up-stream intronic base pairs, was inputted in the program. DNA sequence of each exon was obtained from a suitable transcript (generally the longest coding transcript available with a consensus CDS (CCDS) identifier) downloaded from UCSC Genome Browser (https://genome.ucsc.edu/).

PCR was performed using 10 μl Faststart PCR Master (Roche Applied Sciences), 2 μl of forward and reverse primers at a dilution of 5 pmol/μl, 5 μl of double distilled water and genomic DNA at a final concentration of 20-30ng. DMSO was added to the mix for amplification of amplicons GC-rich. Each PCR reaction was performed using a program that had been demonstrated to optimally amplify the product.

3.3 Agarose Gel Electrophoresis

Agarose gel electrophoresis was used to check whether the PCR reaction was successful and verify the quality and size of PCR amplification product. 10x TBE (tris-borate-EDTA solution) solution was prepared using 121.1g of Trizma base (Sigma), 61.8g Boric Acid (Sigma), 7.4g of Ethylenediaminetetraacetic acid (EDTA) (Sigma) and dissolved in 1 litre of distilled water. A 1.5% gel was prepared using Ultrapure Agarose (Invitrogen) and TBE 1X buffer and stained with gel red (Cambridge bioscience). 3μl of PCR product and 3μl of X6 Orange DNA loading dye (Thermo scientific) were mixed together and loaded into one well of the gel. A DNA ladder (Midrange 100-2000 bp) (Qiagen) was run alongside each lane of the gel and then the samples were run at 100 mV for 45 minutes. DNA fragments are visualized using UV light.

3.4 PCR Purification

PCR cleanup was performed using an enzymatic method. The enzymatic cleanup solution was prepared mixing 200µl of Fast-Alkaline phosphatase (Thermo scientific), which removes unused dNTPs, 50µl Exonuclease I (Thermo scientific), which removes single strand DNA from PCR products, and 750µl of purified water. 5µl of PCR product was added to 2µl of the enzymatic solution and then run on a thermal cycler at 37°C for 30 minutes followed by 80°C for 15 minutes.

3.5 Sanger Sequencing

The sequencing Reaction mix was prepared combining 0.5µl BigDye Terminator v3.1 (Applied Biosystems), 2µl 5x Sequencing Buffer (Applied Biosystems), 1µl forward or reverse primers at 5 pmol/µl and 3µl of purified PCR product and 2.15µl of PCR grade water. The standard thermo-cycler program recommended by Applied Biosystems was used to run the Sequencing reaction. Sequencing purification was performed through the Sephadex method. A hydrated solution of Sephadex was prepared mixing 40ml of autoclaved water and 2.9 grams of Sephadex G-50 powder (Sigma-Aldrich). It was then vigorously mixed and allowed to hydrate, resting for at least 30 minutes at room temperature. Next, 350µl of the Sephadex solution was placed into each well of a Corning FiltrEXTM 96 well filter plates (0.66 mm glass fibre filter). The Corning FiltrEXTM filter plate was placed on top of an empty collection plate and centrifuged for 3 minutes at 750xg. The Corning FiltrEXTM was then placed on top of a new PCR plate. The entire sequencing reaction volume was then pipetted onto the Sephadex columns and the plates were then centrifuged again for 5 minutes at 910xg.

Sanger sequencing reaction products were then read on a 3730 DNA analyser (Applied Biosystems, Foster City, CA, USA) and electropherograms were visualised using Sequencher software (Gene Codes Corporation, MI, USA, version 5.0.1).

3.6 Multiplex Ligation-Dependent Probe Amplification

Multiplex Ligation-Dependent Probe Amplification (MLPA) analysis is is a multiplex PCR method used to determine exon copy number of genes of interest.

In this thesis I used the MLPA probemix P051-D1 (MRC-Holland, Amsterdam, the

Netherlands), which screens for the presence of exon deletions and duplications in *SNCA, PARK2, PINK1*, *PARK7* (Djarmati *et al.*, 2007). In addition, it contains probes that will only generate a signal when the *SNCA* p.Ala30Pro and *LRRK2* p.Gly2019Ser mutation are present.
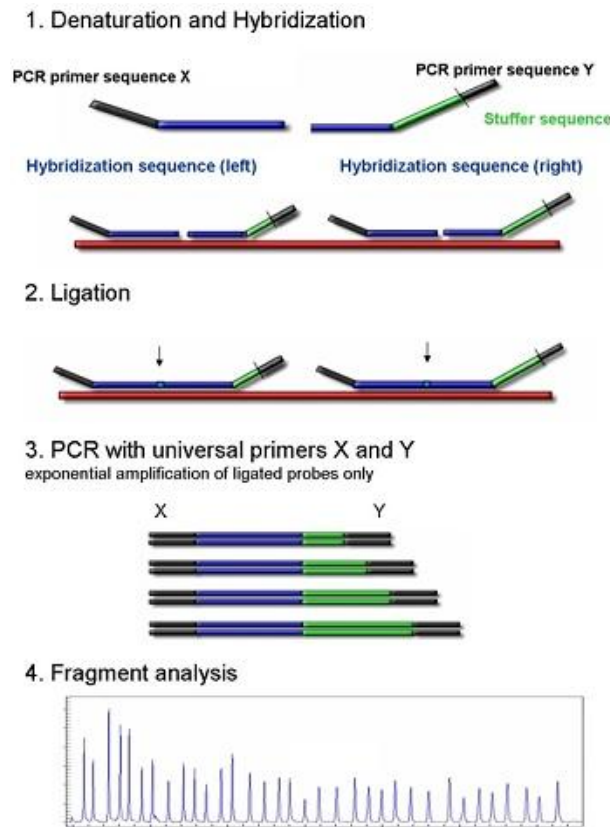
Figure 3-1 Steps of the MLPA reaction
Reproduced from mlpa.com

The MLPA reaction can be divided in five major steps (Figure 3-1): 1) DNA denaturation and hybridisation of MLPA probes. During this step, the DNA of the probands is first denatured at 98°C and then incubated overnight with a mixture of MLPA probes and MLPA buffer. MLPA probes consist of two separate oligonucleotides, each containing one of the PCR primer sequences. 2) Ligation reaction; this reaction can occur only if the two probe oligonucleotides are both hybridised to their adjacent targets. 3) PCR reaction; because only ligated probes will be exponentially amplified during this reaction, the number of probe ligation products is a measure for the number of target sequences in the sample. 4) Separation of PCR amplification products, after combining it with a mix of Hi-Di Formamide (Thermo Fisher Scientific) and marker Liz500 (Thermo Fisher Scientific) by electrophoresis on the 3730 DNA analyser. 5) Data

91

analysis; the results of the analysis are checked and interpreted using Genemarker software (Softgenetics).

3.7 Analysis of Microsatellites

Microsatellites are DNA sequences located in non-coding genomic regions and formed by mono, di, tri or tetra-nucleotides repeated in multiple tandem copies. Microsatellites are abundant and dispersed through the genome. The number of repeats is highly variable amongst different individuals in a population, whereas they tend to be stable between generations and are transmitted in a Mendelian fashion. Microsatellites are therefore widely used as genetic markers in genetic familial study. In this thesis microsatellites were used to define and compare the haplotype surrounding specific mutations in different families. Microsatellites were selected in UCSC genome browser. Primers to amplify the regions containing the microsatellite of interest were designed using Primer3. One primer for each reaction was labelled with a fluorescent dye (6-FAM). PCR reactions were performed as previously described. 0.5μl of undiluted PCR product was mixed with 12 μl of Hi-Di Formamide and 0.3μl of Liz500, denaturated at 98°C for 3 minutes and analysed by electrophoresis on the 3730 DNA analyser. The size of the microsatellites was assessed using the GeneMapper software (Thermo Fisher Scientific).

3.8 DNA Array SNP Analysis

Two types of DNA array SNP beadchips were used. For whole genome linkage analysis, I used Human CytoSNP beadchips (Illumina), which contains probes for ~220,000 markers. For detection of copy number variants or small chromosomal rearrangements, I used HumanOmni2.5-8 BeadChips (Illumina), which contains probes for ~2,500,000 markers.

For each sample, 10 μl of DNA at a concentration of ~75 ng/μl were prepared. Samples were processed, hybridized and scanned in accordance with the manufacturers instructions at UCL Genomics. Clustering, normalization and genotype calls were performed using Genome Studio 2010.3 Genotyping module (Illumina).

A Genome Studio project was created for each family project with default parameters.

CNVs analysis was performed using the plugin CNV partition 2.4.4 und results were

applied as bookmarks in genome viewer. PLINK output files, to be used for whole-genome linkage analysis, were created in Genome Studio through the PLINK report plug-in.

3.9 Genome-Wide Parametric Multipoint Linkage Analysis

Quality control checks were performed through PLINK. SNPs with low call rates (<90%) and monomorphic SNPs (MAF <0.5%) were removed using the commands –-maf 0.05 –-geno 0.1. ~6000 single nucleotide polymorphisms (SNP) equally distributed across the genome were then randomly selected using the command –-thin.

Linkage analysis was performed using the software MERLIN (http://www.sph.umich.edu/csg/abecasis/merlin/tour/linkage.html) (Abecasis *et al.*, 2002).

A .ped, .dat, .map and .model files were generated following the instructions. The .ped file contains information about the affection status of each individual included in the analysis (specified with a number: 1=unaffected and 2=affected 0=unknown), the sex of the individual (1=male, 2=female). Furthermore, the .ped file contains information about the pedigree structure, indicated by assigning every individual a unique number and specifying for each subject the identifiers of his/her father and mother. The .map files contains the list of SNP markers used for the linkage analysis and their genetic position expressed in centimorgans (cM). The model file contains information regarding the assumed mode of inheritance (autosomal dominant vs recessive) together with the estimated disease allele frequency and the probability of being affected for individuals with 0, 1 and 2 copies of the disease allele (penetrances).

The PEDSTATS function (http://csg.sph.umich.edu//abecasis/PedStats/) was used to validate the input formats and pedigree consistency using the command:

pedstats –d file.dat –p file.ped

To identify Mendelian errors (genotyping errors), which can lead to misleading inferences about gene flow in pedigrees and reduce the power of pedigree analysis, I used the command:

merlin -d file.dat -p file.ped -m file.map –error

Then, to erase from the input files the genotypes flagged as problematic I run the command:

pedwipe -d error.dat -p error.ped

MERLIN was then used to perform genome wide parametric linkage analysis using the command:

merlin –d file.dat –p file.ped –m file.map –model file.model –markernames –-pdf –-tabulate

This produces an output file containing LOD scores for each marker and a PDF graphical representation of the results. At least three randomly generated sets of markers were generated to perform linkage analysis.

Haplotype analysis allows to reconstructing the haplotype of a region of interest and checking segregation in the pedigree of the disease-associated haplotypes with disease status. Furthermore, it allows to possibly identifying recombination event, which could further narrow down the genomic intervals (fine mapping).

Fine mapping and haplotype reconstruction were performed for chromosomal loci identified by linkage analysis with LOD scores >0. First, for each locus, a list of SNPs spanning the linked region was compiled and this was used to generate a new of input files (.ped, .map, and .dat) using PLINK.

Haplotype analysis was then performed using the MERLIN command:

merlin -d haplo.dat -p haplo.ped -m haplo.map –-best –-horizontal

3.10 Whole-Exome Sequencing

WES was performed using the next-generation sequencing platform at Institute of Neurology. WES experiments were performed by Deborah Hughes and preliminary bioinformatics analysis by Dr Alan Pittman. The Truseq Exome Enrichment Kit (Illumina) was used for WES and run on an Illumina Hiseq 2000. This kit targets 64Mb of genomic sequence, including exons, exons-introns boundaries and UTRs and micro-RNAs. This kit offers on average more than 90% coverage of the exons, as defined in the latest version of the CCDS and Refseq database.

The first of WES is the library preparation (Figure 3-2). In brief, 3μg of genomic DNA must be sheared to form fragments, either by mechanical (Covaris) or enzymatic methods. This was followed by blunting of ragged ends of the DNA fragments and binding of the sequencing adapters. The latters contain unique indexes, which are unique for each sample and are essential in the next steps of the data analysis. After a series of PCR amplification, purification steps (to eliminate leftover adapters, enzymes and primers) and normalization (to ensure equal coverage of each sample in the total data), the libraries are ready for the enrichments stage.
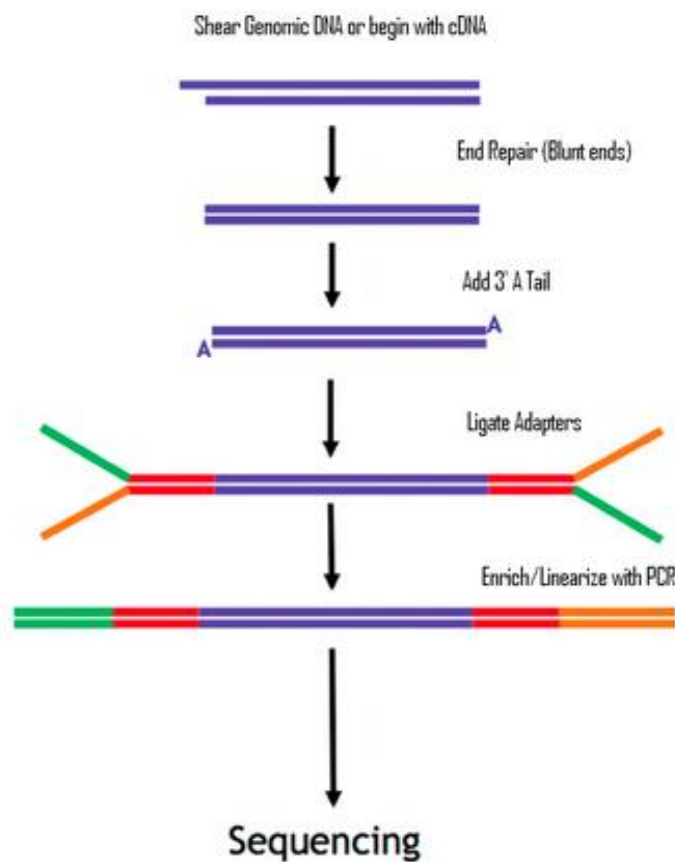
Figure 3-2 Scheme of the library preparation using the Truseq Illumina kit
Reproduced from (http://tucf-genomics.tufts.edu/home/faq)

The first step of enrichment is hybridization, during which the DNA fragments are first denatured to single strands and then bound to biotin-labelled probes specific for the target exome region. This is flowed by a series of capture and washing steps through a magnetic beads system and then the library is amplified through a final PCR step. After a last washing step, the libraries are ready for cluster generation, which is completed

95

within the Illumina cBOT. To form the clusters, the single-stranded, single-molecule template are primed and extended and subsequently the immobilized templates undergo bridge amplification with immediately adjacent primers (Figure 3-3).

A flow cell consists of eight lanes and is covered with a lawn of specific oligos to capture libraries as they are passed through the flow cell. Multiple samples can be pooled together and loaded in the same lane. The more libraries are pooled together the poorer will be the coverage.
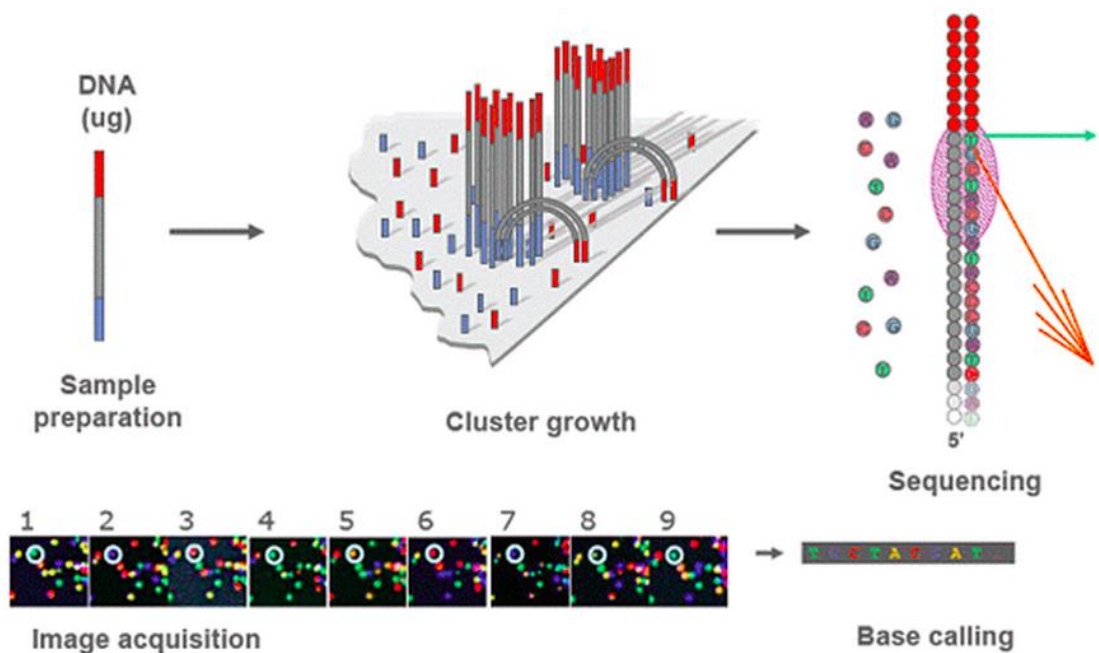
Figure 3-3 Cluster generation, bridge amplification and imaging
Reproduced from Openwetware.org

Following cluster generation and bridge amplification, the flow cell is loaded into the HiSeq 2000 for sequencing and imaging. After sequencing and imaging are terminated, the individual sample reads are de-multiplexed based on their unique indexes (Casava 1.8.2).

3.11 Bioinformatic Analysis of Whole-Exome Sequencing

In order to obtain a final list of variants the WES raw data was run and analysed through a bioinformatics pipeline, constructed by Dr. Vincent Plagnol and optimized by Dr Alan Pittman. The pipeline is schematically represented in Figure 3-4.

The WES data generated by the HiSeq 2000 is stored in a FASTQ file, a text-based format for storing nucleotide sequence.

Paired-end sequence reads are aligned with Novoalign (www.novocraft.com) against the reference human genome (UCSC hg19). Generation of duplicate DNA sequencing reads, which are due to PCR-induced duplication, is one of the most relevant technical artifacts of the capture-sequencing procedure. Duplicate read needs to be removed so that they do not influence variant calling and this step is performed with Picard software package (http://picard.sourceforge.net/).
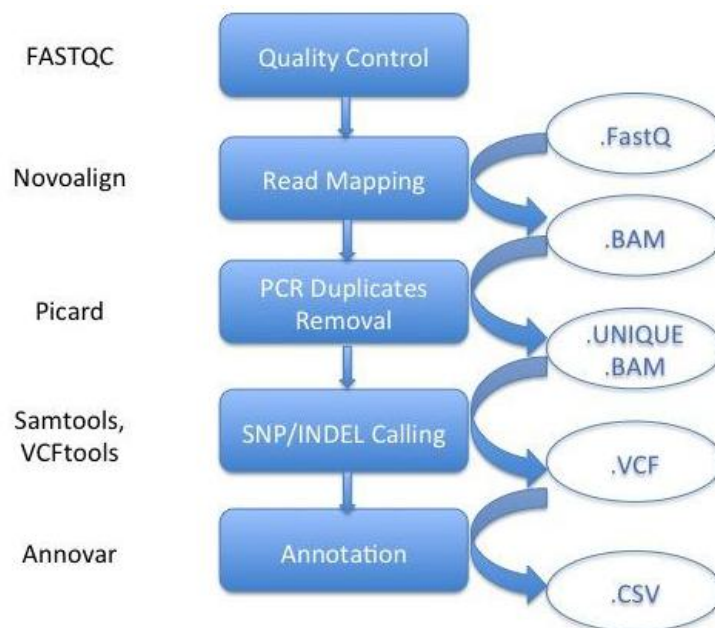
Figure 3-4. Bioinformatic pipeline for WES analysis.

Information regarding the project, the genome and an alignment section, which includes mapping position and information on mismatches, are contained into tab-delimitated text files, called SAM files (.sam). A BAM file (.bam) is the binary version of a SAM file. BAM files, rather than SAM, are the recommended format for visualisation software.

After the alignment is completed, variant calling is performed comparing at each genomic position the aligned SAM/BAM file to the reference genome. SAMTOOLS package (http://samtools.sourceforge.net/) is used to recalibrate base quality scores, perform local realignments around possible indels, and to call and filter the variants.

The outcome of the analysis is a Variant Call Format (VCF) file, which holds the list of identified genetic variants and the associated quality scores that take into account both base calling and mapping scores.

ANNOVAR software is used to perform functional annotation the variants (Wang *et al.*, 2010). Annotated variant files are generated including a comparison to several publicly available reference databases of genetic variation, including the Exome Aggregation Consortium (ExAC; http://exac.broadinstitute.org/), dbSNP version 129 and 137 (www.ncbi.nlm.nih.gov/projects/SNP), 1000 Genomes project (1kGP; www.1000genomes.org), NHLBI Exome Variant Server (EVS; evs.gs.washington.edu) and Complete Genomics 69 (www.completegenomics.com/public-data/69-Genomes).

In silico prediction of pathogenicity is assessed using SIFT (http://sift.jcvi.org/) (Kumar *et al.*, 2009), PolyPhen2 (http://genetics.bwh.harvard.edu/pph2/) (Adzhubei *et al.*, 2010), Provean (http://provean.jcvi.org/) (Choi *et al.*, 2012), MutationTaster (http://www.mutationtaster.org/) (Schwarz *et al.*, 2014) and CADD (http://cadd.gs.washington.edu/home) (Kircher *et al.*, 2014). Evolutionary conservation of nucleotides involved by variants is score using PhiloP (Pollard *et al.*, 2010) and GERP++ (Davydov *et al.*, 2010).

Copy number variants (CNV) were called in WES data using the Exome depth algorithm (Plagnol *et al.*, 2012).

3.12 Regional Gene Expression Profiling in Brain Tissue

To add further support to the causal role of newly identified gene variants, regional gene expression profile across various brain regions in humans was assessed using an in-house and other publicly available datasets. The in-house dataset originated from the work of Dr Mina Ryten and Dr Daniah Trabzuni. This dataset was generated using Affymetrix Exon 1.0 ST Arrays and brain tissue originating from 134 control individuals, collected by the Medical Research Council (MRC) Sudden Death Brain and Tissue Bank, Edinburgh, UK, and the Sun Health Research Institute (SHRI), an affiliate of Sun Health Corporation, USA. Ten brain regions were analyzed: putamen (PUTM), frontal cortex (FCTX), temporal cortex (TCTX), hippocampus (HIPP), substantia nigra (SNIG), medulla (specifically inferior olivary nucleus, MEDU), intralobular white matter (WHMT), thalamus (THAL), and cerebellar cortex (CRBL). A full description of

the samples used and the methods of RNA isolation and processing can be found in (Trabzuni *et al.*, 2011).

As described therein, all arrays were preprocessed using Robust Multi-array Average (RMA) quantile normalisation with GC background correction and log2 transformation in Partek's Genomics Suite v6.6 (Partek Incorporated, USA). Regional differences in gene-level expression were investigated using Partek's mixed-model ANOVA with gender and batch effects (date of hybridization and brain bank) included as co-factors.

RNA expression changes during the course of human brain development were assessed accessing the data available through the Human Brain Transcriptome (HBT) database (Johnson *et al.*, 2009, Kang *et al.*, 2011). The brain regions analyzed are the striatum (STR), amygdala (AMY), neocortex (NCX), hippocampus (HIP), mediodorsal nucleus of the thalamus (MD), and cerebellar cortex (CBC). The data is publicly available accessing the HBT website (http://hbatlas.org/).

Chapter 4. Exploring the Genetics of Parkinson Disease

4.1 Outline Of The Chapter

This chapter describes the work I conducted to expand our knowledge of the genetic basis of PD.

The specific aims of the study were:

1) To assess the contribution of genetic variation in *GBA* in the Queen Square cohort of early-onset PD

 2) To characterise genetically the Queen square cohort of PD patients who underwent treatment with DBS and assess whether the genetic status influence the outcome of the treatment and disease progression;

3) To assess the relationship between mutations in *GCH1*, the gene responsible for the childhood-onset disease DOPA-responsive dystonia, and PD.

4.2 *GBA* Mutational Analysis In Early Onset Parkinson Disease

4.2.1 Statement Of Contribution

I participated to the design of this study and ascertained the cases to be included in this study. I performed the *GBA* sanger-sequencing analysis in the PD cases. Dr Raquel Duran performed the *GBA* sanger-sequencing analysis in the Gaucher disease (GD) cohort and in control samples.

4.2.2 Background

Patients with EOPD, in comparison to patient with late-onset PD (LOPD) tend to progress more slowly in terms of motor features and generally have a longer disease course, often with preservation of cognitive function. On the other hand, L-DOPA induced complications, including motor fluctuations and dyskinesias, tend to appear earlier and be more severe (Schrag and Schott, 2006).

As previously discussed in this thesis, mutations in several genes have been associated with EOPD, in particular autosomal recessive genes, including *PARK2*, *PINK1* and *PARK7* (Bonifati, 2012). *PARK2* is by far the most commonly mutated gene in EOPD, whereas mutations in *PINK1* and *PARK7* are significantly more rare (Abou-Sleiman *et al.*, 2003, Healy *et al.*, 2004, Alcalay *et al.*, 2010).

PARK2 mutations are particularly common (frequency ~50%) in familial cases and in patients with very early onset (e.g. onset at age < 30), whereas their frequency drops (frequency ~10-15%) in sporadic cases and patients with later onset (e.g. onset at age > 30 and < 50) (Lucking *et al.*, 2000).

The different clinical course of EOPD, together with pathological reports showing in most *PARK2* mutations carriers the absence of the characteristic LBs (Doherty *et al.*, 2013), suggest that EOPD may represent a distinct clinical and pathological entity.

Loss-of-function mutations in the acid β glucocerebrosidase gene (*GBA*), which are responsible for the autosomal recessive lysosomal disorder GD (Grabowski, 2008), represent the most prevalent genetic risk factor for PD identified to date (Sidransky *et al.*, 2009). So far genetic analysis has suggested that all *GBA* mutations causing GD can equally predispose to PD, the assumption being that variants that do not cause GD in the homozygous would not predispose to PD.

In this this study, a complete sequence analysis of the open reading frame of *GBA* was performed in a cohort of 185 PD cases with early onset PD (EOPD; defined by an age at onset of ≤50 years). These data were compared with those obtained from 283 controls and 73 patients with type 1 GD from the same geographic region (Duran *et al.*, 2012).

This study had two main aims; first, to assess and quantify the contribution of *GBA* mutations in EOPD; second, to compare the spectrum of *GBA* mutations found in PD cases versus that of GD cases. Indeed, possible differences in the type of mutations found in the two disease groups may shed light onto the underlying pathogenic mechanisms responsible for PD and GD.

4.2.3 Subjects, Materials and Methods

Subjects

The cohort included in this study was formed by 185 unrelated PD cases with an onset age ≤ 50 who attended the Movement Disorders clinics at the National Hospital Queen

101

Square. They were all diagnosed with PD following the UK Brain Bank Clinical Criteria, presenting with at least 2 of 3 cardinal signs of tremor, rigidity, and bradykinesia, as well as a positive response to L-DOPA therapy (Hughes *et al.*, 1992). The age-at-onset was on average 40 ± 7.2 years (range $16 - 50$). A positive family history compatible with PD in at least a first or second-degree relative was reported in 27.5% of patients (51/185) reported.

Controls were age-matched subjects. This series of controls has been previously described (Neumann *et al.*, 2009) with the addition of twenty-six age-matched spouse controls. Controls were neurologically intact. All cases and controls were of UK Caucasian origin with no reported Jewish Ashkenazim background. GD patients were 73 unrelated subjects, affected with the type 1 form of the disease (non-neuronopathic), attending the National GD clinics at the Royal Free and Addenbrookes Hospitals. 16 were Ashkenazi Jewish (22%) and 4 had Eastern European ancestry (5.7%); the remainder were white UK citizens without Ashkenazi ancestry. The results of the *GBA* mutational screening of this cohort have been published independently (Duran *et al.*, 2012). Written informed consent was taken from each participant.

Genetic Analysis

The open reading frame (11 exons) of the *GBA* gene (RefSeq accession number NM_000157.3) was entirely sequenced in cases and controls. For PCR amplification of *GBA*, three different long-range PCR reactions were performed. To avoid amplification of the pseudogene, primers were designed to bind to DNA regions exclusively present within *GBA*. Primer sequences are listed in the appendix. Allele names refer to the processed protein, excluding the 39-residue signal peptide.

Statistical Analysis

Frequencies of coding and splice-site *GBA* variants in cases and controls were compared by means of Fisher's exact (statistical significance set at P value < 0.05 using a two-tailed test) and odds ratios (OR) and 95% confidence intervals (CI) were calculated. Analyses were performed using the statistical analysis program R (http://www.r-project.org/).

4.2.4 Results

The results of the genetic analysis are summarised in Table 4-1. In this population of early-onset PD, a surprisingly high proportion of cases carried a *GBA* variant (25.94 %; 48/185 individuals; odds ratio for carriers of any variant in cases versus controls: 7.9, 95% confidence interval 4.1 - 15.4, P < 0.0001). 14 of the *GBA* mutation carriers (29.7%) had a positive family history for PD, though we could not check segregation of the mutations in other affected family members due to unavailability of genetic material.

Among the *GBA* mutation carriers, 22 cases had a known GD-causing pathogenic mutation (20 carried one mutation and two each carried two mutations), a proportion significantly higher than in a late-onset PD cohort from the same population reported by our group (11.9%; 22/185 individuals versus 3.8%; 30/790, p = 0.0001) (Neumann *et al.*, 2009).

The most frequent GD-causing mutations found in the PD cohort was the N370S (p.Asn409Ser) that was observed in 5 cases, followed by R463C (p.Arg502Cys) and the recombinant allele Rec*N*ciI (L444P [p.Leu483Pro] + A456P [p.Ala495Pro] + V460V [p.Val499Val]), which were each present in 3 cases, and by L444P (p.Leu483Pro) and R131C (p.Arg170Cys), each found in 2 cases. All the other GD-causing mutations were each found in single individuals. In the control group the N370S (p.Asn409Ser) and the

R257Q (p.Arg314Gln), each found in 1 subject, were the only GD-causing mutations detected.

Of relevance, one PD case carried the N370S (p.Asn409Ser) mutation in the homozygous state and, although this genotype is known to cause GD, he did not display any feature of GD. This is not entirely surprising, as the clinical spectrum in GD is wide and there are studies suggesting that patients homozygous for mild mutations, such as N370S, may actually never develop the disease (Cormand *et al.*, 1997). Furthermore, individuals with two pathogenic *GBA* variants, presenting with typical PD but showing no signs of GD, have already been reported in the literature (Lesage *et al.*, 2011).

The second important finding is that the single most common mutation in the PD group was E326K (p.Glu365Lys), which was detected at a frequency of 7.57% in cases (14/185 individuals; 12 were heterozygote, including one in combination with L444P and 2 homozygote) versus 2.47% in controls (7/283 individuals). To confirm this observation, a further 202 controls were screened for this variant and the frequency in this new cohort was 2.97 % (6/202). Taking into account both sets, the total frequency in controls was 2.68% (13/485 individuals), indicating a significant association of this variant with PD (p = 0.0059, odds ratio 2.97, 95 % confidence interval 1.3 -6.4).

However, despite the high frequency in both PD and control groups, E326K (p.Glu365Lys) was not detected at all in the GD cohort (Duran *et al.*, 2012). Consistent with previous reports (Park *et al.*, 2002), this finding clearly indicates that this variant does not cause GD. Further supporting this conclusion, the two PD cases homozygote for the E326K did not have any of the clinical or haematological features of GD and their white blood cell GCase enzymatic activity was at the lower limit of normal range. Interestingly, a number of other variants, not present in GD group and never associated with GD, were also detected in the PD cohort. Of these E388K (p.Glu427Lys), G113A (p.Gly152Ala), T369M (p.Thr408Met), S465P (p.Ser504Pro) have been previously reported in both PD cases or controls, whereas L(-14)V (p.Leu25Val), V172L (p.Val211Leu), S177T (p.Ser216Thr), L217P (p.Leu256Pro), L354P (p.Leu393Pro), V375G (p.Val414Gly), c.1506-4 C>T, c.1506-12 C>T are novel. Collectively, these variants of undetermined clinical significance were more frequent in cases than in controls (OR 7.0 - confidence interval 1.8-31.6; p = 0.001).

Table 4-1 Proportion of cases and controls with *GBA* mutations

GBA variants	% in PD (n=185)	% in controls (n=283)	% in type 1 GD (n=73)	OR (95%CI)*
N370S	2.70 (5)	0.35 (1)	86.30 (63)	7.8 (0.9-67.6)
Rec*Nci*I (L444P+A456P+V460V)	1.6 (3)	0 (0)	10.96 (8)	Ø
R463C	1.62 (3)	0 (0)	5.48 (4)	Ø
L444P	1.08 (2)	0 (0)	24.66 (18)	Ø
Other Gaucher's causing mutations	5.4 (10) [2]	0.35 (1) [3]	45.2 (33)	16.1 (2.04-126.97)
E326K	7.57 (14)	2.47 (7) [1]	0 (0)	3.2 (1.2-8.1)
Other variants with unproven pathogenicity	7.03 (13) [4]	1.06 (3) [5]	0 (0)	7.0 (1.8-31.6)
Total	25.94 (48)	4.24 (12)	100 (100)	7.9 (4.1-15.4)

The number of carriers for each GBA variant is in brackets

*OR: Odds ratio calculated for PD patients versus controls. CI: confidence interval. Ø: OR cannot be calculated, as all carriers were cases

1Additionally further 202 individuals were screened for just this variant and the frequency in these additional samples was 2.97 % (6/202). The total frequency, taking into account both sets of controls, was 2.68% (13/485 individuals).

2 IVS2+1 (1), R131C (2), W184R (1), N188S (1), H255Q (1), R257Q (1), D409H (2), RecTL (1)

3 R257Q (1)

4 E388K (1), G113A (2), T369M (1), S465P (1), L(-14)V (1), V172L (2), S177T (1), L217P (1), L317L (1), L354P (1), V375G (1), IVS10-4 C>T(1), IVS10-12 C>T(1).

5 E340A (1), T369M (1) and V458L (1).

4.2.5 Discussion

This study reports the largest series of early-onset PD cases in which the *GBA* gene was entirely sequenced and shows that the frequency of *GBA* mutations is much higher than in late-onset patients from the same geographic area. Prior to this work, only one study had screened the entire *GBA* open-reading frame in EOPD cases, but in a much smaller cohort (Clark *et al.*, 2007). Consistent with the results of this project, Clark and colleagues found that the frequency of *GBA* mutations was 22.2% in subjects with EOPD, compared with 9.7% in cases with classic LOPD. This indicates that *GBA* mutations represent by far the most common genetic alteration in EOPD, in particular in subjects with an onset of symptoms at ages between 30 and 50 years. As will be discussed more extensively in the next chapter, this finding bears important clinical consequences. It has been reported that EOPD cases often have a more benign disease course, in particular with regard to the risk of developing dementia (Schrag *et al.*, 1998). However, this may not be true for carriers of *GBA* mutations, as it is now recognized that the risk of progression both to dementia and major motor difficulties (i.e. balance loss) is significantly greater in *GBA* mutation carriers (Alcalay *et al.*, 2012, Winder-Rhodes *et al.*, 2013).

Importantly, the *GBA* variant E326K was by far the most common variant found in this cohort (7.5% of cases screened), indicating that in north European populations this mutation may be the single most frequent predisposing factor for PD.

The possibility that the E326K could be a risk factor for PD was raised before, but discarded as in previous studies it was *a priori* considered a benign polymorphism or the association with PD was not as robust as we describe in this study (Nichols *et al.*, 2009, Lesage *et al.*, 2011). These data confirm those initial observations and put uncertainty beyond doubt, demonstrating that indeed this variant does increase the risk of PD. Consistent with this results, similar data were presented by Pankratz and colleagues as part of a large meta-analysis of the existing available PD GWAS datasets, in which the E326K reached genome-wide significance (OR=1.71; p=5 $\times$ 10^{-8}) and hence was highlighted as a susceptibility allele for PD (Pankratz *et al.*, 2012).

These results are in apparent contrast with the large meta-analysis of *GBA* in PD performed by Sidransky *et al.*, which failed to demonstrate this association (Sidransky *et al.*, 2009). This difference could be due to the heterogeneity of populations included

in that study. Indeed, it was enriched with subjects from populations (e.g. Asian, Jewish, Portuguese) in which the E326K is absent or very rare (Clark *et al.*, 2007, Bras *et al.*, 2009, Mitsui *et al.*, 2009).

Although biochemical observations have demonstrated that the E326K is a subtle loss-of-function variant (Montfort *et al.*, 2004, Horowitz *et al.*, 2011), this reduction of the activity is clearly not severe enough to lead to disease in the tissues where GD is associated with lysosomal storage dysfunction. However, when E326K is detected on the same allele with another mutant variant (e.g. L444P, N188S, or N370S), it does not act as a neutral allele, and instead contributes to GD severity by further reducing the residual enzymatic activity (Grace *et al.*, 1999, Chabas *et al.*, 2005, Rozenberg *et al.*, 2006, Liou and Grabowski, 2012).

The association of the E326K with PD and its absence in the GD cohort, together with the presence of many other novel rare *GBA* variants in the PD group not associated with GD, may suggest a possible dissociation of the pathogenic molecular mechanisms that underlie these two diseases.

However, it is not clear whether the mild loss-of-function of the allele E326K is the cause of the increased risk for PD or whether other, still undetermined, effects of the mutation on lysosomal function are contributing to nigral neuron degeneration. Recent studies suggest that heterozygous *GBA* mutations may contribute to the pathogenesis of PD through a gain of function effect that may include endoplasmic reticular stress (Gegg *et al.*, 2012).

Interestingly, an overall enrichment of variants of undetermined clinical relevance was detected in the PD group. Although further population studies and functional analyses are warranted to substantiate this observation, these data indicate that there may be other *GBA* variants that predispose to PD but are not associated with GD. It is also possible that, as PD is a frequent disorder and a higher number of PD cases, compared to GD, are screened for *GBA* mutations, some of these variants are actually GD-causing mutations, simply not observed yet in GD cases.

In conclusion, this study shows that *GBA* mutations are the most common genetic abnormality in patients with PD with an age at onset below 50. These results strongly link the pathogenesis of EOPD to that of LOPD and suggest that both forms are part of the disease spectrum associated with the same underlying pathogenic process.

Furthermore, these results incontrovertibly establish a pathogenic role for the allele E326K. The latter extends the relevance of *GBA* dysfunction to a much larger number of PD patients than previously thought, bearing crucial implications for the development and application of future treatment targeting lysosomal dysfunction in PD. Finally, these data reflects the need to accurately explore the contribution of all *GBA* rare variants to the increased risk of PD and not just alleles that have been previously associated to GD.

4.3 Genotype-Phenotype Correlation in A Cohort Of Parkinson Disease Patients Treated With Deep-Brain Stimulation

4.3.1 Statement of Contribution

I performed all the genetic experiments and analysed the genetic data. Dr Aikaterini Angeli performed the clinical assessment and Dr Thomas Foltynie performed the clinical data analysis.

4.3.2 Background

Patients with PD may present significant heterogeneity in their clinical features, in particular with relation to their motor phenotype, their rate of disease progression and the development of non-motor symptoms (e.g. cognitive decline) (Foltynie *et al.*, 2002). From a clinical viewpoint, the purpose of identifying PD subtypes is to aid individually tailored prognosis and to understand whether different subtypes of PD may show different responses to treatments.

Previous authors have attempted to classify subgroups of PD patients based on clinical features, such as "Tremor Dominant PD" or "Akinetic-Rigid PD" (Jankovic *et al.*, 1990).

However, despite the recognition of the existence of PD heterogeneity, there has been little translation of theories into practice, largely because of the lack of consensus regarding how best to sub-classify PD based on clinical phenotype. Techniques other than clinical examination have been used to help explore PD heterogeneity, including neuro-physiological techniques (Morgante *et al.*, 2006), CSF examination (Jellinger, 2012), structural (Jubault *et al.*, 2011) & functional imaging (Brooks and Pavese, 2011) biomarkers as well as clinico-pathological correlations have all been explored (Selikhova *et al.*, 2009). However, to date there have been no convincing demonstrations that any of these methods can reliably distinguish subtypes of disease.

It is possible that some features of PD phenotype heterogeneity could depend on the underlying genetic background, with superimposed effect of other environmental or stochastic inter-individual modifiers. A number of studies have described the phenotype of specific genetic mutations carriers and compared it to non-carriers (Lesage *et al.*, 2011, Marras *et al.*, 2011), but a direct comparison of PD phenotype between carriers of

mutations in different genes are few (Gan-Or *et al.*, 2010).

Functional neurosurgery has embraced PD heterogeneity in day-to-day practice for many years. PD tremor responds very well to Deep Brain Stimulation (DBS) of the motor thalamus (Benabid *et al.*, 1993), severe disabling dyskinesia responds very well to Globus Pallidum pars interna (GPi) DBS (Krack *et al.*, 1998), whereas the Akinesia/ Rigidity of PD is best relieved through targeting the Subthalamic nucleus (STN) (Limousin *et al.*, 1995). Given that the risks of neurosurgery become higher with advancing age, patients undergoing DBS are a very skewed group of PD patients, necessarily having had many years of PD but nevertheless still remaining young and judged fit enough to undergo neurosurgery. Consequently PD patients undergoing DBS tend to have relatively young onset disease and may contain an over-representation of genetic forms of PD. Furthermore, as part of the pre-operative workup, patients undergo a systematic evaluation of PD severity both in the absence and presence of medication, as their drug responsiveness is a helpful predictor of subsequent DBS response.

I performed an extensive genetic characterization of a series of patients with PD undergoing DBS surgery in a single centre. Cases were screened for point mutations in *PARK2, GBA*, for exonic rearrangements in *SNCA* and *PARK2* and for the presence of the *LRRK2* variants c.6055 G>A; p.Gly2019Ser.

The clinical phenotype among the carriers of different genetic mutations both on and off dopaminergic medication, as well as assessing the range of responses to DBS, was compared. In addition, a subgroup of these patients with complete longitudinal follow up assessments allows us to evaluate the natural history of PD following DBS according to genotype with respect to, perhaps the most important long term outcome, cognitive decline.

4.3.3 Subjects, Materials and Methods

Subjects

94 patients who underwent DBS for PD were included in the study. The mean age at PD onset of the cohort was 40.4±8.2 (range 7-58). Of these 31 (32.9%) had a positive family history for PD in a first or second degree relative.

Clinical assessment

All patients included in this series were followed-up at the National Hospital for

Neurology and Neurosurgery (NHNN), Queen Square. As part of their routine assessment, details were recorded regarding their basic demographics such as age at onset, initial symptoms and disease duration. The L-DOPA equivalent dose was derived using standard formulae (Tomlinson *et al.*, 2010).

As part of the decision making process regarding appropriateness of DBS, all patients underwent detailed assessments including a formal L-DOPA challenge comparing scores on motor part of the Unified Parkinson's disease rating scale (UPDRS) in the practically defined "Off state"- (overnight free from dopaminergic medication) and the "On state" after a L-DOPA challenge (250mg of oral dispersible L-DOPA). Additional assessments included a detailed battery of Neuropsychological assessments including the Mattis Dementia Rating Scale (DRS-2). From the UPDRS motor scale, sub-scores were derived to quantify tremor (based on the sum of items 20 and 21), akinesia and rigidity (based on the sums of items 22-26 and 31), and axial features (based on the sum of Items 18, 19, & 27-30). Part 4 of the UPDRS was divided into 2 sub-scores; items 32 to 34 for dyskinesia and items 35-39 to reflect OFF periods.

The optimal DBS target was chosen according to the frequency and severity of OFF-symptoms, dyskinesias, tremor, speech-intelligibility, and cognition. STN was targeted in the majority of patients requiring DBS. However, the presence of severe dyskinesias was an indication to target the bilateral internal globus pallidus (GPi), whereas severe tremor, especially if unresponsive to L-DOPA and in the absence of other disabling PD symptoms, is an indication for DBS of motor thalamus (VIM DBS).

Post-operative assessments were performed at 12 months after DBS implantation. A subgroup of patients with longer follow-up after DBS surgery was recruited to repeat cognitive assessment, including the DRS-2. Their mean annual change in cognitive performance between baseline and follow up was calculated as follows (DRS-2 score at baseline – DRS-2 score at follow up)/ number of years between assessments.

Genetic analysis

The coding regions and the flanking intronic sequences of *PARK2* and *GBA* were analysed by PCR amplification and subsequent direct Sanger sequencing, as described in Materials and Methods. Primer sequences are listed in the appendix. Exonic rearrangements (deletions/duplications) in *SNCA, PARK2, PINK1, PARK7* and the presence of the p.Gly2019Ser mutation in *LRRK2* were screened using a multiplex

ligation-dependent probe amplification (MLPA), as described in Materials and Methods. Patients found by MLPA to be positive for *LRRK2* p.Gly2019Ser mutation had this result confirmed by Sanger sequencing.

Statistical analysis

Chi-squared test was used to make comparisons between categorical data. Continuous data were checked for normality using Shapiro-wilk test. For normally distributed variables, one way analysis of variance (ANOVA) was used to compare genetic subgroups. Post hoc pair wise comparisons were performed using Sidak's method. For non-normally distributed variables, Kruskal-Wallis & non-parametric post hoc pair wise comparisons were used. Analyses were performed using the statistical analysis program R (http://www.r-project.org/).

4.3.4 Results

Genetic results

27 out 94 patients included in the study (29%) carried at least one mutation in the genes I tested. The results of the genetic screening are summarised in Table 4-2.

Eight individuals (8.5% of the cohort) had at least one pathogenic mutation in *PARK2*. Of these six had homozygous or compound heterozygous mutations (phase of the mutations unknown), while two patients had a single mutation only (one of whom also had a *GBA* T369M mutation). Given the controversial role of single heterozygous *PARK2* mutations (Klein *et al.*, 2007), only patients with bi-allelic *PARK2* mutations were included in the phenotypic analysis.

Eighteen patients (19.1% of the cohort) had at least one mutation in the *GBA* gene. Amongst the *GBA* mutation carriers, ten carried GD-causing mutations (of these one had the L444P combined with E326K) and five carried the pathogenic common risk factor E326K (four heterozygotes and one homozygote; see previous section of this chapter for further discussion about this variant). One case carried the novel variant L271P, predicted pathogenic by *in silico* prediction scores and therefore likely to be a deleterious variant. Two cases carried the variants T369M and E388K, respectively. Given the uncertainty regarding the clinical relevance of the two variants (Walker *et al.*, 2003) (Paciotti *et al.*, 2012), these two cases were excluded as well from further phenotypic analysis.

Five patients (5% of the cohort) carried the common pathogenic mutation in *LRRK2* p.Gly2019Ser. One of the cases with p.Gly2019Ser also carried the E326K *GBA* mutation. This patient developed PD symptom at age 35, the youngest age at onset from the group of *LRRK2* positive patients reported in this study and overall much earlier than the average age at onset of the *LRRK2* mutation carriers (Healy *et al.*, 2008). This finding possibly suggests a synergistic effect of the two variants on the onset anticipation.

The remaining 67 patients had no mutation detected using the genetic tests performed.

Phenotypes

The mean age at onset of the bi-allelic *PARK2* carriers (26.6 years) was significantly lower than *GBA* mutation carriers (p=0.0009), *LRRK2* p.Gly2019Ser mutation carriers (p=0.0008) and gene negative (p=0.006) patients (Table 4-3). There was no significant difference in the age at onset between the other groups.

The mean duration of PD in patients undergoing DBS surgery was 15.0 ± 6.6 years (range 3.8-38.0 years). Patients with *PARK2* mutations had a longer duration of disease at the time of surgery than all other subgroups (p=0.007). On the contrary, *GBA* mutation carriers had a significantly shorter mean duration of disease at the time they needed DBS surgery compared to all other sub-groups (p=0.001) (Table 4-3). There was no difference in duration of disease between the *LRRK2* p.Gly2019Ser and gene negative groups.

Table 4-2 Description of the genetic mutations in *PARK2*, *GBA* and *LRRK2* in a cohort of PD patients with DBS surgery.

Genetic test results	n	Description	Age at symptom onset ± SD
PARK2 (Compound heterozygotes/ homozygotes)	6	Homozygous c.101_102delAG	30
		p.Gly430Asp+p.Arg275Trp	20
		c.337_376del+c.465_466del	36
		Homozygous del exons 3-4	27
		p.Arg275Trp+het dup of exon 6	7
		c.337_376del +p.Ala82Glu	39
			(Mean 26.5±11.6)
PARK2 (Single mutation carriers)	2	p.Arg334Cys	41
		p.Pro437Leu + *GBA* T369M[a]	39
*GBA**	16	R463C	45
		L444P+E326K	34
		N370S	45
		D409H	39
		rec*Nci*I	40
		R463C	45
		N188S	49
		R275Q	42
		IVS2+1 G>A	41
		L444P	45
		E326K/E326K	42
		E326K	36

		E326K	51
		E326K	58
		E326K+*LRRK2* p.Gly2019Ser[a]	35
		L217P	39
			(Mean 42.9±6.2)
LRRK2	5	p.Gly2019Ser	40
		p.Gly2019Ser	36
		p.Gly2019Ser	49
		p.Gly2019Ser	55
		p.Gly2019Ser +*GBA* E326K[a]	35
			(Mean 43±8.7)
No mutation found	67		(Mean 40.8±7.2)

Numbers add up to 96 since 2 individuals marked with [a] are represented twice in the table in view of their carrying 2 mutations.

* Allele names refer to the processed protein, excluding the 39-residue signal peptide

As part of the preoperative assessment for DBS, all patients underwent an L-DOPA challenge. All patients in this series had a good response to L-DOPA (mean UPDRS part 3 improvement of 68% in the group as a whole), independently from the mutational status. This is not surprising, as a positive L-DOPA challenge represents an essential part of the basis for predicting a beneficial response from DBS surgery and therefore only patients with an excellent L-DOPA responsiveness were included in the cohort.

Dyskinesia scores were higher in the *PARK2* bi-allelic mutations carriers, in spite of the lower doses of L-DOPA they were taking.

All patients in this series had baseline neuropsychological performance that was judged to be clinically acceptable for DBS surgery.

During pre-operative assessment in the off phase, there were no overt differences in the motor phenotype according to mutational status. Tremor was present in all subgroups, and the proportion of tremor compared with akinesia/rigidity or axial features was similar in each group.

Chi-squared analysis showed a significant difference in targeted brain region for DBS according to mutational status ($p<0.001$), with an excess of *PARK2* and *GBA* patients that received bilateral GPi DBS rather than STN DBS.

There were no significant differences in the level of improvement obtained with STN DBS between gene negative patients and patients with *PARK2*, *GBA* or *LRRK2* mutations.

Longitudinal 5-year follow up data regarding cognitive performances were available for 35 subjects, all treated with STN DBS, and amongst them six were *GBA* mutations carriers. The mean reduction in Mattis DRS-2 scores in patients with GBA mutations was 4.4±7.3 points per year, compared with 0.5±0.9 points per year among gene negative patients, although this did not reach threshold for significance.

Table 4-3 Pre-operative UPDRS scores and response to L-dopa according to genetic subgroup

Genetic results	Duration of PD at DBS assessment yrs (SD)	L-dopa Equivalent Dose; mg (SD)	UPDRS part 1 (SD)	UPDRS part 2 OFF meds (SD)	UPDRS part 2 On meds (SD)	UPDRS Part 3 Off meds (SD)	UPDRS part 3 On meds (SD)	Percentage improvement UPDRS part 3 with L-dopa	UPDRS Part 4 Dyskinesia score (SD)	UPDRS Part 4 Off Score
PARK2 (N=6)	25.2 (12.8)	960 (611)	1.7 (2.0)	24.3 (4.0)	6 (6.2)	57.0 (11.2)	21.0 (6.4)	61.0 (18.3)	5.3 (3.9)	3.5 (1.3)
GBA (N=16)	11.2 (5.0)	1143 (540)	1.5 (1.5)	24.6 (11.3)	10.9 (12.3)	51.3 (14.0)	18.0 (15.4)	66.9 (18.6)	3.2 (2.7)	4.9 (1.9)
LRRK2 (N=5)	12.1 (1.8)	1317 (803)	1.3 (1.3)	26.8 (7.9)	4.5 (4.3)	65.4 (14.9)	10.8 (5.1)	84.9 (5.5)	3.5 (3.1)	4.8 (0.9)
No mutations found N=67	15.1 (5.5)	1280 (548)	2.0 (1.7)	22.7 (7.9)	8.0 (7.3)	47.4 (14.7)	15.6 (11.3)	68.5 (19.3)	3.2 (2.3)	4.5 (1.2)

4.3.5 Discussion

This study shows the usefulness of studying a cohort of cases undergoing DBS as a valuable resource for detecting genetic forms of PD. DBS is usually performed in patients with advanced PD that has been refractory to non-invasive therapies, and yet patients are also selected on the basis that they are still young enough to tolerate invasive neurosurgery. Therefore, it is not surprising that EOPD are over-represented in this cohort.

While some of the Mendelian forms of PD can present in later decades, it is indeed well established that, overall, mutations in most Mendelian genes tend to be associated with an earlier onset of symptoms (Alcalay *et al.*, 2010). This could explain in part why the frequency of PD genes mutation carriers is much higher in this cohort (27/94 patients; 29%), than in population representative cohorts of PD (Winder-Rhodes *et al.*, 2013). Although it is widely known that both *GBA* mutations (Sidransky *et al.*, 2009) and *LRRK2* mutations (Ozelius *et al.*, 2006) are more common in Jewish populations, this was not the reason for the high rate of gene positive subjects in our cohort.

While the use of DBS cohorts represents a clear advantage in terms of facilitating a rapid identification of gene positive patients, there are some biases to consider that may impact on the relevance of these data to the broader PD population. Patients with major cognitive, main psychiatric problems or lack of L-DOPA response are excluded during the selection process, and therefore this limits the ability to comment whether these features are more or less frequent according to mutational status. However, in this study it was therefore possible to explore the underlying PD phenotype and disease progression in patients undergoing with DBS with different genetic forms of PD, without the major bias of dopamine replacement. Patients were indeed routinely systematically evaluated On and Off medication as part of their DBS work-up, and thus it was possible to observe and evaluate their Off medication phenotype.

Apart from confirming the known *PARK2*-related feature of younger age at onset and earlier and more severe L-DOPA induced dyskinesias (Doherty *et al.*, 2013), any consistent phenotypic difference between carriers of mutations in different genes and gene negative cases were not identified *at a single time point*. This includes evaluating the relative distribution of tremor, akinesia/rigidity and axial features as well as the degree of L-DOPA responsiveness.

However, a number of interesting observations were made through analysis of the longitudinal data. Duration of disease at time of needing DBS surgery was significantly different between genetic subgroups. As mentioned, *PARK2* mutation carriers had an earlier age at onset of disease and earlier dyskinesias, however they also have a longer duration until requiring DBS, which indicates a more benign form of disease. As observed in this study, *PARK2* patients have been previously reported to respond well to DBS (Capecci *et al.*, 2004, Romito *et al.*, 2005, Lohmann *et al.*, 2008, Moro *et al.*, 2008), though these series restricted their reports to response to STN DBS. In this series the GPi target was favoured, given the greater severity of dyskinesias in *PARK2* cases.

Importantly, PD patients carrying *GBA* mutations needed DBS significantly earlier in their disease course than any other mutation group. At the time of needing DBS, *GBA* mutations carriers presented off-medication comparable clinical features to other groups, while with a significantly shorter duration of disease. This suggests a more aggressive form of the disease in PD patients with *GBA* mutations. This is in keeping with data obtained from an unselected population of PD cases from the UK showing that PD patients with *GBA* mutations have a faster rates of progression to major motor end-points (Hoehn and Yahr stage 3) in cases followed longitudinally (Winder-Rhodes *et al.*, 2013). At one-year follow-up, the response to both STN DBS and GPi DBS was not different between *GBA* patients and the other groups. However, longer follow up showed that patients undergoing STN DBS with *GBA* mutations may develop far greater cognitive impairment than any other group. This possibly suggests there may be an interaction between *GBA* status and risk of subsequent decline following DBS. Consistent with this observation, a previous report of three *GBA* patients undergoing STN DBS also identified a more aggressive process that lead to both cognitive impairment and axial impairments (Weiss *et al.*, 2012).

Patients with *LRRK2* mutations have been previously shown to have a good response to STN DBS (Schupbach *et al.*, 2007, Gomez-Esteban *et al.*, 2008, Breit *et al.*, 2010). Consistent with previous data, this study confirms that G2019S mutation carriers have indeed an excellent response to STN DBS, without risk of major cognitive decline. The particular suitability of *LRRK2* G2019S mutation carriers to DBS treatment may explain the surprisingly high frequency of the mutation in this cohort (~5%), compared to unselected PD case from the UK (~1%) (Healy *et al.*, 2008).

In conclusions, from a longitudinal perspective, differences in phenotype between carriers of mutations in different genes appear to clearly emerge. *PARK2* mutation carriers have a younger onset of disease and more severe dyskinesias, but overall a more indolent disease course. On the other hand, patients with *GBA* mutations have a more aggressive motor disease needing earlier intervention with therapies such as DBS and are likely to have more rapid cognitive impairment following STN DBS implantation.

4.4 Mutational Analysis of the GTP cyclohydrolase-1 Gene in Parkinson Disease

4.4.1 Statement of Contribution

I designed the research, performed the genetic analysis and collected the clinical information concerning the four pedigrees reported in the first section of the study, performed clinical assessment and DNA and RNA analysis in family 1, and analysed the whole-exome sequencing data, generated and provided by the International Parkinson Disease Genetic Consortium (IPDGC) and UCL-exomes. Dr Ioannis Isaias performed the analysis and quantification of the dopaminergic imaging data.

4.4.2 Background

GTP cyclohydrolase 1 (GTPCH), encoded by the *GCH1* gene (14q22.1-q22.2; OMIM 600225), is the enzyme controlling the first and rate-limiting step of the biosynthesis of tetrahydrobiopterin (BH_4), the essential cofactor for the activity of tyrosine hydroxylase, and for dopamine production in nigrostriatal cells (Kurian *et al.*, 2011).

Mutations in *GCH1* are the commonest cause of dopa-responsive dystonia (DRD) (Clot *et al.*, 2009), a disorder that presents typically in childhood with lower limb dystonia and subsequent generalisation (Nygaard, 1993). An excellent and sustained response to small doses of L-DOPA, generally without the occurrence of motor fluctuations generally observed in patients with PD, is the classic hallmark of the disease (Trender-Gerhard *et al.*, 2009).

The diagnosis of GTPCH-deficiency may be supported by low cerebrospinal fluid (CSF) levels of pterins, dopamine and serotonin metabolites (Assmann *et al.*, 2003) or by an abnormal phenylalanine-loading (PLT) (Bandmann *et al.*, 2003).

Inheritance is usually autosomal dominant with incomplete penetrance (Furukawa et al., 1998), though recessive cases have been described (Opladen *et al.*, 2011). Dominant *GCH1* mutations result in a significant reduction of GTPCH activity through a dominant negative effect of the mutant protein on the normal enzyme (Hwu *et al.*, 2000).

Neuropathological examination, in a limited number of DRD cases, revealed marked reduction of melanin pigment and dopamine content in nigrostriatal neurons, but no

evidence of nigral cell loss or degeneration (Furukawa *et al.*, 1999).

Parkinsonian features are common in patients with DRD (Tassin *et al.*, 2000) and carriers of *GCH1* mutations may develop adult-onset parkinsonism in absence of dystonia (Nygaard *et al.*, 1990). Based on previous studies, the prevailing hypothesis was that parkinsonism represented an atypical, age-specific, presentation of DRD without nigral degeneration (Nygaard and Wooten, 1998).

The aim of this work was to explore the relationship between *GCH1* mutations and parkinsonism and investigate whether adult *GCH1* mutation carriers are actually at increased risk of developing true *neurodegenerative* PD.

4.4.3 Subjects, Materials and Methods

Family Study

Pedigrees

DRD pedigrees were included in the study, where family members affected with adult-onset parkinsonism were available for clinical and genetic examination and in whom dopaminergic studies had been performed. Local ethics committees approved the study and informed consent for genetic testing was obtained in all cases.

Genetic Analysis

Probands were screened for *GCH1* mutations (NCBI transcript NM_000161.2) by standard bi-directional Sanger sequencing of all 6 coding exons and exon-intron boundaries. Dosage analysis for *GCH1* exonic deletions and duplications was performed by MLPA. Sanger sequencing and MLPA were performed as described in the Materials and Methods.

To test the effect of the splice-site variant c.343+5G>C identified in family-A, messenger RNA (mRNA) was extracted from peripheral blood of individuals II-1 and III-1 using the PAXgene Blood RNA System (Qiagen/PreAnalytix). Following RNA extraction, complementary DNA (cDNA) was synthesized using the Applied Biosystems High-Capacity cDNA reverse transcription kit. The *GCH1* transcript was amplified using exonic primers in exon 1 and exon 3 in both cases and two controls (supplementary Fig. 1A). Following separation by agarose gel electrophoresis, the mutant bands from the patient samples were extracted and sequenced.

Transcript PCR primers

GCH1_exonic_1F	GGGAGTGTGATCTAAGCAG
GCH1_exonic_3R	AAGTTTGCTGAGGCCAAGG

A SYBR Green PCR assay was designed to establish if the c.343+5G>C mutation caused retention of GCH1 intron 1. Two PCRs were employed, each using the same reverse primer in exon 3 (GCH1_rt_Exon3_R), and a forward primer in either intron 1 (GCH1_rt_Intron1_F) or exon 1 (GCH1_rt_Exon1_F).

rtPCR primers

GCH1_rt_Intron1_F	catgttactaaagcaagcctctga
GCH1_rt_Exon1_F	TCTTCACCAAGGGCTACCAG
GCH1_rt_Exon3_R	AAGTTTGCTGAGGCCAAGG

Real-Time PCR was performed on a RotorGene 6000, measuring product accumulation after each amplification cycle. All PCRs for the standard curves and samples were performed in triplicate, the results for sample replicates were averaged. Serial dilutions of control cDNAs were prepared for each PCR over a 27- 490 fold range. Standards and patient samples were amplified on the same experimental run. Rotor-Gene 6000 Series Software 1.7 was used to calculate the cycle threshold (Ct) at which exponential amplification was occurring in the PCRs and a standard curve was plotted for each PCR (log DNA concentration vs. Ct) from the serial dilutions. The relative concentration of each transcript was then calculated for all samples by interpolating from the standard curves. The ratio of immature/mutant transcript : Wild-Type transcript abundance was then derived for each sample.

Dopamine transporter imaging studies

Dopaminergic striatal innervation was evaluated as dopamine reuptake transporter (DAT) density by means of Single Photon Computed Tomography (SPECT) and [123I]N-ω-fluoropropyl-2β-carbomethoxy-3β-(4-iodophenyl) tropane ([123I]FP-CIT).

SPECT data acquisition and reconstruction has been described in details elsewhere (Isaias *et al.*, 2010). To obtain comparable measurements among different centers, [^{123}I]FP-CIT binding values for the caudate nucleus and putamen were calculated by means of the Basal Ganglia Matching Tool (Nobili *et al.*, 2013).

Whole-exome sequencing study

Participants and study design

The study initially involved 1337 unrelated subjects with PD and 1764 controls of European origin or North American of European descent that underwent whole-exome sequencing.

Patients, originating mainly from the USA, UK, Holland and France, were recruited by the IPDGC). A further 190 PD cases were recruited through a community-based epidemiological study of PD in Estonia (University of Tartu, Estonia).

Patients with PD were clinically diagnosed according to the UK Parkinson disease Society Brain Bank (UKPDSBB) criteria (Hughes *et al.*, 1992).

Control samples were collected by the UCL-exomes. Controls had no diagnosis of PD, DRD or any other movement disorder. Whole-exome sequencing data from additional 4300 North American individuals of European descent were analysed from the publicly available from the NHLBI Exome Sequencing Project Exome Variant Server (EVS) database.

Procedures

Whole exome-sequencing was performed as described in the Materials and Methods.

Statistical analysis

Frequencies of coding and splice-site *GCH1* variants in cases and controls were compared by means of Fisher's exact (statistical significance set at *P* value < 0.05 using a two-tailed test) and odds ratios (OR) and 95% confidence intervals (CI) were calculated. Analyses were performed using the statistical analysis program R (http://www.r-project.org/).

4.4.4 Results

Family study

<u>Family A</u>

The proband (III-1, Figure 4-1A) is a British 18-year-old man who had a difficult caesarean birth, with perinatal distress and subsequent developmental delay. At 18 months he developed inward turning of his feet with walking difficulties and frequent falls. He was diagnosed clinically with DRD at the age of 3 and administration of L-DOPA (300mg/day) markedly improved his symptoms. [123I]FP-CIT SPECT, performed at the age 17, was normal. The proband's father (II-1), who was initially thought to have cerebral palsy due to a birth injury, was subsequently diagnosed at age 42 with DRD. The proband's grandfather (I-1) is a 65 year-old man with a six-year history of progressive asymmetric rest tremor in the right upper limb. Examination showed signs of typical PD with hypomimia, unilateral rest tremor and asymmetric bradykinesia. He did not present signs of dystonia. [123I]FP-CIT SPECT showed bilateral reduced tracer uptake more marked on the left, consistent with nigrostriatal dopaminergic denervation. He responded well to L-DOPA therapy (300mg/day).
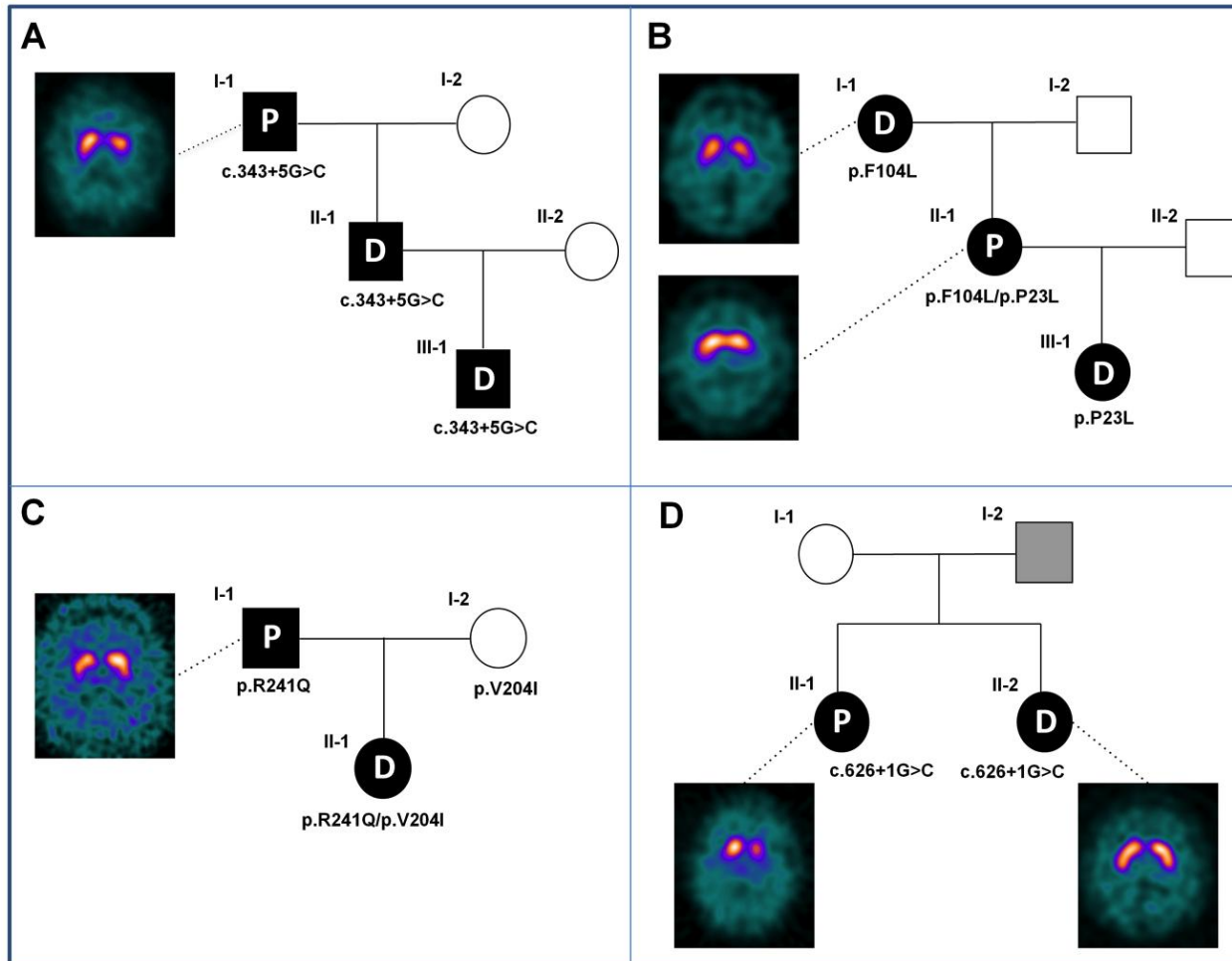
Figure 4-1 Pedigrees and [^{123}I]FP-CIT SPECT scan images of the four families with *GCH1* mutations involved in this study
P=Parkinson disease. D=DOPA-responsive dystonia

GCH1 analysis revealed a heterozygous splice site mutation (c.343+5G>C) in the three affected individuals. We previously detected c.343+5G>C in a recessive pedigree, carried by the unaffected mother of two very severely affected children who also inherited the K224R mutation from their unaffected father (Bandmann *et al.*, 1996, Trender-Gerhard *et al.*, 2009). However the c.343+5G>C mutation has not been previously described in DRD dominant pedigrees, making its pathogenicity uncertain.

To test the pathogenic effect of this variant on splicing, messenger RNA (mRNA) was extracted from peripheral blood of individuals II-1 and III-1 and the *GCH1* transcript was amplified using exonic primers in exon 1 and exon 3 in both cases and two controls (Figure 4-2A). Following separation by agarose gel electrophoresis, the mutant bands from the patient samples were extracted and sequenced. Sequencing of the upper mutant band (352 bp) revealed a mutant transcript whereby exon 2 is spliced to base c.50 of exon 1, splicing-out 293 bp of exon 1 that would be predicted to cause a premature truncation of the protein after 8 out-of-frame amino acids (Figure 4-2A and B). Sequencing of the second mutant transcript at ~200 bp failed.

The low intensity of the mutant bands in Figure 4-2A prompted us to consider other possible effects of this mutation. A SYBR Green PCR assay was designed to establish if the c.343+5G>C mutation caused retention of *GCH1* intron 1. As illustrated in figure 1, the Intron 1 – Exon 3 PCR captured any transcripts in which at least some splicing had occurred (exon 2 to exon 3), but in which intron 1 had not been spliced-out. This is referred to as 'immature/mutant transcript'. The ratio of the abundance of the transcripts was derived and indicates that the mutant/immature transcript is significantly more abundant relative to WT transcript in the patients than controls (Figure 4-2C), confirming that the c.343+5G>C mutation abolishes splicing of intron 1 and is therefore likely to lead to haploinsufficiency.
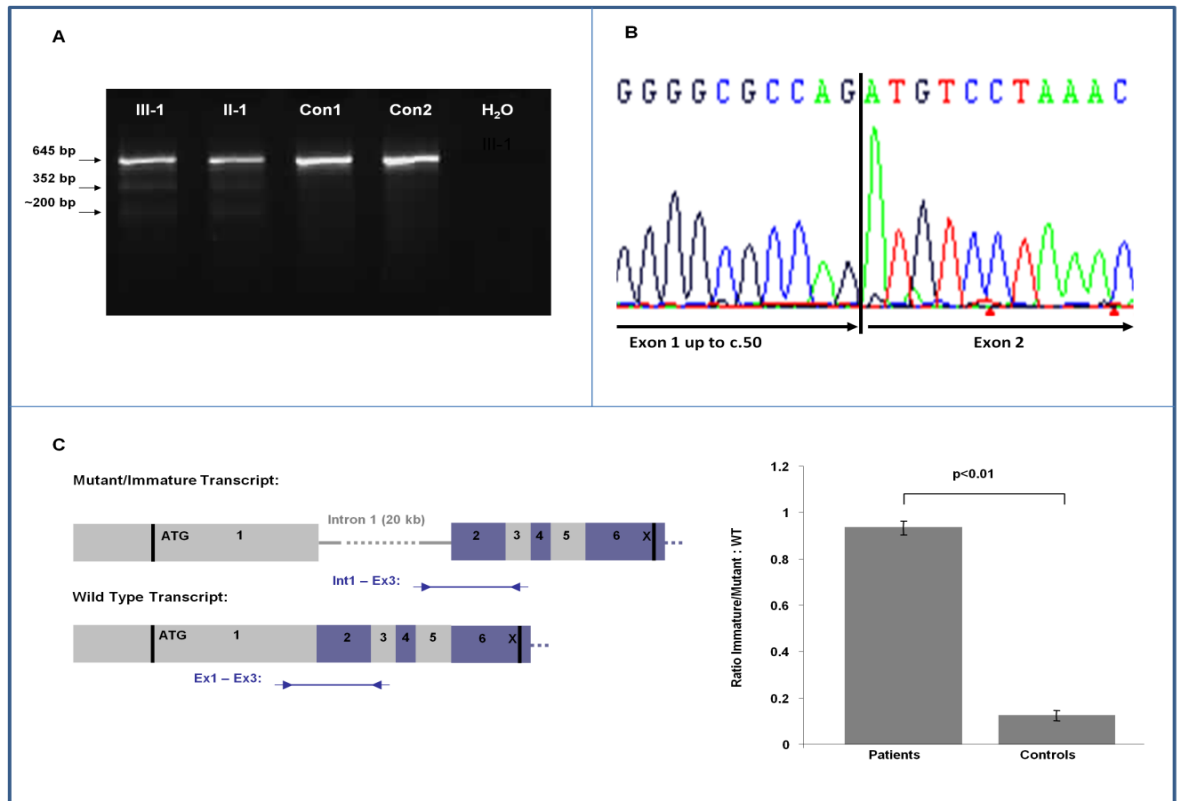
Figure 4-2 RNA analysis performed in family-A

A) Transcript PCR: PCR from GCH1 exon 1 to exon 3 revealed additional bands in the patients carrying the c.343+5G>C mutation compared to controls (Con1 and Con2) at 352 bp and ~200 bp. (B) Mutant Transcript Sequencing: Sequencing electropherogram screenshot showing mutant *GCH1* transcript from patient III-1 whereby exon 2 is aberrantly spliced to c.50 of exon 1. If translated, this would result in 16 in-frame amino acids, followed by 8 out-of-frame amino acids before a premature stop codon. (C) Intron 1 Retention: Two *GCH1* cDNA PCRs each used a common reverse primer in exon 3 and a forward primer either in intron 1 (to detected incompletely-spliced or mutant transcript) or exon 1 (to detect wild-type (WT) transcript). Transcripts are shown with exons 1 to 6 alternately shaded and numbered, the translational start (ATG) and stop (X) sites are indicated with vertical lines. Each SYBR Green PCR was performed on cDNA from patients II-1 and III-1 (two independent extractions from each) and 6 controls. The ratio of the abundance of the transcripts was derived and indicates that the mutant/immature transcript is significantly more abundant relative to WT transcript in the patients than controls (Mean +/- SE; Student's t-test).

<u>Family B</u>

The proband (III-1; Figure 4-1B) is a 12-year-old right-handed female of German origin with DRD, with an onset at age 11 with writing and foot dystonia. Her mother (II-1) presented at age 39 with progressive loss of dexterity and slowness in her right arm and dystonic posturing of the right foot. Examination showed an asymmetric rigid-akinetic parkinsonian syndrome without tremor and severe right foot fixed dystonia. L-DOPA therapy resulted in marked improvement of both dystonic and parkinsonian symptoms. $[^{123}I]$FP-CIT SPECT revealed an asymmetric bilateral reduced tracer uptake, more marked in the left striatum. There was sustained response to L-DOPA therapy although there was an increase in dose requirement (up to 800mg/day). L-DOPA -induced dyskinesias developed 6 years after initiation of L-DOPA. Examination of the proband's 66-year-old grandmother (I-1) revealed oromandibular dyskinesias and upper limb dystonic features. She declined a trial of L-DOPA. Her $[^{123}I]$FP-CIT SPECT displayed border-line reduced DAT values in both putamens.

GCH1 screening in this family revealed two variants: c.68C>T; p.Pro23Leu (carried by III-1 and II-1) and c.312C>A;p.Phe104Leu (carried by II-1 and I-1). There were no *GCH1* exonic rearrangements. F104L is absent in public control datasets and has been previously reported in association with DRD (Clot *et al.*, 2009). p.Pro23Leu (rs41298432) is a benign polymorphism present in population controls at a frequency of 1-2% (Jarman *et al.*, 1997, Hauf *et al.*, 2000).

To confirm GTPCH deficiency, PLT (100 mg/kg) was performed in individuals I-I and II-I and showed pathologically elevated phenylalanine/tyrosine ratios in both cases (Figure 4-3). CSF analysis, performed in individual III-I, displayed low levels of BH_4 (13 nmol/l; 18-53 nmol/l) and neopterin (6nmol/l; 10-31 nmol/l), consistent with GTPCH deficiency. Given the benign nature of p.Pro23Leu, we hypothesize that the GTPCH deficiency confirmed in this patient may be the result of an as yet unidentified non-coding causative mutation.
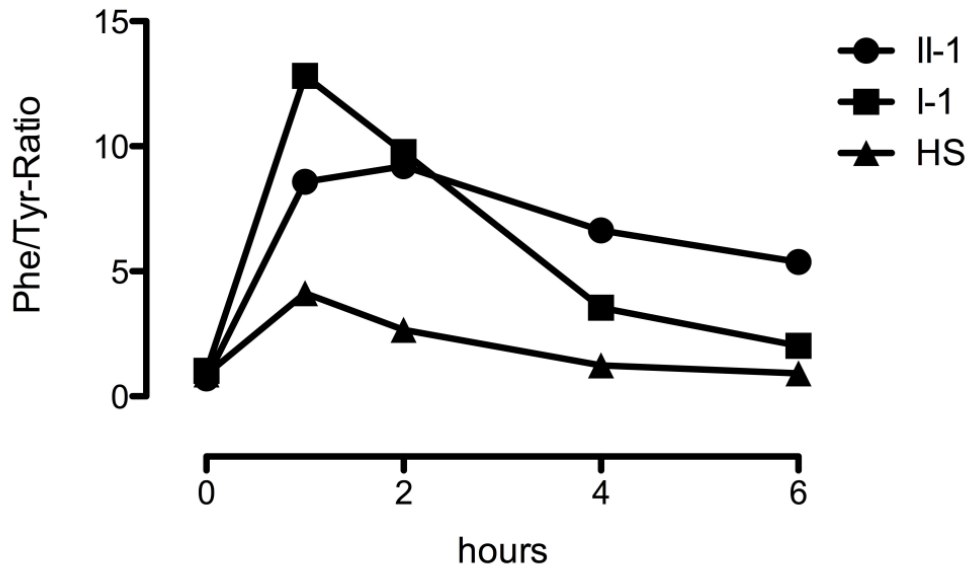
Figure 4-3 Phenylalanine-loading test performed in family B
Abnormally elevated ratios of phenylalanine (Phe) and tyrosine (Tyr) plasma levels at 1, 2, 4, and 6 hours after oral loading with phenylalanine (100mg/kg) in individual I-1 (c.312C>A;p.Phe104Leu), II-1 (c.68C>T;p.Pro23Leu and c.312C>A;p.Phe104Leu) of family B compared to healthy subjects (HS).

<u>Family C</u>

The proband (II-1, Figure 4-1C) is a German 41-year-old lady, affected by DRD, who presented at age four with bilateral foot inversion on walking. Her father (I-1) is a 67-year old man with a one-year history of typical PD with left hand rest tremor, bilateral rigidity and bradykinesia and mild gait difficulties. There was no dystonia. [^{123}I]FP-CIT SPECT examination revealed asymmetrically reduced DAT-density in the striatum. Rasagiline and pramipexole were started with good response. The mother (I-2), aged 62, had a normal neurological examination.

The proband was compound heterozygous for two *GCH1* missense variants, c.610G>A; p.Val204Ile, inherited from the asymptomatic mother, and the novel variant c.722G>A; p.Arg241Gln, which was paternally inherited. p.Arg241Gln is absent in all public control datasets, is predicted deleterious by all *in silico* prediction tools and involves an amino acid residue conserved down to invertebrate species. Furthermore a pathogenic mutation at the same residue has already been reported (Bandmann *et al.*, 1998).

CSF analysis in the parkinsonian case supported a pathogenic effect of the p.Arg241Gln mutation on GTPCH activity: pterin analysis revealed low BH_4 (8 nmol/L; 18-53), but

normal neopterin (24 nmol/L; 10-31); neurotransmitter analysis showed low homovanillic acid (95 nmol/L; 115-455) and 5-hydroxyindolacetic acid (59 nmol/L; 61-204), which are metabolites of dopamine and serotonin respectively.

Family D

The proband is an Italian 58-year-old lady (II-1, Figure 4-1D), who developed progressive tremor and clumsiness in the right arm at age 44. Clinical examination showed typical PD with hypomimia, hypophonia and asymmetrical bradykinesia and rigidity. Action dystonic tremor (right>left), poor postural reflexes and slow gait were also evident and there was a sustained response to L-DOPA. The dose was gradually increased up to 400 mg/day after which rotigotine 4 mg/day was added. Dyskinesias and wearing-off symptoms developed 6 years after L-DOPA initiation. [123 I]FP-CIT SPECT revealed asymmetrically reduced DAT binding values in the striatum.

Her sister (II-2; Figure 4-1D), aged 60, had a childhood onset of mild walking difficulties. At age 55, she developed exercise-induced left foot dystonia and dystonic tremor in both arms. She had no bradykinesia or other parkinsonian signs. Low-dose L-DOPA (100mg alternate days) was started with excellent symptom control. [123I]FP-CIT SPECT was normal. Their father was reported to have a tremulous condition but was not available for clinical or genetic examination. *GCH1* sequencing revealed that both sisters were heterozygous for the previously reported pathogenic mutation c.626+1G>C (Garavaglia *et al.*, 2004).

The structure of the four pedigrees is shown in Figure 4-1. DAT binding values are reported in Table 4-4.. The main clinical features of the *GCH1* mutation carriers with adult-onset parkinsonism and abnormal [123I] FP-CIT SPECT imaging are summarized in Table 4-5. Their clinical features fully met the UKPDSBB criteria for definite PD diagnosis. None of these cases presented significant diurnal fluctuations, worsening of symptoms in the evening or substantial sleep benefit, features often recognised in DRD cases (Kurian *et al.*, 2011).

Table 4-4 DAT binding values of *GCH1* mutation carriers evaluated in this study

Subject	Phenotype	L-putamen	R-putamen	L-caudatus	R-caudatus
Family A/ I-1	PD	2.08 [b]	2.74 [a]	3.51	4.28
Family B/ II-1	PD	2.63 [b]	3.73 [a]	4.72	4.94
Family B/ I-1	DRD	2.85 [a]	2.96 [a]	3.95	3.95
Family C/ I-1	PD	1.86 [b]	1.64 [b]	2.52 [b]	2.19 [b]
Family D/ II-1	PD	1.53 [b]	2.63 [b]	3.29 [a]	4.5
Family D/ II-2	DRD	5.38	5.27	5.71	5.82

Values are expressed as the ratio of [^{123}I]FP-CIT specific uptake in the region of interest/background. [^{123}I]FP-CIT binding values for the caudate nucleus and putamen were calculated by means of the Basal Ganglia Matching Tool.
[a] Value below 97% inferior confidence limit of healthy controls
[b] Value below 90% inferior confidence limit of healthy control

Table 4-5 Characteristics of PD cases with *GCH1* pathogenic variants and abnormal dopaminergic imaging described in this study and present in the literature

Origin	Sex/Age at scan/Age at onset (y)	Mutation	Relatives with DRD	Age at L-DOPA start (y)	Current treatment dose (mg/day)	Parkinsonian features	Dystonic features	L-DOPA-induced complications	Scan Result	Reference
UK	M/65/59	c.343+5G>C/w	Son and grandson	60	L-dopa 300	Hypomimia, R hand rest and re-emergent postural tremor, and bilateral rigidity and bradykinesia (R>L)	No	No	Bilateral (L>R) reduced DAT density	Present study (Family A)
Germany	F/47/39	p.Phe104Leu/ p.Pro23Leu	Daughter, mother (?)	41	L-dopa 800	Hypomimia, bilateral rigidity, bradykinesia, reduced arm swinging (R>L), and mild gait difficulties	R foot dystonia	Dyskinesias after 6 y of therapy	Bilateral (L>R) reduced DAT density	Present study (Family B)
Germany	M/67/66	p.Arg241Gln/w	Daughter	/	Rasagiline 1 Pramipexole 0.375	Hypomimia, L hand rest tremor, bilateral bradykinesia and rigidity (L>R), and mild gait difficulties	No	No	Bilateral (R>L) reduced DAT-density	Present study (Family C)
Italy	F/58/44	c.626+1G>C/w	Sister	53	L-dopa 400 Rotigotine 4	Hypomimia, bilateral rigidity and bradykinesia (R>L), mild postural instability, and gait difficulties	Bilateral (R>L) upper limb dystonic tremor	Dyskinesias after 6 y of therapy	Bilateral (L>R) reduced DAT density	Present study (Family D)
Japan	M/54/39	p.Arg184His/w	No	40	L-dopa 600	Cogwheel rigidity, akinesia, and postural instability	Dystonic posture in the four limbs (R>L)	Wearing-off and dyskinesias after 10 y of therapy	Bilateral reduced FD intake	Kikuchi et al.

Denmark	M/38/28	p.Pro199Ser/w	Brother	33	L-dopa 350 Entacapone Selegiline 5	Bradykinesia and rigidity in the L arm	Dystonia of neck, trunk and four limbs, action tremor (L>R)	Dyskinesias after 2 y of therapy	Bilateral (R>L) reduced DAT density	Hjermind et al.
Germany	F/65/50	Complete deletion of the *GCH1* gene/w	Daughter	60 (for 10 y on dopamine agonist only)	L-dopa 200 Selegiline 5	Tremor in the R hand, reduced dexterity and mild gait disturbance	No	No	Bilateral (L>R) reduced DAT density	Eggers et al.
Italy	M/59/NA	Deletion of exons 5-6/w	Son with DRD, sister with MSA	NA	NA	Hypomimia, L hand rest tremor. bradykinesia (L>R), mild gait difficulties	No	Dyskinesias after 10 y of therapy	Bilateral reduced DAT density	Ceravolo et al.

NA=not available; DRD=dopa-responsive dystonia; H&Y=Hoehn and Yahr; F=female; M=male L=left; R=right; MSA=multiple-system atrophy; y=years; w=wild-type.

Whole-exome sequencing study

To investigate if pathogenic variants in *GCH1* could be found in PD subjects without a family history for DRD, I analysed whole-exome sequencing data of a large cohort of patients predominantly affected by early-onset or familial PD and controls.

After quality control checks (removal of gender mismatches, duplicate, related and non-Caucasian samples, samples with low call rate or excess of heterozygosity), 1318 PD cases and 1635 controls remained. Additional control data (n = 4300) were obtained from the publically available EVS dataset.

In total 1318 cases and 5935 controls were analysed for the presence of *GCH1* coding (including small insertions/deletions, missense and stop-gain changes) or splice-site variants (± 5 base pairs from the coding exons).

The mean age of subjects with PD was 55.7 ± 13.9 years (range 17-101; data available for 970 cases) and the mean age at onset was 46.7 ± 13.8 years (range 6-98; data available for 1194 cases). 423/1194 (35.4%) were early-onset cases (age at onset ≤ 40 years) and ~630 were familial cases (positive family history for PD in a first or second degree relative).

Coverage of the six *GCH1* coding exons (NCBI transcript NM_000161.2) was similar in the three datasets as shown in Table 4-6.

Coverage of exon 1 was sub-optimal, being the average read depth only 12 in the IPDGC data, 17.9 in the UCL-ex data and 6 in the EVS data. Visual inspections of aligned reads of IPDGC and UCL-ex data (BAM files opened with Genome Browse software, Golden Helix) revealed that the first ~150 coding nucleotides of exon 1 were barely covered (average depth 1-2 reads) in the majority of samples. Similar coverage data were evident for the EVS data (Figure 4-4). The coverage of the rest of the exon was good (read depth ≥ 8). No common variants (frequency >1%) were identified. The benign polymorphisms p.Pro23Leu (rs41298432) and p.Pro69Leu (rs56127440), detected at similar frequencies in cases and controls, were not included in the analysis.

Table 4-6 Average exome sequencing coverage of the six *GCH1* exons.

Exon	Genomic coordinates	IPDGC (n=1318)	UCL-ex (n=1645)	EVS (n=4300)
1	chr14:55369016-55369405	12 (65.4%)	18 (61.8%)	6 (59.1%)
2	chr14:55332045-55332154	89 (99.6%)	48 (87.4%)	98 (99.7%)
3	chr14:55326326-55326528	58 (99.6%)	45 (97.1%)	85 (86.3%)
4	chr14:55313798-55313934	14 (81.8%)	35 (77.3%)	20 (83.3%)
5	chr14:55312427-55312630	94 (100%)	114 (98.9%)	93 (95%)
6	chr14:55310683-55310913	53 (99.2%)	22 (80%)	133 (99.5%)

IPDGC=International PDGenetic Consortium; UCL-ex= University College of London exomes consortium; EVS= NHLBI Exome Variant Server; chr=chromosome

Data are expressed as the average read depth per region of interest. In brackets is the percentage of samples that had a read depth ≥8 reads.
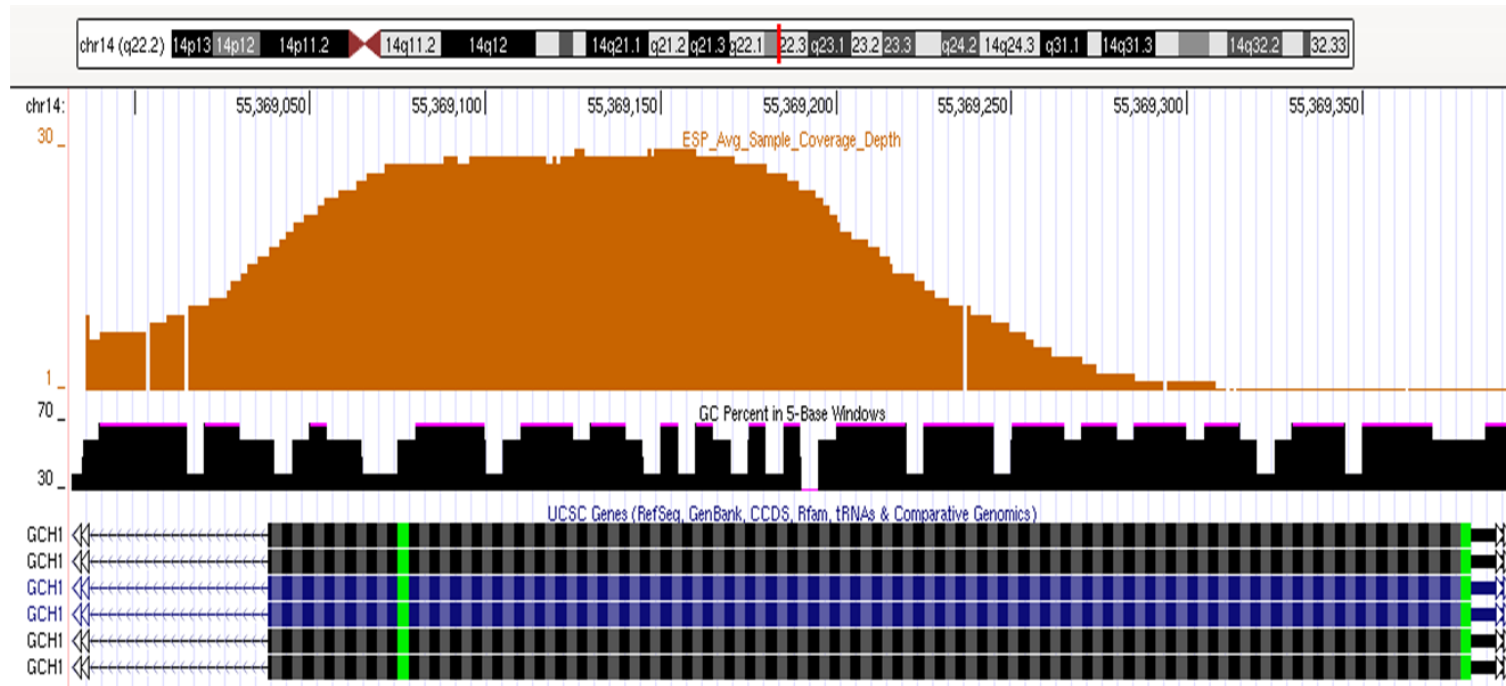
Figure 4-4 Visual representation of coverage depth for *GCH1* exon 1

NHLBI exome variant server sample average coverage depth, showing significantly reduced coverage is evident at the 5' end of the exon, most likely due to the high GC content (greater than 70%)

The main results of the *GCH1* analysis are summarized in Table 4-7.

Combining cases and controls, 11 unique heterozygous *GCH1* variants (ten missense and one stop-gain mutation) were identified in 16 individuals. Six variants were found only in PD cases (p.Gln110*, p.Gln110Glu, p.Ala120Ser, p.Asp134Gly, p.Gly217Val and p.Met230Ile), three in controls alone (p.Thr112Ala, p.Ile154Val and p.Arg198Gln) and two were detected in both groups (p.Val204Ile, p.Lys224Arg).

The frequency of *GCH1* variants was significantly higher in PD cases (10/1318; 0.75%) than in individual (UCL-ex controls 1/1635; 0.06%; P = 0.003; OR 12.4 95% CI 1.7-541.1; EVS database 5/4300; 0.11%; P = 0.0004; OR 6.5, 95% CI 2.0-24.5) and combined datasets of controls (6/5935; 0.1%; P = 0.0001; OR 7.5, 95% CI 2.4-25.3).

All carriers of variants in *GCH1* were negative for pathogenic mutations in all known genes associated with Mendelian forms of parkinsonism. The presence of copy number variants in the *SNCA*, *PARK2*, *PARK7*, and *PINK1* genes was excluded by MLPA in all cases. One case carried the *GBA* mutation E326K.

The main features of the ten PD cases with pathogenic or possibly pathogenic *GCH1* variants are listed Table 4-8. The age at onset of *GCH1*-mutated cases was 43.2 ± 13.4 years (range 17-61). Seven had a positive family history of PD. DNA of other family members was available for only one case and we showed segregation of the same *GCH1* mutation (p.Gln110*) in the affected sister of the index case. All cases exhibited a variable combination of asymmetrical bradykinesia, rigidity, rest and postural tremor, walking difficulties, postural instability and excellent response to dopaminergic treatment, consistent with a clinical diagnosis of PD (Lees *et al.*, 2009).

The two subjects with the youngest age at onset of symptoms (case 4 and 9, who developed symptoms at age 32 and 17 respectively) presented with dystonic features in the lower limbs at onset, a well-recognised characteristic of young-onset PD cases (Bozi and Bhatia, 2003). One case (case 5) developed lower limb dystonia in off periods over the course of the disease. The remainder did not present with any symptoms or signs of dystonia.

Detailed information about treatment was available for eight cases: the two cases (case 1 and 7) with the shortest disease duration (≤ 5 years) were treated only with a

dopamine-agonist, whereas the other cases were taking a combination of L-DOPA and other anti-parkinsonian drugs.

Mean disease duration was 17.6 ± 15.4 years (range 4-56). Patients with longer disease duration displayed a more severe clinical picture with some degree of postural instability (Hoehn and Yahr score ≥ 3), indicating disease progression in spite of the dopaminergic treatment.

In those patients taking L-DOPA and for whom follow up information was available (*n* = 7), all developed clinically relevant motor complications of chronic L-DOPA treatment, including wearing off, motor fluctuations and dyskinesias. Dyskinesias in case 4 were so disabling that he required treatment with deep brain stimulation of the subthalamic nuclei at age 60.

Most cases exhibited some of the typical non-motor features often recognised in PD, such as cognitive difficulties (case 5), hyposmia (case 3, 4, 5, 6 and 10) constipation (case 4 and 10), urinary problems (case 5, 6 and 9), fatigue (case 2 and 5) and sleep disturbances (case 4, 5, 6 and 10).

Mutation	Exon	dbSNP	Prediction score[b]	Previously described in DRD?	PD patients (n=1318)	UCL-ex controls (n=1635)	OR (95% CI)	p-value	EVS controls (n=4300)	OR (95% CI)	p-value	Total controls (n=5935)	OR (95% CI)	p-value
All variants					10 (0.75%)	1 (0.06%)	12.4 (1.7-541.1)	0.003	5 (0.11%)	6.5 (2.0-24.5)	0.0004	6 (0.1%)	7.5 (2.4-25.3)	0.0001
c.328C>T; p.Gln110*	1		NA	Yes, in dominant and recessive pedigrees	1	0			0			0		
c.328C>G; p.Gln110Glu	1		2	No	1	0			0			0		
c.334A>G; p.Thr112Ala	2	rs199990434	2	No	0	0			1			1		
c.358G>T; p.Ala120Ser	2		4	No	1	0			0			0		
c.401A>G; p.Asp134Gly	2		4	No	1	0			0			0		
c.460A>G; p.Ile154Val	3		2	No	0	1			0			1		
c.593G>A; p.Arg198Gln	5	rs201238926	0	No	0	0			1			1		
c.610G>A; p.Val204Ile	5	rs200891969	4	Yes, in sporadic and recessive cases	3	0			1			1		
c.650G>T; p.Gly217Val	6		4	No	1	0			0			0		

c.671A>G; p.Lys224Arg	6	rs4129 8442	2	Yes, in dominant and recessive pedigrees	1	0	2	2
c.690G>A; p.Met230Ile	6		4	Yes, in a sporadic case	1	0	0	0

NA=not applicable; DRD=dopa-responsive dystonia; PD=Parkinson disease; UCL-ex= University College of London exomes consortium; EVS=Exome Variant Server; OR=odds ratio; CI=confidence intervals. *p*-values were calculated by means of Fisher's exact test

[a] NCBI transcript NM_000161.2. This count includes all detected coding and splice-site variants at any frequency, but the two benign variants P23L and P69L

[b] This score, ranging from 0 to 4, indicates the number of tools (Polyphen-2, SIFT, LRT and Mutation Taster) predicting a pathogenic effect on the protein function

Table 4-8 Clinical features of PD cases with GCH1 variants identified in the exome-sequencing study

Case	Sex/Age / Age at onset (y)	*GCH1* mutation	Family history of PD	Age at L-dopa start (y)	Current treatment (mg/day)	Parkinsonian features	H&Y score	Cognitive symptoms	Other non-motor features	Dystonia	Levodopa-induced complications
1	F/47/43	p.Met230Ile	No	/	Pramipexole 0.75	Asymmetric onset, bilateral involvement with rest and postural tremor, bradykinesia and rigidity, mild gait difficulties	2	No	No	No	No
2	M/55/37	p.Lys224Arg	Yes (father)	NA	NA	Asymmetric onset, moderate bilateral involvement with rest tremor, bradykinesia and rigidity, postural instability and gait difficulties	3	No	Fatigue	No	Dyskinesias and wearing-off
3	M/49/35	p.Gly217Val	No	43	L-dopa 600, Tolcapone 400, Pramipexole 3.15	Asymmetric onset, slurred speech, mild L arm rest and postural tremor, moderate bilateral bradykinesia and rigidity, postural instability	3	Subjective loss of memory (MMSE 29/30)	Hyposmia, ICD	No	Initial dyskinesias and wearing-off
4	M/63/32	p.Val204Ile	Yes (1st degree cousin)	36	DBS, L-dopa 200 Amantadine 100 Rotigotine 8	Asymmetric onset, hypomimia, slurred speech, hypophonia, marked bilateral rest and postural tremor, moderate bilateral rigidity and bradykinesia, postural instability	4	No	Hyposmia, constipation, RBD	Right foot exercise-induced dystonia at onset	Disabling dyskinesias and on-off fluctuations
5	M/75/61	p.Val204Ile	Yes (mother)	61	L-dopa 400, Pramipexole 3.15	Asymmetric onset, rest and postural tremor (R>L), bradykinesia and rigidity, mild gait disorder, hypomimia	3	Mild cognitive impairment	Hyposmia, fatigue, sleep and bladder disorder	Lower limb off-dystonia	On-off fluctuations (30% of waking day in off-state)
6	M/72/59	p.Val204Ile	Yes (mother)	65	L-dopa 600 Entacapone 800	Asymmetric onset, bilateral bradykinesia and rigidity (L>R), no tremor. Mild gait difficulties and postural instability	3	No	Hyposmia, sleep and bladder disorder	No	Dyskinesias (30-40% of waking day), wearing-off

7	M/57/52	p.Asp134Gly	Yes (father and paternal aunt)	/	Ropinirole 14	Asymmetric onset, unilateral left arm rest tremor, bradykinesia and rigidity. Reduced arm swing	1	No	NA	No	No
8	F/59/51	p.Ala120Ser[a]	Yes (mother)	NA	NA	Asymmetric onset, bilateral bradykinesia and rigidity. No tremor. Mild gait difficulties	2	No	NA	No	NA
9	F/73/17	p.Gln110X*	Yes (sister; father had tremor)	49	L-dopa 600 Trihexyphenidyl 6	Bilateral rest and postural tremor (L>R), bilateral rigidity and bradykinesia. Some postural instability	3	No	Urinary urgency	Lower limb dystonia at onset	Marked limb and truncal dyskinesias, off phases in the morning
10	M/58/45	p.Gln110Glu	No	55	L-dopa 400 Entacapone 800 Rasagiline 1 Amantadine 300	Bilateral severe bradykinesia and rigidity, postural instability, mild tremor, hypomimia	3	No	Hyposmia, constipation, fatigue, sleep disorder	No	Mild dyskinesias and wearing-off

NA=information not available; M=male; F=female; PD=Parkinson disease, y=years, ICD=Impulse control disorder, DBS=deep brain stimulation, RBD=REM behavioural sleep disorder, H&Y=Hoehn and Yahr. [a]This case also carries in the heterozygous state the *GBA* E326K variant

4.4.5 Discussion

Family study

I report here four unrelated DRD pedigrees in which loss-of-function *GCH1* mutations (two splice-site mutations and two missense mutations, confirmed to be pathogenic by metabolic or CSF studies) were found in individuals, asymptomatic for DRD during childhood, who developed adult-onset parkinsonism. They all met the UKPDSBB clinical criteria for a definite diagnosis of PD and had imaging evidence of a PD-like nigrostriatal dopaminergic denervation.

A parkinsonian syndrome in the absence of dystonia has been reported in adults who are first-degree relatives of children with DRD. In a series of 21 families, Nygaard showed that 7/50 (14%) individuals older than 40 years had parkinsonism (Nygaard, 1993) and Hagenah and colleagues reported that 8/23 (34.7%) patients of their series had a positive family history for PD (Hagenah *et al.*, 2005). *GCH1* mutations have also been shown to segregate in pedigrees with multiple individuals affected by isolated parkinsonism (Irie *et al.*, 2011).

This study provides evidence that in most of the cases the parkinsonian phenotype in adult *GCH1* mutation carriers is likely due to nigrostriatal degeneration, rather than being part of the phenotypic spectrum of metabolic GTPCH-related striatal dopamine deficiency. This is consistent with other previous isolated reports of adult-onset parkinsonism in *GCH1* mutation carriers with abnormal nigrostriatal imaging (features summarized in table 1) (Kikuchi *et al.*, 2004, Hjermind *et al.*, 2006, Eggers *et al.*, 2012, Ceravolo *et al.*, 2013).

Our imaging findings are however in apparent contrast to a previous report by Nygaard and colleagues (Nygaard *et al.*, 1992). The authors described a large DRD pedigree, in which three subjects had a late-onset benign parkinsonism, two of which had normal nigrostriatal dopaminergic function determined by means of ^{18}F-fluorodopa (FD) PET.

Compensatory mechanisms at the presynaptic level (e.g. increased dopamine-intake and dopamine-decarboxylation activity) may result in relatively higher striatal FD uptake in the initial phase of PD, underestimating the degree of nigral cell decrease (Nandhagopal *et al.*, 2011). DAT values are therefore a more precise indicator of dopaminergic innervation loss (Ito *et al.*, 1999). I speculate that *GCH1*-parkinsonian cases with

normal FD-PET scan could have up-regulated compensatory dopaminergic activity at the presynaptic level, possibly masking the presence of striatal denervation.

In agreement with these findings, Gibb and Lees reported a case that presented with juvenile-onset parkinsonism and dystonia with good response to L-DOPA (commenced at the age of 30) and occurrence of disabling dyskinesias after one year of treatment. The patient died at 39 years and pathological examination showed a striking combination of low melanin content in nigral neurons and devastating neuronal loss with reactive gliosis. Furthermore, LBs were found in surviving nigral cells and in the locus coeruleus (Gibb *et al.*, 1991). This case was subsequently demonstrated to be carrier of a heterozygous mutation in *GCH1* (c.276delC) (Segawa *et al.*, 2004).

Whole-exome sequencing study

I subsequently showed, in a large cohort of PD patients without family history of DRD, that rare *GCH1* coding variants are associated with PD and increase the disease risk by seven-fold on average.

Among the *GCH1* variants identified by exome sequencing, two (p.Gln110* and Lys224Arg) have been shown to cause GTPCH deficiency and DRD in dominant pedigrees (Leuzzi *et al.*, 2002, Saunders-Pullman *et al.*, 2004) and two (p.Val204Ile and p.Met230Ile) have been reported in heterozygous sporadic or in recessive cases with DRD (Segawa *et al.*, 2004, Trender-Gerhard *et al.*, 2009, Opladen *et al.*, 2011).

The other heterozygous variants identified in this study could not be functionally investigated (e.g. PLT or CSF analysis), therefore their effect on GTPCH activity remains undetermined. However, three of the four novel variants (p.Ala120Ser, p.Asp134Gly and p.Gly217Val) detected in PD cases were located at amino acid positions that are fully conserved through species down to invertebrates and were predicted to be pathogenic by all *in silico* prediction tools, whereas this was not the case for any of the novel mutations present in controls.

Nevertheless, the limitations of prediction tools in reliably distinguishing benign from pathogenic missense changes are well known and therefore we did not exclude any variant from the association test based on predictions scores, possibly underestimating the effect size of *GCH1* pathogenic variants.

The p.Pro23Leu (rs41298432) and p.Pro69Leu (rs56127440) variants were excluded from the exome sequencing analysis as several data argue against their pathogenic role.

p.Pro23Leu has been reported in population controls at a frequency of 1-2% (Jarman *et al.*, 1997, Hauf *et al.*, 2000), it affects a non-conserved amino acid residue and functional studies have shown that it does not affect *GCH1* enzymatic activity (Furukawa *et al.*, 1999). It was also shown not to segregate with the clinical phenotype in a large dominant dystonia kindred and GTPCH deficiency was excluded in affected carriers by CSF analysis (Hauf *et al.*, 2000). In this study it was detected in only 1/1318 (0.07%) cases and 4/5915 controls (0.06%; difference not significant), due to very poor sequencing coverage of the first part of exon 1.

The p.Pro69Leu variant, despite its relatively high frequency in the general population, has been described only in two published DRD cases; Clot et al. detected it in the heterozygous state in a sporadic case, but in the same study it was also found at a similar frequency in controls (Clot *et al.*, 2009); it was also found in an apparently recessive pedigree, in trans with a pathogenic frameshift mutation, but the phenotype of the carriers was not as severe as usually reported in recessive GTPCH deficient cases (Furukawa *et al.*, 2004). In this study it was detected in 3/1318 (0.22%) cases and 10/5935 controls (0.17%; difference not significant). Among the three cases identified in this study with p.Pro69Leu, two had a positive family history for PD. Segregation analysis was performed in one pedigree for which DNA of multiple affected members was available. The mutation did not segregate with the clinical phenotype and no carriers presented features of DRD.

Previous studies investigating the contribution of rare coding *GCH1* variants in small cohorts of PD cases have reported negative results although these were insufficiently powered to draw conclusions (Bandmann *et al.*, 1996, Hertz *et al.*, 2006, Cobb *et al.*, 2009).

The association between *GCH1* variants and PD is further strengthened by the recent identification, through the meta-analysis of GWAS data deriving from approximately 13,000 cases and 95,000 controls, that *GCH1* is also a low-risk susceptibility locus for PD (Nalls *et al.*, 2014). This finding potentially extends the role of GTPCH deficiency in the pathogenesis of PD beyond carriers of rare deleterious coding mutations.

The mechanism whereby *GCH1* mutations could predispose to nigral cell degeneration is a matter of speculation. Biochemical evidence of GTPCH deficiency and reduced dopamine production has been reported in asymptomatic carriers of *GCH1* mutations (Takahashi *et al.*, 1994, Furukawa *et al.*, 2004). It is therefore possible that GTPCH deficiency and the consequent chronic dopamine deficiency could directly predispose to nigral cell death. This would suggest that normal levels of dopamine exert a protective role on the survival of nigral neurons. There is increasing evidence that L-DOPA is not toxic to nigral neurons as was previously thought (Parkkinen *et al.*, 2011). Furthermore, activation of dopamine receptors may have a strong antiapoptotic effect and increase survival of dopaminergic neurons (Nair *et al.*, 2003, Vaarmann *et al.*, 2013) (Nair *et al.*, 2003, Vaarmann *et al.*, 2013). In animal models, L-DOPA has been shown to promote recovery of nigrostriatal denervation (Datla *et al.*, 2001).

Another possibility is that *GCH1* mutation carriers who do not develop symptoms of DRD in childhood may have compensatory mechanisms that allow for normal nigrostriatal dopaminergic transmission. The maintenance of these mechanisms may increase nigral cell vulnerability to aging or other environmental and genetic factors, favouring degeneration.

It is also possible that the reduced striatal basal dopamine levels found in *GCH1* mutation carriers may simply lower the threshold of nigral cell loss before parkinsonian symptoms are exhibited.

Lastly, we cannot exclude that other yet unrecognized cellular pathways, not related to dopamine synthesis, may be disrupted by GTPCH and BH_4 deficiency.

With this regard, Ryan and colleagues have recently proposed that different cellular mechanisms secondary to BH_4 deficiency, other than reduced dopamine levels, could be contributing to the death of nigral dopaminergic neurons (Ryan *et al.*, 2015). BH_4 acts as an antioxidant itself (Milstien and Katusic, 1999) and is an essential cofactor for nitric oxide synthases (NOS) activity (Crabtree *et al.*, 2009). Furthermore decreased BH_4 levels have been demonstrated to lead to NOS uncoupling which results in increased oxidative and nitrative stress (Chen *et al.*, 2014). In addition to these mechanisms, Ryan and colleagues have recently demonstrated that α-synuclein modulates cellular BH_4 levels by regulating GTPCH activity (Ryan *et al.*, 2014). This supports the compelling hypothesis that a pathogenic cascade may occur in nigral

neurons, whereby increased levels of α-synuclein and mitochondrial dysfunction lead to decreased GTPCH activity and BH$_4$ levels, which in turn may result in increased oxidative stress and cell death.

There are some important limitations in this study that need to be acknowledged.

Firstly, dopamine transporter imaging was not available for the PD cases with *GCH1* variants identified in the exome sequencing study. It remains a possibility therefore that some of these cases (in particular case 9, who presented at age 17, with lower limb dystonia and parkinsonism) may represent DRD cases with a parkinsonian phenotype, which may have been misdiagnosed as PD.

However, removal of the aforementioned case from the statistical analysis did not change substantially the significance of the association ($P = 0.0003$). Furthermore, most of the patients for whom clinical follow-up data were available showed a progressive disease course with increasing L-DOPA requirements, emergence of motor complications due to chronic treatment with L-DOPA and presence of classic non-motor features of PD, strongly supporting nigrostriatal cell loss as the underlying pathology. Although dyskinesias have been very rarely described also in DRD cases, these are significantly different from the ones generally observed in PD. Indeed they tend to appear at the beginning of the treatment and subside after dose reduction without reoccurring with subsequent slow dose increase (Furukawa *et al.*, 2004, Lee *et al.*, 2013).

Secondly, the effect of the *GCH1* variants detected in the exome sequencing study on pterin and dopamine metabolism could not be determined at the individual level. Reduced penetrance of *GCH1* pathogenic variants for the DRD phenotype is a well-established feature. Nevertheless it has been repeatedly reported, through analysis of brain tissue (Furukawa *et al.*, 2002), CSF (Takahashi *et al.*, 1994) and urine (Leuzzi *et al.*, 2013), that even completely asymptomatic carriers of *GCH1* mutations have abnormal metabolism of biopterins and dopamine, although to a lesser extent than DRD cases. This indicates the existence of a metabolic *endophenotype*, which we speculate could be the pathogenic mechanism underlying the increased risk for PD.

Thirdly, a cohort enriched with early-onset and familial PD cases was evaluated. Thus the frequency of detected *GCH1* variants may not reflect the frequency in late-onset

sporadic cases.

Finally, I did not assess our samples for the presence of *GCH1* copy number variants, possibly underestimating the frequency of *GCH1* mutations.

In conclusion, I demonstrate that rare *GCH1* coding variants should be considered as a risk factor for PD. This is derived both from imaging evidence of striatal dopaminergic denervation in *GCH1* pathogenic variant carriers with a clinical diagnosis of definite PD (in DRD pedigrees) and from exome sequencing data which show a significant association between *GCH1* coding variants and an increased risk for the disease.

These findings expand the clinical and biological relevance of GTPCH deficiency, suggesting a role not only in biochemical dopamine depletion and DRD, but also in nigrostriatal degeneration. The question as to how the same variants known to cause a Mendelian disease may also exist as risk alleles in PD may be explained by the well-known reduced penetrance of *GCH1* pathogenic variants. Whether additional genetic or epigenetic factors play a role in determining the clinical phenotype of *GCH1* variant carriers should be addressed by future studies.

Chapter 5. Exploring the Genetics Basis of Myoclonus-Dystonia

5.1 Outline of the Chapter

This chapter describes my efforts to identify novel genetic causes responsible for Myoclonus-Dystonia (M-D).

The chapter begins with an overview of the clinical and genetic features of M-D. The specific aims of the study were:

1) To identify the underlying causative mutation in a pedigree with genetically unexplained autosomal dominant M-D;

2) To identify the genetic cause in a recessive pedigree with genetically unexplained M-D;

3) To assess the role of the missense variant p.Arg1389His in *CACNA1B*, a newly identified M-D genetic cause, in a large international cohort of patients with M-D.

5.2 Overview of Myoclonus-Dystonia

M-D is a very rare condition with a suggested prevalence about 2 per million in Europe. M-D is clinically characterized by a variable combination of non-epileptic myoclonic jerks and dystonic movements (Asmus and Gasser, 2004).

The first locus for autosomal dominant M-D (DYT11) was mapped on chromosome 7q21-q31 (Nygaard *et al.*, 1999). Heterozygous mutations (including nonsense, missense, deletions, and insertions) in the *SCGE* gene (MIM 604149) were subsequently identified as the genetic cause responsible for DYT11 and represent a major cause of inherited autosomal dominant M-D (Zimprich *et al.*, 2001). Usually *SGCE* mutation carriers manifest the first symptoms in childhood with brief lightning-like myoclonic jerks affecting the upper body often being the most prominent symptom (Asmus *et al.*, 2002). Dystonia, presenting as cervical dystonia or writer's cramp, generally appears later and is generally of mild to moderate intensity. Cranial, laryngeal and lower limb

dystonia are conversely more rarely reported (Roze *et al.*, 2008). Additional features such as alcohol responsiveness of jerks and psychiatric co-morbidities (depression, anxiety and obsessive-compulsive disorder, alcohol addiction and attention deficit and hyperactivity disorder) are frequently present in *SGCE*-mutation carriers (Peall *et al.*, 2013).

Asmus and colleagues recognised that large heterozygous deletions of *SGCE*, undetectable by direct Sanger sequencing, may account for a substantial portion (~25%) of the genetically unexplained cases with familial M-D (Asmus *et al.*, 2005). Large deletions on the 7q21.13-21.3 region, encompassing not only *SGCE* but also other neighbouring genes (e.g. *KRIT1, COL1A2, SHFM1, DLX6 and DLX5*), are associated with a M-D plus presentation, which include other clinical features, such as hearing loss, short stature, joint laxity and microcephaly, skeletal deformities and cavernous cerebral malformations on cranial MRI (Asmus *et al.*, 2007, Grunewald *et al.*, 2008, Saugier-Veber *et al.*, 2010, Peall *et al.*, 2014). Penetrance of mutations in the *SGCE* is reduced and related to maternal imprinting. Transcription occurs almost exclusively from the paternal allele, whilst transcription from the maternal allele is silenced by promoter methylation (Grabowski *et al.*, 2003). Individuals with paternally inherited loss-of-function *SGCE* mutations exhibit M-D, whereas individuals with maternally inherited mutations are asymptomatic. This particular pattern of inheritance explains why patients with M-D due to *SGCE*-mutations may lack a positive family history.

The *SGCE* gene encodes the 438-aminoacid protein ε-sarcoglycan, member of the sarcoglycan gene family. In the brain *SGCE* mutations are thought to lead to mislocalisation of the protein from the plasma membrane to the endoplasmic reticulum and to promotion of its degradation by the proteasome (Esapa *et al.*, 2007).

SGCE mutations, including both point mutations and large deletions, are detected in only ~30-50% of familial cases, suggesting genetic heterogeneity and the existence of other still unidentified disease-associated genes (Schule *et al.*, 2004, Tezenas du Montcel *et al.*, 2006, Carecchio *et al.*, 2013, Peall *et al.*, 2014). An additional locus on chromosome 18p11 (DYT15; MIM 607488) has been linked to M-D in a single large Canadian family, but the causative mutation has not been identified as of yet (Han *et al.*, 2007). A frameshift mutation in *TOR1A* and a missense mutation in the *DRD2* gene have been proposed as possible causes for M-D in single pedigrees, but then dismissed

as in both pedigrees pathogenic *SGCE* were subsequently detected (Klein *et al.*, 2002).

Other autosomal dominant M-D syndromes include some cases of benign hereditary chorea due to *NKX2-1* mutations, with additional signs such as delayed motor milestones and later chorea (Armstrong *et al.*, 2011) and one family with *GCH1* mutations, which presented with L-DOPA-responsive M-D and later developed parkinsonism (Leuzzi *et al.*, 2002). With regard to AR disorders, M-D is described in one case with Vitamin E deficiency (Angelini *et al.*, 2002), that later developed ataxia. When myoclonus and dystonia are only part of the phenotype a number of mitochondrial (Hanna and Bhatia, 1997, Garcia-Cazorla *et al.*, 2008) or neurometabolic disorders (e.g. Lafora body disease, GM2 gangliosidosis, Niemann-Pick disease) should be considered in the differential diagnosis (Gouider-Khouja *et al.*, 2010).

Recently, Groen and colleagues identified two missense variants, p.Arg1389His (rs184841813) in *CACNA1B* and p.Thr1904Met (rs114190729) in *RELN,* each in a single autosomal dominant Dutch pedigree with M-D lacking mutations in *SGCE,* as the likely causative mutations (Groen *et al.*, 2015, Groen *et al.*, 2015). However, the pathogenic role of these variants is not confirmed as yet.

5.3 Linkage Analysis and Exome Sequencing Identify A Novel Cause Of Familial Myoclonus-Dystonia

5.3.1 Statement of contribution

The index case of the family described in this chapter was recruited in Professor Kailash Bhatia's clinic at the National Hospital for Neurology, London. I examined and recruited all other available family members. I performed all the genetic analysis and the functional studies in fibroblasts. I performed stable transfection of SH-SY5 cell lines and immunocytochemistry, in collaboration with Dr Anselm Zdebik. The WGCNA analysis was performed by Dr Conceicao Bettencourt based on the data generated by Dr Paolo Foraboschi, Dr Mina Ryten and Dr Trabzuni.

5.3.2 Introduction

I describe here the work that resulted in the identification of the genetic cause in a large British four-generation pedigree affected with autosomal dominant M-D, without mutations in *SGCE*. Through a combination of linkage analysis and WES, I identified a single missense mutation in *KCTD17* as a novel cause for M-D.

5.3.3 Subjects, Materials and Methods

Index Family

The clinical characteristics of the patients and the family pedigree are described in the Results. Out of 19 living family members from the index family, 13 subjects were assessed and recruited. Six children of unaffected individuals were not examined. Assessment included a detailed medical interview and a full videotaped neurological examination, with focus on movement disorders. All videos were subsequently blindly reviewed by two experts in movement disorders (Professor Kailash P. Bhatia and Dr Tom Foltynie). After obtaining informed consent, a blood sample was collected and DNA was extracted from 13 family members and 4 spouses. Samples were collected with the written consent of participants and formal ethical approval by the relevant research ethics committee (UCLH Project ID number 06/N076).

Linkage Analysis

Genome-wide linkage analysis was performed in a standard manner as described in the Materials and Methods section.

Whole-Exome Sequencing

WES (TruSeq SBS chemistry sequenced on the Illumina HiSeq 2000) was performed in the two most distantly related affected individuals (V-3 and IV-14), as described in the Materials and Methods chapter.

Sanger Sequencing

Sanger sequencing was performed to validate WES results, check variants segregation in the index family and screen other M-D cases. Sanger sequencing was performed as described in Materials and Methods section. Primers were designed the entire coding region of *KCTD17* (9 exons; transcript NM_001282684.1). The primers used are listed in the Appendix.

Selection of Additional Cases for Mutational Screening

A cohort of M-D cases was selected to search for further confirmatory mutations in candidate genes. Cases were selected from a bank of DNA samples donated with research consent, which are held at NHNN Neurogenetics Department. Additional cases were provided by international collaborators (Prof. Thomas Gasser, University of Tubingen; Prof. Christine Klein, University of Lubeck; Prof. Nardo Nardocci, Istituto Neurologico Carlo Besta). All selected cases fulfilled the proposed diagnostic criteria for M-D (Kinugawa *et al.*, 2009). All samples included in this project had previously undergone diagnostic testing for mutations in *SGCE* (both point mutations and copy number variants) and were negative. In total 87 unrelated probands with familial M-D (defined by a family history of M-D in at least a first or second degree relative) and 358 sporadic cases of British, German and Italian origin were selected. The study was approved by the relevant local ethics committees and informed consent was provided by all participants in accordance with local guidelines.

Expression Profiling of KCTD17 In Brain Tissue

Brain expression profiling data was collated for *KCTD17* as described in Materials and Methods section.

Generation of stably transfected SH-SY5 cell lines

To assess subcellular distribution of KCTD17, a major splice variant from mouse brain was cloned. Total RNA was isolated from TRIZOL lysate, which was purified using the Zymo Direct-zol RNA mini kit (Cambridge Bioscience, UK) and quality assessed by non-denaturing agarose gel electrophoresis. Following poly-dT primed transcription

using Superscript III (Invitrogen, UK) on 5 ug total RNA, we amplified the full-length cDNA with primers containing unique restriction sites. The mutation c.434 G>A p.Arg145His was inserted by recombinant PCR. Either N- or C-terminal HA tagged wild-type and mutant cDNAs were inserted with a 1-step recombinant PCR into pcDNA3.1 constructs for expression in mammalian cells. Stable SH-SY5 cells were generated by electroporating 5 μg linearized tagged wild-type and mutant plasmids into ~1 million cells and G418 (InvivoGen) selection at 250 mg/l over at least 4 weeks and at least 6 passages. A control cell line expressing the empty vector was obtained in parallel.

Immunocytochemistry

Immunocytochemistry was performed on cells seeded on glass coverslips (13 mm diameter) coated with Cultrex basement membrane extract (R&D systems, USA). After fixation with either 4% PFA in PBS or ice-cold 50% methanol/50% acetone, cells were blocked in PBS+2% BSA%, 3% normal goat serum, 1% NP-40, 0.5% sodiumdesoxycholate for 30 minutes and primary antibodies. The Roche 3F10 or 12Ca5 monoclonal antibodies were used for detection of the HA tag, at 1:1000 or 1:300 dilutions, respectively. Subcellular marker antibodies were used at 1:1000 dilution. After washing, secondary detection used Alexa-dye labelled, highly cross-absorbed anti-rat (Invitrogen, UK) in 0.5x block, with 1 mg/l DAPI. Coverslips were mounted using Prolong Gold (Invitrogen, UK) after 4 washes with PBS. Microscopy was performed on a Zeiss confocal microscope.

Weighted Gene Co-expression Network Analysis

Weighted Gene Co-expression Network Analysis (WGCNA) was performed based on the UKBEC human brain mRNA expression data. In brief, this systems biology analytic approach uses brain regional whole-transcriptome gene expression data and establishes the degree of gene neighbourhood sharing, as defined on the basis of co-expression relationships. This approach allows to identify in an unsupervised and unbiased manner modules of genes that are highly co-expressed and co-regulated and therefore likely to be functionally related (Oldham *et al.*, 2006). Microarray data on 19152 transcripts (corresponding to 17247 genes), generated from 788 brain samples obtained from 101 neuropathologically healthy individuals was used for weighted gene co-expression network analysis (WGCNA). The WGCNA network was constructed for each brain region to achieve a scale-free topology, as previously described (Forabosco *et al.*,

2013). A dissimilarity matrix based on topological overlap measure was used to identify gene modules (i.e., densely interconnected and co-expressed genes) through a dynamic tree-cutting algorithm. A detailed description of the methods used to generate the dataset is available in the manuscript of Forabosco and colleagues.

Calcium Imaging in Fibroblasts

After obtaining informed consent, fibroblasts were isolated from a skin biopsy taken from a carrier of the *KCTD17* Arg145His mutation (index family, III-2). Two unrelated age- and passage-matched controls were selected from in-house cell lines. The fibroblasts were cultured in Dulbecco's modified Eagle's medium GlutaMAX supplemented with 10% heat-inactivated fetal bovine serum and 1% penicillin-streptomycin. They were maintained at 37°C in a humidified atmosphere of 5% CO_2 and 95% air, media changed twice a week. Calcium homeostasis was assessed using the ratio-metric calcium (Ca^{2+}) dye, Fura-2, AM (Molecular Probes, Paisley, UK), which indicates intracellular Ca^{2+} concentration and allows recordings of Ca^{2+} fluxes upon application of different pharmacological stimuli. Fibroblasts were loaded at room temperature for 30 minutes with 5mM fura-2 AM and 0.005% Pluronic in HBSS composed of (mM): 156 NaCl, 3 KCl, 2 $MgSO_4$, 1.25 KH_2PO_4, 2 $CaCl_2$, 10 glucose and 10 HEPES (pH adjusted to 7.35 with NaOH). Fluorescence measurements were obtained on an epifluorescence inverted microscope equipped with a 20x fluorite objective. Analysed areas were randomly chosen, and at least three independent experiments were performed for each condition. Ca^{2+} was monitored in single cells using excitation light provided by a Xenon arc lamp, with the beam passing monochromator centred at 340 and 380 nm (Cairn Research, Kent, UK). Emitted fluorescence light was reflected through a 515 nm long-pass filter to a cooled CCD camera (Retiga, QImaging, Surrey, BC, Canada). All imaging data were collected and analysed using software from Andor (Belfast, UK). ATP (100 mM) was used for stimulating Ca^{2+} signals in fibroblasts via purinoceptors and for releasing calcium from the endoplasmic reticulum (ER) via IP3 receptors. In a second round of experiments thapsigargin (1 mM), in Ca_{2+}-free medium (plus 0.5 mM EGTA), was used for inducing the release of calcium from the ER to the cytosol and thus for estimating the size of the reticular Ca_{2+}pool. After stimulation with thapsigargin, Ca_{2+} (2mM) was added to the medium for stimulating the plasma membrane store-operated Ca_{2+} channels and assessing the store-operated calcium entry.

5.3.4 Results

Clinical phenotype of the index family

The family pedigree is shown in Figure 5-1. The 71-year-old index case (subject III-2) was first seen in clinic at age 56. She was born without complications after an uneventful pregnancy and had a normal development as a child. Her symptoms started during childhood with involuntary jerky movements of her arms. She always felt clumsier than other children. In her fifties, she developed constant head jerks and head deviation to the left. In her sixties her speech became involved, with changes of tone and stops during conversation. She also noticed that her balance was not as good as before. Involuntary movements worsened while performing voluntary actions, particularly while walking, and improved when relaxed. Touching her chin or the back of her head reduced the jerks markedly. Occasional use of alcohol did not have an impact on symptoms. On examination she had spasmodic dysphonia, perioral myoclonus and blepharospasm. She had a left torticollis and frequent irregular head myoclonic jerks. There was dystonic posturing of the hands with some writhing movements of the fingers and occasional low amplitude jerks. When she walked her trunk was slightly tilted to the left and backwards and she presented bilateral foot dystonia with feet turning inwards. She walked with a wide base and felt that walking backwards was easier. While standing she developed jerks in her legs.

A broad range of genetic investigations resulted negative, including testing for SCA 1,2,3,6 and 7, HD, DRPLA, DYT1, DYT6 and DYT11 (including sequencing of all coding exons and adjacent intronic regions and MLPA to detect copy number variants). Her brain MRI showed minor age-linked atrophy and some non-specific high signal spots in subcortical areas. She also had normal EEG, nerve conduction studies, EMG and central motor and sensory conduction times. She had a trial of oral L-DOPA (up to 600 mg/day for at least a month) without improvement. She was treated with local Botulinum Toxin injections for her cervical dystonia, with some improvement. Because of progressive worsening of her symptoms she was considered for globus pallidus internus (GPi) deep brain stimulation and, after the appropriate assessment, she was operated, at the age of 70. Following surgery her cervical dystonia improved considerably but her other symptoms, particularly her gait problems, remained unchanged.

Six other family members displayed signs of dystonia and/or myoclonus, and were accordingly categorized as affected (see Table 5-1). Age of onset of movement disorder symptoms ranged from 5 to 20 years. All affected family members initially presented with jerks or a jerky tremor, with mild dystonic features presenting later in life. All cases fulfilled the currently proposed clinical criteria for a definite diagnosis of M-D (Kinugawa *et al.*, 2009), except individual IV-3, who upon examination displayed isolated cervical dystonia, although she reported intermittent jerky arm tremor. Myoclonus involved predominantly the arms. Dystonia predominantly affected the cranio-cervical region and upper limbs. Older individuals (>60 years; III-2 and III-5) were more severely affected and also showed laryngeal involvement. None of the affected subjects reported improvement of symptoms with alcohol. No other individuals presented with psychiatric symptoms. Case IV-12 aged 42 when clinically assessed, was considered to be unaffected with the family condition by both Professor Bhatia and Dr Foltynie. He had strabismus and benign congenital nystagmus. He showed no myoclonus or dystonia, but exhibited a mild bilateral postural hand tremor, consistent with a diagnosis of essential tremor. A similar tremor was also observed in his father, spouse of the affected individual III-5, suggesting that this feature is likely to be unrelated from the condition affecting the other family members. The remaining individuals were asymptomatic and had an entirely normal neurological examination.
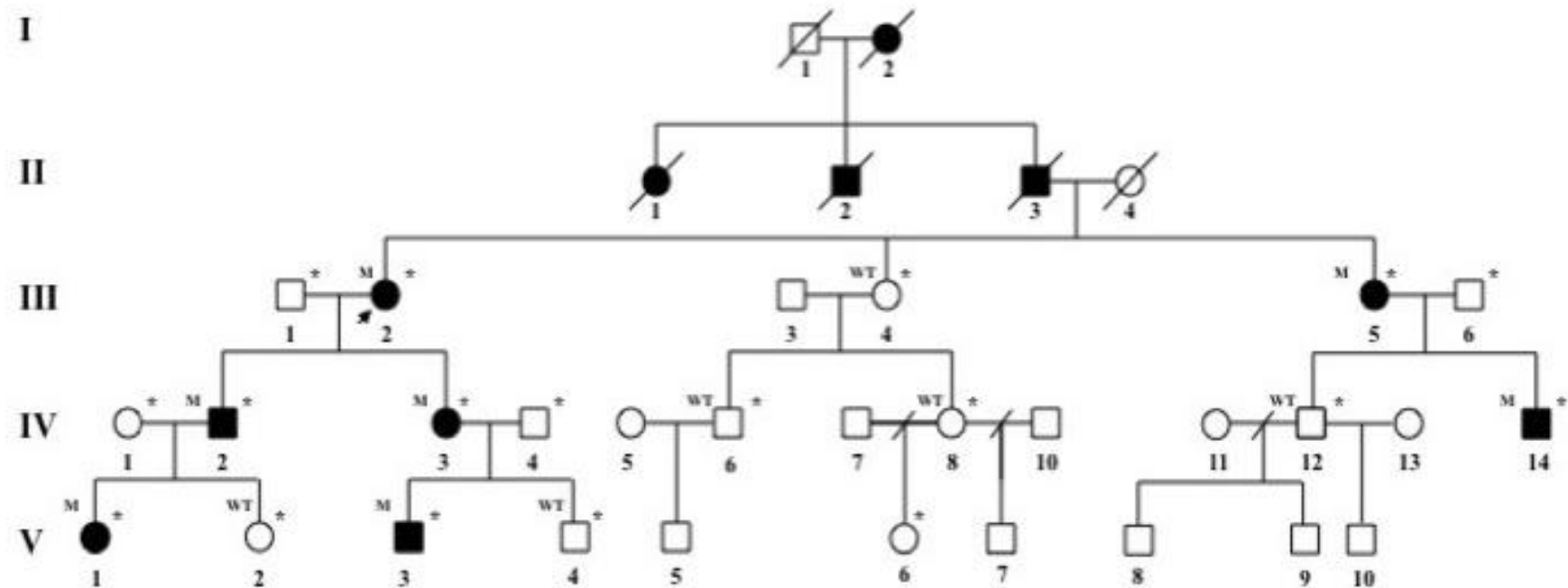
Figure 5-1 Pedigree of the index family where the *KCTD17* c.434 G>A p.Arg145His mutation was identified.

159

Table 5-1 Clinical features of cases carrying the *KCTD17* c.434 G>A p.Arg145His mutation

Subject	III-2	III-5	IV-2	IV-3	IV-14	V-1	V-3	II.2 (Germany)
Sex	F	F	M	F	M	F	M	M
Age at last examination (y)	70	65	46	44	35	20	19	62
Age at onset (y)	10	6	10	20	10	5	5	10
Presenting symptoms	Jerks; Arms	Jerks; Arms	Jerks; Arms	Jerky tremor; Arms	Jerky tremor; Arms	Jerks; Arms	Jerks; Arms	Jerks, Arms
Dystonic features	Yes	Yes	Yes	Yes	Yes	Yes	No	Yes
Involved areas	Cranial, Cervical, Brachial, Truncal, Crural	Cranial, Cervical, Brachial	Brachial	Cervical	Cervical, Brachial	Brachial	NA	Cranial, Cervical, Brachial, Truncal
Myoclonus	Yes	Yes	Yes	No	Yes	Yes	Yes	Yes
Involved areas	Cranial, Cervical, Brachial	Cranial, Brachial	Brachial	NA	Cranial, Brachial	Brachial	Cervical, Brachial	Brachial

Linkage analysis

Genotype from seven affected individuals (III-2, III-5, IV-2, IV-3, IV-14, V-1 and V-3), five unaffected (III-4, IV-6, IV-8, IV-12 and V-4) and four spouses (III-1, III-6, IV-1, IV-4) was included in the analysis. The unaffected subject V-2 was not included as she was too young (17 when last examined) to exclude or confirm disease status. Linkage was performed under the assumption of an autosomal dominant inheritance with 90% penetrance and a disease allele frequency of 0.0001%. One single locus with a LOD score > 2 was identified on chromosome 22q13 (LOD score 2.4, the maximal expected value given the pedigree size; Figure 5-2). Fine mapping identified a segregating haplotype delimitated by SNP markers rs926543 and rs3213584 and spanning 6.7Mb (chr22: 36989327-43716324; UCSC hg19 Genome Build), which contained 132 protein-coding genes. In addition, 5 other regions presented with uninformative multipoint LOD scores, ranging from -0.9 to +0.14 (see Table 5-2), but haplotype analysis excluded co-segregation of these regions with the disease.

Table 5-2 Summary of position, size and genetic content of the regions with a LOD score > -2

Chromosome	Start position (Hg19)	Stop position (Hg19)	LOD score
3	100410724	101569726	-0.8111
12	58842292	60028954	0.1474
12	70112707	70517723	-0.7314
12	70422480	71099936	-0.9131
12	72641784	73373089	-0.7143
22	36989327	43716324	2.4082
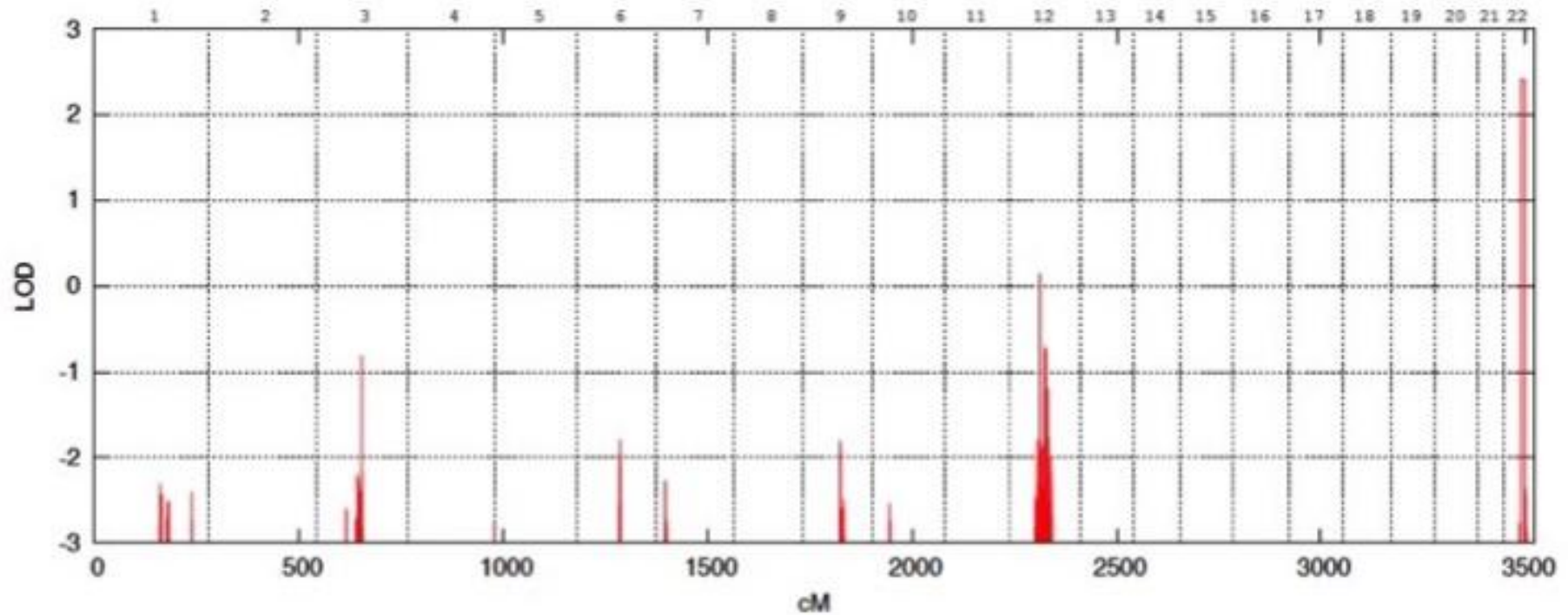
Figure 5-2 Linkage analysis results

LOD score plot for genome-wide linkage analysis in the British index pedigree showing a single linkage peak on chromosome 22q13 with a maximum LOD score of 2.4. An autosomal dominant model was specified with an estimated allele frequency of 0.00001 and 90% penetrance. The chromosome is indicated across the top of the plot; chromosomal distance in centiMorgans (cM) is indicated on the x-axis; and the LOD score is indicated on the y-axis.

Whole-exome sequencing

To identify the disease-causing variant, WES was performed in the two most distantly related affected individuals (V-3 and IV-14). In total, 83,572,847 (V-3) and 81,527,162 (IV-14) unique reads were generated. According to the Consensus Coding Sequences hg19 definition of the 'TruSeq exome', the average read depth of both exomes was > 70, > 95% of the target bases were covered at a read depth of 2x and > 90% at a depth of 10x. A total of 22,857 (V-3) and 22,946 (IV-14) exonic/splicing variants were detected. A summary of the WES metrics can be found in Table 5-3.

Table 5-3 Summary of results from exome sequencing

Patient	V-3	IV-14
Unique reads	83,572,847	81,527,162
Aligned Reads (%)	87.6	87.2
Mean depth	73	71
Target covered at least 2x	96	95
Target covered at least 10x	92	91
Total variants	22,857	22,946
Excluding synonymous variants	11,710	11,737
Novel variants	154	140
Shared novel variants	4	4
Shared novel variants within the linkage peak on 22q	1	1

All synonymous changes and those not shared by the two affected individuals were filtered out. Then, under the assumption that the mutation causing this rare autosomal dominant disease is extremely rare and not present in the general population, I also excluded variants that are present in databases of sequence variations publicly available databases of sequence variations (dbSNP version 129, 1000 Genomes project, NHLBI Exome Variant Server and Complete Genomics 69). Furthermore, I excluded variants found in our own in-house exomes (n=200) from individuals with unrelated diseases.

After applying filtering criteria, only four novel missense variants shared by the two affected individuals were left (see Table 5-4): c.10976 C>T; p.Ser3659Phe in *FLG* (filaggrin; RefSeq NM_002016.1), c.1055 T>G; p.Phe352Cys in *OBSCN* (obscurin; RefSeq NM_052843.3), c.1076 A>C; p.Lys359Thr in *LRRC6* (leucine rich repeat containing 6; RefSeq NM_012472.4) and c.434 G>A; p.Arg145His in *KCTD17* (potassium channel tetramerisation domain containing 17; RefSeq NM_001282684.1). Of these variants, only the missense change in *KCTD17* was located within the linked chromosomal locus on chromosome 22q. No shared rare copy number variants in exome sequencing data were detected using the Exome depth algorithm.

Sanger sequencing of the *KCTD17* variant (see Figure 5-3) in all available family members confirmed perfect co-segregation of the variant with the disease-phenotype, being the nucleotide change present in all affected individuals and absent in all unaffected (including subject V-2, initially excluded from the linkage analysis). Segregation analysis of the other three novel variants, shared by individuals V-3 and IV-14 but located outside the identified linkage peak, was also performed. As expected, none of them fully segregated: the *LRRC6* variant was not carried by affected individuals (IV-2 and V-1) and the *OBSCN* and *FLG* variants were carried by unaffected subjects V-4 (*OBSCN* and *FLG*) and IV-12 (*FLG*), aged 20 and 40 respectively when last examined. Although the KCTD17 p.Arg145His substitution falls in a functionally uncharacterized portion of the protein, it lies in an extremely conserved amino acid motif, not only completely conserved down to invertebrate species, but also identical in the *KCTD17* human paralogs *KCTD2* and *KCTD5* (see Figure 5-4).
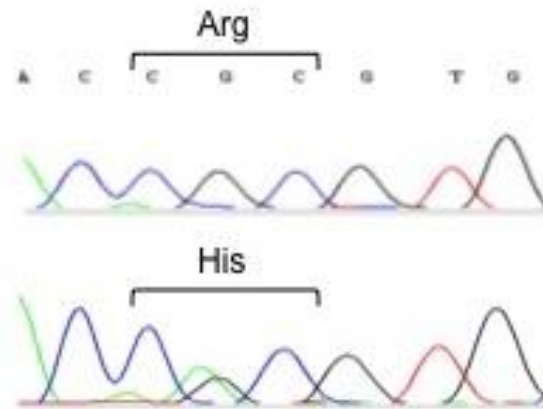
Figure 5-3 Sanger sequencing confirmation of the *KCTD17* c.434G>A p.Arg145His mutation.

The variant is absent in over 3,700 individuals of European origin without movement disorders, who were exome sequenced by the UCL-exomes consortium, and in a further > 61,000 individuals listed in the Exome Aggregation Consortium database (last accessed in March 2016). All *in silico* tools consistently predicted a deleterious effect of the substitution (see Table 5-4).

Figure 5-4 Interspecies protein sequence alignment

Multiple-sequence alignment showing complete conservation of protein sequence across species and human paralogs (KCTD2 and KCTD5) in the region of KCTD17 where the disease-segregating mutation p.Arg145His was identified. The amino acid involved by the mutation is marked in red. The residues that are not completely conserved are highlighted in yellow. In blue the residues completely conserved.

Table 5-4 Summary of novel variants detected by whole-exome sequencing and shared by individuals V-3 and IV-14.

Chr	Position (hg19)	Gene (Transcript)	Variant	GERP score[a]	CADD C-score[b]	SIFT	Provean	PolyPhen-2 HumVar	Mutation Taster	Gene previously associated with disease?	Linkage analysis (LOD score)
1	152276386	*FLG* (NM_002016.1)	c.10976 C>T; p.Ser3659Phe	2.48	11.15	T (0.06)	N (-0.8)	D (0.78)	P (0.99)	Yes, skin diseases (e.g. ichthyosis vulgaris, and/or eczema)	< -2
1	228401208	*OBSCN* (NM_052843.3)	c.1055 T>G; p.Phe352Cys	5.58	21	D (0)	D (-3.8)	D (0.94)	D (0.99)	Hypertrophic cardiomyopathy	< -2
8	133622476	*LRRC6* (NM_012472.4)	c.1076 A>C; p.Lys359Thr	3.5	15.74	D (0.01)	D (-3.1)	B (0.39)	D (0.99)	Recessive primary ciliary dyskinesia	< -3
22	37453460	*KCTD17* (NM_001282684.1)	c.434 G>A; p.Arg145His	4.46	28.8	D (0)	D (-4.8)	D (0.53)	D (0.99)	No	2.4

B=benign; D=deleterious/damaging/disease-causing; N=neutral; P=polymorphism; T=tolerated

[a] Positive scores represent a substitution deficit and indicate that a site may be under evolutionary constraint. Negative scores indicate that a site is probably evolving neutrally. Positive scores scale with the level of constraint, such that the greater the score, the greater the level of evolutionary constraint inferred to be acting on that site.

[b] C-scores greater or equal 10 indicates that the variant is predicted to be the among the 10% most deleterious substitutions that you can do to the human genome; a score of greater or equal 20 indicates the 1% most deleterious

Sanger Sequencing of KCTD17 in a Cohort of Phenotypically Similar Myoclonus-Dystonia Cases

The entire coding region of *KCTD17* was subsequently sequenced by Sanger sequencing in a further 87 unrelated probands with familial *SGCE*-negative M-D. Exon 4 only (containing the c.434 G>A mutation) was sequenced in a further 358 sporadic M-D cases. This analysis revealed the presence of the same *KCTD17* mutation, c.434 G>A p.Arg145His, in the index case of a German family with autosomal dominant M-D (Figure 5-5). No further pathogenic mutations in KCTD17 were identified.
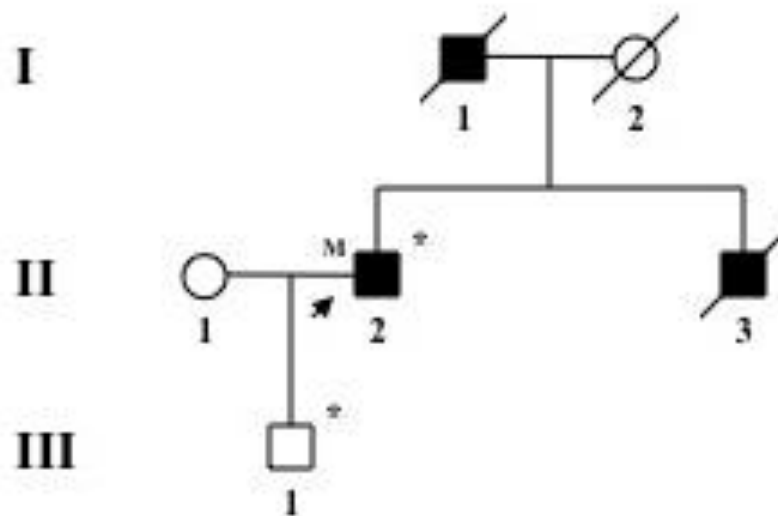
Figure 5-5 Pedigree of the German families with the *KCTD17* c.434 G>A p.Arg145His mutation.

The clinical presentation of this case closely resembled that of III-2 and III-5, the older affected subjects from the British family. He reported arm jerks and difficulty writing, starting in childhood. Right torticollis and a jerky head tremor appeared around age 40, becoming progressively debilitating. There was no response to alcohol or psychiatric comorbidities. He underwent surgery for bilateral pallidal deep brain stimulation at age 58, which resulted in marked improvement of cervical dystonia and myoclonus of the upper limbs. Clinical examination at age 62 showed generalized dystonia, with prominent cranio-cervical involvement, and myoclonic jerks involving the upper limbs.

His father was also affected with a movement disorder, presenting with perioral dyskinesia in his forties. The proband's brother had M-D, with similar clinical features, including generalized jerks, cervical dystonia and dysarthria. Unfortunately, DNA

samples of the deceased father and brother were not available for segregation analysis. The 25-years old proband's only son, who had no signs upon examination, refused genetic testing.

To determine whether the *KCTD17* c.434 G>A; p.Arg145His occurred on the same haplotype in the British and in the German kindreds, SNP markers located 0.5 Mb up- and down-stream the mutation were compared (see Table 5-5). In the British family, the haplotype of the identified *KCTD17* mutation was reconstructed. The German case was genotyped using the same array. In the German case SNP phasing was possible only for homozygous alleles, due to lack of genetic data on other family members. Different alleles were located at markers rs5756477 and rs228924 (45.9 kb upstream and 53 kb downstream of *KCTD17*, respectively), delimitating a small region of approximately 99 kilobases (Kb) of a possibly shared haplotype. Further analysis with a highly polymorphic microsatellite (19xAG; chromosomal position 22:37,446,300-37,446,339), located only 1.4 Kb upstream of the 5' end of the *KCTD17* open reading frame, revealed that the two pedigrees had different alleles.

Table 5-5 Disease haplotype of the families with the *KCTD17* c.434 G>A; p.Arg145His

Marker	Chromosomal position (hg19)	Genotype UK family	Genotype German family
rs5756370	37242476	A	A
rs6000449	37251377	A	A
rs4821542	37252918	G	G
rs909483	37260474	A	A
rs2413429	37289869	G	A
rs4821558	37308785	G	A
rs11705394	37329676	A	A
rs9622506	37338286	A	G
rs8137446	37347959	G	G
rs9622521	37350881	G	G

rs4821576	37357169	G	G
rs8142593	37363121	A	A
rs877166	37369148	C	C
rs5756437	37375668	G	G
rs1157557	37381674	G	G
rs5756477	37407527	G	A
rs5756492	37424991	G	G
Microsatellite 19xAG	37446300	17[a]	18/14[a]
KCTD17 c.434G>A	37453460	A	A
rs2160906	37493178	G	G
rs228924	37507250	A	G
rs11914132	37509087	G	G
rs228942	37524619	C	C
rs3218258	37544245	A	G
rs229483	37553619	G	A
rs12167757	37567490	G	G
rs229518	37577872	A	A
rs11913300	37580627	A	A
rs5756540	37582205	G	G
rs5756546	37589805	G	G
rs64547	37592504	A	A
rs9610680	37621951	A	G
rs8137698	37624236	G	A

rs739042	37625419	G	G
rs2285110	37628145	G	G
rs9607431	37629938	C	A
rs5995404	37632938	C	C

All alleles where the haplotype of the UK family differs from that of the German family are highlighted in yellow. [a]These values indicate the number of AG repeats

Brain expression analysis

KCTD17 gene expression was evaluated in 10 brain regions from 134 normal individuals using our in-house data from the UK Brain Expression Consortium. *KCTD17* mRNA expression throughout the course of human brain development was assessed using the data available in the Human Brain Transcriptome (HBT) database. *KCTD17* mRNA expression was high across all brain regions, but it was highest in the putamen followed by the thalamus (Figure 5-6A). There was a 3.2-fold difference (p value $< 3.5^{-71}$) between the striatum and the cerebellum, the regions with respectively the highest and lowest expression. These findings are consistent with the data available in the HBT database, showing increasing *KCTD17* brain mRNA levels in the striatum and the thalamus from early midfetal development (between 21 and 25 post-conception weeks of age) to adolescence (between 12 and 20 years of age) in the striatum and the (Figure 5-6B).
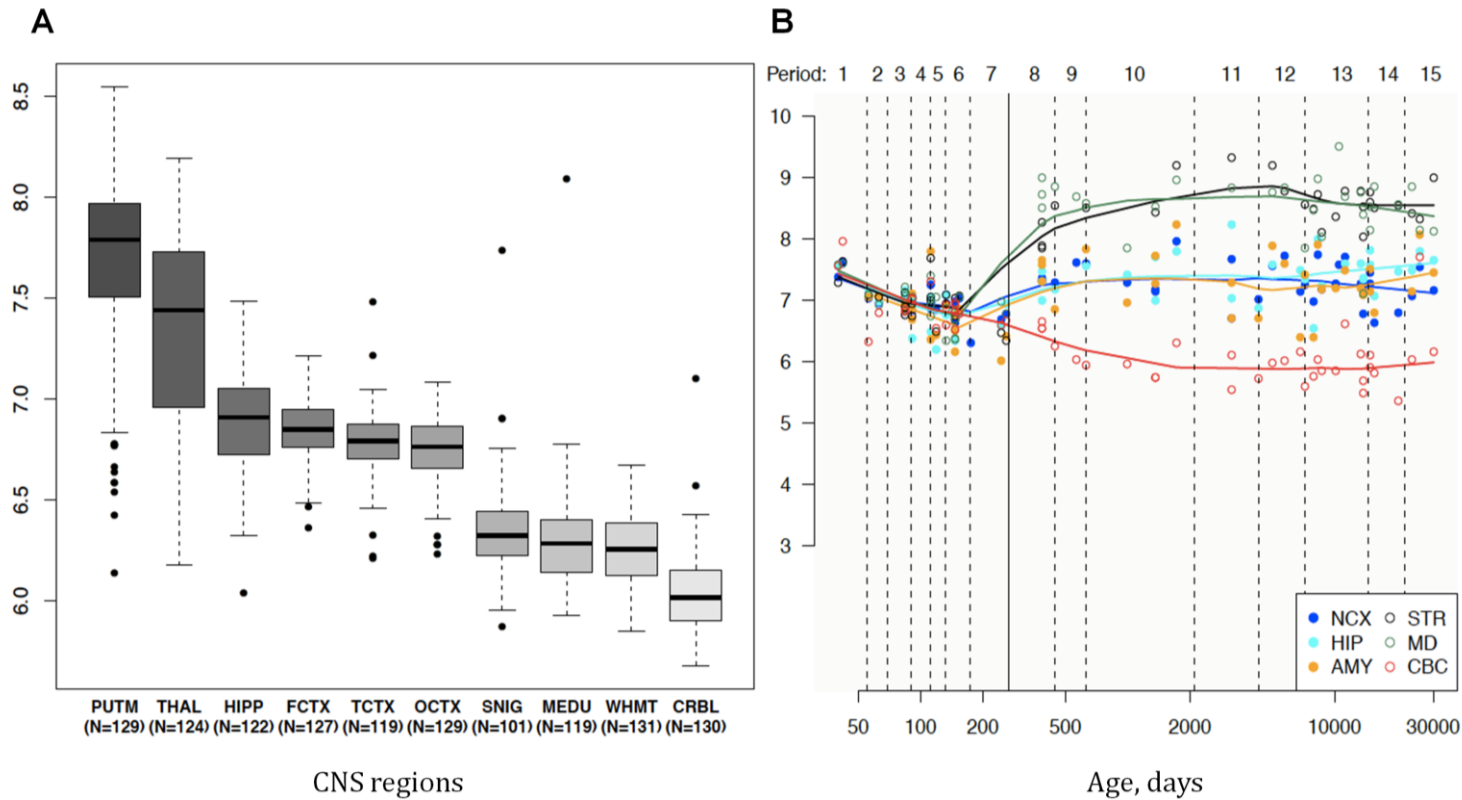
Figure 5-6 *KCTD17* brain regional mRNA expression data

(A) Box plot of mRNA expression levels for *KCTD17* in 10 adult brain regions, based on exon array experiments and plotted on a log2 scale (y axis). The plot shows significant variation in *KCTD17* transcript expression across the 10 CNS regions analysed. "N" indicates the number of brain samples analysed to generate the results for each CNS region. KCT17 expression is higher in the putamen, followed by the thalamus. Whiskers extend from the box to 1.53 the interquartile range. (B) Graph to show mRNA expression levels for *KCTD17* in 6 brain regions during the course of human brain development, based on exon array experiments and plotted on a log2 scale (y axis).

Immunocytochemistry

Stably transfected SH-SY5 cells were generated by incorporating either N- or C-terminally HA-tagged wild-type and mutant *KCTD17* cDNAs. KCTD17 staining with anti-HA primary monoclonal antibodies showed that the protein is diffusely distributed in the cytosol with fine reticular pattern and does not localize at the plasma membrane (Figure 5-7). We did not observe significant changes in subcellular localization of mutant versus wild-type KCTD17, indicating that the amino acid substitution does not lead to cellular mislocalisation of the protein.
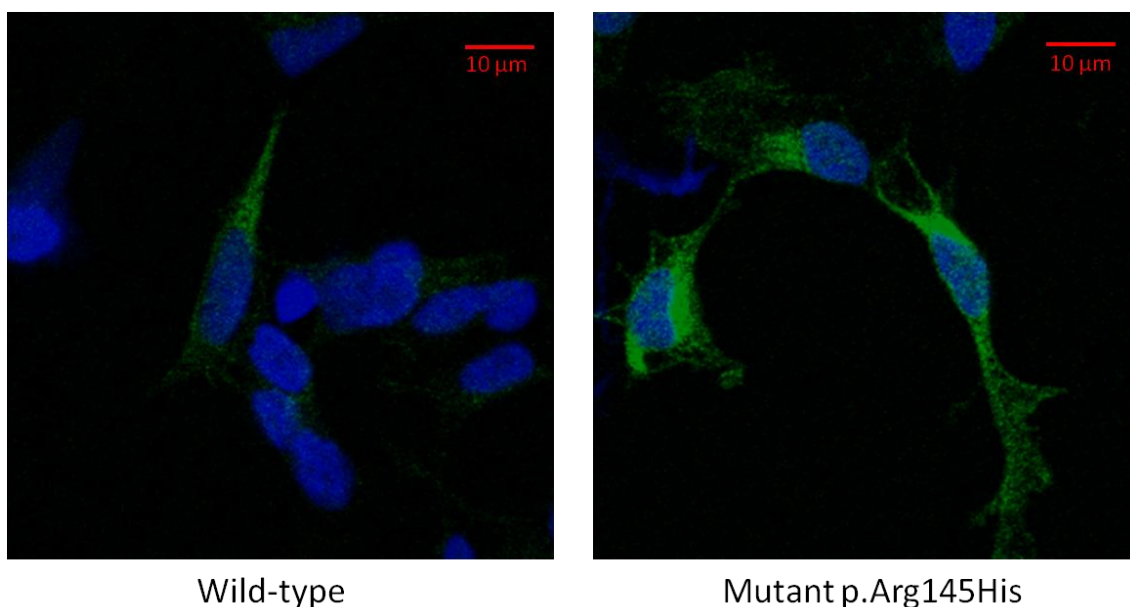
Figure 5-7 Immunocytochemistry in stably transfected SH-SY5 cells
These experiments show no difference between wild-type and mutant KCTD17 subcellular localization. HA-tagged KCTD17 is shown in green. Cellular nuclei are stained with DAPI and are shown in blue.

Weighted Gene Co-expression Network Analysis

KCTD17, in common with other dystonia genes (e.g. *ANO3, GNAL* and *HPCA*), shows the highest expression in the putamen and this brain structure has an established role in the pathogenesis of dystonia. I therefore focused the analysis on the putamen module including *KCTD17*.

This module contains 179 transcripts (equating to 172 genes; see Figure 5-8 for a graphic representation of the module).

Figure 5-8 Network representation of the putamen *KCTD17*-containing gene module
Shown are all genes in the putamen *KCTD17*-containing module connected with a topological overlap measure exceeding 0.03. The dystonia genes in the module (*KCDT17* and *HPCA*) and all the direct connections of *KCTD17*, based on topological overlap values, are highlighted in red. Larger circles represent the most interconnected genes in the module, including *KCTD17*.

I first assessed if the module was enriched for genes linked to Mendelian forms of dystonia. The analysis focused on the nine genes known to be associated with dystonia (*TOR1A*, *THAP1*, *SGCE, TUBB4A, CIZ1, ANO3, GNAL, ATP1A3, HPCA*). I did not include in the analysis genes causing DOPA-responsive dystonia (*GCH1*, *TH*, and *SPR*) as their established functional role in nigrostriatal dopamine synthesis, together with the specificity of the clinical presentation, clearly identifies them as a separate entity.

Importantly, the putamen *KCTD17*-module showed significant clustering of dystonia genes (*KCTD17* and *HPCA*; Fisher's exact test $P = 5 \times 10^{-3}$), suggesting the relevance of this gene network to the molecular pathogenesis of dystonia. The module was poorly preserved across other brain regions, indicating its specificity to the putamen (Figure 5-9).

Figure 5-9 Putamen KCTD17-containing module preservation across other brain regions
Module preservation statistics were calculated (z score) to assess how well modules from one tissue are reproducible (or preserved) in another brain region (Langfelder *et al.*, 2011). Previously proposed thresholds were considered (z score of <2 indicates no evidence of module preservation, z score between 2 and <10 indicates weak to moderate evidence, and z score of ≥10 indicates strong evidence). The module is poorly conserved across other brain regions, indicating its specificity to the putamen

To infer the biological and functional relevance of the putamen *KCTD17* gene network, functional annotation enrichment analysis was then carried out using the online tool g:Profiler (Reimand *et al.*, 2011). This analysis allowed the identification of over-represented genes assigned to specific Kyoto Encyclopedia of Genes and Genomes (KEGG) pathways, namely "Circadian entrainment" (KEGG:04713; g:Profiler's custom threshold $P = 5.13 \times 10^{-3}$) and "Dopaminergic synapse" (KEGG:04728; g:Profiler's custom threshold $P = 2.71 \times 10^{-2}$). This suggests the involvement of the genes in the module with these molecular pathways.

Ca²⁺ imaging in Patient Fibroblasts

Disruption of calcium (Ca^{2+}) homeostasis has been recently implicated in the pathogenesis of several genetic forms of dystonia (eg. *TOR1A*, *ANO3*, *HPCA*) (Charlesworth *et al.*, 2012, Iwabuchi *et al.*, 2013, Charlesworth *et al.*, 2015). As the putamen *KCTD17*-module included *HPCA*, a gene with an established role in intracellular Ca^{2+}-dependent signalling (Palmer *et al.*, 2005), I hypothesized that the

KCTD17 p.Arg145His substitution may have a significant impact on intracellular Ca^{2+} homeostasis.

For this purpose, fibroblasts were isolated from a skin biopsy taken from a subject with the *KCTD17* p.Arg145His mutation and two unrelated age- and passage-matched controls. The expression of *KCTD17* in fibroblasts was confirmed by RT-PCR (data not shown). I observed that stimulation with ATP (50μM), which stimulates P2Y receptors and releases Ca^{2+} from the ER via IP_3 receptors, resulted in significantly reduced and delayed cytosolic Ca^{2+} signal (one-way ANOVA $P < 0.01$; Figure 5-10A and B) in cells carrying the p.Arg145His mutation when compared to both control cells, indicating a smaller calcium pool within the ER.

To further prove this finding, a second round of experiments using thapsigargin (1μM) in Ca^{2+}-free medium (plus 0.5 mM EGTA) was subsequently carried out. Thapsigargin is an inhibitor of the ER calcium ATPase (SERCA) and induces the release of calcium from the ER to the cytosol, allowing an estimation of the ER Ca^{2+}-pool. Ca^{2+} was then added at the end of the experiment to stimulate elevation of cytosolic Ca^{2+} through opening of store operated calcium channels. Thapsigargin stimulation resulted in a significantly smaller Ca^{2+} signal in fibroblasts bearing the p.Arg145His mutation when compared to controls (one-way ANOVA $P < 0.01$; Figure 5-10C and D), confirming that the Ca^{2+} pool in the ER of mutation-carrying fibroblasts is reduced.

Furthermore, stimulation of the store-operated Ca^{2+} channels induced a smaller Ca^{2+} influx in mutated fibroblasts (Figure 5-10C), possibly suggesting an insufficient Ca^{2+} influx across the plasma membrane in response to the fall in Ca^{2+} concentration within the ER lumen.
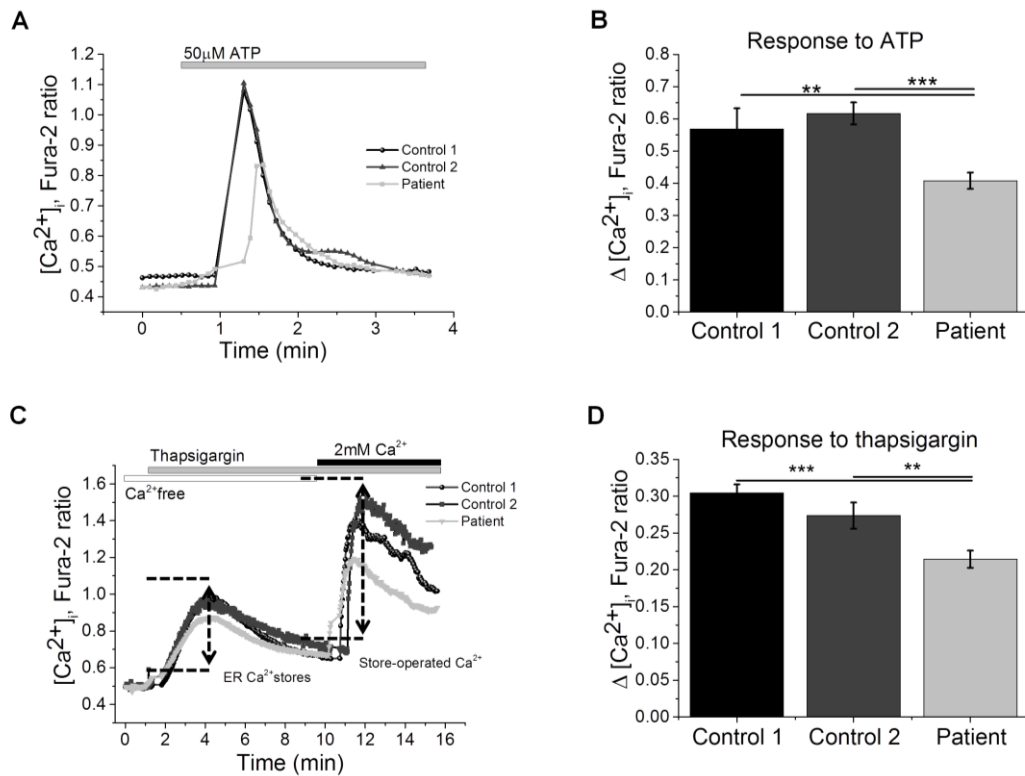
Figure 5-10 Functional studies showing abnormalities of endoplasmic reticulum calcium signalling in *KCTD17* p.Arg145His substitution bearing fibroblasts

All experiments were carried out in triplicate. Data are represented as the mean ± SEM. ''n'' indicates the total number of cells analysed. The asterisks indicate P < 0.05 (*), P < 0.01 (**) and P < 0.001 (***). (A) Typical trace of [Ca2+]c in control and KCTD17-mutant fibroblasts in response to the application of 50 mM ATP. (B) Histograms showing a significantly decreased [Ca2+]c response upon ATP stimulation in mutation-bearing fibroblasts (n=56) versus controls (control 1 n=41; control 2 n=35), as measured by changes in Fura-2 fluorescence intensity. (C) Typical trace of [Ca2+]c in control and KCTD17-mutant fibroblasts in response to the application of thapsigargin (1 μM), and subsequent Ca2+ challenge (2 mM). (D) Histograms demonstrating a significant reduction in ER calcium pool in response to thapsigargin in mutation-bearing fibroblasts (n=53) versus controls (control 1 n=51; control 2 n=65), as measured by changes in Fura-2 fluorescence intensity.

5.3.5 Discussion

Several lines of evidence support the pathogenic role of the *KCTD17* p.Arg145His.

1) In the discovery pedigree, the p.Arg145His variant was located within the only segregating chromosomal locus and Sanger sequencing confirmed perfectly co-segregation with dystonia. This was not the case for any other variant identified by WES that survived the filtering strategy. These latter variants were either not carried by definitely affected subjects (*LRRC6*) or carried by clinically unaffected subjects (*FLG* and *OBSCN*). Given the high penetrance of the disease indicated by the pedigree structure (no obligate unaffected carriers observed over four generations) and the onset of symptoms in the first decade in all affected individuals, we consider extremely

176

unlikely the possibility of the causative mutation for this pedigree being carried by unaffected adults. Furthermore the identified *FLG* and *OBSCN* variants are located in large and polymorphic genes tolerating a high burden of genetic variation (2560 and 4135 rare [MAF < 0.01] non-synonymous variants spread across *FLG* and *OBSCN*, respectively, are listed in the ExAC database versus 71 rare variants observed in *KCTD17*), arguing against a pathogenic role of these changes. Moreover, pathogenic variants in *FLG* and *OBSCN* have been previously linked to diseases unrelated to dystonia, respectively skin diseases (Irvine *et al.*, 2011) and cardiomyopathy (Marston *et al.*, 2015).

2) A screening of the *KCTD17* gene in a cohort of *SGCE*-negative M-D cases revealed the same nucleotide change in the index case of an additional unrelated pedigree with an autosomal dominant pattern of inheritance. In this second pedigree I could not prove segregation due to unavailability of the other affected family members. However, given the striking clinical similarity between this case and the affected individuals of the index family, together with the absence of the variant in over 65,000 internal and publicly available controls, it is highly unlikely this variant could merely represent a private benign polymorphism.

Importantly, I demonstrated that the two families with the p.Arg145His mutation did not share a common founder haplotype and therefore two independent mutational events must have occurred. This is relevant for two reasons; firstly, I can exclude that the *KCTD17* p.Arg145His variant is in linkage with the actual causative mutation but it is not itself pathogenic. Secondly, were the two families to be linked by an ancestral common founder, given the high penetrance of the mutation, I would expect a much higher prevalence of the p.Arg145His mutation as a cause of familial M-D across the British and German population. This is the case, for instance, for the recurrent *GOSR2* G144W mutation, a widespread cause of progressive myoclonus-ataxia syndrome in Nordic populations (Boisse Lomax *et al.*, 2013).

3) *KCTD17* is abundantly expressed in all brain regions and the highest expression was observed in putamen and thalamus. In light of the current view about the neuroanatomical bases of dystonia, seen as a network disorder originating from disrupted circuits involving the sensory-motor cortex, the basal ganglia and the cerebellum (Neychev *et al.*, 2011), this pattern of expression is highly relevant and

supports the pathogenic role of *KCTD17* in the pathogenesis of M-D. Furthermore, focal ischemic lesions of the thalamic subnuclei have been causally linked to the development of a movement disorder that closely resembles M-D (Lehericy *et al.*, 2001). This strengthens the relevance of high *KCTD17* expression in the thalamus and supports the hypothesis of a crucial role for disrupted thalamic pathways in the pathogenesis of *KCTD17*-associated M-D.

KCTD17 encodes for a member of a recently identified family of 26 closely related and highly conserved proteins, the potassium channel tetramerisation domain (KCTD)-containing proteins. KCTD proteins are characterized by the presence of a N-terminal *b*ric-a-brack, *t*ram-track, *b*road complex/*po*xvirus *z*inc finger (BTB/POZ) domain, homologous to the cytoplasmic domain T1 of voltage-gated potassium channels (Liu *et al.*, 2013). The BTB/POZ domain is known to permit protein-protein interactions, either promoting self-oligomerisation or facilitating interaction with other biological partners (Stogios *et al.*, 2005). KCTDs are small soluble proteins, which are not predicted by their structure to form transmembrane domains. Despite the homology reflected in their names, a direct interaction with potassium channels has not been shown for most members of the family and was explicitly excluded for KCTD5, a paralog 85% identical to KCTD17 (Dementieva *et al.*, 2009).

KCTD proteins, despite the high level of sequence similarity, are involved in a surprisingly wide spectrum of cell functions, including regulation of cellular proliferation, gene transcription, cytoskeleton organization, protein degradation targeting via the ubiquitin-proteasome system, and regulation of G protein-coupled receptors (Skoblov *et al.*, 2013). Several members of the KCTD family have a primary role in the central nervous system (Schwenk *et al.*, 2010, Matsui *et al.*, 2013) and a growing number of neurological diseases have been linked to mutations in KCTD genes. *KCTD7* (MIM 611725) mutations cause recessive progressive myoclonic epilepsy (Van Bogaert *et al.*, 2007, Kousi *et al.*, 2012, Krabichler *et al.*, 2012). Copy number variants in *KCTD13* (MIM 60894) have been associated with size of the head, autism disorder and epilepsy (Golzio *et al.*, 2012). More recently a homozygous missense mutation in *KCTD3* (MIM 613272) was identified as the likely cause in a pedigree with severe psychomotor retardation, seizure, and cerebellar hypoplasia (Alazami *et al.*, 2015).

The precise cellular localization and function of the KCTD17 protein are largely unknown. Recent work has shown that KCTD17 contributes to the ubiquitin-proteasome machinery, acting as an adaptor for the CUL3-RING E3 ligase and targeting substrates for degradation through poly-ubiquitinylation (Kasahara *et al.*, 2014). Although most of the KCTD17-CUL3 substrates are currently unknown, CUL3 has been implicated in the elaboration of dendrite branching and neurite terminal morphogenesis in drosophila models (Zhu *et al.*, 2005, Djagaeva and Doronkin, 2009).

A number of cellular pathways, encompassing abnormalities of the cell-cycle and transcriptional regulation, endoplasmic reticulum and nuclear envelope function and control of synaptic function, are thought to underlie molecular pathogenesis of primary genetic dystonias (Ledoux *et al.*, 2013).

How *KCTD17* abnormal function could contribute to dystonia disease mechanisms is currently not known. WGCNA analysis indicates that *KCTD17* may closely interact with *HPCA*, another recently identified dystonia-gene that is involved in calcium signalling (Charlesworth *et al.*, 2015). Through live-cell imaging experiments in patients fibroblast I showed that the presence of the *KCTD17* p.Arg145His mutation reduces Ca^{2+} storage in the ER and opening of store-operated calcium channels. Importantly, our group recently showed very similar defects of ER Ca^{2+} storage in fibroblasts bearing a pathogenic mutation in *ANO3*, another dystonia gene (Charlesworth *et al.*, 2012). This indicates that defective ER calcium signalling may represent a converging pathogenic mechanism in genetically unrelated forms of dystonia.

WGCNA also showed that the putamen *KCTD17* module is enriched with genes involved in dopaminergic signalling, suggests the involvement of the genes in the module with these molecular pathway. Recent work in drosophila strongly reinforces the results of WGCNA and further suggests a relevant contribution of KCTD17 to regulation of dopaminergic transmission in the putamen. *Insomniac* (the *KCTD17* fly homolog) is an essential regulator of sleep homeostasis through the control of the dopaminergic arousal pathways (Stavropoulos and Young, 2011, Pfeiffenberger and Allada, 2012). More specifically, *insomniac* seems to regulate dopaminergic signalling at the post-synaptic level, possibly controlling the turnover of dopamine receptors or their downstream effectors (Pfeiffenberger and Allada, 2012).

Importantly, abnormal post-synaptic dopaminergic signalling in the basal ganglia is one of the main themes in molecular dystonia pathogenesis, a concept recently strengthened by the identification of mutations in *GNAL* causing dystonia (Fuchs *et al.*, 2013). Fitting well with this model, all the genes in the putamen *KCTD17* module assigned to the KEGG "Dopaminergic synapse" pathway (*CACNA1C, PPP1R1B, AKT1, GNAO1,* and *GNB2*) localize and act at the post-synaptic level.

The *KCTD17/HPCA* putaminal module is not preserved across brain regions, which indicates it is a putamen-specific gene network. Importantly, the brain regional specificity of this module may suggest why mutations in *KCTD17* and *HPCA* manifest purely as a dysfunction of the basal ganglia (i.e. dystonia), in spite of the ubiquitous expression in the human brain.

Finally, the molecular pathogenic mechanism whereby the identified *KCTD17* p.Arg145His mutation could lead to M-D is still unclear. Our data shows that the protein stability or subcellular localization is unaltered in presence of the p.Arg145His p.Arg145His. The substitution falls outside the BTB/POZ domain. However it lies in an extremely highly conserved amino acid motif, which is not only completely conserved throughout all species down to *Drosophila*, but is also identical in human paralogous genes (*KCTD2* and *KCTD5*), suggesting an essential role for the protein function.

Notably, recent studies highlighted that tetramerisation is not a prerogative of the BTB/POZ domain but also the C-terminal domain of KCTD proteins may be able to promote tetramers assembly (Correale *et al.*, 2013). Hence, it is possible that p.Arg145His mutation might prevent a correct oligomerisation or interaction with specific protein partners. Alternatively, the KCTD17 p.Arg145His substitution could abrogate the interaction with CUL3, resulting in abnormal degradation of specific substrates via the ubiquitine-proteasome system. For instance, this mechanism has been recently shown for a *KCTD7* pathogenic mutations located outside the BTB/POZ domain (Staropoli *et al.*, 2012).

In conclusion, through a combination of genome-wide linkage analysis and WES in large British kindred, I showed that the missense mutation p.Arg145His in *KCTD17* represents a novel genetic cause for inherited autosomal dominant M-D. The clinical features of the *KCTD17*-mutated cases, although fully consistent with a clinical diagnosis of M-D, were distinct in many ways from the usual phenotype of subjects

with *SGCE* mutations. Dystonia dominated the clinical picture and showed a progressive course, worsening over time and spreading to other sites (including speech involvement), a course unusual for *SGCE*-related M-D. Myoclonus, despite being the presenting symptom in most cases, was overall mild and not as disabling as in *SGCE*-mutated subjects. These phenotypic differences may be explained by the different functions of the two genes, but also by the clearly distinct patterns of brain regional expression. *SGCE* is highly expressed in the cerebellum, whereas its expression is low to moderate in putamen and globus pallidus (Ritz *et al.*, 2011). On the other hand, *KCTD17* expression is high in the putamen and thalamus but relatively low in the cerebellum. Intriguingly, this could be the explanation for the scarce response to alcohol consumption in *KCTD17*-mutated cases, as alcohol probably exerts its beneficial effect in M-D secondary to *SGCE* mutations by modulating cerebellar activity (Ritz *et al.*, 2011).

Preliminary data suggest an involvement of KCTD17 in dopamine synaptic transmission regulation and an effect of the p.Arg145His substitution on ER-derived Ca^{2+} signalling. Further insight into the physiological role of KCTD17 and a better understanding of the pathogenic effect of the p.Arg145His substitution will shed light onto the mechanisms leading to abnormal neuronal activity underlying M-D. Furthermore, the identification of KCTD17 interactors will possibly highlight new potential pharmacological targets for the treatment of dystonia.

Mutational screening of additional cohorts of M-D cases will help to define the frequency and the spectrum of *KCTD17* mutations. *KCTD17* mutations should be considered in cases without mutations in *SGCE* presenting with myoclonus, dystonia or a combination of both, particularly if there is predominant cranio-cervical and laryngeal involvement.

5.4 Tyrosine Hydroxylase Deficiency Causes Autosomal Recessive, DOPA-Responsive, Myoclonus-Dystonia

5.4.1 Statement of Contribution

Dr Stamelou and I examined the family described in this chapter. I performed all the genetic analysis.

5.4.2 Background

I describe here the genetic analysis I conducted in a second, highly informative, family with *SGCE*-negative M-D. While the pattern of transmission was autosomal-dominant in the pedigree described in the previous chapter, in this family the disease was clearly transmitted in an autosomal recessive fashion (see Figure 5-11); three out of four siblings presented with a severe, early-onset movement disorders, while both parents were undoubtedly unaffected.

An important clinical clue toward the identification of the underlying genetic abnormality in this family was the reported L-DOPA-responsiveness of symptoms in all affected subjects, which raised the suspicion of an atypical form of DRD. As discussed in the *Introduction* chapter, mutations in four genes have been convincingly demonstrated to cause DRD: *GCH1* (GTP Cyclohydrolase 1), *TH* (Tyrosine Hydroxylase) and *SPR* (Sepiapterin Reductase) and *DDC* (DOPA decarboxylase).

Although M-D has only been described once in a single family with DRD due to GTP Cyclohydrolase 1-deficieny (Leuzzi *et al.*, 2002), given the strong clinical suspicion of a disorder of the dopamine synthesis pathway, after the exclusion of pathogenic *SGCE* mutations, I sequenced the coding regions of the genes mentioned above and identified compound-heterozygous mutations in *TH*.

5.4.3 Subjects, Materials and Methods

Index family

The clinical characteristics of the patients and the family pedigree are described in the Results. All living family members from the index family were assessed and recruited. Two children of an unaffected individual were not examined. Assessment included a detailed medical interview and a full videotaped neurological examination, with focus on movement disorders. The University College London Hospitals/University College

London ethics committee (University College London Hospitals project ID number 06/N076) approved the study, and all family members gave their informed consent. After obtaining informed consent, a blood sample was collected and DNA was extracted from all examined family members.
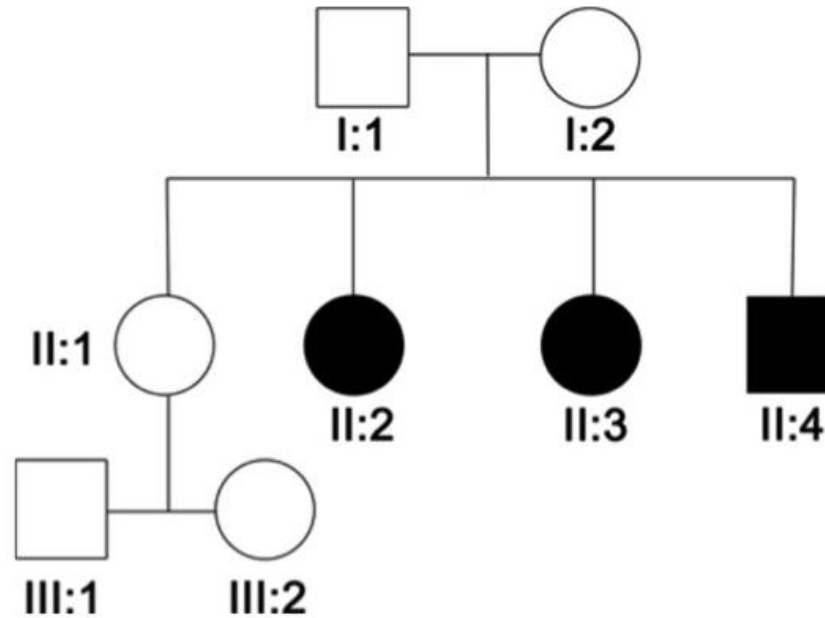
Figure 5-11 Pedigree of a family with recessive L-DOPA responsive Myoclonus-Dystonia

Genetic analysis

Sanger sequencing was performed as described in Materials and Methods section. Primers were designed to amplify all coding exons and splicing sites of the *GCH1* (ENST00000491895; 6 coding exons), *TH* (ENST00000381178; 14 coding exons), *SPR* ENST00000234454; 3 coding exons), and *DDC* (ENST00000444124; 14 coding exons). The primers used in this study are listed in the Appendix.

5.4.4 Results

Clinical description

Patient II-2, the index case, is a 27-year-old, female, who had normal birth. At the age of 6 months she was floppy with poor head control, and subsequently never properly reached normal motor milestones. She then went on and developed prominent and violent myoclonic jerks in all four limbs, trunk and neck. She also developed dystonia, which was most prominent on the upper limbs and face without diurnal fluctuation. She would also have intermittently painful spasms, with extension of all four limbs and

trunk that occurred several times daily, lasted up to several hours, and were accompanied by oculogyric crises and double incontinence and exacerbated by fever, infections or tiredness. Magnetic resonance imaging (MRI) brain and dopamine transporters imaging were normal. *TOR1A* genetic testing was performed and resulted negative.

At the age of 13, she first tried L-DOPA, initially at a dose of 100 mg and subsequently increased up to 800 mg over about 5 years. This led to a gradual but significant improvement of dystonia and myoclonic jerks. She also started speaking and became able to control the electric wheelchair with her left hand, but she could still not use her right hand due to myoclonic jerks. The spasms improved in frequency and severity (5-7 times a week). After the introduction of L-DOPA, cognition improved and she was able to attend a special school and later college. Given the marked response to L-DOPA, the suspicion of dopamine synthesis defect was raised. A phenylalanine loading test was normal. Lumbar puncture was performed under treatment with L-DOPA since the patient refused to stop treatment for investigations and consequently; CSF showed normal pterins; homovallinic acid (HVA) was in the lower normal range 71 nmol/L (normal range: 71-565) and 5-hydroxyindoleacetic acid (5-HIAA) was lower than normal 28 nmol/L (normal range: 58-220) and 3-methyl DOPA was markedly elevated, due to L-DOPA treatment.

She was first seen at the NHNN at age 18. On examination eye movements were normal, she had dystonic grimacing and dysarthria; she had generalized dystonia more prominent on the upper limbs with occasionally choreo-athetoid movements; generalized non-stimulus sensitive, spontaneous and action-induced myoclonus was more prominent in the right side, mostly in the right leg. There was slowing in finger-tapping but not true bradykinesia. She could walk some steps with help. The rest of the examination was unrevealing. Follow-up over the next 9 years revealed no progression of the symptoms. She is still taking 800 mg L-DOPA/daily and occasionally up to 1000/mg, when the spasms are more severe. She has no dyskinesias or further side effects from L-DOPA.

Two of her siblings were similarly affected; case II-3 is a 24 year-old female with an identical picture to patient II-2. She was started on L-DOPA at age 8 years with similar improvement to patient II-2, but significantly better improvement of the jerks. On

examination she had similar findings to the index case, but less myoclonic jerks. Patient II-4 is now 19 and is the youngest sibling. He developed similar symptoms at the same age as II-2 and II-3, with generalized dystonia and prominent myoclonus, but he was treated earlier on L-DOPA at the age of 4. The jerks nearly disappeared. Both II-2 and II-3 are treated with 800 mg L-DOPA/daily (occasionally up to 1000 mg), with no dyskinesias or other side effects.

The older sister, aged 29 and who has two healthy children aged 6 and 8, is unaffected. The father (originally from Nigeria) and the mother (British Caucasian) are asymptomatic and did not show any neurological sign upon detailed examination.

Given the results of the phenyalalanine loading test and CSF analysis, a diagnosis of *GCH1*-related DRD was considered unlikely. The presence of the DYT1 mutations was excluded. However, the analysis of *SGCE* revealed the presence of the splice-site variant c.391-3T>C in the index case, which was interpreted as the likely cause of the disease (Valente *et al.*, 2005). Therefore, when I first started working on this project, the consensus was that this was a family with an atypical, particularly severe, form of *SGCE*-related M-D.

Identification of the Causative Mutation

As a detailed analysis of the segregation of the *SGCE* splice-site variant had not been performed in all available family members, I first checked whether the variant segregated in the remaining subjects (both parents, the affected brother II-4, and the healthy sister II-1). *S*equencing of the variant was performed using primers previously designed and used by our own diagnostics laboratory.

Importantly, I showed that the variant did not segregate, being present in the father, the unaffected sister and absent in the affected subject II-4. Furthermore, the variant is reported at a MAF of 0.2786 in African subjects (as per the ExAC database), thus completely ruling out a pathogenic role and the initial diagnosis of *SGCE*-related M-D was incorrect.

Subsequently, based on the marked L-DOPA responsiveness, we decided to direct the genetic analysis based on the clinical suspicion of a disorder of the monoamine synthesis pathway. Although the CSF analysis was not indicative of any specific neurotransmitter deficiency, this was performed while the patient was on L-DOPA

treatment, thus making unreliable the dosage of dopamine degradation products.

Analysis of *GCH1*, *SPR* and *DCC* genes did not reveal any pathogenic change. However, *TH* analysis revealed that all three affected siblings carried two mutations: a previously described point mutation (c.1-71 C>T) in the promoter region (Ribases *et al.*, 2007, Verbeek *et al.*, 2007) and a novel missense mutation in exon 12 (c.1282G>A, p.Gly428Arg). The chromatograms of the mutations are shown in Figure 5-12A.
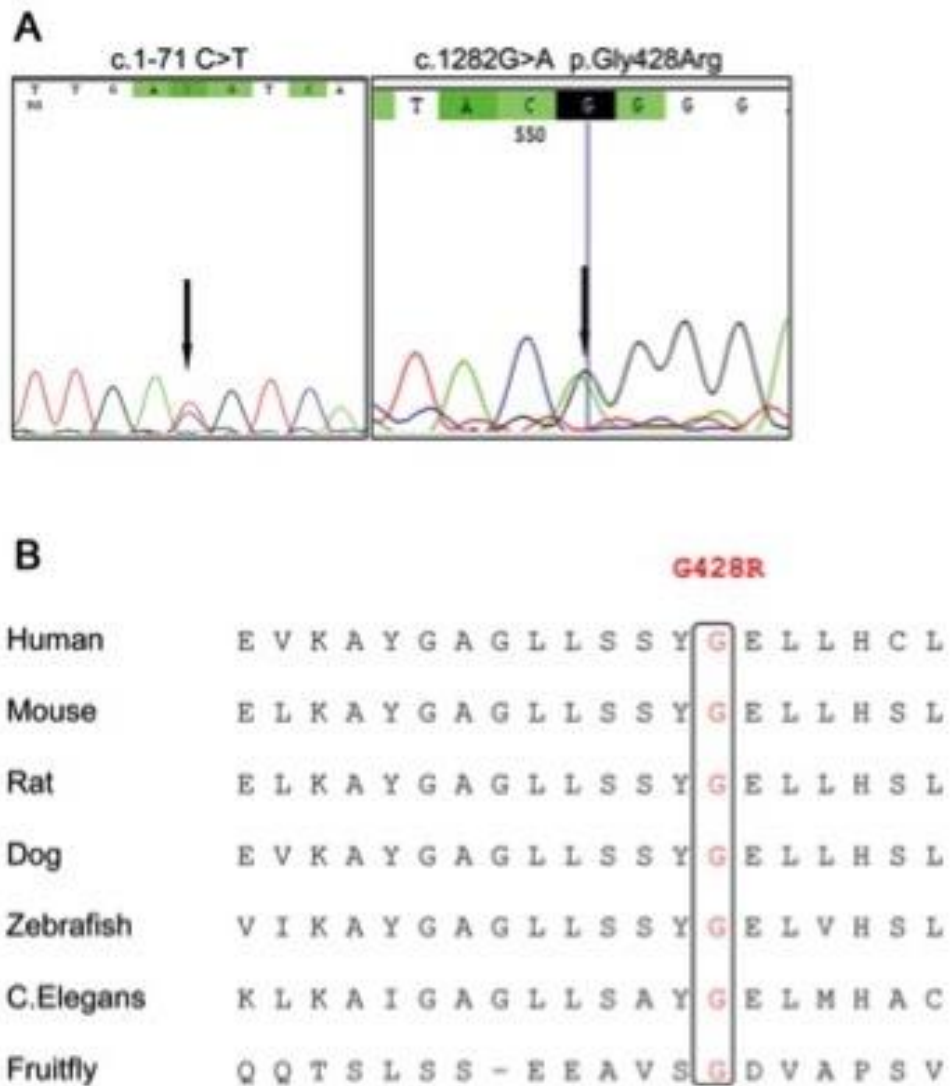
Figure 5-12 Genetic results

(A) Chromatograms of *TH* mutations identified in the present study. (B) Amino acid alignment of *TH* protein showing conservation of the p.Gly428Arg residue in different species.

Segregation analysis confirmed that the patients were compound heterozygotes, being the c.1-71 C>T mutation inherited from the mother and the c.1282G>A inherited from the father. The unaffected sister was heterozygote for the latter mutation. The identified mutation in the gene promoter lies in the Cyclic Adenosine Monophosphate Response Element (CRE), a highly conserved octomer (TGA**C**GTCA→TGA**T**GTCA) located at -74 to -68 upstream the transcription initial codon. The novel variant identified in exon12 p.Gly428Arg is not reported in the ExAC database (containing WES data from more than 10,000 subjects of African ethnical background) and it affects an amino acid highly conserved throughout species. It is consistently predicted by both SIFT, Polyphen-2 and MutationTaster to have a deleterious effect.

5.4.5 Discussion

I report here three members of a family Tyrosine hydroxylase deficiency (THD) who presented with severe myoclonus accompanied by dystonia, consistent with a diagnosis of M-D, as the predominant feature.

It is important that this unusual THD phenotype is recognised and considered in the differential diagnosis of early-onset M-D, as early treatment with L-DOPA is crucial for the final motor outcome in THD (Willemsen *et al.*, 2010). This may be reflected here by the fact that although all three patients were similarly affected before the introduction of L-DOPA, and were subsequently treated with the same L-DOPA dose, the motor outcome is significantly different; the patient that was treated earliest (II-4, 4 years old) showed better response with regard to both the myoclonus and the dystonia than the one that was treated at age 9 years (II-3), and both of them showed a better outcome than the index case (II-2), who was first treated at the age of 13.

Due to presence of a splice-site variant in *SGCE*, this pedigree was initially labelled as atypical *SGCE*-related M-D. When the variant was first found in this family, it was not observed in 384 control chromosomes and therefore the variant was interpreted as likely pathogenic and responsible for the phenotype (Valente *et al.*, 2005). Furthermore, L-DOPA-responsiveness has been reported before in cases with M-D (Luciano *et al.*, 2009). Hence, this feature did not put off the treating clinicians from the diagnosis.

However, in spite of its rarity in European population controls (MAF in EXAC 0.001), the variant is common in African controls. This element, together with the complete

analysis of the variant segregation in all family members, completely ruled out the pathogenic role for the variant and discarded the initial diagnosis of *SGCE*-related M-D.

THD is a rare autosomal recessive, DRD secondary to mutations in *TH* (Iwata *et al.*, 1992, Brautigam *et al.*, 1998). Tyrosine hydroxylase is the enzyme responsible for catalysing the conversion of the amino acid L-tyrosine to L-DOPA and therefore *TH* loss-of-function mutations result in reduced production L-DOPA and dopamine in nigrostriatal neurons.

The phenotype of THD is thought to be a spectrum with overlap of clinical features between two main phenotypes (Willemsen *et al.*, 2010); on the one hand, a progressive hypokinetic-rigid syndrome with onset of symptoms in the first year, usually presenting with a combination of generalized dystonia and parkinsonism and a good response to L-DOPA; on the other a more 'complex encephalopathy', with earlier onset and featuring perinatal abnormalities, diurnal fluctuations, autonomic disturbances and less pronounced response to L-DOPA (Willemsen *et al.*, 2010) (Brautigam *et al.*, 1999, De Lonlay *et al.*, 2000, de Rijk-van Andel *et al.*, 2000, Diepold *et al.*, 2005, Zafeiriou *et al.*, 2009, Yeung *et al.*, 2011).

Despite the large phenotypic variability of THD (Willemsen *et al.*, 2010), prominent myoclonus is not considered classically to belong to THD phenotype. There is one case with 'jerks' reported, however, those presented in the concept of severe encephalopathy, rigidity, spasticity, no response to L-DOPA and death at the age of 9 (Hoffmann *et al.*, 2003).

A recent review of all genetically confirmed THD cases, revealed no phenotype-genotype correlations (Willemsen *et al.*, 2010). Our family showed compound heterozygosity of a point mutation in the promoter region (c.1-71 C>T) and a novel non-synonymous substitution in exon 12 (c.1282G>A, p.Gly428Arg). Mutations in the promoter region of the *TH* gene have been reported previously; mutagenesis studies in rats and cell lines clearly point out that each nucleotides substitution in the CRE of the TH gene results in a drastic reduction of the basal transcription (Lazaroff *et al.*, 1995, Nagamoto-Combs *et al.*, 1997). The c.1-71 C>T mutation has been found to cause a reduction of 90% of basal transcription of the TH promoter (Tinti *et al.*, 1997) allowing a residual activity, which explains the good response to L-DOPA. This variant has been reported previously in two cases, one in the homozygous and one in the compound

heterozygous state (Verbeek *et al.*, 2007). The novel variant detected in exon 12 p.Gly428Arg is highly unlikely to be benign: it is absent in all publicly available databases (over 130,000 chromosomes studied), it affects an amino acid completely conserved throughout species down to invertebrates, and it is predicted by all *in silico* tools to have a deleterious effect.

TH pathogenic variants reported up to now are often private mutations confined to single or small number of pedigrees and, apart from a common mutation (c.698G>A, p.Arg233His) in the Dutch population (van den Heuvel *et al.*, 1998), and one reported in three Greek families (c.707T>C, p.L236P) (Pons *et al.*, 2010), no other founder effects have been described. Consequently, despite most of THD having been reported in Western Europe, the disease is expected to occur worldwide (Willemsen *et al.*, 2010) and the novel mutation described here is the first pathogenic *TH* mutation in patients of African ancestry.

In conclusion, THD should be included in the differential diagnosis of early-onset M-D. This is crucial for an early initiation of L-DOPA treatment, which could influence the motor and cognitive outcome of patients.

5.5 Assessment of The Role Of The *CACNA1B* Arg1389His Variant In a large Myoclonus-Dystonia Cohort

5.5.1 Statement of Contribution

I performed all the genetic analysis described in this chapter.

5.5.2 Background

Recently Groen and colleagues identified the missense variant c.4166G>A; p.Arg1389His (rs184841813) in *CACNA1B* as the likely causative mutation in a Dutch pedigree with five subjects affected by autosomal dominant M-D lacking mutations in *SGCE* (Groen *et al.*, 2015). Unique features in the pedigree were lower limb orthostatic high-frequency myoclonus, attacks of limb painful cramps and cardiac arrhythmias in 3 of the affected subjects (Groen *et al.*, 2011). As *CACNA1B* mutations have not bee identified in other unrelated pedigrees, the implication of mutations in this gene as a cause for M-D is not confirmed.

In this study, we assessed the frequency of the *CACNA1B* c.4166G>A; p.Arg1389His variant in a large multicentric cohort of M-D cases without mutations in *SGCE*. The results of this analysis do not support a causal association between the variant and M-D.

5.5.3 Subjects, Materials and methods

Patients

A total of 520 M-D cases of British, German and Italian origin were recruited for this study in four tertiary movement disorders centres (London, Lübeck, Tübingen and Milan). This cohort is the same described in the previous chapter, with some additional samples recruited by the Tubingen centre. 146 cases (28%) had a positive family history of M-D. 489 white healthy controls of UK and US origin were provided by the International Parkinson's Disease Genomic Consortium (IPDGC). All participants provided written informed consent. Additionally, I assessed the frequency of the variant in European cases listed in publicly available datasets of genetic variation (1000 Genomes, Exome Variant Server and Exome Aggregation Consortium).

Genetic analysis

Given the large size of the entire *CACNA1B* open-reading frame (47 coding exons) and that only one variant has been described to date in M-D, I decided to perform Sanger

sequencing only of the coding exon (exon 28; RefSeq NM_000718.3), which contains the c.4166G>A; p.Arg1389His variant. Primers used for this study are listed in the Appendix.

5.5.4 Results

None of the 146 probands with familial M-D carried the *CACNA1B* c.4166G>A; p.Arg1389His variant. However, the variant was detected only in a single female case of UK origin with sporadic M-D (Figure 5-13). The clinical features of this case are an onset in her mid 30s of tremulous cervical dystonia and myoclonic jerks in the upper limbs. She had no family history for M-D or any other movement disorder. No other family members were available for segregation analysis of the variant.

The total carrier frequency in our M-D cohort, including familial and sporadic cases, is 0.19% (1/520 cases). Surprisingly, the variant was found at a similar frequency in our healthy controls (0.2%; 1/489 individuals). The control carrier of the variant is a 38-year old male without any neurological disease and with no relevant family history of movement disorders.

The variant was found at similar frequencies in the 1000 genome project (0.26%; 1/379 individuals) and Exome Variant Server (0.28%; 12/4,203 individuals) databases. In the Exome Aggregation Consortium database, c.4166G>A; p.Arg1389His is present in 0.11% (38/33,367) of the European subjects (difference to M-D cases not significant; Fisher's exact test $p = 0.4$).
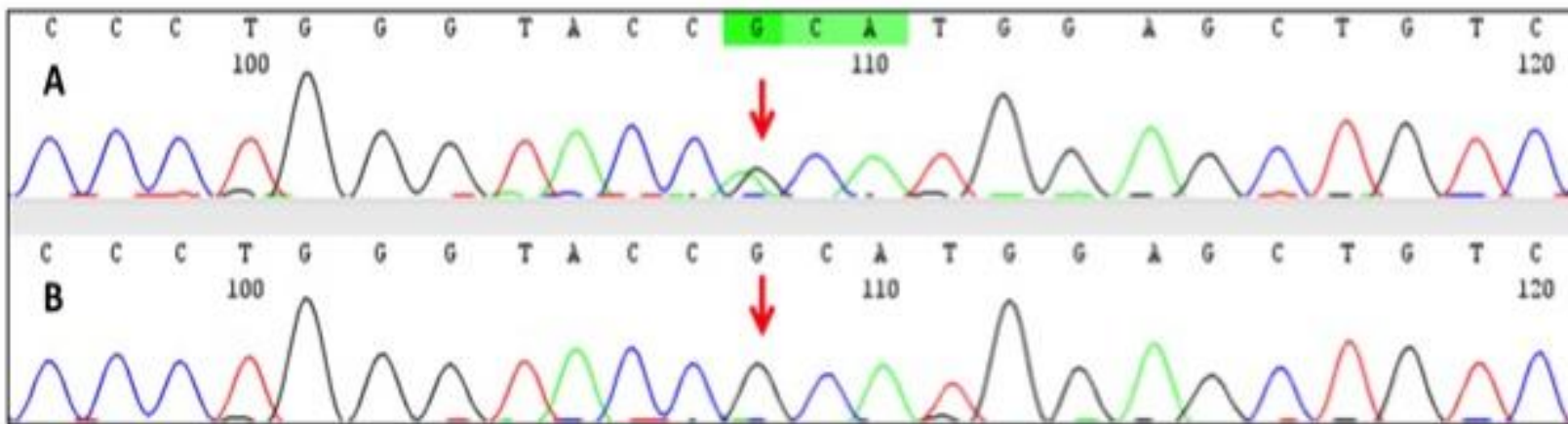
Figure 5-13 Chromatograms showing the *CACNA1B* c.4166G>A; p.Arg1389His variant (A) and a control sequence (B).

5.5.5 Discussion

The c.4166G>A; p.Arg1389His variant was identified by Groen and colleagues combining WES and linkage analysis (13 chromosomal regions identified, with a maximum LOD score of 1.2) in a single dominant M-D pedigree. Sanger sequencing of the *CACNA1B* exons coding for the protein portion spanning from III-S5 to III-S6 failed to reveal other mutations in a further 47 M-D cases.

CACNA1B encodes neuronal voltage-gated calcium channels CaV2.2, which have a key role in controlling synaptic neurotransmitter release (Beuckmann *et al.*, 2003). Furthermore *CACNA1A* mutations in the homologous region of the gene cause familial hemiplegic migraine (Carrera *et al.*, 1999) and episodic ataxia type 2 (Jen *et al.*, 2001).

The *CACNA1B* p.Arg1389His substitution represents therefore an excellent candidate as a disease-causing mutation for M-D.

While assessment of co-segregation with disease of the candidate variant represents the first requirement to prove causality in family-based studies, co-segregation in a single pedigree does not establish with certainty its pathogenic role, especially if other co-segregating coding variants and the possibility of a separate undetected pathogenic variant in linkage disequilibrium cannot be convincingly ruled out. This is the case in the pedigree reported by Groen et al., where two other rare missense changes, c.10355A>G; p.Gln3452Arg in *VPS13D* and c.5308C>T; p.Arg1770Cys in *SPTAN1*, perfectly co-segregated with the disease. However, given the clinical presentation pointing towards a possible channelopathy, the authors assumed that the causative variant was the one in *CACNA1B*.

De novo mutations in *SPTAN1* have been shown to cause a neurological phenotype (West syndrome with severe cerebral hypomyelination, spastic quadriplegia, and developmental delay) (Saitsu *et al.*, 2010) and more recently a microdeletion encompassing *SPTAN1* was detected in a child with epileptic encephalopathy and severe dystonia (Matsumoto *et al.*, 2014). Furthermore, its frequency in the ExAC database is significantly lower (2/33,360 European subjects) than the *CACNA1B* p.Arg1389His. Therefore, the *SPTAN1* could also represent a good candidate gene responsible for M-D.

A candidate variant responsible for a rare disease should be found at a low frequency in

population controls, consistent with the proposed model of inheritance and disease prevalence. As previously mentioned, M-D is a very rare disorder with a suggested prevalence of around 2 per million in Europe (Asmus and Gasser, 2010). I would therefore anticipate highly penetrant mutations causing dominant forms of M-D to be absent or extremely rare in the general population. Yet, this is not the case for p.Arg1389His, which is present at a considerable frequency in our healthy controls and all publicly available databases (~0.1-0.3%). According to the Exome Aggregation Consortium database, the carrier frequency of this variant in Europeans is ~4 times higher than the *TOR1A* c.904_906delGAG deletion (0.026%), which is by far the most common single mutation responsible for dystonia described to date (Valente *et al.*, 1998). Given this frequency, if c.4166G>A; p.Arg1389His were a pathogenic variant, it would be expected to be responsible for a large proportion of familial M-D cases. However, in our cohort not only was the variant not identified in any of the probands with familial M-D, but the overall frequency of the variant did not differ between M-D cases and healthy controls. This does not support a pathogenic effect of the variant even assuming a reduced penetrance.

These results strongly question the pathogenic role of the *CACNA1B* variant p.Arg1389His as a cause for M-D. Despite its compelling biological role, fitting very well with the current themes in dystonia pathogenesis (i.e. abnormal calcium signalling), further genetic evidence is needed before designating *CACNA1B* mutations as a cause for dominant M-D. In the era of NGS, the rate of identification of rare genetic variants has hugely increased. Hence, to avoid false assignment of pathogenicity, a close scrutiny is necessary before causally linking a candidate variant to a disease.

Groen and colleagues performed functional work (whole-cell and single-channel patch recording studies) showing that the identified *CACNA1B* variant affected the normal activity of the channel (i.e. the mutant channel carried less current when open). However, the frequency of this variant in controls is simply incompatible with a dominant variant causing a disease with an aggregate frequency of 1 per 500,000, even if incomplete penetrance is posited. As such there is no remaining support for *CACNA1B* as a causal gene for M-D.

Chapter 6. Exploring the Genetics of Benign Hereditary Chorea

6.1 Outline of chapter

This chapter describes the work I performed to characterise the genetic aetiology, and where possible to identify novel genetic causes, in a cohort of patients with benign hereditary chorea (BHC). As discussed below, *NKX2-1* represents the only gene that has been incontrovertibly associated with familial BHC.

The chapter begins with an overview on BHC. The specific aims of the study were:

1) To define the frequency of *NKX2-1* mutations in the BHC Queen Square cohort

2) To evaluate whether mutations in *ADCY5,* the gene responsible for the condition Familial Dyskinesias with Facial Myokymia, are a cause of BHC

3) Identify novel genetic causes of BHC

6.2 Benign Hereditary Chorea

The term BHC was first introduced in the medical literature in 1967. The authors described a "non-progressive syndrome of inherited childhood-onset chorea with a good outcome in the absence of an underlying progressive disease" affecting 14 individuals, members of a large autosomal dominant 5-generation African American pedigree (Haerer *et al.*, 1967). A similar presentation, with different patterns of inheritance, was subsequently observed in a number of other families, (Nutting *et al.*, 1969, Chun *et al.*, 1973, Bird *et al.*, 1976, Burns *et al.*, 1976).

A single epidemiological study in the Welsh population has tried to establish the frequency of BHC (Harper, 1978). BHC appears to be a very rare syndrome with an estimated prevalence of 1 in 500,000, although this figure is likely to be an underestimate due to poor recognition of the syndrome.

Based on the analysis of 42 individuals with BHC reported in the medical literature since 1967, Kleiner-Fisman and Lang outlined the phenotype of BHC. BHC is mainly

characterized by the onset during infancy or early childhood of a choreic syndrome, often preceded by hypotonia and delay in reaching motor milestones. Affected children are often described as clumsy and report several falls. BHC cases, differently for neurodegenerative forms of choreas, present relatively scarce progression of symptoms and the absence of other major neurological deficits, in particular severe mental retardation or cognitive decline. In some families improvement of chorea can be observed over time (Kleiner-Fisman and Lang, 2007).

After mapping the disease locus to chromosome 14q (de Vries *et al.*, 2000, Fernandez *et al.*, 2001), mutations in the *NKX2-1* gene, encoding the thyroid transcription factor 1 (TTF-1), were recognized in 2002 as a major cause for autosomal dominant BHC (Breedveld *et al.*, 2002). At the same time, a second independent group also identified *NKX2-1* point mutations in cases with congenital hypothyroidism and who also suffered from choreoathetosis, muscular hypotonia, and pulmonary problems (Krude *et al.*, 2002). This discovery represented a major breakthrough in the recognition and diagnosis of this condition. To date ~190 cases and ~100 *NKX2-1* mutations (both point mutations and large deletions; Figure 6-1) have been reported, allowing a better definition and an expansion of the phenotype associated with mutations in this gene (Inzelberg *et al.*, 2011, Gras *et al.*, 2012, Thorwarth *et al.*, 2014). It is now well recognized that *NKX2-1* mutations often lead to a complex multisystem disease, defined brain-lung-thyroid syndrome, which features hypothyroidism, pulmonary defects and a variety of neurological symptoms (including not only chorea, but also hypotonia, neurodevelopmental delay, learning disabilities, behavioural problems, dystonia, myoclonus, tics and ataxia; Figure 6-2) (Gras *et al.*, 2012). In particular, a series of clinical observations have consistently pointed out that dystonic features and EMG-confirmed myoclonic jerks are often present in carriers of *NKX2.1* mutations (Asmus *et al.*, 2007, Armstrong *et al.*, 2011, Gras *et al.*, 2012). Importantly, as chorea tends to improve during adulthood, myoclonus-dystonia (M-D) symptoms may become the most prominent features in adult individuals with *NKX2.1* mutations, leading to significant diagnostic difficulties in differentiating BHC from M-D secondary to *SGCE* mutations.

Around 97% of cases reported in the literature present neurological symptoms, with only a minority of cases presenting with isolated lung involvement (Devriendt *et al.*, 1998, Iwatani *et al.*, 2000, Hamvas *et al.*, 2013). However, it is important to acknowledge that this figure may reflect an ascertainment bias due to selection of cases

196

to be screened for *NKX2.1* mutations mainly based on the presence of neurological involvement. The two larger case series reported to date have demonstrated the presence of thyroid dysfunction in ~70% of mutation positive cases and slightly lower frequency of pulmonary involvement (Gras *et al.*, 2012, Thorwarth *et al.*, 2014). The full triad of brain, thyroid and lung involvement is observed in ~30% of patients, whereas isolated chorea in observed in only ~20% of mutation carriers. Pathogenic *NKX2.1* are often loss-of-function and lead to haploinsufficiency. Missense mutations affect the ability of the protein to bind to DNA (Provenzano *et al.*, 2016).
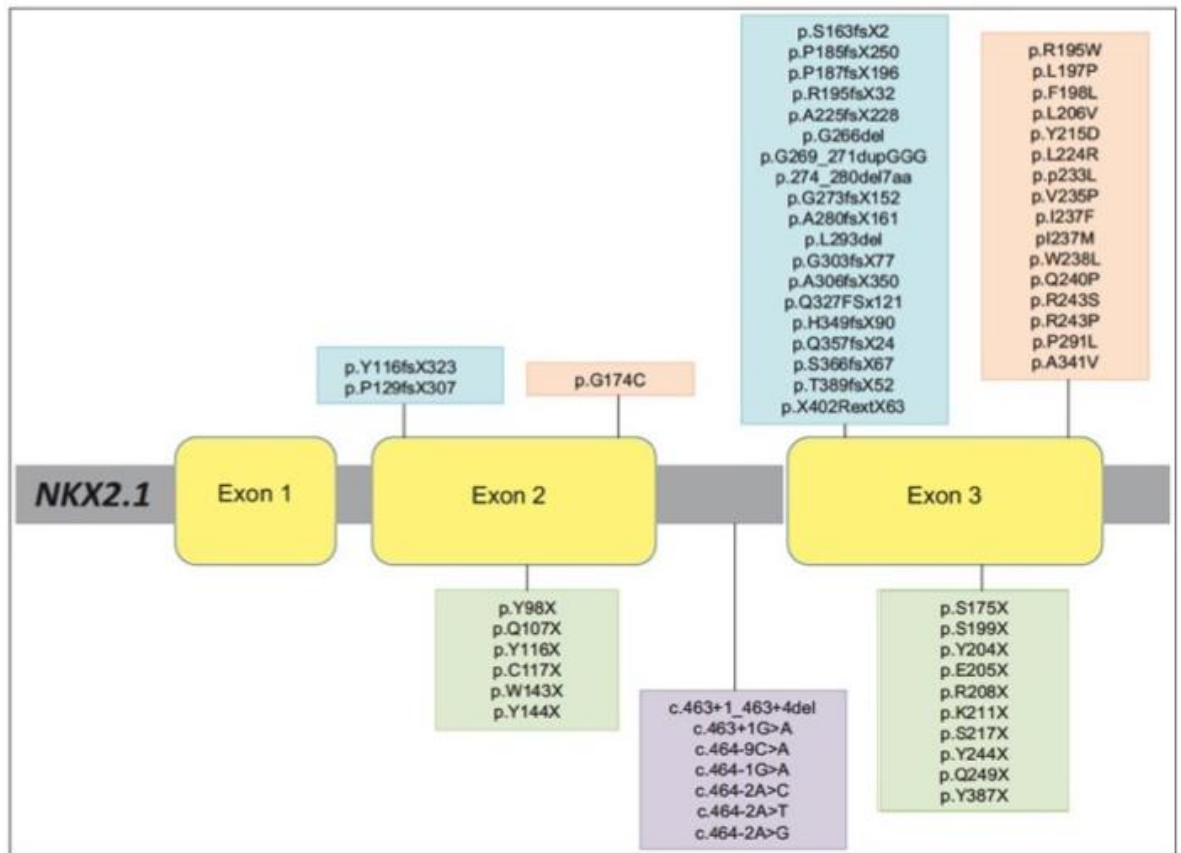
Figure 6-1 Schematic representation of *NKX2-1* point mutations reported to date.
Reproduced from (Peall and Kurian, 2015)

NKX2.1 is a transcription factor gene essential for a correct early development of lungs, thyroid, and forebrain regions, in particular the basal ganglia. *NKX2-1* is expressed in brain, especially in striatal cholinergic neurons. Pathological analysis in one case with genetically confirmed *NKX2-1* associated BHC showed normal gross macroscopic and microscopic appearances, though with reduced count of striatal interneurons (Kleiner-Fisman *et al.*, 2003, Kleiner-Fisman *et al.*, 2005). In mice, homozygous *Nkx2-1* gene deletion results in a lethal phenotype, featuring pulmonary hypoplasia, absence of functional thyroid tissue and complex malformations of brain structures, including the basal ganglia (Kimura *et al.*, 1996).
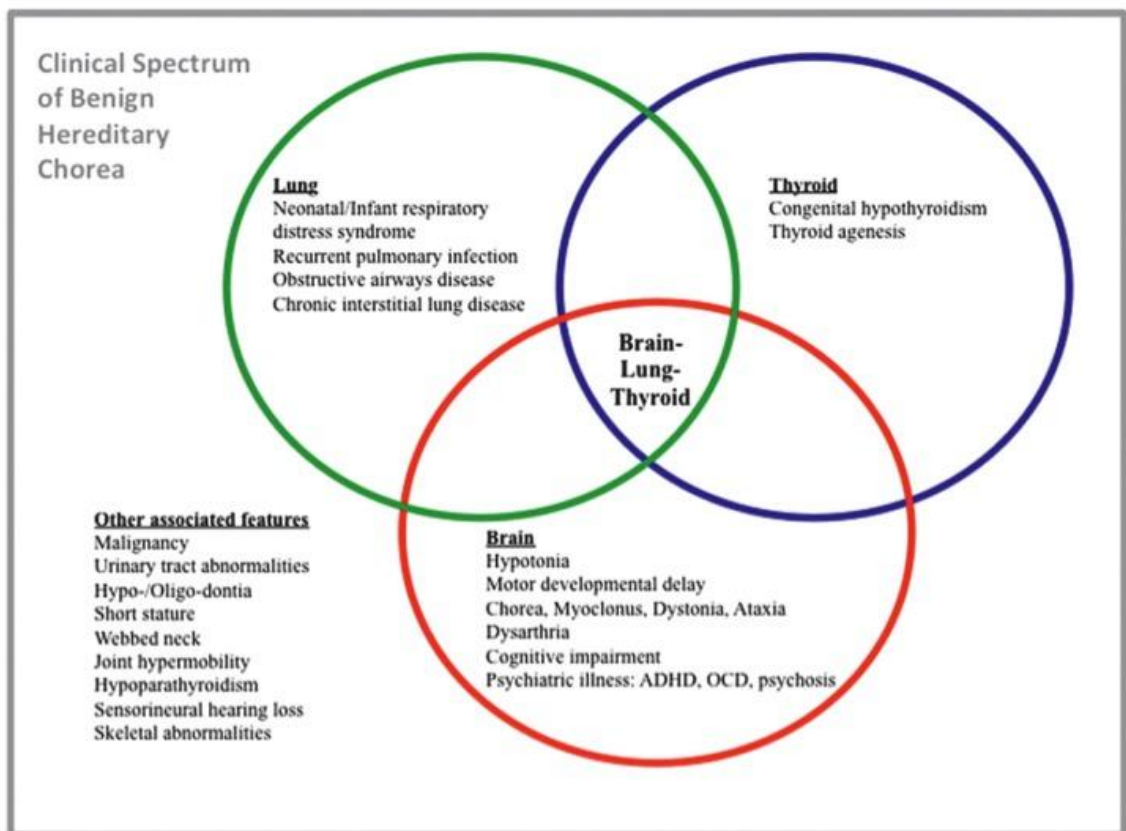
Figure 6-2 Clinical features described in cases with *NKX2-1* mutations
Reproduced from (Peall and Kurian, 2015)

Importantly, a significant number of BHC families do not carry mutations affecting the coding sequence of *NKX2-1*. Breedveld et al. failed to demonstrate linkage to chromosome 14 in four dominant BHC families (Breedveld et al., 2002). Bauer and colleagues did not identify *NKX2-1* mutations in 18 patients with chorea of unknown origin, including the index cases of three families with dominant benign chorea (Bauer *et al.*, 2006). Genetic linkage analysis mapped an alternative disease associated locus on chromosome 8 (8q21.3-q23.3; locus named benign hereditary chorea 2 - BHC2) in two unrelated Japanese families with autosomal dominant non-progressive chorea (Shimohata *et al.*, 2007). However, the clinical phenotype in these pedigrees differed from that of classic BHC, as the disease onset was in adult years and not in childhood. Finally, Thorwarth and colleagues recently completed an extensive clinical and genetic study in a large cohort of 101 cases with suspected BHC cases, clinically ascertained based on the presence of a variable combination of chorea, thyroid and lung disturbances. They identified *NKX2-1* point mutations in 17 cases and large deletions in 10 cases (Thorwarth *et al.*, 2014). Of 74 cases without *NKX2-1* mutations, 15 presented the full triad of brain-thyroid-lung involvement, 34 had brain-thyroid involvement and 8 brain-lung involvement (Figure 6-3), suggesting the existence of variants in *NKX2-1* enhancer and/or promoter region or mutations in other yet unknown genes.
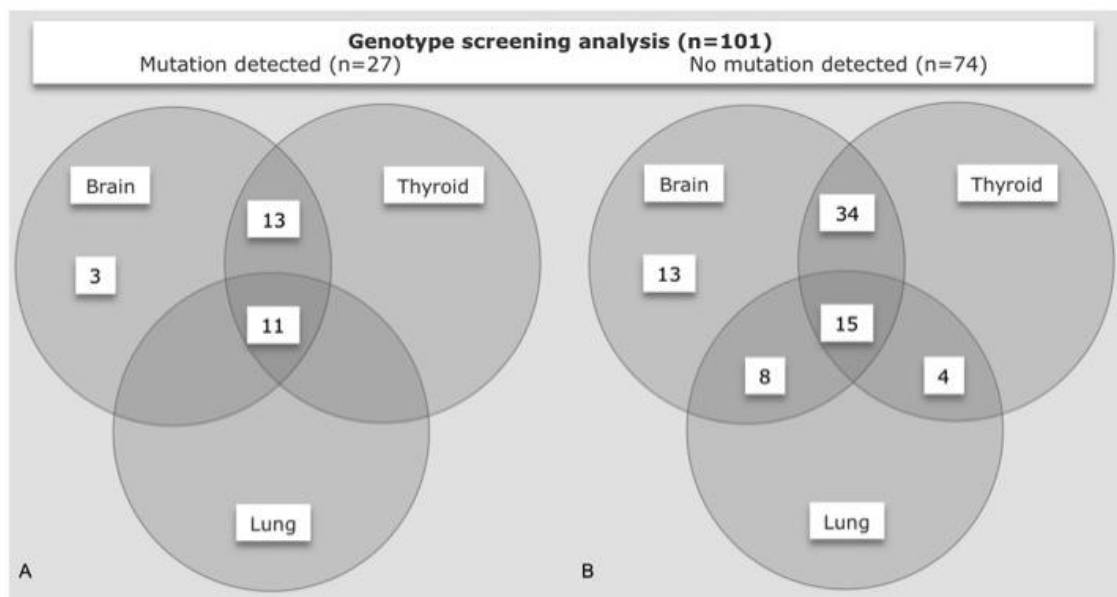
Figure 6-3 Brain, thyroid and lung involvement in index patients and family members, with and without *NKX2-1* mutations, in the largest cohort of Benign Hereditary Chorea cases screened to date
Reproduced from (Thorwarth *et al.*, 2014).

Intriguingly, 2 of the deletions detected in BHC cases were neighboring but not including the *NKX2-1* coding region. One deletion was de novo, while the other segregated in a large pedigree with chorea of dominant inheritance. This finding confirms previous isolated observations of chromosomal deletions neighboring but not including *NKX2-1* in 2 other BHC cases (Barnett *et al.*, 2012, Dale *et al.*, 2012). The pathogenic mechanism of such deletions is currently not clear. The deletions may remove essential regulatory elements downstream of *NKX2-1* and critically affect *NKX2-1* gene expression. The only coding gene encompassed by all deletions not *NKX2-1* reported to date is *MBIP,* which encodes MAP3K12 binding inhibitory protein, a histone acetyltransferase complex involved into chromatin modifications (Suganuma *et al.*, 2010). In situ hybridisation of MBIP in early mice embryos revealed the same expression pattern of *NKX2-1*, including the basal ganglia, forebrain, thyroid and lung, making *MBIP* a plausible cause of a *NKX2-1* deficiency like phenotype (Thorwarth *et al.*, 2014).

6.3 *NKX2-1* Mutational Analysis in the Queen Square Benign Hereditary Chorea Cohort

6.3.1 Statement of Contribution

All participants to this study were clinically characterized and diagnosed by Professor Niall Quinn and Professor Kailash P. Bhatia. Dr Liana Veneziano and I performed the *NKX2.1* mutational analysis.

6.3.2 Background

The Queen square cohort of BHC, consisting of ten families (7 dominant and 3 recessive) and four sporadic cases, was first characterised and published in 2000 (Schrag *et al.*, 2000), before the identification of *NKX2-1* mutations as the underlying genetic cause of BHC. Surprisingly, a systematic mutational analysis of *NKX2-1* was never performed. In this section, I describe the *NKX2-1* analysis performed in the BHC Queen Square cohort.

6.3.3 Subjects, Materials and Methods

Selection of cases for the project

Of the 14 cases reported by Schrag and colleagues, DNA was available for only seven subjects (five familial and two sporadic cases).

A search of the NHNN Neurogenetics database revealed an additional 16 cases, recruited after the publication of the initial series, with a clinical description consistent with BHC. These cases were clinically diagnosed as BHC based on the presence of a movement disorder, with onset prior to the age of 20, predominantly characterized by chorea in the absence of other major neurological features. In particular, none of the selected cases presented significant cognitive decline. Amongst these six had a positive family history for a similar disorder consistent with an autosomal dominant transmission, whereas ten cases were sporadic. In total, 23 cases (11 familial cases and 12 sporadic) were included in the study. Amongst these, four familial cases and one sporadic case had evidence of extra-neural involvement, namely thyroid and lung defects.

All these cases had been extensively investigated for acquired causes of chorea, without reaching a conclusive diagnosis. All cases had previously tested negative for the HD

triplet repeat expansion. Furthermore, given the reported clinical overlap with Myoclonus-Dystonia, all cases had been screened for *SGCE* mutations and were negative. All cases included in this study were recruited at the Movement disorder center of the National Hospital for Neurology and Neurosurgery, Queen Square, London and had given written consent and formal ethical approval by the relevant research ethics committee.

Genetic Analysis

I performed direct Sanger sequencing of the *NKX2-1* coding exons (3 coding exons; transcript ENST00000354822) in all 23 BHC cases, as described in the Materials and Methods section. MLPA analysis to detect *NKX2-1* copy-number variants was performed by Dr Liana Veneziano at the Institute of Translational Pharmacology in Rome.

6.3.4 Results

NKX2-1 mutational analysis

This analysis revealed a total of five different heterozygous *NKX2-1* mutations in five out of 23 BHC cases (21.7%). All mutations were found in cases with familial autosomal dominant BHC (5/11; 45.4%). The identified mutations were a missense mutation (c.605A>G; p.Gln202Arg), two STOP-gain mutations (c.622C>T;p.Arg208* and c.817A>T; Lys241*), one splice-site mutation (c.463+1G>C;p?), and one intronic variant (c.464-24A>C). Two point mutations (c.463+1G>C and p.Arg208*) have been previously described in BHC cases and are therefore established pathogenic variants, whereas the other variants are reported here for the first time. All variants are absent in all publicly available datasets (including ExAC). Segregation analysis supported a pathogenic role for all the identified variants as they were all found in other affected family members (see below). The missense change Gln202Arg is predicted pathogenic by Polyphen-2, SIFT and MutationTaster, and affects an amino acid completely conserved down to invertebrates. The effect of the two intronic mutations on splicing was evaluated *in silico* using Human Splicing finder (http://www.umd.be/HSF3/). The software predicted a highly detrimental effect for the c.463+1G>C (i.e. broken wild-type donor site, most probably affecting splicing). Conversely, the *in silico* prediction tool did not highlight any significant splicing motif alteration determined by the c.464-24A>C variant, suggesting that this mutation may not have any impact on splicing.

However, the variant segregated in other two affected family members and is completely absent in all publicly available datasets. As we did not have access to RNA to test experimentally the effect of the mutation on splicing, the pathogenic role of this variant remains uncertain.

Transmitted and *de novo* large deletions neighbouring, but not encompassing, the *NKX2-1* coding region have been recently described in cases with familial and sporadic BHC (Thorwarth *et al.*, 2014). Thus, all cases without *NKX2-1* point mutations or large deletion were genotyped using a dense array HumanOmni 2.5 (Illumina). However, no deletions were detected (Figure 6-4).

Figure 6-4. Array data of patient with BHC showing no deletions either encompassing or neighbouring the *NKX2-1* locus

Clinical presentations of cases with NKX2-1 mutations

<u>Family-1</u>

This pedigree has been reported before (Robinson and Thornett, 1985) and represents family 7 in the paper of Schrag and colleagues.

The proband, aged 46 when last examined, is the product of a normal pregnancy and his birth was uncomplicated. His motor milestones were delayed and as a child he suffered with several falls per day. He developed involuntary movements and upper limb jerks early in childhood, which progressed until age 11. After that, the movement disorder began to improve. When last assessed, the involuntary movements would still represent a source of social embarrassment, but they were not functionally invalidating. He had no cognitive difficulties. On examination he had generalised dystonia affecting the face, hands and feet, with super-imposed myoclonic jerks, mainly distributed in the upper body. He had a dystonic gait. Dystonia dramatically improved with a small dose of trihexyphenidyl (4 mg/day) combined with a small dose of L-DOPA (600 mg/day), with an almost complete resolution of symptoms.

His son, who carried the same mutation, reported a similar medical history, with delayed motor milestones, frequent falls in childhood and an onset of the movement disorder very early in life. On examination, at age 22, he displayed generalised chorea, frequent stutter and gasps. He was not on any treatment when last assessed. Nobody else in the family was affected. The available medical notes did not mention any lung or thyroid involvement. Both cases carried the pathogenic splice site mutation c.463+1G>C.

<u>Family-2</u>

This family represents family 8 in the paper of Schrag et al. This 38-year-old woman was the product of a normal pregnancy and delivery. She had delayed reaching of motor milestones, with walking independently only at 3 and ½ years. As a child she would have multiple falls per day and she was clumsy and poorly coordinated. She was unable to run or ride a bicycle. Involuntary movements appeared at a very early age and these would affect mainly lower limbs, making her balance worse. Over the years the condition worsened, forcing her to use a wheelchair outdoors to prevent falls. Due to the presence of significant learning difficulties she had to attend special schools.

Her examination showed mild jerky choreic movements affecting the face, the trunk and

the four limbs. Her speech was slurred, but the rest of the cranial nerve examination was unremarkable, including eye movements. There was mild posturing of hands and feet. Gait was choreic with superimposed elements of ataxia. A trial of L-DOPA up to 600mg/day was not beneficial and therefore trihexyphenidyl was prescribed, though no information about the response to this treatment is available in the patient's notes.

She carried the pathogenic mutation p.Arg208*, which was also carried by her similarly affected mother and brother.

Family-3

This family represents family 10 in the paper of Schrag and colleagues

Unfortunately, I was not able to retrieve any relevant clinical information for this pedigree. The pedigree consists of two siblings and their mother, all affected. They all had onset of symptoms in the first two years of life and all had delayed motor milestones and experienced many falls per day during childhood. Intellectual functioning was reported to be low average. The disease symptoms slightly improved with age in all family members. They all carried the intronic variant c.464-24A>C, of uncertain clinical significance.

Family-4

The proband is a 49-year old lady born via an uncomplicated delivery after a normal pregnancy. She was a 'floppy' baby. Her motor milestones were delayed, with delayed independent walking. At age 2 she was diagnosed with cerebellar ataxia. She experienced lifelong balance problems and, at around age 16, the balance worsened due to the appearance of choreic movements. Benztropine was then started resulting in improved symptoms. Hypothyroidism was diagnosed around age 40 and treated successfully with levothryoxine. She took no medications for the movement disorder.

On examination, her gait was mildly ataxic and she had clear chorea and dystonic movements of her head and shoulders and dystonic posturing of the hands while walking. Eye movement examination revealed ocular apraxia with difficulty initiating saccades, broken pursuit movements, hypometric saccades and gaze impersistence. She had mild dysarthria. Here daughter was also affected and both cases carried the p.Lys248* mutation, which was not found in her parents, brothers and sisters (all

unaffected). After identifying the *NKX2-1* variant in this case, I was informed that a genetic diagnosis had actually already been reached and the clinical description of this case had already been published (Veneziano *et al.*, 2014).

<u>Family-5</u>

This case, aged 35 when last assessed, was born 3 weeks premature and initially fed with difficulty. She had a chest infection as a new-born and her initial motor milestones were delayed. Twitching choreic movements in here limbs were noticed since birth and, as soon as she started walking, she began to experience several falls per day. Her symptoms gradually improved with age. On examination she had a mix of chorea and dystonic posturing affecting the four limbs. She was not taking any medication for the movement disorder. Her daughter was similarly affected and both carried the novel missense change p.Gln202Arg.

6.3.5 Discussion

While several studies are available in the literature describing ~ 200 BHC cases caused by *NKX2-1* mutations (recently reviewed in [Peall and Kurian, 2015]), surprisingly few studies have systematically assessed the contribution of *NKX2-1* mutations in cohorts of clinically defined BHC cases.

In this chapter I report the results of a detailed screening of *NKX2-1,* by means of Sanger sequencing and MLPA analysis, of the BHC Queen Square cohort. All these cases fully met the current clinical definition of BHC, as they all presented in childhood with a non-acute onset, predominantly choreic, movement disorder, which was scarcely progressive and did not include prominent additional neurological features, in particular cognitive decline. As dystonia, in combination with chorea, has been observed in genetically proven *NKX2-1*–mutation cases (Fung *et al.*, 2006, Armstrong *et al.*, 2011), this feature was not considered as an exclusion criterion for the study.

The study included both familial and sporadic cases as it has been recently shown that a high proportion of mutated cases carry de novo mutations and therefore the absence of a positive family history should not excluded a diagnosis of *NKX2-1*–related disease (Gras *et al.*, 2012). All sporadic cases had all been extensively investigated for acquired causes of chorea.

Importantly, I show that only five out of 23 BHC cases carried variants in the gene. All

cases had a positive family history for the condition and mutations were shown to segregate in additional affected family members, strongly supporting their pathogenic role. Four of the five identified mutations are either established pathogenic changes or are clear loss-of-function variants, and therefore pathogenic by definition. More controversial is the role of the intronic variant found in family 3, as *in silico* tools did not predict an obvious effect on splicing and I did not have access to patients' RNA to establish experimentally the effect on splicing. However, in support of its pathogenic effect, the mutation is completely absent in all publicly available datasets and segregated in the three available family members. Furthermore, the role of deep intronic mutations in Mendelian diseases is increasingly recognised (Akman *et al.*, 2015, Stepensky *et al.*, 2016).

Although the yield of mutation positive cases (21.7%) of this study could look surprisingly low, it is actually in line with what has been reported by other groups. In particular, Thorwarth and colleagues have recently completed an extensive clinical and genetic study in a large cohort of 101 cases with clinically suspected BHC cases and found that 74 cases (73% of the cohort), of which 15 presented with the full triad of brain-thyroid-lung involvement, actually did not carry mutations in *NKX2-1* (Thorwarth *et al.*, 2014). Similarly, in our cohort, three out five cases with brain-thyroid-lung disease, two of which with a clear autosomal dominant family history, did not carry *NKX2-1* point mutations or deletions, or the recently described deletions of the chromosomal region neighbouring *NKX2-1*. These results clearly indicate the existence of either undetected variants in *NKX2-1* (e.g. in the enhancer and/or promoter region or deep intronic mutations) or mutations in other yet unknown genes that critically interact with *NKX2-1* for the correct development of striatal neurons and of thyroidal and pulmonary tissues.

Interestingly, part of this cohort (and three of *NKX2-1*-mutated cases; family 1,2, and 3) had been reported back in 2000, before the discovery of *NKX2-1* mutations (Schrag *et al.*, 2000). While all three families had at some point been labelled as affected with typical BHC, several cases from all three families, when clinically reappraised for the paper of Schrag and colleagues, were re-assigned to other diagnostic categories, such as M-D or generalised dystonia. This element clearly suggests the difficulty of recognising genetic entities on clinical grounds alone. Furthermore, it highlights the broad clinical heterogeneity associated with mutations in *NKX2-1*.

In conclusion, while the term BHC is often used to imply the presence of *NKX2-1* mutations, a significant number of sporadic cases and families with BHC do not carry mutations in this gene. Furthermore, *NKX2.1*-mutated cases can frequently present with movement disorders other than chorea.

6.4 *ADCY5* Mutational Analysis in a Cohort of Benign Hereditary Chorea Cases

6.4.1 Statement of Contribution

I performed all the genetic analysis described in this section.

6.4.2 Introduction

In 2001 Fernandez and colleagues described a North American 5-generation pedigree of German origin with 18 members affected with a childhood-onset autosomal dominant movement disorder. The clinical presentation in this family was that of a hyperkinetic movement disorder featuring predominantly chorea and dystonia involving the limbs, neck, and face. Perioral and periorbital twitching was also observed in some family members and needle electromyogram (EMG) in two individuals revealed what was initially thought to be myokymia (Fernandez *et al.*, 2001). The disease was consequently named Familial Dyskinesia with Facial Myokymia (FDFM).

In 2009 the disease locus was subsequently mapped to chromosome 3p21-3q21 (Raskind *et al.*, 2009), but only recently Chen and colleagues identified using WES a missense variant in *ADCY5,* encoding adenyl cyclase 5 (AC5), as the causative mutation (Chen *et al.*, 2012). Prior to the identification of facial myokymia as one of the core features, individuals from the original FDFM kindred had been described as affected with familial essential ("benign") chorea (Bird *et al.*, 1976). Hence, given the large phenotypic overlap between FDFM and BHC, I hypothesised that *ADCY5* mutations could be responsible for BHC in cases lacking mutations in *NKX2-1*.

I therefore performed a mutational analysis of *ADCY5* in the Queen Square cohort of *NKX2-1*-negative BHC cases and in a second cohort of *NKX2-1*-negative BHC cases of Italian origin.

6.4.3 Subjects, Materials and Methods

Samples

The eighteen BHC cases that did not carry *NKX2-1* mutations (see previous section), including six with an autosomal dominant family history and 12 sporadic, were initially selected for this study. An additional cohort of 35 cases of Italian origin, clinically diagnosed by Prof Nardo Nardocci's and Dr Carlo Fusco's groups, was subsequently

studied. Dr Liana Veneziano and Dr Barbara Garavaglia's laboratories had previously performed the *NKX2-1* analysis in the Italian cohort, including Sanger sequencing and MLPA analysis.

Genetic Analysis

WES was performed in ten of the BHC cases. Cases were prioritised for WES if they had an autosomal dominant family history (five cases) and/or an age at onset < 10 years (five cases), assuming that a genetic aetiology would be more likely for these cases.

In the Queen Square BHC cohort, the search for *ADCY5* mutations was performed either by interrogating WES data or by Sanger sequencing of the *ADCY5* coding region (21 exons; transcript ENST00000462833). As WES poorly covered exon 1 due to its high GC content, Sanger was used to sequence exon 1 in all cases. Visual inspection revealed that all other exons were adequately covered by WES.

In the Italian cohort I screened by Sanger sequencing only *ADCY5* exons 2 and 10. This strategy was undertaken as these two exons are likely to represent mutational hotspots.

WES and Sanger sequencing were performed as described in the Materials and Methods chapter. The primers used to amplify the coding exons and splice sites of *ADCY5* are listed in the appendix.

Segregation analysis was performed in all available relatives of mutation positive-cases.

Expression Profiling of ADCY5 and NKX2-1 in Brain Tissue

Brain *ADCY5* and *NKX2-1* mRNA regional distribution and expression in the normal adult human brain and longitudinal expression changes during the course of human brain development were determined using microarray analysis of human post-mortem brain tissue from the UK Human Brain Expression Consortium and the Human Brain Transcriptome database, as previously detailed in the Materials and Methods chapter.

6.4.4 Results

Genetic Analysis

The search for mutations in the entire *ADCY5* coding region in the Queen square BHC cohort revealed the presence of five different heterozygous mutations.

The c.1252C>T; p.Arg418Trp variant was identified in two unrelated cases. This amino

acid change has been previously reported in association with FDFM (Chen *et al.*, 2014) and is absent in all publicly available datasets of population controls (dbSNP, 1000genome project, NHLBI exome variant server and Exome Aggregation Consortium). All *in silico* prediction tools (Polyphen-2, SIFT and Mutation Taster) consistently predict a deleterious effect of the mutation.

Another missense variant (c.2117C>T; p.A706V) was detected in the index case of a pedigree with autosomal dominant BHC (brain-lung-thyroid syndrome). This variant is novel, as it is not reported in any of the databases of genetic variations.

The variant was predicted benign and tolerated respectively by Polyphen-2 and SIFT, but disease causing by MutationTaster. Segregation analysis in the family showed that the mutation was absent in the affected mother and was inherited by the unaffected father, thus ruling out any pathogenic relevance. A non-coding variant in the 5' UTR (c.1-5G>C; rs566725675) together with the missense variant c.29C>T; p.P10L (rs143905423) (phase of the mutation not know) were detected in a sporadic case of African ancestry. The phase of the two mutations is not known. Both variants are reported with a MAF $\geq$ 1% in control individuals of African ancestry as reported by the ExAC, thus excluding a pathogenic role.

In total 2/18 probands (11.1%) from the Queen Square cohort carried pathogenic *ADCY5* variants, both located in exon 2.

The analysis of exons 2 and 10 in the Italian BHC cohort revealed that three probands (3/35; 8.5%) carried pathogenic *ADCY5* missense mutations, all involving the same amino acid residue, Arg418. The variant c.1252C>T; p.Arg418Trp, the same change identified in the two Queen Square cases, was also found in one Italian sporadic case. Two novel variants, c.1253G>A; p.Arg418Gln and c.1252C>G; p.Arg418Gly were found in a sporadic and in a familial case, respectively. Both variants are absent in all publicly available datasets and are predicted pathogenic by Polyphen-2, SIFT and MutationTaster.

Clinical Presentations of Cases with Pathogenic ADCY5 Mutations
Clinical information of the patients with pathogenic *ADCY5* mutations identified in this study is summarized in Table 6-1.

<u>Family-1</u>

The clinical description of this pedigree has been previously published in 1981, as part of a report describing a series of families with benign (non-paroxysmal) familial chorea (Sleigh and Lindenbaum, 1981). The index case is a British 36-year old man. His birth and early development throughout infancy were normal. In the first year of life he progressively developed brief choreic movements at rest, involving the face and the four limbs. Movements were markedly worsened by excitement, stress or tiredness. Around the age of 18 he also developed painful spasms of the four limbs, particularly frequent and severe upon awakening. Symptoms progressed over the years and neurological examination at the age of 28 revealed dysarthric speech and severe abnormal involuntary movements comprising generalized chorea with facial grimacing and marked dystonic features. Both chorea and dystonia were present at rest, but action significantly exacerbated movements in the limbs. Eye movements were abnormal with gaze impersistence and use of head thrust to initiate saccades. Gait was unsteady with both choreic and dystonic features, but cerebellar testing was otherwise normal. He never displayed facial myokymia and EMG of periorbital and perioral regions failed to show either myokymia or other signs of motor neuron hyperexcitability. Over the years different medications were tried without major improvements, including trihexyphenidyl, tetrabenazine, baclofen, L-DOPA and clonazepam. He is currently on a combination of trihexyphenidyl (3 mg/day) and tetrabenazine (75 mg/day), which he finds helpful in reducing the intensity and frequency of the spasms. His 64-year old father also developed hyperkinetic movements in the first year of life. His neurological examination mainly consisted of generalized chorea, but no dystonic posturing. Overall, his clinical presentation was much milder than his son's one. Besides chorea, on examination he had marked ocular and motor impersistence and tandem walking difficulties. Cerebellar testing was otherwise normal. At the last follow-up, when he was 61, occasional twitches were observed in the periorbital areas, but an EMG performed on the same day did not show myokymia. A low dose of tetrabenazine was tried but was not tolerated due to the developed of depression. He is currently taking trihexyphenidyl (7.5 mg/day), with satisfactory control of the dyskinesias. Higher doses were not tolerated due to the occurrence of cognitive difficulties. There was no history of movement disorders in other family members, including both paternal grandparents of the index case.

The heterozygous *ADCY5* c.1252C>T; p.Arg418Trp mutation was found by WES and confirmed by Sanger sequencing in subject III-1. However, Sanger sequencing surprisingly failed to detect the mutation in the affected father (Figure 6-5). Mosaicism has been previously reported in patients with mild presentation of Mendelian disorders (Beicht *et al.*, 2013). We therefore suspected that Sanger sequencing might have missed the mutation in the father due to low-grade somatic mosaicism.

As next-generation sequencing has been shown to be a more sensitive method to detect this type of mutations (Beicht *et al.*, 2013; Miyatake *et al.*, 2014), WES was subsequently performed also in subject II-1. Interestingly, this disclosed the presence of the mutated allele in 9/110 of the sequence reads (~8% versus ~40% in his son; Figure 6-5), confirming the presence of low-level somatic mosaicism. This suggests that the mutation arose in the father during early stages of embryogenesis. Sanger sequencing analysis showed that the unaffected mother and sister of the index case did not carry the mutation.

Family-2

This is a 22-year-old man of Pakistani ethnicity. He is the son of a consanguineous marriage (parents are first degree cousins) and he is the first of four siblings. He is the only affected member in the family. He had delayed motor milestones with walking at approximately 20 months. Since then his gait has always been abnormal, being mainly characterized by arching of the trunk, walking on tiptoes and inversion of both feet. Around the age of 2 he developed constant involuntary movements involving all four limbs and trunk, which became progressively more evident over the years. Movements were largely exacerbated by stress and anxiety. Around the age of 10, he developed "fits" of violent hyperkinetic movements and painful spasms of all four limbs, mainly occurring at night. A polysomnographic study performed to investigate their nature excluded any epileptic activity and showed that the attacks occurred when the patient was awake. Neurological examination showed he had moderate generalized chorea at rest, and intermittent distal dystonic posturing in the four limbs. The hyperkinetic movements were dramatically increased by action. Gait was unsteady, but cerebellar testing was otherwise normal. Cranial nerve examination showed ocular impersistence and frequent facial choreic movements were also observed. The patient declined an EMG of the facial muscles.

He is currently taking trihexyphenidyl (30 mg/day) and tetrabenazine (50 mg/day), which partially reduced the intensity of the dyskinesias and the frequency of the spasms.

WES and subsequent Sanger sequencing analysis showed the presence of the *ADCY5* c.1252C>T; p.Arg418Trp change in the heterozygous state in the affected. The mutation was *de novo*, as Sanger sequencing showed its absence in both healthy parents and in the three unaffected siblings.

Family-3

The proband is a 14-year-old Italian girl born pre-term (38th week) from healthy parents. She presented with psychomotor delay and could walk independently at around age 3. At age 4, she developed a generalized hyperkinetic movement disorder featuring a combination of chorea and dystonia, which made ambulation difficult and caused frequent falls. Pyramidal signs were present in the lower limbs together with a bilateral foot dystonia, requiring splints and regular botulinum toxin injections. Since the first months of life, this patient presented severe paroxysmal worsening of chorea upon falling asleep, which could happen in clusters of 2-10 attacks lasting up to 30 seconds each with spontaneous remission. In addition, she later presented two different kinds of paroxysms, one occurring mainly during sleep (generalized dystonia and dyskinesias with facial grimacing and no sleep interruption, with onset around age 4), and one during the day (multiple sudden falls due to give-way of legs without premonitory sensation, with onset around age 11). All the types of attacks were favored by tiredness and emotions, but no clear triggering factors were reported.

Examination at age 14 showed generalized chorea involving also the perioral muscles, upper and lower limbs dystonic posturing and fixed dystonia (in turning and plantar flexion) of the left foot. Scissoring gait with pyramidal signs in the lower limbs were present and speech was markedly dysarthric.
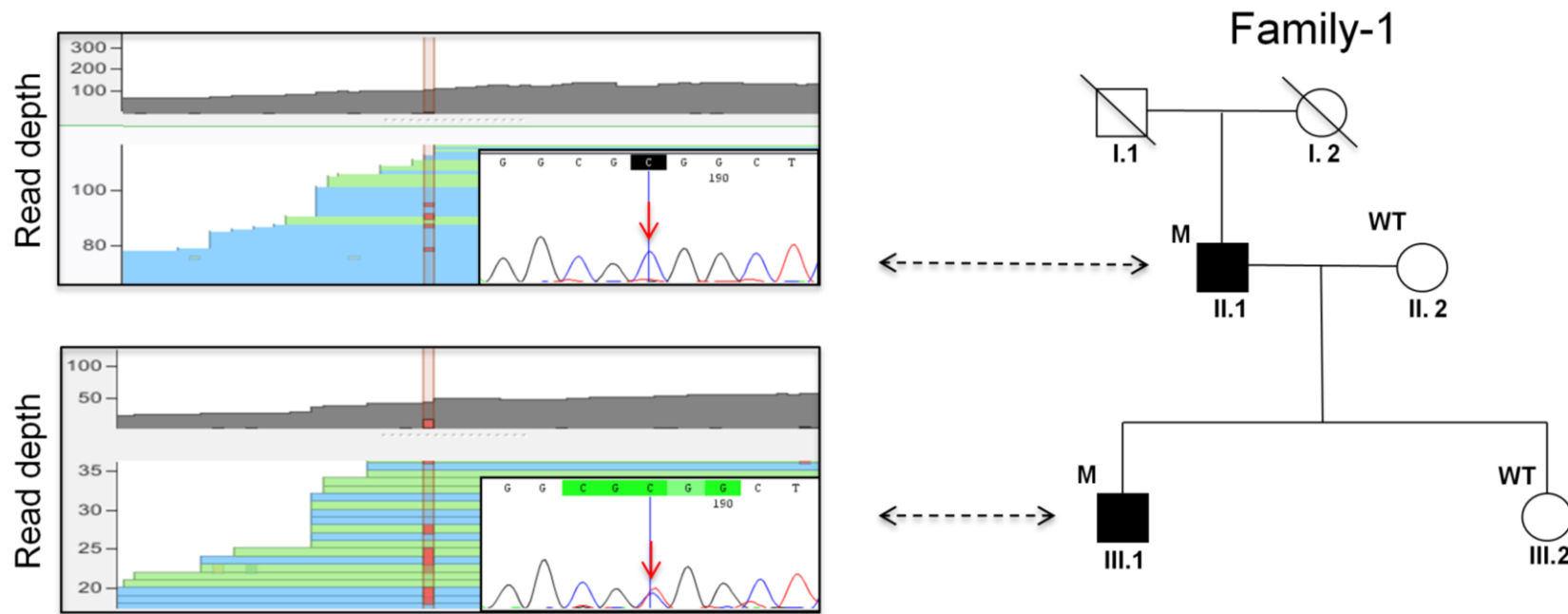
Figure 6-5 Pedigree and genetic results of family 1

On the left the visual output of the WES data and Sanger sequencing results in the affected individuals carrying the p.Arg418Trp mutation. In the top section of each box the read depth of the exonic portion of *ADCY5* involved by the mutation is shown. In the bottom part of each box, samples of the reads carrying the mismatching allele are displayed. The mutant T replacing a C is highlighted in red. Sanger sequencing failed to show the mutation in individual II-1.

Overall, the severity of movement disorder was reduced as compared to infancy, and so was the frequency of nocturnal paroxysms; however, diurnal paroxysms were very disabling and could occur several times per day. She was on Trihexyphenidyl 32 mg/day.

Sanger sequencing showed she carried the p.Arg418Trp change, which was demonstrated to be de novo.

Family-4

The proband is an 18-year-old boy of Italian origin born from healthy parents. He presented with delayed motor milestones and a tendency to tiptoe walking around the age of 18 months. Since his first months of life, nocturnal paroxysms characterized by generalized dystonia with inconsolable crying, lasting for hours, disrupted his sleep. During infancy he developed generalized chorea and myoclonic jerks also involving facial muscles. Episodic worsening of dyskinesias without specific triggers accompanied by hyperventilation was noticed during childhood with a weekly frequency. Examination at age 17 showed generalized asynchronous, non-stimulus sensitive myoclonic jerks at rest, mild dysarthria, scissoring gait with pyramidal signs in the lower limbs and dystonia of upper limbs and the trunk. Diurnal and nocturnal paroxysms were still present, albeit at a decreased frequency (one episode per year). Overall no progression in the severity of his movement disorder was noticed as compared to infancy, though choreic movements decreased and myoclonic and dystonic aspects became more prominent. He carried the novel p.Arg418Gln substitution, which was not found in both his parents and therefore confirmed to be a de novo mutation.

Family-5

The proband is a 2-year-old-boy of Italian origin. He was born normally after a normal pregnancy. Generalised choreic and myoclonic movements appeared in the first months of life. Motor and language development were severely delayed. He is currently able to sit, but not to stand without support. The neurological examination showed axial hypotonia, diffuse chorea and myoclonic jerks and dystonic posturing in the four limbs. A tendency to tiptoe walking was noted. A trial with trihexyphenidyl was unsuccessful.

His father, currently aged 47, is affected with generalised dystonia mixed with choreic elements, started around age 3. Differently from his child, his motor and language development were entirely normal. He presented frequent facial twitches and severe

dysarthria. The dyskinesias are markedly worsened by action, emotions and stress. Paroxysmal episodes of severe and painful dyskinesias are triggered by strong emotions and sleep. Several pharmacological trials (including trihexyphenidyl, L-DOPA and tetrabenazine) were ineffective. Both father and son have recently started a therapeutical trial with acetazolamide.

Both cases were found to carry the novel change p.Arg418Gly. Interestingly visual inspection of the chromatograms shows an imbalanced ratio between the wild-type and the mutated allele, with the latter significantly less represented (Figure 6-6). This was not observed in the son, suggesting that the father could be mosaic for the mutation.
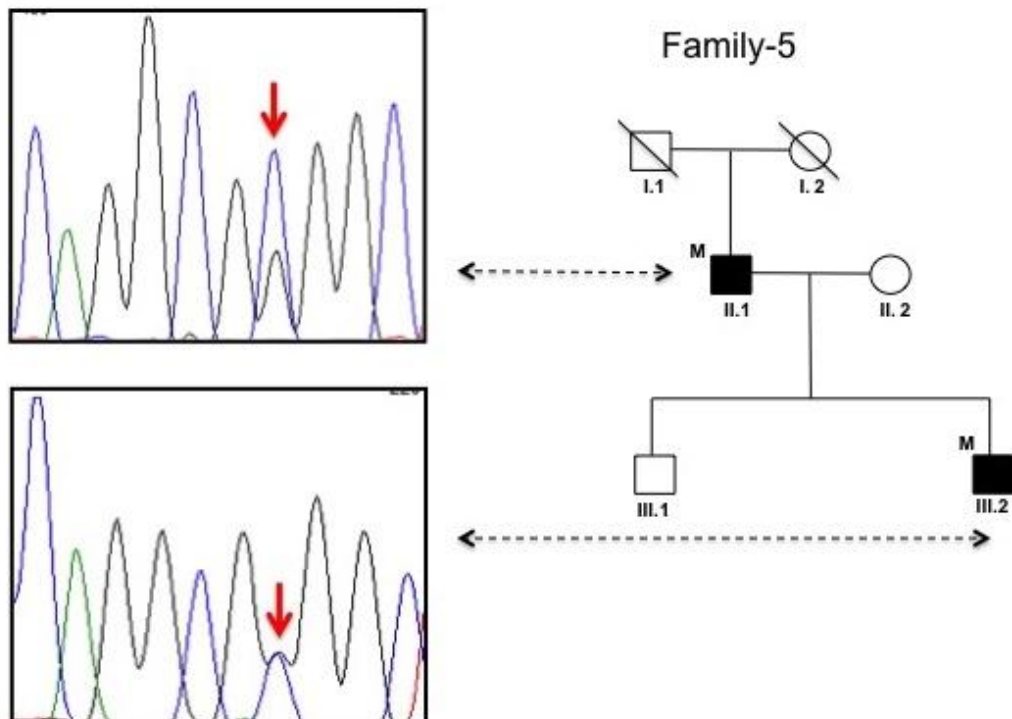
Figure 6-6. Pedigree of family 5 with the novel Arg418Gly mutation
The electropherogram of the affected father clearly shows an unbalance ratio between the wild-type and the mutant allele (top panel), with the wild-type significantly more represented and suggesting somatic mosaicism. This was not observed in the proband where the chromatograms of the normal and mutated allele are equivalently represented (bottom panel).

Table 6-1 Clinical features of cases with pathogenic *ADCY5* mutations

	Family-1 - Father	Family-1 Son	Family-2	Family-3	Family-4	Family-5 - Father	Family-5 - Son
Ethnic origin	UK-Caucasian	UK-Caucasian	UK-Pakistani	Italian-Caucasian	Italian-Caucasian	Italian-Caucasian	Italian-Caucasian
Age at onset (y)	1	1	2	4	1	3	1
Age at examination(y)	64	36	22	14	18	47	2
Mutation	c.1252C>T; p.Arg418Trp (low-level mosaicism)	c.1252C>T; p.Arg418Trp	c.1252C>T; p.Arg418Trp	c.1252C>T; p.Arg418Trp	c.1253G>A; p.Arg418Gln	c.1252C>G; p.Arg418Gly (mosaicism)	c.1252C>G; p.Arg418Gly
Symptoms at onset	Chorea	Chorea	Chorea and lower limb dystonia	Violent dyskinesias upon falling asleep	Chorea, dystonia	Chorea, dystonia	Chorea
Developmental milestones	Normal	Delayed	Delayed	Delayed	Delayed	Normal	Delayed
Dysarthria	No	Yes	Yes	Yes	Yes	Yes	Not applicable
Facial dyskinesias	Yes	Yes	Yes	Yes	Yes	Yes	No
Chorea	Yes, mild	Yes, severe and worsened by action and anxiety	Yes, severe and worsened by action and anxiety	Yes	Yes, mild	Yes, worsened by action	Yes
Dystonia	No	Yes	Yes	Yes, severe	Yes,	Yes, severe	Yes

Other features	Gaze impersistence, difficulty initiating saccades	Gaze impersistence, difficulty initiating saccades	Gaze impersistence	Pyramidal signs in the lower limbs	Frequent myoclonic jerks and pyramidal signs in the lower limbs	No	Severe language development
Paroxysmal events	Ballistic episodes and spasms upon awakening	Ballistic episodes and spasms upon awakening	Ballistic episodes and spasms at night	Triggered by sleep, favoured by emotions	Triggered by stress and sleep	Triggered by stress and sleep	No
Gait	Mild difficulty on tandem walking	Abnormal due to lower limb choreo-dystonia	Abnormal due to lower limb choreo-dystonia	Dystonic and pyramidal features, frequent falls	Mildly affected with dystonic features	Dystonic	Not applicable

Brain expression data

In order to investigate the differences in the phenotype and clinical course between BHC due to *ADCY5* and *NKX2-1* mutations, the expression of the two genes across multiple brain regions and during the course of development was compared.

Consistent with the observed phenotype, mainly characterized by chorea and dystonia with preserved cognition and no other major neurological features, both *ADCY5* and *NKX2-1* mRNA expression profiling in 10 brain regions showed the highest regional expression in the putamen (Figure 6-7 and Figure 6-8). When comparing *ADCY5* to *NKX2-1* expression, *ADCY5* had a much higher expression in adult striatum. Furthermore, longitudinal analysis of mRNA expression during brain development showed opposite trends for *ADCY5* and *NKX2-1*, with *ADCY5* expression progressively increasing in the striatum from 50 to 500 days post-conceptualization and *NKX2-1* progressively decreasing (Figure 6-7 and Figure 6-8).

6.4.5 Discussion

I report here the results of the *ADCY5* mutational analysis in a cohort of *NKX2-1* negative BHC cases and show that transmitted and *de novo* heterozygous *ADCY5* mutations are an important cause of familial and sporadic BHC. Overall, in this study pathogenic mutations were identified in 5/53 (9.4%) of cases.

The heterozygous mutation p.Ala726Thr in *ADCY5* was identified as the genetic cause in the original FDFM pedigree (Chen *et al.*, 2012). The presentation of the affected members of this family was that of a hyperkinetic choreo-dystonic movement disorder starting from early childhood to late adolescence. A distinctive feature of this disorder was initially thought to be the presence of prominent periorbital and perioral facial myokymia (Fernandez *et al.*, 2001). After the identification of *ADCY5* as the responsible gene in the original FDFM pedigree, the same group identified a second pathogenic missense variant in *ADCY5* (c.1252C>T; p.Arg418Trp), which occurred *de novo* in two unrelated individuals with a sporadic complex hyperkinetic movement disorder (Chen *et al.*, 2014). The phenotype of these cases shared some features with the original FDFM pedigree, but it was more severe and further encompassed delayed motor milestones, axial hypotonia and progressive gait difficulties in one case.
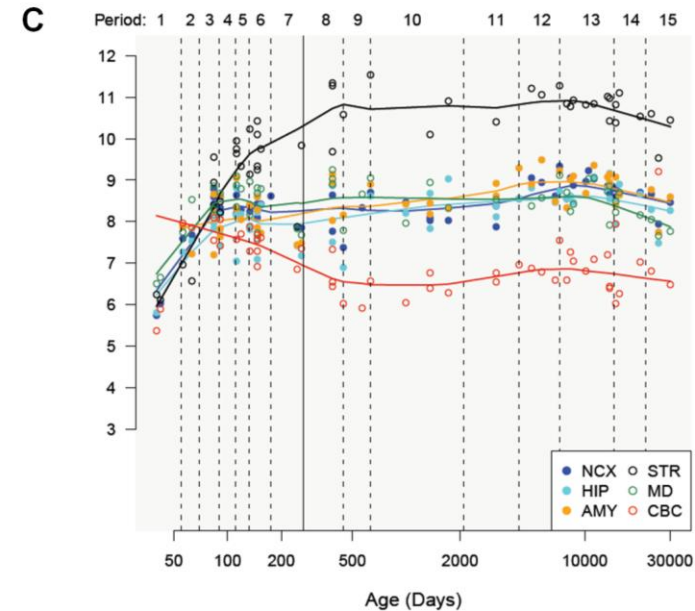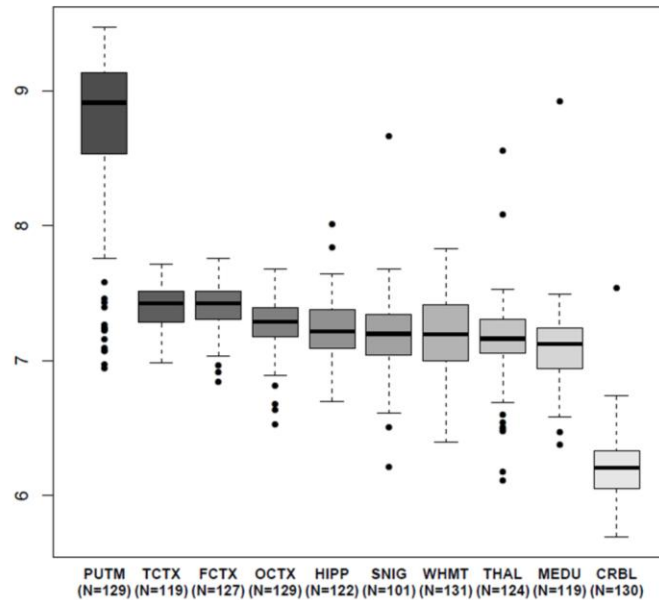
Figure 6-7 Graphical Summary of *ADCY5* Brain Expression Data

On the left box plots representing *ADCY5* mRNA expression levels. The expression levels are based on exon array experiments and are plotted on a log2 scale (y axis). *ADCY5* mRNA expression is higher in the putamen than in all other brain regions. Oh the right, graphs to show *ADCY5* longitudinal mRNA expression in six brain regions during the course of human brain development. The expression levels are based on exon array experiments and are plotted on a log2 scale (y axis). The plots show increasing expression of *ADCY5* mRNA during human brain development, particularly in the striatum, from 50 to 500 days post-conceptualization.
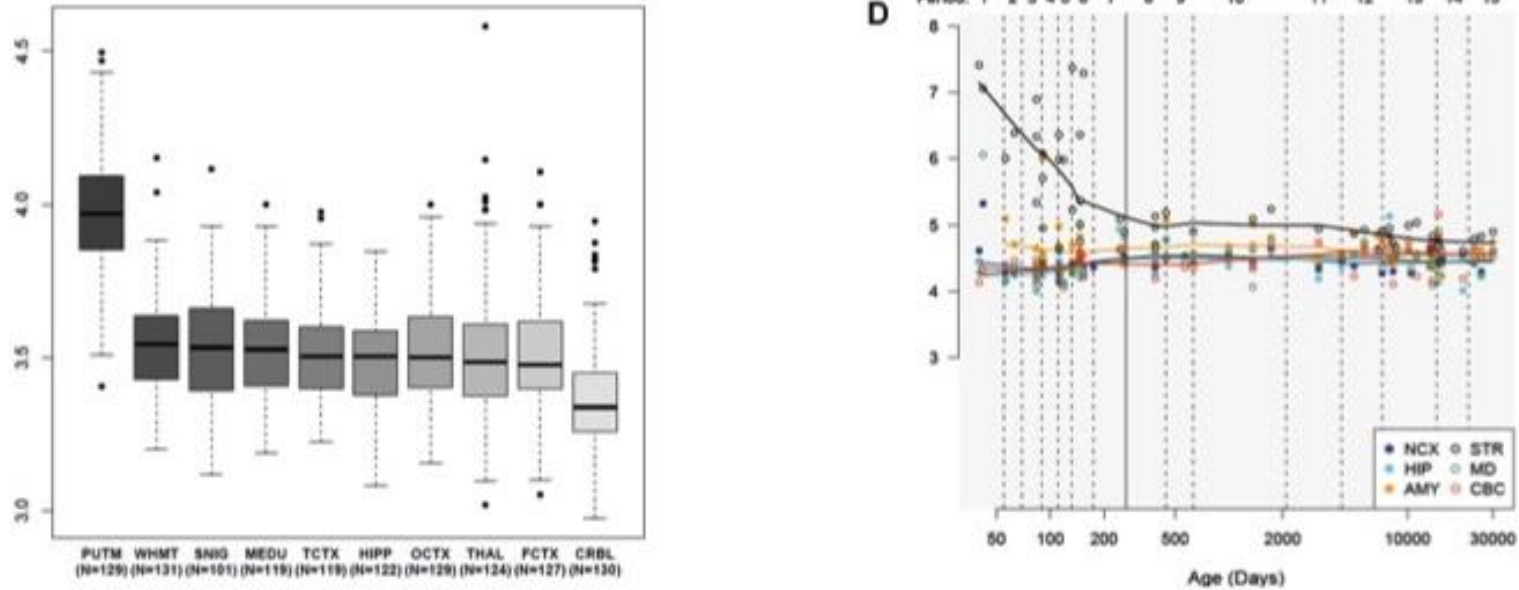
Figure 6-8 Graphical Summary of *NKX2-1* Brain Expression Data

On the left box plots representing *NKX2-1*mRNA expression levels. The expression levels are based on exon array experiments and are plotted on a log2 scale (y axis). *NKX2-1*mRNA expression is higher in the putamen than in all other brain regions. However *NKX2-1* expression in the putamen is significantly lower than *ADCY5*. On the right, graphs to show *NKX2-1* longitudinal mRNA expression in six brain regions during the course of human brain development. The expression levels are based on exon array experiments and are plotted on a log2 scale (y axis). The plots show decreasing expression of *NKX2-1*mRNA during human brain development, particularly in the striatum, from 50 to 500 days post-conceptualization, an opposite trend compared to *ADCY5*.

223

In this chapter, I report seven cases from five unrelated pedigrees bearing pathogenic *ADCY5* mutations. Importantly, all the mutations that I identified involved the same amino acid p.Arg418, highlighting a particular relevance of this residue in the disease mechanisms. Three unrelated cases carried the previously reported Arg418Trp mutation, whereas two others carried the novel mutations Arg418Gln and Arg418Gly.

The clinical phenotype of these cases predominantly featured generalized chorea, though with significant intra- and inter-familial phenotypic variability.

As previously described, three of the four mutated subjects with the *ADCY5* p.Arg418Trp mutation were more severely affected than subjects from the original FDFM pedigree and carriers of the p.Arg418Gln and p.Arg418Gly. The phenotype of these cases with the p.Arg418Trp included axial hypotonia, delayed motor milestones, and disabling choreo-dystonic dyskinesias.

Conversely, subject II-1 from family 1 had a much milder presentation, with very little functional impact from the dyskinesias. Furthermore, he had isolated chorea and no dystonic features. Interestingly, low-level somatic mosaicism is the likely mechanism for the observed milder phenotype. Indeed, WES data showed a significantly reduced number of reads carrying the mutated allele in the latter case, indicating the presence low-level somatic mosaicism. Somatic mosaicism was likely present also in cases II-1 from family 5 (carrier of the p.Arg418Gly), who, differently from his son, had a predominantly dystonic phenotype and normal motor and language development.

Mosaicism has been recently described in two further cases with *ADCY5* mutations and a milder phenotype, suggesting that somatic mosaicism may represent a common explanation for inter- and intra-familial phenotypic variability in *ADCY5* mutation carriers (Chen *et al.*, 2015).

The clinical presentation of the subject with the Arg418Gln mutation, who initially presented in childhood with BHC, is now consistent with a diagnosis of myoclonus-dystonia. A similar evolution was also observed in subject III-1 from family I (with the p.Arg418Trp), who predominantly showed chorea during childhood, while dystonic elements became more prominent over the years.

In some of the previously described cases with *ADCY5* mutations, dyskinesias are

reported as paroxysmal in the initial phase of the disease (Fernandez *et al.*, 2001) (Chen *et al.*, 2014). In contrast, in all the cases described herein, dyskinesias were constantly present from the onset of symptoms, albeit markedly influenced by emotional states and action. However, two subjects developed superimposed diurnal episodic worsening of dyskinesias, triggered by intense emotional stress. Furthermore, six subjects (excluding individual III-2 from family 5, who is currently only 18 months old) presented exacerbations of hyperkinesias at night, sometimes evolving into episodes of violent ballistic movements and painful spasms. The episodes were particularly frequent at night, either upon falling asleep or awakening. Similar episodes have been described in several other cases with *ADCY5* mutations (Chen *et al.*, 2015), indicating that this could be a specific feature of *ADCY5*-related movement disorders.

Facial myokymia was initially highlighted as a distinctive feature of *ADCY5*-related disorder. However, an EMG study of the facial muscles performed in both affected subjects from family 1 (both presenting facial involuntary movements) excluded the presence of myokymia or other signs of motorneuron hyperexcitability. Although EMG was not performed in the other cases, who all reported facial dyskinesias, these were clinically deemed to be choreic and/or myoclonic in nature. This indicates that patients with *ADCY5* mutations present prominent facial hyperkinetic movements in the absence of myokymia. Consistent with this, neither facial myokymia was described in all affected members from the original FDFM kindred nor was recognized as a prominent feature in the other *ADCY5* mutation carriers that were subsequently reported. Importantly, a subsequent EMG study, performed in the same members of the FDFM family in whom myokymia was initially described, failed to confirm the presence of myokymia (Chen *et al.*, 2015).

Importantly, even though the clinical presentation of patients with *ADCY5* mutations is consistent with the clinical definition of BHC, there are several differences that differentiate *ADCY5*-mutation carriers from BHC secondary to variants in *NKX2-1*.

Firstly, although both conditions can have extra-neural involvement, *NKX2-1* carriers often present pulmonary symptoms or evidence of endocrine defects (Inzelberg *et al.*, 2011), whereas cardiac heart failure has been observed in some affected individuals from the original FDFM pedigree (Chen *et al.*, 2012). *ADCY5* overexpression has also been shown to lead to cardiomyopathy in a mouse model (Ho *et al.*, 2010).

Secondly, the clinical progression between the two disorders seems to be different; BHC cases secondary to *NKX2-1* mutations tend to remain relatively mildly affected and often improve after childhood, while we show here that *ADCY5* mutation carriers are often severely affected by the dyskinesias, and may present significant progression of symptoms, at least until the adult age. This difference in the clinical progression is nicely mirrored by the brain transcriptome data. The analysis and comparison of *ADCY5* and *NKX2-1* mRNA regional brain expression showed that, although both genes are most highly expressed in the adult striatum, *ADCY5* levels progressively increase during brain development whereas *NKX2-1* levels show an opposite trend. Thirdly, prominent dystonic and myoclonic features are present in several affected cases with *ADCY5* mutations and may dominate the clinical picture as the disease progresses. Dystonic features can be also observed in some *NKX2-1* cases (Armstrong *et al.*, 2011, Peall *et al.*, 2014), but they are generally not as severe as we observed in *ADCY5* mutation carriers. Lastly, *ADCY5*-related dyskinesias are dramatically worsened by action, excitement or stress. Furthermore, some patients may present frank episodic worsening of the dyskinesias, closely mimicking paroxysmal movement disorders. This feature likely reflects the biological role of AC5. This enzyme catalyzes the formation of cyclic adenosine monophosphate (cAMP) upon β-adrenergic receptor stimulation via G-proteins in striatal cells and pathogenic mutations seem to increase the cyclase activity (Chen *et al.*, 2014).

In conclusion, this study contributes to expand and delineate the phenotype associated with *ADCY5* mutations. I suggest the term FDMD should not be used to refer to *ADCY5*-related movement disorder, as facial myokymias are not part of the phenotype.

A diagnosis of *ADCY5*-related disorder should be always suspected when assessing patients with a choreic disorder with onset in childhood, in particular if neuroimaging is normal and a fluctuating course with severe dyskinetic attacks triggered by drowsiness are described. Differences in the clinical presentation between *ADCY5* mutation carriers may be attributed to distinct molecular effects of different mutations, though somatic mosaicism may explain intra-familial phenotypic variability, as shown in family 1 and 5. Given the possible reported association of *ADCY5* mutations with cardiac involvement, it will be fundamental to closely follow-up *ADCY5* mutation carriers in order to prevent or adequately treat potential cardiac complications.

Importantly, the majority of the BHC cases included in this project did not carry mutations in either *NKX2-1* or *ADCY5*, including four cases with clear autosomal dominant family history. This indicates that more genes responsible for BHC have yet to be identified.

6.5 *De novo* Mutations in *PDE10A* Cause Childhood-Onset Chorea with Bilateral Striatal Lesions

6.5.1 Statement of Contribution

I performed all the genetic analysis performed in this chapter. I performed the *in silico* modelling of the mutations. Dr Haruhide Kimura's team (Takeda Pharmaceutical Company Limited) performed the *in vitro* functional characterisation of the identified PDE10A substitution.

6.5.2 Background

WES can be used to identify the disease-causing gene in series of unrelated cases with a very rare and homogenous phenotype, under the assumption that only few causative genes are involved. For example, this strategy has been successful for the identification of *TUBB4A* (MIM 602662) mutations in cases with hypomyelination with atrophy of the basal ganglia and cerebellum (Simons *et al.*, 2013) or *WDR45* (MIM 300526) mutations in an X-linked form of neurodegeneration with brain iron accumulation (Haack *et al.*, 2012).

In this study I identified *de novo* dominant missense mutations in *PDE10A* as a novel disease-associated additional genetic cause in three subjects without a family history who presented with a similar childhood-onset movement disorder predominantly characterized by chorea and striking bilateral striatal abnormalities on cerebral magnetic resonance imaging (MRI).

6.5.3 Subjects, Materials and Methods

Subjects

I initially analysed WES data from the eight unrelated BHC cases without pathogenic variants in *NKX2-1* and *ADCY5,* including four with autosomal dominant family history and four sporadic cases. The ascertainment criteria of this cohort have been described in the previous sections of this chapter. For three of the familial cases, DNA and WES from at least another affected relative (1st degree relative in one case and 2nd degree in the other two) were available for segregation analysis.

An additional cohort of 60 cases with BHC of Italian, Dutch and UK origin, negative for mutations in *NKX2-1* and *ADCY5*, was included to replicate the finding made in the

initial cohort. The cases of Italian origin are the same subjects described in the previous section of the chapter. Additional cases were recruited by Dr Manju Kurian at UCL Great Ormond Street Hospital, London (United Kingdom) and Dr Lisenka Visser and Dr Michel Willemsen at Radboud University Medical Center, Nijmegen (Netherlands).

Genetic analysis

WES, alignment, variant calling and annotation were performed as previously described in the Materials and Methods chapter. The average read depth of targeted regions was 84.29 and all samples had >95% of the target bases were covered at a read depth of 2x and >90% at a depth of 10x, ensuring high-confidence variant detection. The variant filtration strategy that led to the identification of the *PDE10A* variants is described in the results section.

Expression profiling in brain tissue

Brain mRNA regional distribution and expression in the normal adult human brain were determined using microarray analysis of human post-mortem brain tissue from the UK Human Brain Expression Consortium, as previously detailed in the Materials and Methods chapter.

In silico modelling of the identified PDE10A mutations

In silico modelling of the 3-D structure of the PDE10A GAF-B domain binding pocket and its interaction with the cAMP, was generated with the software PyMol (Schrodinger) using the PDB-file 2ZMF (downloaded from http://www.rcsb.org/pdb/home/home.do).

In vitro functional analysis of the identified PDE10A mutations

Materials

1-NO-cAMP was purchased from Biolog Life Science Institute (Bremen, Germany). cAMP and cyclic guanosine monophosphate (cGMP) were purchased from Sigma–Aldrich (St. Louis, MO). The [^{3}H]-labeled nucleotides, [^{3}H]cAMP (25.9 Ci/mmol) and [^{3}H]cGMP (7.1 Ci/mmol), were purchased from PerkinElmer (Waltham, MA).

Cloning and Expression of Constructs

cDNA for human PDE10A2 (GenBank: NM_001130690) was used as a template and the mutants (c.898T>C; p.Phe300Leu and c.1000T>C; p.Phe334Leu) were constructed by site-directed point mutation. All constructs were cloned into the pcDNA3.1(+)neo

vector (Thermo Fisher Scientific, Inc., Waltham, MA) and transfected into COS-7 cells (ECACC, Salisbury, UK). The membrane fractions were used for the enzyme assay.

In Vitro Phosphodiesterase Enzyme Assay

Phosphodiesterase (PDE) activities were measured using scintillation proximity assay (SPA)-based method (Matthiesen and Nielsen, 2009). In this assay, the product of the PDE reaction, either [^{3}H]AMP or [^{3}H]GMP, can bind directly to yttrium silicate PDE SPA beads (GE Healthcare Ltd. UK), leading to light emission from the scintillant in the beads. The enzyme assays were conducted in a buffer (50 mM HEPES-NaOH, 8.3 mM MgCl$_2$, 1.7 mM EGTA, 0.1% bovine serum albumin (pH 7.4)) in 96-well half-area plates (Corning Inc., Corning NY). For kinetic studies, reaction was conducted at presence of the indicated concentrations of substrate using mixture (20 μL) of [^{3}H]-labelled and unlabelled cAMP or [^{3}H]-labelled and unlabelled cGMP with the 20 μL of membrane fractions of PDE10A-expressing COS-7 cells at room temperature, followed by reaction termination by SPA beads addition (20 μL of 20 mg/mL). The plates were counted for 1 min in a scintillation counter (PerkinElmer). For the purpose of determination of baseline counts, every tested concentration of labelled and unlabelled cyclic nucleotides was run with matching controls having the identical reagent concentrations except for the addition of buffer alone in place of enzyme. Specific enzyme activity was then calculated by subtracting the baseline counts.

To obtain the Michaelis–Menten constants (Km), the initial rates of the reaction were fitted to the following equations using GraphPad Prism (GraphPad Software, Inc., La Jolla, CA): V = Vmax [S] / (Km + [S]), where V is the initial velocity of the enzyme-catalyzed reaction, [S] is the substrate concentration, Vmax is the limiting reaction velocity at saturating substrate concentrations, and Km is the Michaelis–Menten constant (concentration of substrate at 1/2 of Vmax).

The effects of cAMP or its analogue, 1-NO-cAMP, on PDE10A enzyme activity were assessed using [^{3}H]cGMP as a substrate. The indicated concentrations of unlabelled nucleotide (cAMP or 1-NO-cAMP, 10 μL) and 70 nM [^{3}H]cGMP (10 μL) were added to the 20 μL buffer containing membrane fractions of PDE10A-expressing COS-7 cells at 37°C. After 40-min incubation, the reaction was terminated by addition of SPA beads (20 μL of 20 mg/mL) and the plates were counted in a scintillation counter. Activity rates were calculated on the basis of 100% control wells without unlabelled nucleotides

and 0% control wells without enzyme.

6.5.4 Results

Identification of PDE10A mutations in the discovery cohort

A total of 26,387 unique variants were detected in eight exomes of unrelated BHC cases. I excluded from the analysis (i) UTR and intergenic variants outside of canonical splice sites as well as variants that are synonymous, non-frameshift insertions and deletions; (ii) variants that lie in segmental duplication regions, as these are prone to produce false-positive variant calls due to mapping errors; (iii) poor quality variants (quality scores $\leq$ 50 or read depth $\leq$ 5).

Given a dominant family history in four out of eight cases and the fact that mutations in the two currently known BHC genes, *NKX2-1* and *ADCY5*, exert a pathogenic effect in the dominant state, I decided to initially focus the analysis only on single heterozygous changes. Furthermore, based on the extreme rarity of BHC in the general population, I assumed that causative variants would be absent in dbSNP version 137 (provided they were not know disease-associated mutations) and in the publicly available datasets of genetic variations (1000 genome project, EVS, ExAC and CG69). I also excluded novel variants that were observed more than five times in our in-house exome database (~1000) from individuals with unrelated diseases, as these are likely to represent sequencing or alignment artefacts. Variants present in the familial cases that did not segregate in the affected relatives were filtered out.

After applying this filtering strategy, I was left with a list of individual variants that included 18 frameshift indels, 11 nonsense mutations, four mutations affecting canonical splice-sites, and 212 missense variants.

I subsequently focused only the genes that contained at least a variant in more than one sample. This filtering strategy left us with only three candidate genes (see Table 6-2), each containing a variant in two unrelated samples, *PDE10A* (phosphodiesterase 10A) on chromosome 6, *THSD1* (thrombospondin, type I, domain containing 1) located on chromosome 13, and *PRMT7* (protein arginine n-methyltransferase 7) on chromosome 16.

I then explored the regional expression of these three genes in the normal adult human brain. This analysis showed that *PDE10A* expression is exceptionally high in the striatum (Figure 6-9A), whereas this is not the case for *THSD1* and *PRMT7* (see Figure 6-10). These data are consistent with the data available on the Allen Mouse Brain Atlas (Lein *et al.*, 2007) (see Figure 6-9B and C) and previous work in the literature, demonstrating high and selective expression of *PDE10A* in the striatum (Fujishige *et al.*, 1999), particularly in MSNs (Seeger *et al.*, 2003), which makes *PDE10A* an excellent candidate gene for chorea.

The two cases with *PDE10A* mutations carriers were both sporadic and carried the exact same heterozygous change, c.898T>C; p.Phe300Leu.

Sanger sequencing confirmed the presence of the mutation in both cases. The mutation was demonstrated to be *de novo* in the first case, as it was absent in both parents and in the unaffected 19-year old sister. To confirm that no other variants could be responsible for chorea in this subject, WES was performed in all family members, including the two parents and the healthy sister. Importantly, I could not identify other putatively damaging mutations (defined as nonsense, frameshift, canonical splice site, predicted damaging missense mutations based on CADD scores >20; with a MAF <1% in ExAC), assuming either a de novo or a recessive pattern of transmission.

Parents of the second individual were both deceased and therefore not available for DNA analysis. However, DNA analysis in six siblings, all unaffected with chorea, demonstrated that they were all homozygous for the reference allele. Furthermore, haplotype analysis using three microsatellites (Marker 1 – chr6:166069747-166069785; Marker 2 – chr6:165862198-165862227; Marker 3 - chr6:165839259-165839288) spanning the *PDE10A* locus identified the four parental haplotypes and revealed that the individual carrying the mutation shared one of the haplotypes with two siblings and the other with three other siblings, strongly indicative of the *de novo* occurrence of the mutation also in this case (Figure 6-11). Analysis of the same three microsatellites in the family of case 1, who carries the same *de novo PDE10A* change, indicates the mutation arose on a different background haplotype.

Table 6-2 Summary of variants detected by whole-exome sequencing that survived the filtering strategy.

Gene (Transcript)	Chr	Position (hg19)	Variant	GERP score[a]	CADD C-score[b]	SIFT	PolyPhen-2	Mutation Taster	ExAC constraint metrics	Number of unrelated probands with the variant
PDE10A (NM_001130690)	6	165832223	c.898T>C; p.(Phe300Leu)	4.47	28.7	D (0)	D (0.98)	D (0.99)	Missense: z^c 3.78 LoF: pLi[d] 1.00	2 (both sporadic)
THSD1 (NM_199263)	13	52952435	c.1669_1670del; p.(Ser557fs)[d]	NA	NA	NA	NA	NA	Missense: z^a 0.75 LoF: pLi[b] 0.00	1 (familial)[e]
	13	52952567	c.1379G>A; p.Ser460Asn	5.62	12.16	T (0.57)	B (0.02)	D (0.99)		1sporadic
PRMT7 (NM_001184824)	16	68373391	c.522dupT; p.(Ser174fs)[d]	NA	NA	NA	NA	NA	Missense: z^a0.23 LoF: pLi[b] 0.00	1 (familial)[e]
	16	68382285	c.1214T>C; p.(Ile405Thr)	5.6	24.2	D (0.01)	B (0.03)	D (0.99)		1 (familial)

Chr=chromosome; B=benign; D=deleterious/damaging/disease-causing; B=benign; T=tolerated; NA=not applicable; fs=frameshift; LoF:loss-of-function; pLI= probability of loss-of-function intolerance

[a]Positive scores represent a substitution deficit and indicate that a site may be under evolutionary constraint. Negative scores indicate that a site is probably evolving neutrally. Positive scores scale with the level of constraint, such that the greater the score, the greater the level of evolutionary constraint inferred to be acting on that site.

[b]C-scores greater or equal 10 indicates that the variant is predicted to be the among the 10% most deleterious substitutions that you can do to the human genome; a score of greater or equal 20 indicates the 1% most deleterious.

[c]z-missense scores reflect expected mutation probabilities and are based on deviation of observed standing variation patterns (higher values = more constrained [fewer variants observed than expected]).

[d]The closer pLI is to 1, the more LoF intolerant the gene appears to be.

[e]The two frameshift variants in *THSD1* and *PRMT7* were found in the same individual

De novo mutations in *PDE10A* have not been observed in control individuals (Rauch *et al.*, 2012, Xu *et al.*, 2012, Gulsuner *et al.*, 2013, Genome of the Netherlands Consortium, 2014, Iossifov *et al.*, 2014) and the p.Phe300Leu is neither listed in ExAC, nor in our in-house exomes with unrelated diseases (~1,000), and in 500 exomes from ethnically matched healthy controls. All used *in silico* tools consistently predicted a highly deleterious effect of the substitution. Interspecies alignment of protein sequences revealed that the amino acid substitution lies in an acid motif that is completely conserved down to invertebrate species (see Figure 6-12). Constraint metrics reported in ExAC indicate that *PDE10A* is highly intolerant to both loss-of-function and missense mutations (Samocha *et al.*, 2014).

The frameshift mutations in *THSD1* (p.Ser557fs) and *PRMT7 (*p.Ser174fs) were both found in the same subject with a dominant family history of BHC and were present also in the similarly affected sister (the DNA of the affected father was not available). The missense heterozygous changes in *THSD1* and *PRMT7* were carried by a sporadic case and a familial case, respectively. No family members of the carrier of the *THSD1* missense mutation were available for segregation analysis, whereas the *PRMT7* missense change were inherited from the affected mother and grandmother of the proband. Prediction tools displayed contrasting results for both missense mutations. Importantly, although a pathogenic role for this variant cannot be excluded, the ExAC constraint metrics indicate that both *THSD1* and *PRMT7* are tolerant to missense and loss-of-function variation (see Table 6-2), suggesting it is unlikely that heterozygous mutations in these two genes could be responsible for the phenotype.

Finally, bi-allelic variant variants in *PRMT7* have been recently detected in three pedigree with a recessive condition called Albright hereditary osteodystrophy, which feature mild intellectual disability with obesity and symmetrical shortening of the digits and posterior metacarpals and metatarsals (Akawi *et al.*, 2015). This element further argues against any pathogenic role for the heterozygous *PRMT7* variants I identified in patients with BHC.
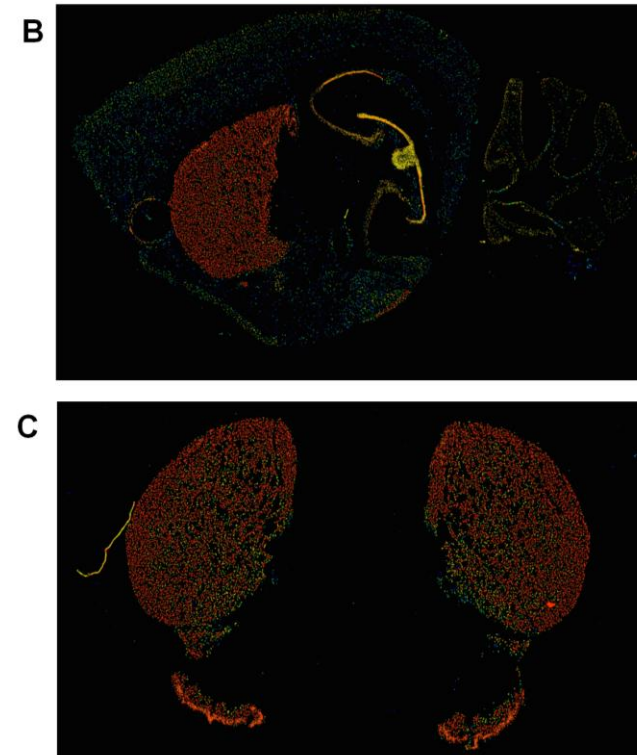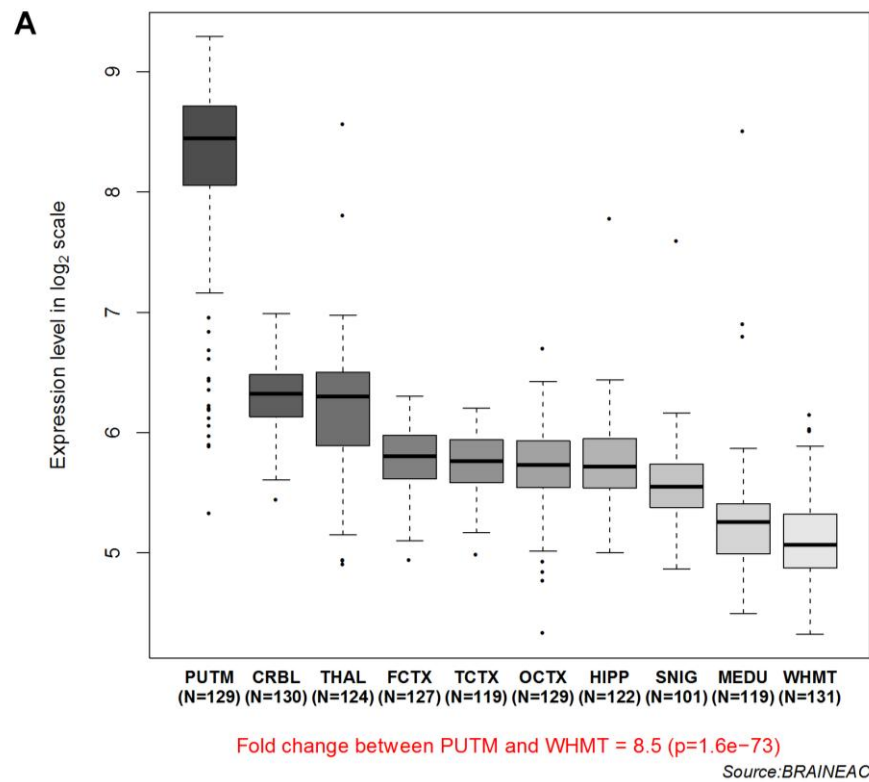
Figure 6-9 Summary of human and mouse brain *PDE10A* mRNA expression data

(A) Box plots of PDE10A mRNA expression levels in 10 adult brain regions. The expression levels are based on exon array experiments and are plotted on a log2 scale (y axis). This plot shows significant variation in *PDE10A* expression across the 10 brain regions analysed, with expression higher in the putamen than in any other region. PDE10A expression in mouse brain in (B) sagittal and (C) coronal sections. PDE10A is very highly and selectively expressed in the striata and in the olfactory tubercula. Images were obtained from the Allen Mouse Brain Atlas website (© 2015 Allen Institute for Brain Science). Expression intensity is color-coded, ranging from blue (low intensity) through green and yellow to red (high intensity).
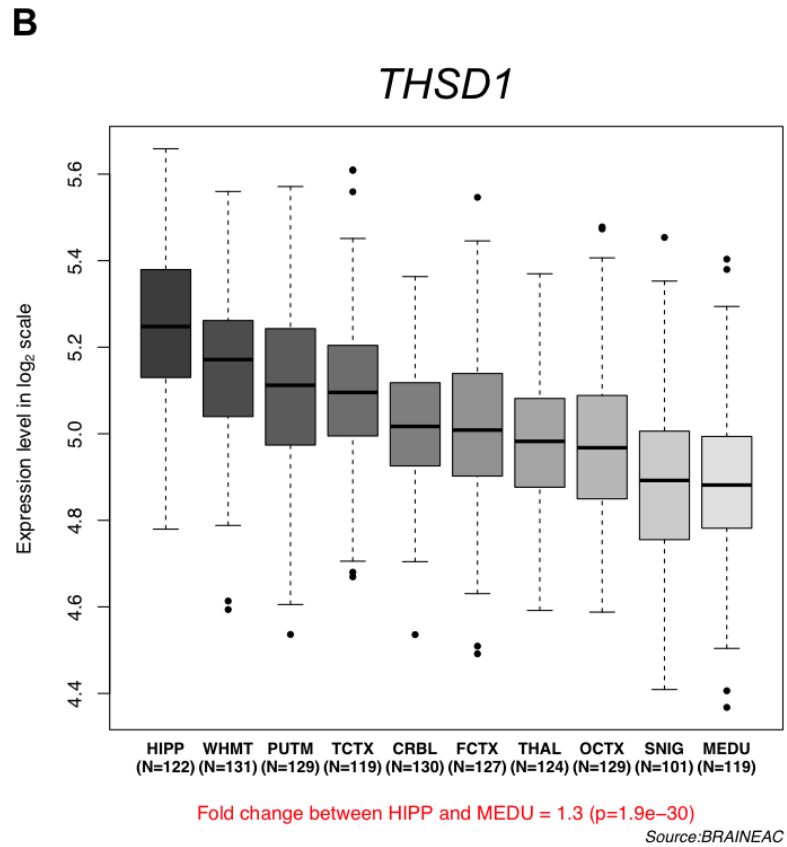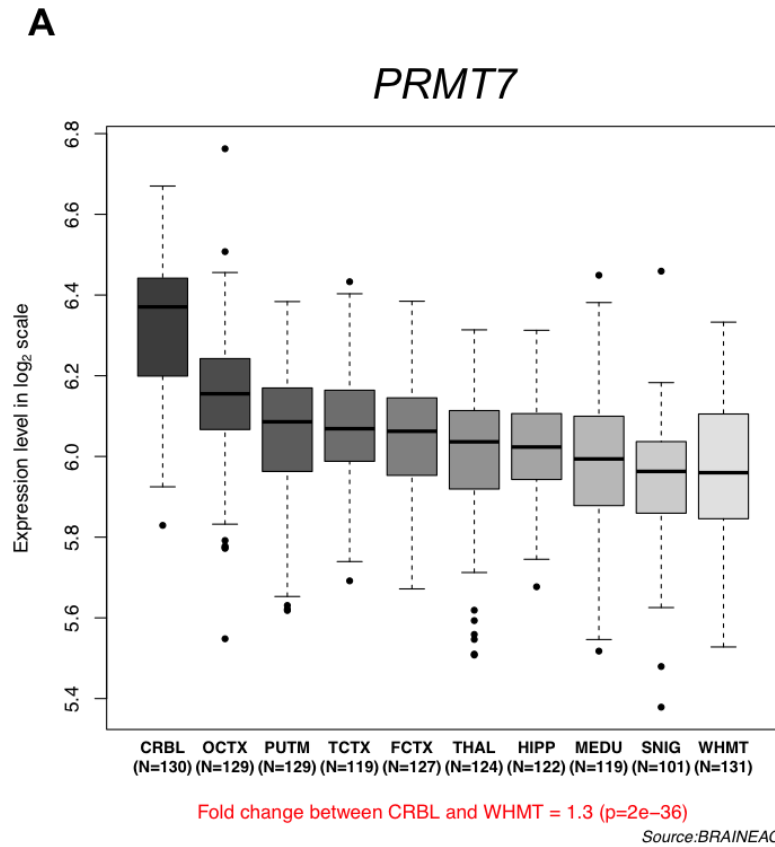
Figure 6-10 Summary of human brain expression of *PRMT7* and *THDS1*

Box plots of mRNA expression levels in 10 adult brain regions showing that the expression in the putamen of *PRMT7* (A) and *THDS1* (B) is significantly lower than *PDE10A*
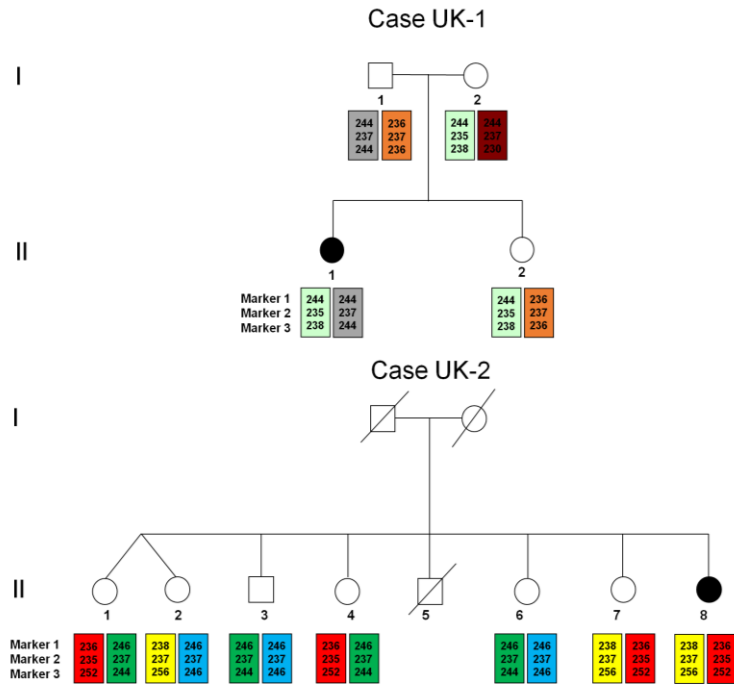
Figure 6-11 Pedigree and haplotype analysis in the families of cases 1 and 2
The four parental haplotypes were reconstructed in both families (each haplotype defined by a different colour). Cases 1 and 2 did not share the haplotype encompassing the c.898C>T variant, suggesting the mutations arose on different haplotype backgrounds. Furthermore, haplotype analysis indicates that case 2, who carries the PDE10A c.898T>C variant, shares one of the allele (marked in yellow) with two unaffected siblings (II-2, II-7) whereas the other allele (marked in red) is shared with three unaffected siblings (II-1, II-4 and II-7).

300   334

| Homo sapiens | IVAIDSLLEHIMIYAKNLVNADRCAL | F | QVDHKNKELYSDLFDIGEEKEGKPVFKKTKEIR | F | SIEKGIAGQVARTGEVLNIPDAYADP |

Mutated residues — L — L

Pan troglodytes	IVAIDSLLEHIMIYAKNLVNADRCAL	F	QVDHKNKELYSDLFDIGEEKEGKPVFKKTKEIR	F	SIEKGIAGQVARTGEVLNIPDAYADP
Papio Anubis	IVAIDSLLEHIMIYAKNLVNADRCAL	F	QVDHKNKELYSDLFDIGEEKEGKPVFKKTKEIR	F	SIEKGIAGQVARTGEVLNIPDAYADP
Rattus norvegicus	IVAIDSLLEHIMIYAKNLVNADRCAL	F	QVDHKNKELYSDLFDIGEEKEGKPVFKKTKEIR	F	SIEKGIAGQVARTGEVLNIPDAYADP
Mus musculus	IVAIDSLLEHIMIYAKNLVNADRCAL	F	QVDHKNKELYSDLFDIGEEKEGKPIFKKTKEIR	F	SIEKGIAGQVARTGEVLNIPDAYADP
Canis familiaris	IVAIDSLLEHIMIYAKNLVNADRCAL	F	QVDHKNKELYSDLFDIGEEKEGKPIFKKTKEIR	F	SIEKGIAGQVARTGEVLNIPDAYADP
Ornithorhynchus anatinus	IVAIDSLLEHIMIYAKNLVNADRCAL	F	QVDQKNKELYSDLFDIGEENEGKPIFKKTKEIR	F	SIEKGIAGQVARTGEVLNIPDAYADP
Gallus gallus	IVAIDSLLEHIMIYAKNLVNADRCAL	F	QVDHKNKELYSDLFDIGEENDGKPVFKKTKEIR	F	SIEKGIAGQVARTGEVLNIPDAYADP
Xenopus tropicalis	IVAIDSLLEHIMIYAKNLVNADRCAL	F	QVDHKNKELYSDLFDIGEEDEGKPVFKKTKEIR	F	SIEKGIAGQVARTGEVLNIPDAYADP
Tetraodon nigroviridis	IVAIDSLLEHIMIYAKNLVNADRCAL	F	QVDHNNKELYSDLFDIGEEKEGRPVFKKTKEIR	F	SIEKGIAGQVAQTGEVLNIPDAYADP
Danio rerio	IVAIDSLLEHIMIYAKNLVNADRCAL	F	QVDHNNKELYSDLFDIGEENEGKPVFRKTKEIR	F	SIEKGIAGQVARTGEVLNIPDAYADP
Caenorhabditis elegans	IVSMDAVIIKVMNFAQKLVDADRASL	F	LVDSKNAQIYARIFDVGDEEHVRVNSEGQKEIR	F	DMSKGIAGYVASTGEGLNIENAYEDE

:::*::: ::* :*:::***.:* * ** :* ::*: :**:*:*.. : .   **** * .:.***** ** *** *** :** *

Figure 6-12 Interspecies alignment of the identified pathogenic *PDE10A* mutations

Interspecies alignment showing the complete conservation down to invertebrates of the amino acid residues involved by the substitutions. Asterisks indicate invariant residues (full conservation), whereas a colon (:) and period (.) represent strong and moderate similarities, respectively.

Sanger Sequencing of PDE10A in a Cohort of Childhood-Onset Chorea Cases

As these results outlined in the previous section strongly support the pathogenic role of the *PDE10A* c.898T>C; p.Phe300Leu mutation, I then Sanger sequenced the entire coding sequence and the exon-intron boundaries of *PDE10A* in a further 60 cases with BHC without mutations in *NKX2-1* and *ADCY5*.

Importantly, this analysis revealed the presence of two additional variants: the unreported c.1000T>C; p.Phe334Leu was found in a Dutch case, and the c.1459C>G; the p.Pro487Ala (rs61733392) was found in an Italian case.

Sequencing in the parents of the carrier of the c.1000T>C; p.Phe334Leu variant showed that it was absent in both subjects, demonstrating the *de novo* occurrence of the mutation and highly supporting its pathogenic role. WES was performed also in this family and no other possibly pathogenic mutations, de novo or bi-allelic, were found.

This mutation is absent in all publicly available datasets, in all our exomes from healthy controls and in all exomes from cases with unrelated diseases. Furthermore, the change is predicted pathogenic by all *in silico* tools (Polyphen-2, SIFT and MutationTaster) and has a CADD score of 31. Interspecies alignment showed complete interspecies conservation (see Figure 6-12).

The p.Pro487Ala is a rare benign coding polymorphism, present in 478 European alleles reported in ExAC (MAF 0.007; two subjects are homozygotes) and is predicted benign by both Polyphen-2 and SIFT.

Clinical and Neuroradiological Features of Carriers of Pathogenic PDE10A mutations

Case 1, carrier of the Phe300Leu substitution, is a 22-year-old woman who developed generalized chorea around the age of 8. Although developmental motor milestones were reached normally, she had mild difficulties with speech and coordination during childhood. She now suffers from anxiety with some obsessive features. On examination she showed selective upgaze hypometric saccades and a mixed movement disorder consisting mainly of generalised chorea associated with some myoclonic jerks.

Case 2, carrier of the Phe300Leu substitution, is a 60-year-old woman who developed chorea around the age of 5. She had a normal birth and normal developmental

milestones. The chorea remained stable over the years, with parkinsonian symptoms becoming apparent in her fifth decade with freezing and falls. Striatal dopamine reuptake transporter density imaging was bilaterally abnormal, consistent with nigrostriatal dopaminergic denervation. On her last examination, there was generalised chorea, most prominently in the orofacial area, with motor and gaze impersistence and severe dysarthria. She also had generalised bradykinesia, more prominent in the lower than in upper limbs, and marked axial parkinsonian symptoms (freezing and postural instability), which responded well to a L-DOPA treatment (600 mg/day), without worsening of the choreic movements.

Case 3, carrier of the p.Phe334Leu substitution, is an 11-year-old, who developed an isolated non-progressive choreic disorder at around age 5. He had normal motor and language development.

Very importantly, brain MRI consistently showed striking bilateral T2 hyperintensity within the striatum in all three cases (Figure 6-13). It is noteworthy that the MRI images of case 3 (aged 11 when scanned) showed slight swelling of the striata (Figure 6-13A), together with restricted diffusion (Figure 6-13B and C), suggesting an active disease process. Conversely, MRI of case 1 (aged 22 when scanned) demonstrated modest atrophy of the putamina (Figure Figure 6-13D) and normal diffusion (Figure Figure 6-13 E and 1F), suggesting a more advanced stage of disease. The MRI of case 3 (aged 53 when scanned) was markedly degraded by movement artefacts, but also showed T2 bilateral hyperintensities within the posterolateral putamina, albeit less dramatic than in the two younger cases.
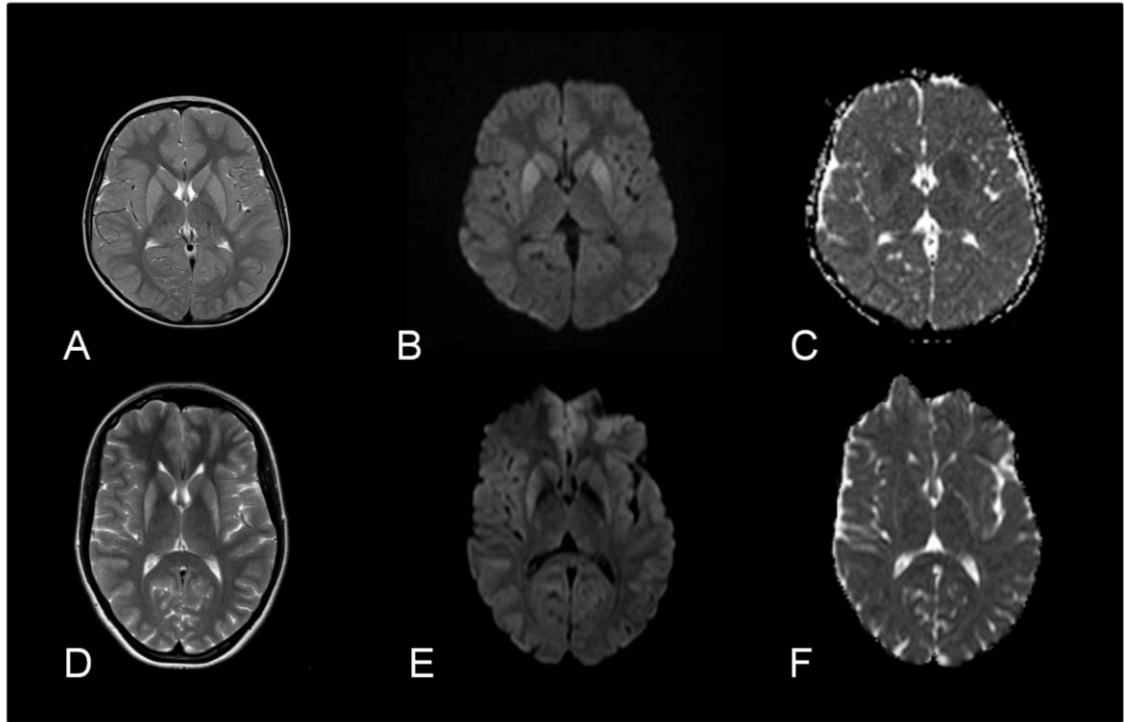
Figure 6-13 MRI features associated with de novo dominant *PDE10A* mutations
Axial MR images of case 3 (A-C) and 1 (D-F). There is increased signal intensity within the striatum on T2-weighted images (A, D) and diffusion-weighted images (DWI) (B, E). In case 3, the putamen and caudate nucleus appear slightly swollen (A) and high signal on DWI (B) is confirmed to represent abnormal restricted diffusion on the ADC map (C). In case 1, the abnormal signal is principally located in the postero-lateral putamina, which also appear atrophic (D). There is no corresponding restriction of diffusion on the ADC map (F), and appearances suggest a more chronic disease stage.

Overall, the three individuals presented with a very similar and unique clinical presentation of childhood-onset chorea and characteristic brain MRI (Table 6-3), strongly supporting *PDE10A* mutations as the unitary aetiology underlying all three cases.

Table 6-3 Clinical and genetic features of cases with *PDE10A* mutations

		Case 3	Case 1	Case 2
Age at most recent clinical examination (*years*)		11	22	60
Gender		Male	Female	Female
Descent		European (Dutch)	European (British)	European (British)
PDE10A mutation	Genomic[a]	Chr 6:165829768 A>G	Chr 6:165832223 A>G	Chr 6:165832223 A>G
	cDNA[b]	c.1000T>C	c.898T>C	c.898T>C
	Protein	p.Phe334Leu	p.Phe300Leu	p.Phe300Leu
	Inheritance	*de novo*	*de novo*	*de novo*[d]
CADD score[c]		31.0	28.7	28.7

Neurology

	Case 3	Case 1	Case 2
Developmental milestones	Normal	Normal	Normal
Cognition	Normal	Normal	Normal
Chorea (age of onset, yrs)	+ (5)	+ (8)	+ (5)
Other	No	Anxiety	Adult-onset parkinsonism

MRI

	Case 3	Case 1	Case 2
Bilateral striatal hyperintensities	+	+	+
Bilateral striatal swelling	+	-	-
Restriction of diffusion	+	-	N.A.
Bilateral striatal atrophy	-	+	+

+=present; N.A.=not available
[a](GRCh37)
[b]Ref Seq ID: NM_001130690.2
[c]Haplotype analysis in unaffected siblings suggests the *de novo* occurrence of the mutation in case 3

In silico Modelling of the Identified PDE10A Mutations

PDE10A encodes a member of the cyclic nucleotide (cNMP) phosphodiesterase (PDE) family, consisting of 21 different genes, grouped into 11 sub-families based on their affinity for the type of cNMP (cAMP and/or cGMP), cellular regulation, expression and tissue distribution (Lakics *et al.*, 2010). cNMPs are ubiquitously expressed intracellular second messengers, which modulate a broad range of cellular functions and pathways (Beavo and Brunton, 2002). The intracellular concentration of cNMPs is tightly regulated through a fine balance between their synthesis, controlled by the activity of adenylyl/guanylyl cyclases (Koesling *et al.*, 1991, Steegborn, 2014), and degradation, mediated by PDEs which hydrolyse the cNMPs into their corresponding monophosphate nucleoside (Soderling and Beavo, 2000).

PDEs function as homodimers, with the dimer interface extending over the entire length of the molecule, and all share a highly similar catalytic domain located in the C-terminal portion of the protein. Conversely, the N-terminal portion, which contains the regulatory domains, is variable and differs between different PDE families (Bender and Beavo, 2006).

PDE10A contains two N-terminal domains, GAF-A and GAF-B, of which the latter binds to cAMP (Figure 6-14A) (Gross-Langenhoff *et al.*, 2006, Heikaus *et al.*, 2009). cAMP binding increases the enzyme activity of the PDE10A catalytic domain (Jäger *et al.*, 2012). Although details of the GAF-B dependent modulation of PDE10A enzyme activity are currently unclear, a general mechanism for the regulation of all PDEs has been postulated. In the non-activated state the dimerised catalytic domains are packed against each other at the dimer interface, occluding the catalytic pockets. The binding of cAMP to the GAF-B domain induces a rotating movement of the catalytic domains, enabling substrate access to the catalytic pockets and a consequent increase of cNMP hydrolysis (Pandit *et al.*, 2009).

The crystal structure of the PDE10A-GAF-B domain and its interaction with cAMP has been elucidated and consists of six stranded anti-parallel β-sheet (β3, β2, β1, β6, β5, β4), sandwiched between a three-helix bundle (α1, α2, and α5) on one side and three short helices (α3, α4, 3_{10}) on the other side (Handa *et al.*, 2008). The cAMP molecule is almost completely buried deep into a tight binding pocket, the floor of which is formed by the β-sheets and the roof by two α-helices (α3 and α4). Importantly, the amino acids

p.Phe300 and p.Phe334 are located in the β1 and β3 sheets, positioned deep into the cAMP binding pocket of GAF-B and in very close proximity to the cAMP molecule (Figure 6-14B). It is therefore postulated that the substitutions severely affect the morphology of the GAF-B binding pocket and/or alter its affinity for cAMP.
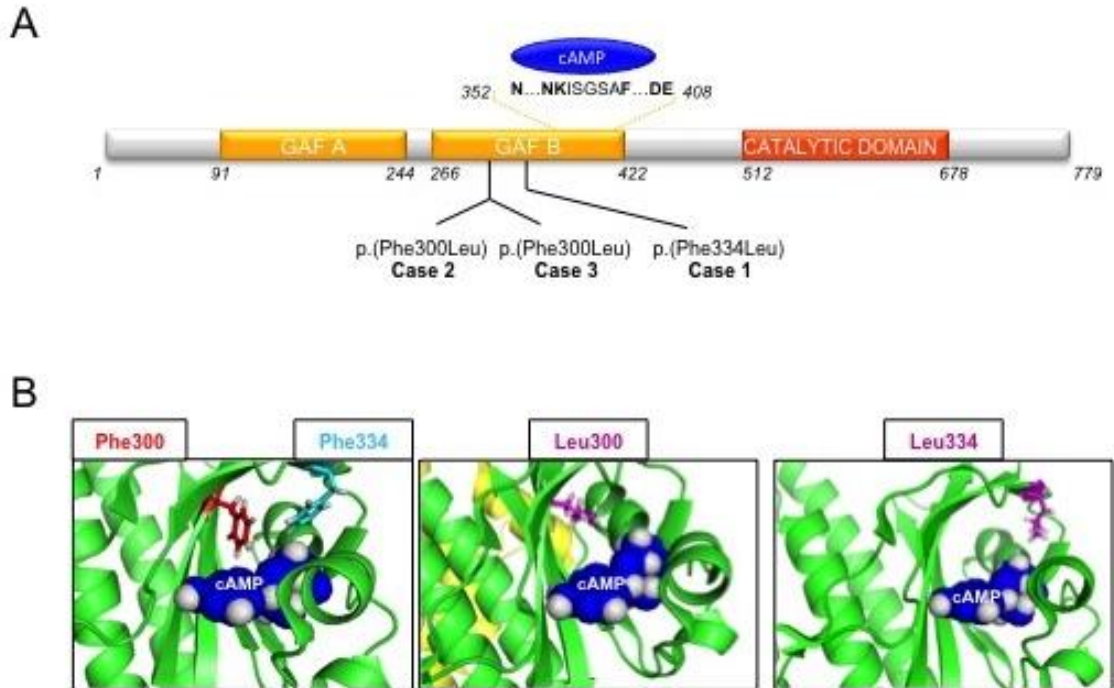
Figure 6-14 Schematic representation of the PDE10A protein and *in silico* modelling of the 3D structure of the PDE10A GAF-B domain
(A) A schematic representation of the PDE10A protein showing its organization in three domains, the regulatory GAF-A and GAF-B domains located in the N-terminal portion of the protein and the catalytic domain located in the C-terminus. (B) In silico modelling of the 3-D structure of the GAF-B domain binding pocket and its interaction with the cyclic adenosine monophosphate (cAMP; shown in blue). The mutated residues p.Phe300 and p.Phe334 and their aromatic side chains, located in the β1 and β3 sheets forming the floor of the cAMP binding pocket, are shown in red and cyan respectively. Both mutated residues (in magenta) are located in very close proximity to the cAMP molecule and are therefore likely to play an essential role in nucleotide binding.

In vitro Functional Analysis of the Identified PDE10A Mutations

To assess *in vitro* the functional effect of the identified PDE10A substitutions, we investigated whether they affect (i) PDE basal enzyme activity and/or (ii) the stimulatory effect on PDE catalytic activity mediated by cAMP binding to the GAF-B domain.

Reactions for kinetic studies were performed using a mixture of [^{3}H]-labelled and unlabelled cAMP or cGMP together with either WT or mutant PDE10A-expressing COS-7 cell membrane fractions. Km values for cAMP and cGMP in wild-type PDE10A were 152.5 ± 17.1 nM and 1.7 ± 0.3 μM, respectively. There were no statistically significant differences in Km values among the wild-type and the mutant PDE10As (Figure 6-15), suggesting that both p.Phe300Leu and p.Phe334Leu do not affect substantially basal PDE10A enzyme activity.

We then explored whether the identified substitutions affect the stimulatory properties of cAMP binding to the GAF-B domain. Experiments were conducted using only [^{3}H]cGMP as a substrate to avoid the binding of [^{3}H]cAMP substrate to the GAF-B domain and the cAMP analogue 1-NO-cAMP, which has a higher selectivity for the GAF-B domain over the catalytic site compared to cAMP (247-fold for 1-NO-cAMP vs. 8.7-fold for cAMP). These experimental conditions were chosen as, on the one hand, cAMP activates PDE10A enzyme activity via its binding to GAF-B and, on the other hand, competes at the catalytic domain with radio-labelled substrates and thus inhibits their degradation.

Wild-type and mutant PDE10As were incubated in the presence of various concentrations of 1-NO-cAMP with 70 nM [^{3}H]cGMP, and then catalytic activities were measured. 1-NO-cAMP markedly increased (approximately 2.7-fold over the basal levels) the enzyme activity of WT PDE10A, whereas this effect was almost completely abolished for both mutant PDE10As (Figure 6-16). These experiments demonstrate that p.Phe300Leu and p.Phe334Leu severely affect the positive regulatory mechanism of cAMP binding to the GAF-B domain on PDE catalytic activity.
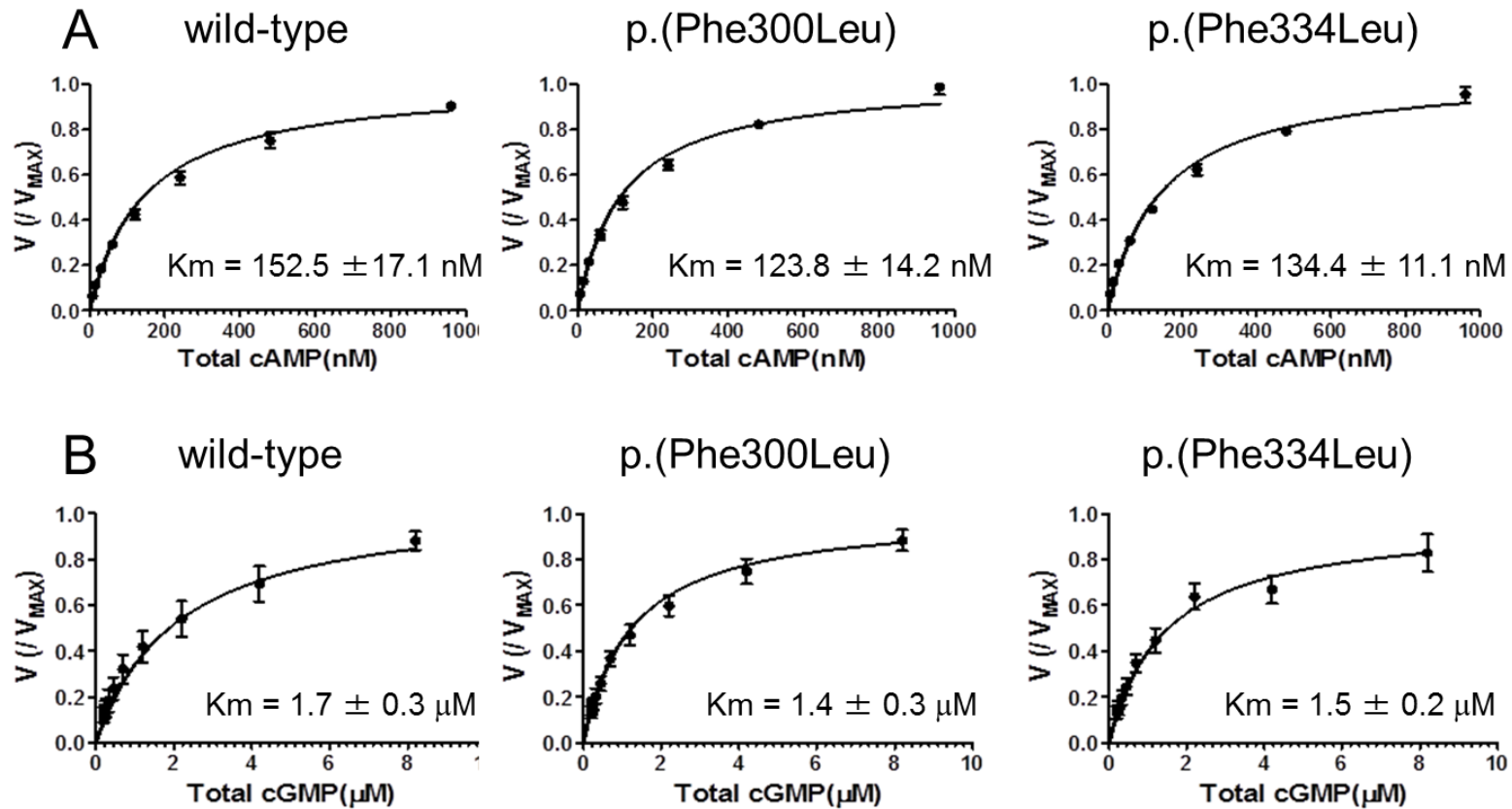
Figure 6-15 Enzyme Kinetics of Wild-Type and Mutant PDE10As.

PDE10A enzymes was incubated at presence of mixture of unlabelled cAMP and [3H]cAMP (A) or unlabelled cGMP and [3H]cGMP (B) with the total concentration as indicated. The velocity was divided by each Vmax value. Km values for cAMP (A) and cGMP (B) were determined by fitting to the Michaelis-Menten equation using GraphPad Prism. Each data point represented as mean ± SEM of five (for cAMP) or four (for cGMP) independent experiments. There was no statistically significant difference in Km values among the wildtype and the mutant PDE10As ($p > 0.05$ by Dunnett's test compared with wild-type).
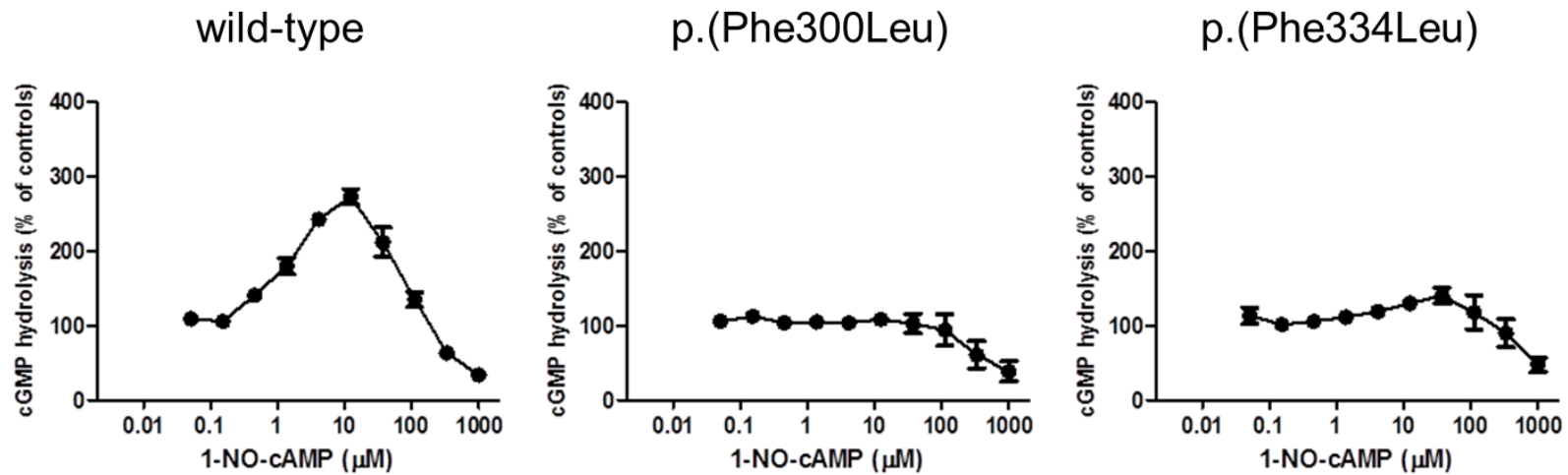
Figure 6-16 Effects of PDE10A substitutions on the modulatory activity of the GAF-B domain

Effect of 1-NO-cAMP on the PDE activity of a wild-type and mutants of PDE10A. Various concentrations of a cAMP analogue, 1-NO-cAMP, was added and catalytic activity of wild-type and mutant PDE10A, p.(Phe300Leu) and p.(Phe334Leu), at presence of 70 nM [3H]cGMP was determined. Each data point represents the means ± SEM for three independent experiments.

6.5.5 Discussion

Strong genetic evidence, fulfilling the recently proposed criteria for inferring causality of genetic variants (MacArthur *et al.*, 2014), supports the pathogenic role of the identified *PDE10A* mutations: (i) segregation analysis confirmed that both variants arose *de novo* in the three mutation carriers; (ii) the changes are otherwise absent in all interrogated public databases and in-house exomes from healthy controls or subjects with unrelated conditions (including more than 70,000 exomes); (iii) the mutations are consistently predicted pathogenic by all *in silico* prediction tools and affect amino acid residues completely conserved in all species homologs; (iv) the substitutions are located in a functionally important regulatory domain of the protein and *in vitro* functional data show that they disrupt the regulatory effect of the GAF-B domain; (v) *PDE10A* is very highly (and almost selectively) expressed in the striatum, the brain area most closely involved in the pathogenesis of choreic movements.

PDEs have previously been implicated in the pathogenesis of neurodegenerative disorders, such as PD and HD (Bollen and Prickaerts, 2012). Mutations in *PDE8B*, a gene highly expressed in the brain and especially in the putamen, causes autosomal dominant striatal degeneration (ADSD, MIM 609161), a disease that clinically presents with adult-onset parkinsonism (Appenzeller *et al.*, 2010, Barsottini *et al.*, 2015). Although the reported MRI abnormalities observed in subjects with ADSD are slightly different from those observed in our cases, it is striking that both diseases are caused by mutations in PDEs leading to clearly visible, largely symmetric, striatal MRI signal abnormalities. Furthermore, the fact that two PDEs are now directly linked to a basal ganglia disease may point towards a crucial role of PDEs in these types of disorders. The latter is of great interest given the pharmacological potential to manipulate PDE activity. Given its high and selective expression in striatal MSNs, PDE10A is a primary target in pharmacological research for diseases where dysregulation of striatal circuits is believed to be crucial (e.g. psychosis, HD, substance abuse and PD) (Chappie *et al.*, 2012).

According to the classic model of basal ganglia motor circuits, chorea may result from dysregulation of the activity of the striatal MSNs (Marsden, 1984). Based on different anatomical projections and biochemical features, MSNs are divided into two classes that constitute two parallel and segregated pathways exiting the striatum; (i) the 'direct pathway', formed by MSNs expressing high levels of the D1 dopamine receptors

(D1DR) and projecting directly to the basal ganglia output nuclei (the substantia nigra pars reticulata and the globus pallidus internal segment); (ii) the 'indirect pathway', mainly formed by MSNs expressing both D2 dopamine receptors (D2DR) and adenosine 2 receptors (A2AR) and projecting indirectly to the globus pallidus internal segment via the globus pallidus external segment and the subthalamic nucleus (Gerfen, 1992).

The two pathways control striatal output in an antagonistic way, the 'direct pathway' being involved in action production and the 'indirect pathway' in action suppression (DeLong and Wichmann, 2007). According to the classic model of basal ganglia motor circuits, chorea mainly results from disruption of the indirect pathway with consequent overactivity of the direct pathway (Marsden, 1984).

Importantly, modulation of MSN activity is largely dependent on cAMP signalling (Threlfell and West, 2013). cAMP synthesis, and thus indirectly its signalling, is promoted by the stimulation of the G protein-coupled receptors D1DR and A2AR, whereas synthesis is inhibited by dopamine stimulation of D2DR (Herve, 2011). The G protein $G\alpha_{olf}$ positively couples D1DR and A2AR to the activation of AC5, the main molecule responsible for cAMP production in MSNs (Lee *et al.*, 2002). Interestingly, the genes encoding $G\alpha_{olf}$ (*GNAL*) and AC5 (*ADCY5*) have both been identified as cause of primary dystonia (Fuchs *et al.*, 2013) and chorea (Chen *et al.*, 2012) respectively.

Mechanistically, *ADCY5* mutations seem to increase the AC5 activity with consequent raised intracellular cAMP levels in cellular models (Chen *et al.*, 2014). As both *PDE10A* and *ADCY5* pathogenic mutations cause chorea, but with PDE10A exerting an opposite effect to AC5 on cAMP levels, one would expect that the p.Phe300Leu and p.Phe334Leu variants exert a deleterious effect on the PDE enzyme activity. Recent studies suggest that PDE10A has two functional states; `active` and `super-active`(Jäger *et al.*, 2012, Russwurm *et al.*, 2015). In presence of high intracellular levels of cAMP, its binding to the GAF-B domain would stimulate the PDE catalytic activity, switching PDE10A from the 'active' to the 'super-active' state. In light of this, PDE10A may function as a 'brake' for MSN activation. Our functional studies show that pathogenic *PDE10A* mutations located in the GAF-B domain severely disrupt this positive regulatory mechanism without affecting the basal PDE enzyme activity. These mutations may therefore have a strong impact on the *in vivo* regulation of MSN activity,

especially when MSNs are activated by high levels of cAMP. Given the homodimerised structure of PDE10A, the mutant proteins could exert a dominant negative effect on the activity of the WT protein. Intriguingly, the *PDE10A* knockout mouse does not show a movement disorder reminiscent of chorea, but conversely presents reduced exploratory activity, more consistent with a parkinsonian phenotype (Siuciak *et al.*, 2006, Siuciak *et al.*, 2008).

In conclusion, I demonstrate here that *de novo* dominant mutations in *PDE10A* are a novel cause of a unique movement disorder characterized by benign childhood-onset chorea and typical MRI abnormalities of the striatum. Of note, PDE10A mutations were not found in cases with a BHC syndrome but with normal brain MRI. This suggests that *PDE10A*-related chorea may represent a distinct genetic clinico-radiological entity. Mutational screening of additional cohorts of cases with such MRI abnormalities is warranted to further define the clinical spectrum associated with *PDE10A* mutations.

Chapter 7. Conclusions

This thesis describes the work I conducted during my PhD to investigate the genetic bases of a range of movement disorders, including PD, dystonia, and chorea, and gain novel insights into the biological mechanisms of these conditions.

I used various combinations of genetic technologies (i.e. Sanger sequencing, WES and linkage analysis) and strategies (i.e. linkage mapping in combination with WES, interrogation of WES data searching for mutations in candidate genes, and analysis of WES from a series of unrelated cases with a specific clinical and radiological presentation).

My research has resulted in the identification of several novel genetic causes for these conditions, including genes harbouring high-risk fully penetrant mutations responsible for Mendelian forms of disease (e.g. *KCTD17* mutations in M-D and *PDE10A* mutations in chorea) and rare variants associated with intermediate risks (e.g. *GCH1* mutations in PD). I also expanded the phenotype associated with known Mendelian genes. I recognised that deficiency of tyrosine hydroxylase is a novel, treatable cause of M-D and mutations in *ADCY5* are not simply responsible for the unique condition Familial Dyskinesias with Facial Myokyimia, but actually represent a frequent cause of chorea with onset in childhood.

The main findings of this thesis are summarised below, together with the implications deriving from this work, both concerning clinical practice and future research into disease mechanisms.

7.1 Genetics of Parkinson Disease

GBA Mutations Are Common in Early-Onset Parkinson Disease and Influence the disease course

I showed that *GBA* mutations are the most common genetic abnormality, not only in patients with the classic late-onset form of the disease, but also in patients with early-onset PD. The frequency of *GBA* mutations in the latter group is actually significantly higher than in patients with classic PD.

This finding possesses an important clinical corollary. *GBA* should be systematically assessed in patients with an early onset of symptoms, as information regarding the mutational status may have crucial implications in terms of prognosis and response to pharmacological or surgical treatments (i.e. DBS). It is thought that patients with early-onset PD, and in particular those carrying mutations in the recessive genes *PARK2* or *PINK1*, tend to have a more indolent and benign disease course, in particular with regard to the risk of developing cognitive decline (Schrag and Schott, 2006).

However, this seems not to be true for *GBA* carriers, both from a motor and cognitive point of view. In our study, PD patients carrying *GBA* mutations, compared to patients with mutations in *PARK2*, *LRRK2* and no mutations, needed DBS significantly earlier in their disease, suggesting a more aggressive form of the disease in PD patients with *GBA* mutations. Furthermore, although the motor response to DBS treatment was comparable to that of the other patients, patients with *GBA* mutations presented a more rapid cognitive impairment following DBS implantation. Although this aspect should be carefully assessed in larger cohorts, these data overall indicate the genetics may be a powerful tool in recognizing and predicting clinical heterogeneity in PD.

The GBA E326K variant predisposes to Parkinson disease

I established incontrovertibly the pathogenic role of the *GBA* E326K variant, which, to date, represents the single most common genetic risk factor for PD with significant clinical relevance (7.5% of the PD cases screened in our study were carriers of the variant; odds ratio ~3). Notably, these results approximately double the proportion of PD patients with *GBA*-related disease, a fact that will have tremendous implications as soon as treatments for addressing *GBA* dysfunction in PD become available.

Confirming my finding, Nalls and colleagues recently demonstrated the association of the E326K with PD-dementia complex and Dementia with LBs (Nalls *et al.*, 2013). Moreover, it has been shown that the presence of the E326K negatively influences both motor disease progression (Winder-Rhodes *et al.*, 2013) and the risk of progression to dementia (Mata *et al.*, 2015).

Finally, the E326K predisposes to PD but does not cause GD (even when inherited in the homozygous state), clearly indicating that other molecular mechanisms, in addition to reduced *GBA* activity, may contribute to the development of PD disease in the presence of *GBA* dysfunction.

Beyond DOPA-responsive dystonia; GCH1 mutations: a novel risk for Parkinson disease

Through the analysis of WES data in a large cohort of PD cases and controls, I have identified rare coding *GCH1* as a novel risk locus for PD. Interestingly, as it was the case for the discovery of *GBA* mutations, this association was first suspected on clinical grounds, thanks to the observation in pedigrees with DRD of striatal dopaminergic denervation in *GCH1* pathogenic variant carriers with a clinical diagnosis of PD.

Interestingly, to date, no genes containing rare variants conferring intermediate risk for PD have been identified through unbiased large NGS studies. Therefore, astute clinical observations remain crucial for driving and inspiring genetic studies.

Since the appearance of this study in the literature, several other reports of DRD families with members affected by PD have been published (Lewthwaite *et al.*, 2015, Terbeek *et al.*, 2015, Someko *et al.*, 2016) and many others have been presented at scientific conferences (personal communication).

Furthermore, a recent study performed within the Canadian population confirmed that rare *GCH1* coding mutations are enriched in PD. The authors identified two variants, the known pathogenic p.Lys224Arg (x2) and the novel variant p.Ala99Asp (likely pathogenic according to in silico prediction tools and interspecies conservation) in three unrelated cases with PD, while no pathogenic changes were found in controls (Guella *et al.*, 2015). The mutational frequency was 0.56% (3/528) in cases versus 0% (0/290) in controls, consistent with the frequency we observed in our study (0.75% in cases versus 0.1% in controls).

The finding that *GCH1* loss-of-function variants are not only responsible for DRD, but are also associated with adult-onset neurodegenerative PD, is strengthened by the recent identification that *GCH1* has also been identified as a low-risk susceptibility locus for PD in the latest GWAS meta-analysis (Nalls *et al.*, 2014). This finding potentially extends the role of GTPCH deficiency in the pathogenesis of PD beyond the rare carriers of deleterious coding mutations.

An outstanding and crucial question remains as to whether patients with DRD eventually develop nigral neurodegeneration, or whether neurodegeneration can be avoided by dopaminergic replacement therapy. This could indeed support a central role

of dopamine deficiency in favouring nigral degeneration, with important therapeutic implications for asymptomatic carriers of pathogenic variants.

To date, no DRD cases treated with L-DOPA since childhood have been shown to develop frank nigral cell loss (Snow *et al.*, 1993, Turjanski *et al.*, 1993, Jeon *et al.*, 1998). This is consistent with post mortem analysis of few cases showing normal nigral cell count and absence of LBs (Furukawa *et al.*, 1999, Grotzsch *et al.*, 2002, Segawa *et al.*, 2013). However, Sawle and colleagues report in six cases with DOPA-responsive dystonia modest but significant reduction in the uptake of ^{18}F-fluorodopa into both caudates and putamen (Sawle *et al.*, 1991). Tadic and colleagues describe that parkinsonian signs are present in DOPA-responsive dystonia cases as a relatively common residual motor sign following treatment, possibly hinting at underlying neurodegeneration (Tadic *et al.*, 2012). Terbeek et al. recently described a 41-year-old patient carrying a known pathogenic *GCH1* variant (p.Tyr75Ser) with onset of classic DRD at age 9 (Terbeek *et al.*, 2015). He was treated with L-DOPA from the age of 11 with good and sustained response. At age 41 dopaminergic imaging (123I-FP-CIT SPECT) was performed showing severe bilateral and asymmetric reduction of putaminal tracer uptake, a pattern typical of idiopathic PD, arguing against a neuroprotective role of dopamine replacement.

I anticipate that post mortem analysis and longitudinal clinical, neuroimaging, and metabolic studies of *GCH1* mutation carriers—including asymptomatic carriers, individuals with classic DRD and cases with adult-onset parkinsonism - will facilitate the understanding of the pathogenesis of *GCH1*–associated PD.

Finally, more work is needed to understand the biological relevance of the GWAS signal in the *GCH1* locus. A functional haplotype at the *GCH1* genomic locus associated with reduced plasma GTPCH activity and BH$_4$ levels has been previously recognised (Antoniades *et al.*, 2008). Interestingly, the most-associated *GCH1* SNP (rs11158026) detected in the GWAS is in moderate linkage disequilibrium (r^2 0.457; D' 0.932) with the SNPs constituting the functional haplotype, suggesting a potential functional basis for the association of this SNP with increased PD risk.

7.2 Genetics of Myoclonus-Dystonia

Mutations in KCTD17 and TH are Novel Genetic Causes for SGCE-negative Myoclonus-Dystonia.

Through a combination of linkage analysis and WES, I identified that a dominant missense mutation in *KCTD17* causes autosomal dominant M-D in families without *SGCE*.

The clinical presentation of the *KCTD17*-mutated cases differs from the phenotype usually observed in *SGCE*-related M-D. All cases initially presented with mild myoclonus affecting the upper limbs. Dystonia showed a progressive course, with increasing severity of symptoms and spreading from the cranio-cervical region to other sites.

Like many other dystonia genes (e.g. *ANO3, GNAL, HPCA*), *KCTD17* is most highly expressed in the putamen, confirming an essential role of this brain structure in the pathogenesis of primary dystonias. Furthermore, a system biology analysis indicates that *KCTD17* is part of a striatal gene network significantly enriched for other dystonia-associated genes and genes involved in post-synaptic dopaminergic signalling in striatal cells. Intriguingly, knock-out of the *KCTD17* homologue in *Drosophila* leads to hyper-arousability and lack of sleep due to increased signaling downstream of the dopaminergic receptors (Stavropoulos and Young, 2011, Pfeiffenberger and Allada, 2012), suggesting that *KCTD17* may interact mechanistically with molecules within the dopaminergic signaling pathway in striatal cells. KCTD17 is known to contribute to the ubiquitin-proteasome machinery, acting as an adaptor for the CUL3-RING-E3 ligase and regulating turnover of substrates (Kasahara *et al.*, 2014). Functional work is warranted to identify the precise substrates of KCTD17 in striatal neurons and the mechanism whereby KCTD17 may regulate post-synaptic dopaminergic signalling. Despite its rarity, the discovery of *KCTD17* mutations as a cause of dystonia may help to elucidate pivotal molecular pathways and novel pharmacological targets to improve treatment of dystonia and other movement disorders.

Finally, the identification of family with tyrosine hydroxylase deficiency presenting with predominant myoclonus-dystonia highlight the importance of consider this treatable condition in the differential diagnosis of M-D, as early treatment with L-DOPA

is crucial for the motor and cognitive outcome of these patients.

The CACNA1B p.Arg1389His Variant Does Not Cause Myoclonus-Dystonia

Through sequencing in a large multi-centric cohort of M-D cases and controls, I show that the *CACNA1B* p.Arg1389His does not a disease-causing mutation for M-D.

The advent of next generation sequencing has led to an extraordinary acceleration in the discovery rate of rare genetic variants, the majority of which are of uncertain clinical significance. Hence, a close scrutiny is necessary before causally linking a candidate variant to a disease. To avoid false assignment of pathogenicity, MacArthur and colleagues have recently proposed guidelines for implicating causality of rare variants in human disease (MacArthur *et al.*, 2014). However, co-segregation of a variant with disease in a single pedigree does not establish with certainty its pathogenic role, especially if other co-segregating coding variants and the possibility of a separate undetected pathogenic variant in linkage disequilibrium cannot be convincingly ruled out (as it was the case in the pedigree where the p.Arg1389His was identified). In addition, a candidate variant responsible for a rare disease should be found at a low frequency in population controls, consistent with the proposed model of inheritance and disease prevalence.

M-D is an exceedingly rare condition. Although *CACNA1B*, by a biological point of view, could be a very plausible candidate gene for M-D and functional work performed by the authors shows that the mutation might affect the properties of encoded channel, the frequency of the *CACNA1B* p.Arg1389His in controls is simply too high to support its role in the pathogenesis of M-D.

7.3 Genetics of Chorea

Benign Hereditary Chorea is Not a Genetic Entity

Surprisingly, a thorough genetic screen of *NKX2-1* in the BHC Queen Square cohort revealed that only five probands (~20% of cohort) carried pathogenic mutations in this gene. A search for the recently described chromosomal deletions neighbouring but not encompassing *NKX2-1* (Thorwarth *et al.*, 2014), did not identify any further mutation carrier.

Importantly, I did not detect mutations in three cases with a clinical presentation fully

consistent with *NKX2-1*-related disease (i.e. presenting the full picture of brain-lung-thyroid disease), of which two had a clear autosomal dominant family history.

These results clearly indicate the existence of other undetected pathogenic variants, either in the *NKX2-1* non-coding regions (e.g. in the promoter, in intronic regulatory regions or in yet uncharacterised deep-intronic splice-site) or in other closely functionally related genes. In the future, WGS analysis in these cases will be potentially revealing for the identification of deep intronic mutations in the *NKX2-1* locus. Currently, WES analysis of the familial cases is ongoing in order to identify coding variants in novel genes responsible for the phenotype. Identification of such genes may shed light on the biological mechanisms essential for the correct development of striatal neurons, lungs and thyroid tissue.

A last remark regards the use of the term BHC. Importantly, the work presented in this thesis, in agreement with previous publications (Thorwarth *et al.*, 2014), demonstrates that ~70% of the cases with a clinical diagnosis of BHC do not carry mutations in this gene. Furthermore, *NKX2-1* mutations have been identified in patients with a range of movement disorders other than chorea, encouraging, overall, to abandon the use of the term BHC to label patients with *NKX2-1* mutations.

The identification of ADCY5 and PDE10A mutations crucially implicates cAMP metabolism in striatal neurons in the pathogenesis of chorea

I describe the identification of pathogenic dominant mutations (both de novo and transmitted) in *ADCY5* and *PDE10A* as important novel genetic causes of chorea with onset in childhood.

From a clinical point of view, *ADCY5* mutations appear to be a relatively common cause of chorea with onset in childhood (~9.4% of the cases I studied here). Importantly, while preparing this thesis, several other papers have appeared in the literature confirming the important clinical role of *ADCY5* mutations and further broadening the phenotype associated with *ADCY5* mutations to also include variable combinations of dystonia, myoclonus and paroxysmal dyskinesias (Carapito *et al.*, 2015, Chen *et al.*, 2015, Chang *et al.*, 2016, Friedman *et al.*, 2016).

Furthermore, a manuscript detailing the identification of recessive *PDE10A* mutations in patients with childhood-onset chorea has been recently published (Diggle *et al.*,

2016). Therein, the authors describe the identification of two homozygous mutations (p.Tyr107Cys and p.Ala116Pro), located in the GAF-A domain, in two consanguineous pedigrees. The phenotype of these cases was more severe than that of the patients I describe. Patients with recessive *PDE10A* mutations showed a much earlier age at onset of chorea (< 1 year), severe dysarthria, axial hypotonia, cognitive and language development delay. The authors also showed that both mutations lead to a reduction in PDE10A levels both in patients and in cellular models. Furthermore, a knock-in mouse model had decreased striatal PDE10A. Interestingly, despite a more severe neurological involvement, the MRI of the cases with recessive mutations did not show the same abnormal signal we observed in the cases with dominant mutations.

ADCY5 and *PDE10A* are almost exclusively expressed in the striatum, the brain region most closely involved in the pathogenesis of chorea and dystonia, and encode the two main enzymes that regulate the synthesis (*ADCY5*) and degradation (*PDE10A*) of cAMP in striatal neurons.

Additionally, mutations in *GNAL* (Fuchs *et al.*, 2013) and *GPR88* (Alkufri *et al.*, 2016), coding for G proteins almost exclusively expressed in striatal neurons that couple dopamine receptors to AC5 activation, have been recently linked to dystonia and chorea. Overall, these results strongly suggest that intracellular cAMP signalling in striatal neurons is crucial for normal activity of basal ganglia circuitry, and that disruptions thereof play an important role in the pathophysiology of hyperkinetic movement disorders. Modulation of the striatal cAMP levels may therefore represent a very attractive target for the development of novel treatments targeting striatal post-receptorial dopaminergic dysregulation in a range of hyperkinetic disorders.

Importantly, modulation of PDE10A activity is already a primary target in pharmacological research of basal ganglia disorders, including HD and PD (Chappie *et al.*, 2012). More specifically, a phase II clinical study (the Amaryllis study) of a PDE10A inhibitor is currently ongoing in HD. Importantly, the identification of loss-of-function *PDE10A* mutations as a cause of chorea suggests that pharmacological inhibition of PDE10A may not be the best option for the treatment of chorea and other hyperkinetic movement disorders. In support of this notion, it has been recently shown that asymptomatic carriers of the HD triplet expansion have reduced striatal levels of PDE10A (Niccolini *et al.*, 2015).

Finally, it will be important to establish whether the observation of EOPD in one of the cases I identified with a *de novo* PDE10A mutation is coincidental or whether individuals with *de novo PDE10A* mutations are also at an increased risk of developing degeneration of nigral neurons. In this regard, recent work has demonstrated that striatal loss of PDE10A expression is associated with PD duration and severity (Niccolini *et al.*, 2015).

References

Abecasis GR, Cherny SS, Cookson WO, Cardon LR. Merlin--rapid analysis of dense genetic maps using sparse gene flow trees. Nat Genet. 2002;30(1):97-101.

Abou-Sleiman PM, Healy DG, Quinn N, Lees AJ, Wood NW. The role of pathogenic DJ-1 mutations in Parkinson's disease. Ann Neurol. 2003;54(3):283-6.

Abou-Sleiman PM, Muqit MM, McDonald NQ, Yang YX, Gandhi S, Healy DG, et al. A heterozygous effect for PINK1 mutations in Parkinson's disease? Ann Neurol. 2006;60(4):414-9.

Adzhubei IA, Schmidt S, Peshkin L, Ramensky VE, Gerasimova A, Bork P, et al. A method and server for predicting damaging missense mutations. Nat Methods. 2010;7(4):248-9.

Ahle S, Ungewickell E. Auxilin, a newly identified clathrin-associated protein in coated vesicles from bovine brain. J Cell Biol. 1990;111(1):19-29.

Akawi N, McRae J, Ansari M, Balasubramanian M, Blyth M, Brady AF, et al. Discovery of four recessive developmental disorders using probabilistic genotype and phenotype matching among 4,125 families. Nat Genet. 2015;47(11):1363-9.

Akman HO, Kakhlon O, Coku J, Peverelli L, Rosenmann H, Rozenstein-Tsalkovich L, et al. Deep intronic GBE1 mutation in manifesting heterozygous patients with adult polyglucosan body disease. JAMA Neurol. 2015;72(4):441-5.

Alazami AM, Patel N, Shamseldin HE, Anazi S, Al-Dosari MS, Alzahrani F, et al. Accelerating Novel Candidate Gene Discovery in Neurogenetic Disorders via Whole-Exome Sequencing of Prescreened Multiplex Consanguineous Families. Cell Rep. 2015;10(2):148-61.

Albanese A, Asmus F, Bhatia KP, Elia AE, Elibol B, Filippini G, et al. EFNS guidelines on diagnosis and treatment of primary dystonias. European journal of neurology : the official journal of the European Federation of Neurological Societies. 2011;18(1):5-18.

Albanese A, Bhatia K, Bressman SB, Delong MR, Fahn S, Fung VS, et al. Phenomenology and classification of dystonia: a consensus update. Mov Disord.

2013;28(7):863-73.

Alcalay RN, Caccappolo E, Mejia-Santana H, Tang M, Rosado L, Orbe Reilly M, et al. Cognitive performance of GBA mutation carriers with early-onset PD: the CORE-PD study. Neurology. 2012;78(18):1434-40.

Alcalay RN, Caccappolo E, Mejia-Santana H, Tang MX, Rosado L, Ross BM, et al. Frequency of known mutations in early-onset Parkinson disease: implication for genetic counseling: the consortium on risk for early onset Parkinson disease study. Arch Neurol. 2010;67(9):1116-22.

Alcalay RN, Dinur T, Quinn T, Sakanaka K, Levy O, Waters C, et al. Comparison of Parkinson risk in Ashkenazi Jewish patients with Gaucher disease and GBA heterozygotes. JAMA Neurol. 2014;71(6):752-7.

Alcalay RN, Siderowf A, Ottman R, Caccappolo E, Mejia-Santana H, Tang MX, et al. Olfaction in Parkin heterozygotes and compound heterozygotes: the CORE-PD study. Neurology. 2011;76(4):319-26.

Alkufri F, Shaag A, Abu-Libdeh B, Elpeleg O. Deleterious mutation in GPR88 is associated with chorea, speech delay, and learning disabilities. Neurology Genetics. 2016;2(3).

Alkuraya FS. The application of next-generation sequencing in the autozygosity mapping of human recessive diseases. Hum Genet. 2013;132(11):1197-211.

Almasy L, Bressman SB, Raymond D, Kramer PL, Greene PE, Heiman GA, et al. Idiopathic torsion dystonia linked to chromosome 8 in two Mennonite families. Ann Neurol. 1997;42(4):670-3.

Andrew SE, Goldberg YP, Kremer B, Telenius H, Theilmann J, Adam S, et al. The relationship between trinucleotide (CAG) repeat length and clinical features of Huntington's disease. Nat Genet. 1993;4(4):398-403.

Angelini L, Erba A, Mariotti C, Gellera C, Ciano C, Nardocci N. Myoclonic dystonia as unique presentation of isolated vitamin E deficiency in a young patient. Mov Disord. 2002;17(3):612-4.

Anheim M, Monga B, Fleury M, Charles P, Barbot C, Salih M, et al. Ataxia with oculomotor apraxia type 2: clinical, biological and genotype/phenotype correlation study of a cohort of 90 patients. Brain. 2009;132(Pt 10):2688-98.

Annesi G, Savettieri G, Pugliese P, D'Amelio M, Tarantino P, Ragonese P, et al. DJ-1 mutations and parkinsonism-dementia-amyotrophic lateral sclerosis complex. Ann Neurol. 2005;58(5):803-7.

Antoniades C, Shirodaria C, Van Assche T, Cunnington C, Tegeder I, Lotsch J, et al. GCH1 haplotype determines vascular and plasma biopterin availability in coronary artery disease effects on vascular superoxide production and endothelial function. J Am Coll Cardiol. 2008;52(2):158-65.

Appenzeller S, Schirmacher A, Halfter H, Baumer S, Pendziwiat M, Timmerman V, et al. Autosomal-dominant striatal degeneration is caused by a mutation in the phosphodiesterase 8B gene. Am J Hum Genet. 2010;86(1):83-7.

Armstrong MJ, Shah BB, Chen R, Angel MJ, Lang AE. Expanding the phenomenology of benign hereditary chorea: evolution from chorea to myoclonus and dystonia. Mov Disord. 2011;26(12):2296-7.

Asmus F, Devlin A, Munz M, Zimprich A, Gasser T, Chinnery PF. Clinical differentiation of genetically proven benign hereditary chorea and myoclonus-dystonia. Mov Disord. 2007;22(14):2104-9.

Asmus F, Gasser T. Inherited myoclonus-dystonia. Adv Neurol. 2004;94:113-9.

Asmus F, Gasser T. Dystonia-plus syndromes. Eur J Neurol. 2010;17 Suppl 1:37-45.

Asmus F, Hjermind LE, Dupont E, Wagenstaller J, Haberlandt E, Munz M, et al. Genomic deletion size at the epsilon-sarcoglycan locus determines the clinical phenotype. Brain. 2007;130(Pt 10):2736-45.

Asmus F, Salih F, Hjermind LE, Ostergaard K, Munz M, Kuhn AA, et al. Myoclonus-dystonia due to genomic deletions in the epsilon-sarcoglycan gene. Ann Neurol. 2005;58(5):792-7.

Asmus F, Zimprich A, Tezenas Du Montcel S, Kabus C, Deuschl G, Kupsch A, et al.

Myoclonus-dystonia syndrome: epsilon-sarcoglycan mutations and phenotype. Ann Neurol. 2002;52(4):489-92.

Assmann B, Surtees R, Hoffmann GF. Approach to the diagnosis of neurotransmitter diseases exemplified by the differential diagnosis of childhood-onset dystonia. Ann Neurol. 2003;54 Suppl 6:S18-24.

Balint B, Bhatia KP. Dystonia: an update on phenomenology, classification, pathogenesis and treatment. Curr Opin Neurol. 2014;27(4):468-76.

Bamshad MJ, Ng SB, Bigham AW, Tabor HK, Emond MJ, Nickerson DA, et al. Exome sequencing as a tool for Mendelian disease gene discovery. Nat Rev Genet. 2011;12(11):745-55.

Bandmann O, Daniel S, Marsden CD, Wood NW, Harding AE. The GTP-cyclohydrolase I gene in atypical parkinsonian patients: a clinico-genetic study. J Neurol Sci. 1996;141(1-2):27-32.

Bandmann O, Goertz M, Zschocke J, Deuschl G, Jost W, Hefter H, et al. The phenylalanine loading test in the differential diagnosis of dystonia. Neurology. 2003;60(4):700-2.

Bandmann O, Nygaard TG, Surtees R, Marsden CD, Wood NW, Harding AE. Dopa-responsive dystonia in British patients: new mutations of the GTP-cyclohydrolase I gene and evidence for genetic heterogeneity. Hum Mol Genet. 1996;5(3):403-6.

Bandmann O, Valente EM, Holmans P, Surtees RA, Walters JH, Wevers RA, et al. Dopa-responsive dystonia: a clinical and molecular genetic study. Ann Neurol. 1998;44(4):649-56.

Barnett CP, Mencel JJ, Gecz J, Waters W, Kirwin SM, Vinette KM, et al. Choreoathetosis, congenital hypothyroidism and neonatal respiratory distress syndrome with intact NKX2-1. Am J Med Genet A. 2012;158A(12):3168-73.

Barrett MJ, Giraldo P, Capablo JL, Alfonso P, Irun P, Garcia-Rodriguez B, et al. Greater risk of parkinsonism associated with non-N370S GBA1 mutations. J Inherit Metab Dis. 2013;36(3):575-80.

Barsottini OG, Martins PM, Chien HF, Raskin S, Nunes RH, da Rocha AJ, et al. Familial striatal degeneration: New mutation and neuroimaging clues. Neurology. 2015.

Batla A, Adams ME, Erro R, Ganos C, Balint B, Mencacci NE, et al. Cortical pencil lining in neuroferritinopathy: a diagnostic clue. Neurology. 2015;84(17):1816-8.

Bauer P, Kreuz FR, Burk K, Saft C, Andrich J, Heilemann H, et al. Mutations in TITF1 are not relevant to sporadic and familial chorea of unknown cause. Mov Disord. 2006;21(10):1734-7.

Beavo JA, Brunton LL. Cyclic nucleotide research -- still expanding after half a century. Nat Rev Mol Cell Biol. 2002;3(9):710-8.

Becanovic K, Norremolle A, Neal SJ, Kay C, Collins JA, Arenillas D, et al. A SNP in the HTT promoter alters NF-kappaB binding and is a bidirectional genetic modifier of Huntington disease. Nat Neurosci. 2015;18(6):807-16.

Becher MW, Rubinsztein DC, Leggo J, Wagster MV, Stine OC, Ranen NG, et al. Dentatorubral and pallidoluysian atrophy (DRPLA). Clinical and neuropathological findings in genetically confirmed North American and European pedigrees. Mov Disord. 1997;12(4):519-30.

Beicht S, Strobl-Wildemann G, Rath S, Wachter O, Alberer M, Kaminsky E, et al. Next generation sequencing as a useful tool in the diagnostics of mosaicism in Alport syndrome. Gene. 2013;526(2):474-7.

Bembi B, Zambito Marsala S, Sidransky E, Ciana G, Carrozzi M, Zorzon M, et al. Gaucher's disease with Parkinson's disease: clinical and pathological aspects. Neurology. 2003;61(1):99-101.

Benabid AL, Pollak P, Seigneuret E, Hoffmann D, Gay E, Perret J. Chronic VIM thalamic stimulation in Parkinson's disease, essential tremor and extra-pyramidal dyskinesias. Acta Neurochir Suppl (Wien). 1993;58:39-44.

Bender AT, Beavo JA. Cyclic nucleotide phosphodiesterases: molecular regulation to clinical use. Pharmacol Rev. 2006;58(3):488-520.

Berman BD, Jinnah HA. Dystonia: Five new things. Neurol Clin Pract. 2015;5(3):232-

40.

Beuckmann CT, Sinton CM, Miyamoto N, Ino M, Yanagisawa M. N-type calcium channel alpha1B subunit (Cav2.2) knock-out mice display hyperactivity and vigilance state differences. J Neurosci. 2003;23(17):6793-7.

Bird TD, Carlson CB, Hall JG. Familial essential ("benign") chorea. J Med Genet. 1976;13(5):357-62.

Blau N, Bonafe L, Thony B. Tetrahydrobiopterin deficiencies without hyperphenylalaninemia: diagnosis and genetics of dopa-responsive dystonia and sepiapterin reductase deficiency. Molecular genetics and metabolism. 2001;74(1-2):172-85.

Boisse Lomax L, Bayly MA, Hjalgrim H, Moller RS, Vlaar AM, Aaberg KM, et al. 'North Sea' progressive myoclonus epilepsy: phenotype of subjects with GOSR2 mutation. Brain. 2013;136(Pt 4):1146-54.

Bollen E, Prickaerts J. Phosphodiesterases in neurodegenerative disorders. IUBMB Life. 2012;64(12):965-70.

Bonafe L, Thony B, Penzien JM, Czarnecki B, Blau N. Mutations in the sepiapterin reductase gene cause a novel tetrahydrobiopterin-dependent monoamine-neurotransmitter deficiency without hyperphenylalaninemia. Am J Hum Genet. 2001;69(2):269-77.

Bonifacino JS, Rojas R. Retrograde transport from endosomes to the trans-Golgi network. Nat Rev Mol Cell Biol. 2006;7(8):568-79.

Bonifati V. Autosomal recessive parkinsonism. Parkinsonism Relat Disord. 2012;18 Suppl 1:S4-6.

Bonifati V, Rizzu P, van Baren MJ, Schaap O, Breedveld GJ, Krieger E, et al. Mutations in the DJ-1 gene associated with autosomal recessive early-onset parkinsonism. Science. 2003;299(5604):256-9.

Bonifati V, Rohe CF, Breedveld GJ, Fabrizio E, De Mari M, Tassorelli C, et al. Early-onset parkinsonism associated with PINK1 mutations: frequency, genotypes, and

phenotypes. Neurology. 2005;65(1):87-95.

Braak H, Del Tredici K, Rüb U, de Vos RAI, Jansen Steur ENH, Braak E. Staging of brain pathology related to sporadic Parkinson's disease. Neurobiol Aging. 2003;24(2):197-211.

Bras J, Guerreiro R, Hardy J. Use of next-generation sequencing and other whole-genome strategies to dissect neurological disease. Nat Rev Neurosci. 2012;13(7):453-64.

Bras J, Paisan-Ruiz C, Guerreiro R, Ribeiro MH, Morgadinho A, Januario C, et al. Complete screening for glucocerebrosidase mutations in Parkinson disease patients from Portugal. Neurobiol Aging. 2009;30(9):1515-7.

Bras J, Verloes A, Schneider SA, Mole SE, Guerreiro RJ. Mutation of the parkinsonism gene ATP13A2 causes neuronal ceroid-lipofuscinosis. Hum Mol Genet. 2012;21(12):2646-50.

Brashear A, Dobyns WB, de Carvalho Aguiar P, Borg M, Frijns CJ, Gollamudi S, et al. The phenotypic spectrum of rapid-onset dystonia-parkinsonism (RDP) and mutations in the ATP1A3 gene. Brain. 2007;130(Pt 3):828-35.

Brautigam C, Steenbergen-Spanjers GCH, Hoffmann GF, Dionisi-Vici C, van den Heuvel L, Smeitink JAM, et al. Biochemical and molecular genetic characteristics of the severe form of tyrosine hydroxylase deficiency. Clinical Chemistry. 1999;45(12):2073-8.

Brautigam C, Wevers RA, Jansen RJ, Smeitink JA, de Rijk-van Andel JF, Gabreels FJ, et al. Biochemical hallmarks of tyrosine hydroxylase deficiency. Clinical chemistry. 1998;44(9):1897-904.

Brautigam C, Wevers RA, Jansen RJ, Smeitink JA, de Rijk-van Andel JF, Gabreels FJ, et al. Biochemical hallmarks of tyrosine hydroxylase deficiency. Clin Chem. 1998;44(9):1897-904.

Breedveld GJ, van Dongen JW, Danesino C, Guala A, Percy AK, Dure LS, et al. Mutations in TITF-1 are associated with benign hereditary chorea. Hum Mol Genet. 2002;11(8):971-9.

Breit S, Wachter T, Schmid-Bielenberg D, Weiss D, Leitner P, Nagele T, et al. Effective long-term subthalamic stimulation in PARK8 positive Parkinson's disease. J Neurol. 2010;257(7):1205-7.

Brooks DJ, Pavese N. Imaging biomarkers in Parkinson's disease. Prog Neurobiol. 2011;95(4):614-28.

Bruno MK, Hallett M, Gwinn-Hardy K, Sorensen B, Considine E, Tucker S, et al. Clinical evaluation of idiopathic paroxysmal kinesigenic dyskinesia: new diagnostic criteria. Neurology. 2004;63(12):2280-7.

Bruno MK, Lee HY, Auburger GW, Friedman A, Nielsen JE, Lang AE, et al. Genotype-phenotype correlation of paroxysmal nonkinesigenic dyskinesia. Neurology. 2007;68(21):1782-9.

Burchell VS, Nelson DE, Sanchez-Martinez A, Delgado-Camprubi M, Ivatt RM, Pogson JH, et al. The Parkinson's disease-linked proteins Fbxo7 and Parkin interact to mediate mitophagy. Nat Neurosci. 2013;16(9):1257-65.

Burns J, Neuhauser G, Tomasi L. Benign hereditary non-progressive chorea of early onset. Clinical genetics of the syndrome and report of a new family. Neuropadiatrie. 1976;7(4):431-8.

Camargos S, Scholz S, Simon-Sanchez J, Paisan-Ruiz C, Lewis P, Hernandez D, et al. DYT16, a novel young-onset dystonia-parkinsonism disorder: identification of a segregating mutation in the stress-response protein PRKRA. Lancet neurology. 2008;7(3):207-15.

Canet-Aviles RM, Wilson MA, Miller DW, Ahmad R, McLendon C, Bandyopadhyay S, et al. The Parkinson's disease protein DJ-1 is neuroprotective due to cysteine-sulfinic acid-driven mitochondrial localization. Proc Natl Acad Sci U S A. 2004;101(24):9103-8.

Cao L, Huang XJ, Zheng L, Xiao Q, Wang XJ, Chen SD. Identification of a novel PRRT2 mutation in patients with paroxysmal kinesigenic dyskinesias and c.649dupC as a mutation hot-spot. Parkinsonism & related disorders. 2012;18(5):704-6.

Capecci M, Passamonti L, Annesi F, Annesi G, Bellesi M, Candiano IC, et al. Chronic bilateral subthalamic deep brain stimulation in a patient with homozygous deletion in

the parkin gene. Mov Disord. 2004;19(12):1450-2.

Caputo A, Caci E, Ferrera L, Pedemonte N, Barsanti C, Sondo E, et al. TMEM16A, a membrane protein associated with calcium-dependent chloride channel activity. Science. 2008;322(5901):590-4.

Carapito R, Paul N, Untrau M, Le Gentil M, Ott L, Alsaleh G, et al. A de novo ADCY5 mutation causes early-onset autosomal dominant chorea and dystonia. Mov Disord. 2015;30(3):423-7.

Carecchio M, Magliozzi M, Copetti M, Ferraris A, Bernardini L, Bonetti M, et al. Defining the epsilon-sarcoglycan (SGCE) gene phenotypic signature in myoclonus-dystonia: a reappraisal of genetic testing criteria. Mov Disord. 2013;28(6):787-94.

Carecchio M, Panteghini C, Reale C, Barzaghi C, Monti V, Romito L, et al. Novel GNAL mutation with intra-familial clinical heterogeneity: Expanding the phenotype. Parkinsonism Relat Disord. 2016;23:66-71.

Carrera P, Piatti M, Stenirri S, Grimaldi LM, Marchioni E, Curcio M, et al. Genetic heterogeneity in Italian families with familial hemiplegic migraine. Neurology. 1999;53(1):26-33.

Ceravolo R, Nicoletti V, Garavaglia B, Reale C, Kiferle L, Bonuccelli U. Expanding the clinical phenotype of DYT5 mutations: Is multiple system atrophy a possible one? Neurology. 2013;81(3):301-2.

Chabas A, Gort L, Diaz-Font A, Montfort M, Santamaria R, Cidras M, et al. Perinatal lethal phenotype with generalized ichthyosis in a type 2 Gaucher disease patient with the [L444P;E326K]/P182L genotype: effect of the E326K change in neonatal and classic forms of the disease. Blood Cells Mol Dis. 2005;35(2):253-8.

Chang FC, Westenberger A, Dale RC, Smith M, Pall HS, Perez-Duenas B, et al. Phenotypic insights into ADCY5-associated disease. Mov Disord. 2016.

Chappie TA, Helal CJ, Hou X. Current landscape of phosphodiesterase 10A (PDE10A) inhibition. J Med Chem. 2012;55(17):7299-331.

Charlesworth G, Angelova PR, Bartolome-Robledo F, Ryten M, Trabzuni D, Stamelou

M, et al. Mutations in HPCA Cause Autosomal-Recessive Primary Isolated Dystonia. Am J Hum Genet. 2015.

Charlesworth G, Bhatia KP, Wood NW. The genetics of dystonia: new twists in an old tale. Brain. 2013;136(Pt 7):2017-37.

Charlesworth G, Mohire MD, Schneider SA, Stamelou M, Wood NW, Bhatia KP. Ataxia telangiectasia presenting as dopa-responsive cervical dystonia. Neurology. 2013;81(13):1148-51.

Charlesworth G, Plagnol V, Holmstrom KM, Bras J, Sheerin UM, Preza E, et al. Mutations in ANO3 Cause Dominant Craniocervical Dystonia: Ion Channel Implicated in Pathogenesis. American journal of human genetics. 2012;91(6):1041-50.

Charlesworth G, Plagnol V, Holmstrom KM, Bras J, Sheerin UM, Preza E, et al. Mutations in ANO3 cause dominant craniocervical dystonia: ion channel implicated in pathogenesis. Am J Hum Genet. 2012;91(6):1041-50.

Chen D-H, Bonkowski E, Korvatska O, Hisama F, Friedman J, Davis M, et al. ADCY5-related movement disorder: broader spectrum and genotype/phenotype correlations including new cases (P2. 140). Neurology. 2015;84(14 Supplement):P2. 140.

Chen DD, Chen LY, Xie JB, Shu C, Yang T, Zhou S, et al. Tetrahydrobiopterin regulation of eNOS redox function. Curr Pharm Des. 2014;20(22):3554-62.

Chen DH, Matsushita M, Rainier S, Meaney B, Tisch L, Feleke A, et al. Presence of alanine-to-valine substitutions in myofibrillogenesis regulator 1 in paroxysmal nonkinesigenic dyskinesia: confirmation in 2 kindreds. Archives of neurology. 2005;62(4):597-600.

Chen DH, Meneret A, Friedman JR, Korvatska O, Gad A, Bonkowski ES, et al. ADCY5-related dyskinesia: Broader spectrum and genotype-phenotype correlations. Neurology. 2015;85(23):2026-35.

Chen WJ, Lin Y, Xiong ZQ, Wei W, Ni W, Tan GH, et al. Exome sequencing identifies truncating mutations in PRRT2 that cause paroxysmal kinesigenic dyskinesia. Nat Genet. 2011;43(12):1252-5.

Chen WJ, Lin Y, Xiong ZQ, Wei W, Ni W, Tan GH, et al. Exome sequencing identifies truncating mutations in PRRT2 that cause paroxysmal kinesigenic dyskinesia. Nat Genet. 2011;43(12):1252-5.

Chen YZ, Friedman JR, Chen DH, Chan GC, Bloss CS, Hisama FM, et al. Gain-of-function ADCY5 mutations in familial dyskinesia with facial myokymia. Ann Neurol. 2014;75(4):542-9.

Chen YZ, Matsushita MM, Robertson P, Rieder M, Girirajan S, Antonacci F, et al. Autosomal dominant familial dyskinesia and facial myokymia: single exome sequencing identifies a mutation in adenylyl cyclase 5. Arch Neurol. 2012;69(5):630-5.

Cheng H, Ma Y, Ni X, Jiang M, Guo L, Ying K, et al. Isolation and characterization of a human novel RAB (RAB39B) gene. Cytogenet Genome Res. 2002;97(1-2):72-5.

Chinnery PF, Crompton DE, Birchall D, Jackson MJ, Coulthard A, Lombes A, et al. Clinical features and natural history of neuroferritinopathy caused by the FTL1 460InsA mutation. Brain. 2007;130(Pt 1):110-9.

Choi Y, Sims GE, Murphy S, Miller JR, Chan AP. Predicting the functional effect of amino acid substitutions and indels. PLoS One. 2012;7(10):e46688.

Chun RW, Daly RF, Mansheim BJ, Jr., Wolcott GJ. Benign familial chorea with onset in childhood. JAMA. 1973;225(13):1603-7.

Cirulli ET, Lasseigne BN, Petrovski S, Sapp PC, Dion PA, Leblond CS, et al. Exome sequencing in amyotrophic lateral sclerosis identifies risk genes and pathways. Science. 2015;347(6229):1436-41.

Claes K, Depuydt J, Taylor AM, Last JI, Baert A, Schietecatte P, et al. Variant ataxia telangiectasia: clinical and molecular findings and evaluation of radiosensitive phenotypes in a patient and relatives. Neuromolecular Med. 2013;15(3):447-57.

Clark LN, Ross BM, Wang Y, Mejia-Santana H, Harris J, Louis ED, et al. Mutations in the glucocerebrosidase gene are associated with early-onset Parkinson disease. Neurology. 2007;69(12):1270-7.

Clark LN, Wang Y, Karlins E, Saito L, Mejia-Santana H, Harris J, et al. Frequency of

LRRK2 mutations in early- and late-onset Parkinson disease. Neurology. 2006;67(10):1786-91.

Clot F, Grabli D, Cazeneuve C, Roze E, Castelnau P, Chabrol B, et al. Exhaustive analysis of BH4 and dopamine biosynthesis genes in patients with Dopa-responsive dystonia. Brain. 2009;132(Pt 7):1753-63.

Clot F, Grabli D, Cazeneuve C, Roze E, Castelnau P, Chabrol B, et al. Exhaustive analysis of BH4 and dopamine biosynthesis genes in patients with Dopa-responsive dystonia. Brain : a journal of neurology. 2009;132(Pt 7):1753-63.

Cobb SA, Wider C, Ross OA, Mata IF, Adler CH, Rajput A, et al. GCH1 in early-onset Parkinson's disease. Mov Disord. 2009;24(14):2070-5.

Cormand B, Grinberg D, Gort L, Fiumara A, Barone R, Vilageliu L, et al. Two new mild homozygous mutations in Gaucher disease patients: clinical signs and biochemical analyses. Am J Med Genet. 1997;70(4):437-43.

Correale S, Esposito C, Pirone L, Vitagliano L, Di Gaetano S, Pedone E. A biophysical characterization of the folded domains of KCTD12: insights into interaction with the GABAB2 receptor. J Mol Recognit. 2013;26(10):488-95.

Corvol JC, Studler JM, Schonn JS, Girault JA, Herve D. Galpha(olf) is necessary for coupling D1 and A2a receptors to adenylyl cyclase in the striatum. J Neurochem. 2001;76(5):1585-8.

Costa Mdo C, Teixeira-Castro A, Constante M, Magalhaes M, Magalhaes P, Cerqueira J, et al. Exclusion of mutations in the PRNP, JPH3, TBP, ATN1, CREBBP, POU3F2 and FTL genes as a cause of disease in Portuguese patients with a Huntington-like phenotype. J Hum Genet. 2006;51(8):645-51.

Cox TM. Gaucher disease: understanding the molecular pathogenesis of sphingolipidoses. J Inherit Metab Dis. 2001;24 Suppl 2:106-21; discussion 87-8.

Crabtree MJ, Tatham AL, Al-Wakeel Y, Warrick N, Hale AB, Cai S, et al. Quantitative regulation of intracellular endothelial nitric-oxide synthase (eNOS) coupling by both tetrahydrobiopterin-eNOS stoichiometry and biopterin redox status: insights from cells with tet-regulated GTP cyclohydrolase I expression. J Biol Chem. 2009;284(2):1136-44.

Cullen V, Sardi SP, Ng J, Xu YH, Sun Y, Tomlinson JJ, et al. Acid beta-glucosidase mutants linked to Gaucher disease, Parkinson disease, and Lewy body dementia alter alpha-synuclein processing. Ann Neurol. 2011;69(6):940-53.

Cummins G, Jawad T, Taylor M, Lynch T. Myoclonic head jerks and extensor axial dystonia in the variant form of ataxia telangiectasia. Parkinsonism Relat Disord. 2013;19(12):1173-4.

Curtis AR, Fey C, Morris CM, Bindoff LA, Ince PG, Chinnery PF, et al. Mutation in the gene encoding ferritin light polypeptide causes dominant adult-onset basal ganglia disease. Nat Genet. 2001;28(4):350-4.

Dale RC, Grattan-Smith P, Nicholson M, Peters GB. Microdeletions detected using chromosome microarray in children with suspected genetic movement disorders: a single-centre study. Dev Med Child Neurol. 2012;54(7):618-23.

Datla KP, Blunt SB, Dexter DT. Chronic L-DOPA administration is not toxic to the remaining dopaminergic nigrostriatal neurons, but instead may promote their functional recovery, in rats with partial 6-OHDA or FeCl(3) nigrostriatal lesions. Mov Disord. 2001;16(3):424-34.

Davydov EV, Goode DL, Sirota M, Cooper GM, Sidow A, Batzoglou S. Identifying a high fraction of the human genome to be under selective constraint using GERP++. PLoS Comput Biol. 2010;6(12):e1001025.

Dawn Teare M, Barrett JH. Genetic linkage studies. Lancet. 2005;366(9490):1036-44.

de Carvalho Aguiar P, Borges V, Ferraz HB, Ozelius LJ. Novel compound heterozygous mutations in PRKRA cause pure dystonia. Mov Disord. 2015;30(6):877-8.

de Carvalho Aguiar P, Sweadner KJ, Penniston JT, Zaremba J, Liu L, Caton M, et al. Mutations in the Na+/K+ -ATPase alpha3 gene ATP1A3 are associated with rapid-onset dystonia parkinsonism. Neuron. 2004;43(2):169-75.

De Lonlay P, Nassogne MC, van Gennip AH, van Cruchten AC, de Villemeur TB, Cretz M, et al. Tyrosine hydroxylase deficiency unresponsive to L-dopa treatment with unusual clinical and biochemical presentation. Journal of Inherited Metabolic Disease. 2000;23(8):819-25.

de Rijk-van Andel JF, Gabreels FJM, Geurtz B, Steenbergen-Spanjers GCH, van den Heuvel L, Smeitink JAM, et al. L-dopa-responsive infantile hypokinetic rigid parkinsonism due to tyrosine hydroxylase deficiency. Neurology. 2000;55(12):1926-8.

de Vries BB, Arts WF, Breedveld GJ, Hoogeboom JJ, Niermeijer MF, Heutink P. Benign hereditary chorea of early onset maps to chromosome 14q. Am J Hum Genet. 2000;66(1):136-42.

Deas E, Wood NW, Plun-Favreau H. Mitophagy and Parkinson's disease: the PINK1-parkin link. Biochim Biophys Acta. 2011;1813(4):623-33.

DeJesus-Hernandez M, Mackenzie IR, Boeve BF, Boxer AL, Baker M, Rutherford NJ, et al. Expanded GGGGCC hexanucleotide repeat in noncoding region of C9ORF72 causes chromosome 9p-linked FTD and ALS. Neuron. 2011;72(2):245-56.

DeLong MR, Wichmann T. Circuits and circuit disorders of the basal ganglia. Arch Neurol. 2007;64(1):20-4.

Dementieva IS, Tereshko V, McCrossan ZA, Solomaha E, Araki D, Xu C, et al. Pentameric assembly of potassium channel tetramerization domain-containing protein 5. J Mol Biol. 2009;387(1):175-91.

Demos MK, van Karnebeek CD, Ross CJ, Adam S, Shen Y, Zhan SH, et al. A novel recurrent mutation in ATP1A3 causes CAPOS syndrome. Orphanet J Rare Dis. 2014;9:15.

Devine MJ, Gwinn K, Singleton A, Hardy J. Parkinson's disease and alpha-synuclein expression. Mov Disord. 2011;26(12):2160-8.

Devriendt K, Vanhole C, Matthijs G, de Zegher F. Deletion of thyroid transcription factor-1 gene in an infant with neonatal thyroid dysfunction and respiratory failure. N Engl J Med. 1998;338(18):1317-8.

Di Fonzo A, Chien HF, Socal M, Giraudo S, Tassorelli C, Iliceto G, et al. ATP13A2 missense mutations in juvenile parkinsonism and young onset Parkinson disease. Neurology. 2007;68(19):1557-62.

Di Fonzo A, Dekker MC, Montagna P, Baruzzi A, Yonova EH, Correia Guedes L, et al.

FBXO7 mutations cause autosomal recessive, early-onset parkinsonian-pyramidal syndrome. Neurology. 2009;72(3):240-5.

Di Fonzo A, Rohe CF, Ferreira J, Chien HF, Vacca L, Stocchi F, et al. A frequent LRRK2 gene mutation associated with autosomal dominant Parkinson's disease. Lancet. 2005;365(9457):412-5.

Diepold K, Schutz B, Rostasy K, Wilken B, Hougaard P, Guttler F, et al. Levodopa-responsive infantile parkinsonism due to a novel mutation in the tyrosine hydroxylase gene and exacerbation by viral infections. Movement Disorders. 2005;20(6):764-7.

Diggle CP, Sukoff Rizzo SJ, Popiolek M, Hinttala R, Schulke JP, Kurian MA, et al. Biallelic Mutations in PDE10A Lead to Loss of Striatal PDE10A and a Hyperkinetic Movement Disorder with Onset in Infancy. Am J Hum Genet. 2016;98(4):735-43.

Djagaeva I, Doronkin S. COP9 limits dendritic branching via Cullin3-dependent degradation of the actin-crosslinking BTB-domain protein Kelch. PLoS One. 2009;4(10):e7598.

Djarmati A, Guzvic M, Grunewald A, Lang AE, Pramstaller PP, Simon DK, et al. Rapid and reliable detection of exon rearrangements in various movement disorders genes by multiplex ligation-dependent probe amplification. Mov Disord. 2007;22(12):1708-14.

Djarmati A, Svetel M, Momcilovic D, Kostic V, Klein C. Significance of recurrent mutations in the myofibrillogenesis regulator 1 gene. Archives of neurology. 2005;62(10):1641.

Dobricic V, Kresojevic N, Marjanovic A, Tomic A, Svetel M, Novakovic I, et al. HPCA-related dystonia: Too rare to be found? Mov Disord. 2016.

Dobricic V, Kresojevic N, Westenberger A, Svetel M, Tomic A, Ralic V, et al. De novo mutation in the GNAL gene causing seemingly sporadic dystonia in a Serbian patient. Mov Disord. 2014;29(9):1190-3.

Doherty KM, Silveira-Moriyama L, Parkkinen L, Healy DG, Farrell M, Mencacci NE, et al. Parkin disease: a clinicopathologic entity? JAMA Neurol. 2013;70(5):571-9.

Donaldson I, Marsden CD, Schneider SA, Bhatia KB. Clinical approach to movement

disorders. In: Donaldson I, Marsden CD, Schneider SA, Bhatia KB, editors. Marsden's Book of Movement Disorders. Oxford, United Kingdom: Oxford University Press; 2012. p. 140-1.

Drouet V, Lesage S. Synaptojanin 1 mutation in Parkinson's disease brings further insight into the neuropathological mechanisms. Biomed Res Int. 2014;2014:289728.

Dufke C, Hauser AK, Sturm M, Fluhr S, Wachter T, Leube B, et al. Mutations in CIZ1 are not a major cause for dystonia in Germany. Mov Disord. 2015;30(5):740-3.

Dufke C, Sturm M, Schroeder C, Moll S, Ott T, Riess O, et al. Screening of mutations in GNAL in sporadic dystonia patients. Mov Disord. 2014;29(9):1193-6.

Duran R, McNeill A, Mehta A, Hughes D, Cox T, Deegan P, et al. Novel pathogenic mutations in the glucocerebrosidase locus. Mol Genet Metab. 2012;106(4):495-7.

Duvoisin RC, Eldridge R, Williams A, Nutt J, Calne D. Twin study of Parkinson disease. Neurology. 1981;31(1):77-80.

Dyment DA, Smith AC, Humphreys P, Schwartzentruber J, Beaulieu CL, Bulman DE, et al. Homozygous nonsense mutation in SYNJ1 associated with intractable epilepsy and tau pathology. Neurobiol Aging. 2015;36(2):1222 e1-5.

Dyment DA, Tetreault M, Beaulieu CL, Hartley T, Ferreira P, Chardon JW, et al. Whole-exome sequencing broadens the phenotypic spectrum of rare pediatric epilepsy: a retrospective study. Clin Genet. 2015;88(1):34-40.

Ebrahimi-Fakhari D, Saffari A, Westenberger A, Klein C. The evolving spectrum of PRRT2-associated paroxysmal diseases. Brain. 2015;138(Pt 12):3476-95.

Edvardson S, Cinnamon Y, Ta-Shma A, Shaag A, Yim YI, Zenvirt S, et al. A deleterious mutation in DNAJC6 encoding the neuronal-specific clathrin-uncoating co-chaperone auxilin, is associated with juvenile parkinsonism. PLoS One. 2012;7(5):e36458.

Edwards TL, Scott WK, Almonte C, Burt A, Powell EH, Beecham GW, et al. Genome-wide association study confirms SNPs in SNCA and the MAPT region as common risk factors for Parkinson disease. Ann Hum Genet. 2010;74(2):97-109.

Eggers C, Volk AE, Kahraman D, Fink GR, Leube B, Schmidt M, et al. Are Dopa-responsive dystonia and Parkinson's disease related disorders? A case report. Parkinsonism Relat Disord. 2012;18(5):666-8.

Ehrlich ME. Huntington's disease and the striatal medium spiny neuron: cell-autonomous and non-cell-autonomous mechanisms of disease. Neurotherapeutics. 2012;9(2):270-84.

Erro R, Hersheson J, Ganos C, Mencacci NE, Stamelou M, Batla A, et al. H-ABC syndrome and DYT4: Variable expressivity or pleiotropy of TUBB4 mutations? Mov Disord. 2015;30(6):828-33.

Erro R, Sheerin UM, Bhatia KP. Paroxysmal dyskinesias revisited: a review of 500 genetically proven cases and a new classification. Mov Disord. 2014;29(9):1108-16.

Esapa CT, Waite A, Locke M, Benson MA, Kraus M, McIlhinney RA, et al. SGCE missense mutations that cause myoclonus-dystonia syndrome impair epsilon-sarcoglycan trafficking to the plasma membrane: modulation by ubiquitination and torsinA. Hum Mol Genet. 2007;16(3):327-42.

Farrer M, Kachergus J, Forno L, Lincoln S, Wang DS, Hulihan M, et al. Comparison of kindreds with parkinsonism and alpha-synuclein genomic multiplications. Ann Neurol. 2004;55(2):174-9.

Fernandez M, Raskind W, Matsushita M, Wolff J, Lipe H, Bird T. Hereditary benign chorea: clinical and genetic features of a distinct disease. Neurology. 2001;57(1):106-10.

Fernandez M, Raskind W, Wolff J, Matsushita M, Yuen E, Graf W, et al. Familial dyskinesia and facial myokymia (FDFM): a novel movement disorder. Ann Neurol. 2001;49(4):486-92.

Ferraris A, Ialongo T, Passali GC, Pellecchia MT, Brusa L, Laruffa M, et al. Olfactory dysfunction in Parkinsonism caused by PINK1 mutations. Mov Disord. 2009;24(16):2350-7.

Foltynie T, Brayne C, Barker RA. The heterogeneity of idiopathic Parkinson's disease. J Neurol. 2002;249(2):138-45.

Foo JN, Liany H, Bei JX, Yu XQ, Liu J, Au WL, et al. Rare lysosomal enzyme gene SMPD1 variant (p.R591C) associates with Parkinson's disease. Neurobiol Aging. 2013;34(12):2890 e13-5.

Forabosco P, Ramasamy A, Trabzuni D, Walker R, Smith C, Bras J, et al. Insights into TREM2 biology by network analysis of human brain gene expression data. Neurobiol Aging. 2013;34(12):2699-714.

Friedman J, Olvera J, Silhavy JL, Gabriel SB, Gleeson JG. Mild paroxysmal kinesigenic dyskinesia caused by PRRT2 missense mutation with reduced penetrance. Neurology. 2012;79(9):946-8.

Friedman JR, Meneret A, Chen DH, Trouillard O, Vidailhet M, Raskind WH, et al. ADCY5 mutation carriers display pleiotropic paroxysmal day and nighttime dyskinesias. Mov Disord. 2016;31(1):147-8.

Fuchs J, Nilsson C, Kachergus J, Munz M, Larsson EM, Schule B, et al. Phenotypic variation in a large Swedish pedigree due to SNCA duplication and triplication. Neurology. 2007;68(12):916-22.

Fuchs T, Gavarini S, Saunders-Pullman R, Raymond D, Ehrlich ME, Bressman SB, et al. Mutations in the THAP1 gene are responsible for DYT6 primary torsion dystonia. Nat Genet. 2009;41(3):286-8.

Fuchs T, Saunders-Pullman R, Masuho I, Luciano MS, Raymond D, Factor S, et al. Mutations in GNAL cause primary torsion dystonia. Nat Genet. 2013;45(1):88-92.

Fujishige K, Kotera J, Omori K. Striatum- and testis-specific phosphodiesterase PDE10A isolation and characterization of a rat PDE10A. Eur J Biochem. 1999;266(3):1118-27.

Funayama M, Hasegawa K, Kowa H, Saito M, Tsuji S, Obata F. A new locus for Parkinson's disease (PARK8) maps to chromosome 12p11.2-q13.1. Ann Neurol. 2002;51(3):296-301.

Funayama M, Ohe K, Amo T, Furuya N, Yamaguchi J, Saiki S, et al. CHCHD2 mutations in autosomal dominant late-onset Parkinson's disease: a genome-wide linkage and sequencing study. Lancet Neurol. 2015;14(3):274-82.

Fung HC, Scholz S, Matarin M, Simon-Sanchez J, Hernandez D, Britton A, et al. Genome-wide genotyping in Parkinson's disease and neurologically normal controls: first stage analysis and public release of data. Lancet Neurol. 2006;5(11):911-6.

Furukawa Y. Update on dopa-responsive dystonia: locus heterogeneity and biochemical features. Adv Neurol. 2004;94:127-38.

Furukawa Y, Filiano JJ, Kish SJ. Amantadine for levodopa-induced choreic dyskinesia in compound heterozygotes for GCH1 mutations. Mov Disord. 2004;19(10):1256-8.

Furukawa Y, Kapatos G, Haycock JW, Worsley J, Wong H, Kish SJ, et al. Brain biopterin and tyrosine hydroxylase in asymptomatic dopa-responsive dystonia. Ann Neurol. 2002;51(5):637-41.

Furukawa Y, Lang AE, Trugman JM, Bird TD, Hunter A, Sadeh M, et al. Gender-related penetrance and de novo GTP-cyclohydrolase I gene mutations in dopa-responsive dystonia. Neurology. 1998;50(4):1015-20.

Furukawa Y, Nygaard TG, Gutlich M, Rajput AH, Pifl C, DiStefano L, et al. Striatal biopterin and tyrosine hydroxylase protein reduction in dopa-responsive dystonia. Neurology. 1999;53(5):1032-41.

Gan-Or Z, Amshalom I, Kilarski LL, Bar-Shira A, Gana-Weisz M, Mirelman A, et al. Differential effects of severe vs mild GBA mutations on Parkinson disease. Neurology. 2015;84(9):880-7.

Gan-Or Z, Bar-Shira A, Mirelman A, Gurevich T, Kedmi M, Giladi N, et al. LRRK2 and GBA mutations differentially affect the initial presentation of Parkinson disease. Neurogenetics. 2010;11(1):121-5.

Gan-Or Z, Giladi N, Rozovski U, Shifrin C, Rosner S, Gurevich T, et al. Genotype-phenotype correlations between GBA mutations and Parkinson disease risk and onset. Neurology. 2008;70(24):2277-83.

Gan-Or Z, Ozelius LJ, Bar-Shira A, Saunders-Pullman R, Mirelman A, Kornreich R, et al. The p.L302P mutation in the lysosomal enzyme gene SMPD1 is a risk factor for Parkinson disease. Neurology. 2013;80(17):1606-10.

Garavaglia B, Invernizzi F, Carbone ML, Viscardi V, Saracino F, Ghezzi D, et al. GTP-cyclohydrolase I gene mutations in patients with autosomal dominant and recessive GTP-CH1 deficiency: identification and functional characterization of four novel mutations. J Inherit Metab Dis. 2004;27(4):455-63.

Garcia-Cazorla A, Duarte S, Serrano M, Nascimento A, Ormazabal A, Carrilho I, et al. Mitochondrial diseases mimicking neurotransmitter defects. Mitochondrion. 2008;8(3):273-8.

Gardella E, Becker F, Moller RS, Schubert J, Lemke JR, Larsen LH, et al. Benign infantile seizures and paroxysmal dyskinesia caused by an SCN8A mutation. Ann Neurol. 2016;79(3):428-36.

Gardiner AR, Jaffer F, Dale RC, Labrum R, Erro R, Meyer E, et al. The clinical and genetic heterogeneity of paroxysmal dyskinesias. Brain. 2015;138(Pt 12):3567-80.

Gegg ME, Burke D, Heales SJ, Cooper JM, Hardy J, Wood NW, et al. Glucocerebrosidase deficiency in substantia nigra of parkinson disease brains. Ann Neurol. 2012;72(3):455-63.

Genome of the Netherlands Consortium. Whole-genome sequence variation, population structure and demographic history of the Dutch population. Nat Genet. 2014;46(8):818-25.

Gerfen CR. The neostriatal mosaic: multiple levels of compartmental organization. J Neural Transm Suppl. 1992;36:43-59.

Ghezzi D, Viscomi C, Ferlini A, Gualandi F, Mereghetti P, DeGrandis D, et al. Paroxysmal non-kinesigenic dyskinesia is caused by mutations of the MR-1 mitochondrial targeting sequence. Human Molecular Genetics. 2009;18(6):1058-64.

Giannandrea M, Bianchi V, Mignogna ML, Sirri A, Carrabino S, D'Elia E, et al. Mutations in the small GTPase gene RAB39B are responsible for X-linked mental retardation associated with autism, epilepsy, and macrocephaly. Am J Hum Genet. 2010;86(2):185-95.

Giasson BI, Covy JP, Bonini NM, Hurtig HI, Farrer MJ, Trojanowski JQ, et al. Biochemical and pathological characterization of Lrrk2. Ann Neurol. 2006;59(2):315-22.

Gibb WR, Narabayashi H, Yokochi M, Iizuka R, Lees AJ. New pathologic observations in juvenile onset parkinsonism with dystonia. Neurology. 1991;41(6):820-2.

Gilad S, Chessa L, Khosravi R, Russell P, Galanty Y, Piane M, et al. Genotype-phenotype relationships in ataxia-telangiectasia and variants. Am J Hum Genet. 1998;62(3):551-61.

Gilks WP, Abou-Sleiman PM, Gandhi S, Jain S, Singleton A, Lees AJ, et al. A common LRRK2 mutation in idiopathic Parkinson's disease. Lancet. 2005;365(9457):415-6.

Giri A, Guven G, Hanagasi H, Hauser AK, Erginul-Unaltuna N, Bilgic B, et al. PLA2G6 Mutations Related to Distinct Phenotypes: A New Case with Early-onset Parkinsonism. Tremor Other Hyperkinet Mov (N Y). 2016;6:363.

Goker-Alpan O, Schiffmann R, LaMarca ME, Nussbaum RL, McInerney-Leo A, Sidransky E. Parkinsonism among Gaucher disease carriers. J Med Genet. 2004;41(12):937-40.

Golbe LI, Lazzarini AM, Spychala JR, Johnson WG, Stenroos ES, Mark MH, et al. The tau A0 allele in Parkinson's disease. Mov Disord. 2001;16(3):442-7.

Goldin E. Gaucher disease and parkinsonism, a molecular link theory. Mol Genet Metab. 2010;101(4):307-10.

Golzio C, Willer J, Talkowski ME, Oh EC, Taniguchi Y, Jacquemont S, et al. KCTD13 is a major driver of mirrored neuroanatomical phenotypes of the 16p11.2 copy number variant. Nature. 2012;485(7398):363-7.

Gomez-Esteban JC, Lezcano E, Zarranz JJ, Gonzalez C, Bilbao G, Lambarri I, et al. Outcome of bilateral deep brain subthalamic stimulation in patients carrying the R1441G mutation in the LRRK2 dardarin gene. Neurosurgery. 2008;62(4):857-62; discussion 62-3.

Goodchild RE, Dauer WT. Mislocalization to the nuclear envelope: an effect of the dystonia-causing torsinA mutation. Proc Natl Acad Sci U S A. 2004;101(3):847-52.

Gouider-Khouja N, Kraoua I, Benrhouma H, Fraj N, Rouissi A. Movement disorders in neuro-metabolic diseases. Eur J Paediatr Neurol. 2010;14(4):304-7.

Govert F, Schneider SA. Huntington's disease and Huntington's disease-like syndromes: an overview. Curr Opin Neurol. 2013;26(4):420-7.

Grabowski GA. Phenotype, diagnosis, and treatment of Gaucher's disease. Lancet. 2008;372(9645):1263-71.

Grabowski M, Zimprich A, Lorenz-Depiereux B, Kalscheuer V, Asmus F, Gasser T, et al. The epsilon-sarcoglycan gene (SGCE), mutated in myoclonus-dystonia syndrome, is maternally imprinted. Eur J Hum Genet. 2003;11(2):138-44.

Grace ME, Ashton-Prolla P, Pastores GM, Soni A, Desnick RJ. Non-pseudogene-derived complex acid beta-glucosidase mutations causing mild type 1 and severe type 2 gaucher disease. J Clin Invest. 1999;103(6):817-23.

Gras D, Jonard L, Roze E, Chantot-Bastaraud S, Koht J, Motte J, et al. Benign hereditary chorea: phenotype, prognosis, therapeutic outcome and long term follow-up in a large series with new mutations in the TITF1/NKX2-1 gene. J Neurol Neurosurg Psychiatry. 2012;83(10):956-62.

Groen J, van Rootselaar AF, van der Salm SM, Bloem BR, Tijssen M. A new familial syndrome with dystonia and lower limb action myoclonus. Mov Disord. 2011;26(5):896-900.

Groen JL, Andrade A, Ritz K, Jalalzadeh H, Haagmans M, Bradley TE, et al. CACNA1B mutation is linked to unique myoclonus-dystonia syndrome. Hum Mol Genet. 2015;24(4):987-93.

Groen JL, Ritz K, Jalalzadeh H, van der Salm SM, Jongejan A, Mook OR, et al. RELN rare variants in myoclonus-dystonia. Mov Disord. 2015;30(3):415-9.

Gross-Langenhoff M, Hofbauer K, Weber J, Schultz A, Schultz JE. cAMP is a ligand for the tandem GAF domain of human phosphodiesterase 10 and cGMP for the tandem GAF domain of phosphodiesterase 11. J Biol Chem. 2006;281(5):2841-6.

Grotzsch H, Pizzolato GP, Ghika J, Schorderet D, Vingerhoets FJ, Landis T, et al. Neuropathology of a case of dopa-responsive dystonia associated with a new genetic locus, DYT14. Neurology. 2002;58(12):1839-42.

Grunewald A, Djarmati A, Lohmann-Hedrich K, Farrell K, Zeller JA, Allert N, et al. Myoclonus-dystonia: significance of large SGCE deletions. Hum Mutat. 2008;29(2):331-2.

Guella I, Sherman HE, Appel-Cresswell S, Rajput A, Rajput AH, Farrer MJ. Parkinsonism in GTP cyclohydrolase 1 mutation carriers. Brain. 2015;138(Pt 5):e349.

Guerreiro R, Wojtas A, Bras J, Carrasquillo M, Rogaeva E, Majounie E, et al. TREM2 variants in Alzheimer's disease. N Engl J Med. 2013;368(2):117-27.

Gulsuner S, Walsh T, Watts AC, Lee MK, Thornton AM, Casadei S, et al. Spatial and temporal mapping of de novo mutations in schizophrenia to a fetal prefrontal cortical network. Cell. 2013;154(3):518-29.

Gusella JF, MacDonald ME, Lee JM. Genetic modifiers of Huntington's disease. Mov Disord. 2014;29(11):1359-65.

Gustavsson EK, Trinh J, Guella I, Vilarino-Guell C, Appel-Cresswell S, Stoessl AJ, et al. DNAJC13 genetic variants in parkinsonism. Mov Disord. 2015;30(2):273-8.

Haack TB, Hogarth P, Kruer MC, Gregory A, Wieland T, Schwarzmayr T, et al. Exome sequencing reveals de novo WDR45 mutations causing a phenotypically distinct, X-linked dominant form of NBIA. Am J Hum Genet. 2012;91(6):1144-9.

Haerer AF, Currier RD, Jackson JF. Hereditary nonprogressive chorea of early onset. N Engl J Med. 1967;276(22):1220-4.

Hagenah J, Saunders-Pullman R, Hedrich K, Kabakci K, Habermann K, Wiegers K, et al. High mutation rate in dopa-responsive dystonia: detection with comprehensive GCHI screening. Neurology. 2005;64(5):908-11.

Hamilton EM, Polder E, Vanderver A, Naidu S, Schiffmann R, Fisher K, et al. Hypomyelination with atrophy of the basal ganglia and cerebellum: further delineation of the phenotype and genotype-phenotype correlation. Brain. 2014;137(Pt 7):1921-30.

Hamvas A, Deterding RR, Wert SE, White FV, Dishop MK, Alfano DN, et al. Heterogeneous pulmonary phenotypes associated with mutations in the thyroid transcription factor gene NKX2-1. Chest. 2013;144(3):794-804.

Han F, Racacho L, Lang AE, Bulman DE, Grimes DA. Refinement of the DYT15 locus in myoclonus dystonia. Mov Disord. 2007;22(6):888-92.

Hanagasi HA, Giri A, Guven G, Bilgic B, Hauser AK, Emre M, et al. A novel homozygous DJ1 mutation causes parkinsonism and ALS in a Turkish family. Parkinsonism Relat Disord. 2016.

Handa N, Mizohata E, Kishishita S, Toyama M, Morita S, Uchikubo-Kamo T, et al. Crystal structure of the GAF-B domain from human phosphodiesterase 10A complexed with its ligand, cAMP. J Biol Chem. 2008;283(28):19657-64.

Hanna MG, Bhatia KP. Movement disorders and mitochondrial dysfunction. Curr Opin Neurol. 1997;10(4):351-6.

Hanna MG, Davis MB, Sweeney MG, Noursadeghi M, Ellis CJ, Elliot P, et al. Generalized chorea in two patients harboring the Friedreich's ataxia gene trinucleotide repeat expansion. Mov Disord. 1998;13(2):339-40.

Hardy J, Singleton A. Genomewide association studies and human disease. N Engl J Med. 2009;360(17):1759-68.

Hauf M, Cousin P, Solida A, Albanese A, Ghika J, Schorderet D. A family with segmental dystonia: evidence for polymorphism in GTP cyclohydrolase I gene. Movement Disorders. 2000;15 (Suppl.3)(P765):154-5.

Healy DG, Abou-Sleiman PM, Gibson JM, Ross OA, Jain S, Gandhi S, et al. PINK1 (PARK6) associated Parkinson disease in Ireland. Neurology. 2004;63(8):1486-8.

Healy DG, Falchi M, O'Sullivan SS, Bonifati V, Durr A, Bressman S, et al. Phenotype, genotype, and worldwide genetic penetrance of LRRK2-associated Parkinson's disease: a case-control study. Lancet Neurol. 2008;7(7):583-90.

Hedera P, Xiao J, Puschmann A, Momcilovic D, Wu SW, Ledoux MS. Novel PRRT2 mutation in an African-American family with paroxysmal kinesigenic dyskinesia. BMC neurology. 2012;12:93.

Heikaus CC, Pandit J, Klevit RE. Cyclic nucleotide binding GAF domains from phosphodiesterases: structural and mechanistic insights. Structure. 2009;17(12):1551-7.

Heinzen EL, Arzimanoglou A, Brashear A, Clapcote SJ, Gurrieri F, Goldstein DB, et al. Distinct neurological disorders with ATP1A3 mutations. Lancet Neurol. 2014;13(5):503-14.

Heinzen EL, Swoboda KJ, Hitomi Y, Gurrieri F, Nicole S, de Vries B, et al. De novo mutations in ATP1A3 cause alternating hemiplegia of childhood. Nat Genet. 2012;44(9):1030-4.

Hempelmann A, Kumar S, Muralitharan S, Sander T. Myofibrillogenesis regulator 1 gene (MR-1) mutation in an Omani family with paroxysmal nonkinesigenic dyskinesia. Neuroscience letters. 2006;402(1-2):118-20.

Hensman Moss DJ, Poulter M, Beck J, Hehir J, Polke JM, Campbell T, et al. C9orf72 expansions are the most common genetic cause of Huntington disease phenocopies. Neurology. 2014;82(4):292-9.

Hermann A, Walker RH. Diagnosis and treatment of chorea syndromes. Curr Neurol Neurosci Rep. 2015;15(2):514.

Hernandez DG, Reed X, Singleton AB. Genetics in Parkinson disease: Mendelian versus non-Mendelian inheritance. J Neurochem. 2016.

Hersheson J, Mencacci NE, Davis M, MacDoanld HN, Trabzuni D, Ryten M, et al. Mutations in the autoregulatory domain of β-tubulin 4a cause hereditary dystonia. Ann Neurol. 2012:n/a-n/a.

Hersheson J, Mencacci NE, Davis M, MacDonald N, Trabzuni D, Ryten M, et al. Mutations in the autoregulatory domain of beta-tubulin 4a cause hereditary dystonia. Ann Neurol. 2013;73(4):546-53.

Hertz JM, Ostergaard K, Juncker I, Pedersen S, Romstad A, Moller LB, et al. Low frequency of Parkin, Tyrosine Hydroxylase, and GTP Cyclohydrolase I gene mutations in a Danish population of early-onset Parkinson's Disease. Eur J Neurol. 2006;13(4):385-90.

Herve D. Identification of a specific assembly of the g protein golf as a critical and regulated module of dopamine and adenosine-activated cAMP pathways in the striatum. Front Neuroanat. 2011;5:48.

Herve D, Levi-Strauss M, Marey-Semper I, Verney C, Tassin JP, Glowinski J, et al. G(olf) and Gs in rat basal ganglia: possible involvement of G(olf) in the coupling of dopamine D1 receptor with adenylyl cyclase. J Neurosci. 1993;13(5):2237-48.

Hjermind LE, Johannsen LG, Blau N, Wevers RA, Lucking CB, Hertz JM, et al. Dopa-responsive dystonia and early-onset Parkinson's disease in a patient with GTP cyclohydrolase I deficiency? Mov Disord. 2006;21(5):679-82.

Hjermind LE, Werdelin LM, Sorensen SA. Inherited and de novo mutations in sporadic cases of DYT1-dystonia. Eur J Hum Genet. 2002;10(3):213-6.

Ho D, Yan L, Iwatsubo K, Vatner DE, Vatner SF. Modulation of beta-adrenergic receptor signaling in heart failure and longevity: targeting adenylyl cyclase type 5. Heart Fail Rev. 2010;15(5):495-512.

Hoffmann GF, Assmann B, Brautigam C, Dionisi-Vici C, Haussler M, de Klerk JBC, et al. Tyrosine hydroxylase deficiency causes progressive encephalopathy and dopa-nonresponsive dystonia. Ann Neurol. 2003;54:S56-S65.

Holmes SE, O'Hearn E, Rosenblatt A, Callahan C, Hwang HS, Ingersoll-Ashworth RG, et al. A repeat expansion in the gene encoding junctophilin-3 is associated with Huntington disease-like 2. Nat Genet. 2001;29(4):377-8.

Horowitz M, Pasmanik-Chor M, Ron I, Kolodny EH. The enigma of the E326K mutation in acid beta-glucocerebrosidase. Mol Genet Metab. 2011;104(1-2):35-8.

Houlden H, Schneider SA, Paudel R, Melchers A, Schwingenschuh P, Edwards M, et al. THAP1 mutations (DYT6) are an additional cause of early-onset dystonia. Neurology. 2010;74(10):846-50.

Hruska KS, LaMarca ME, Scott CR, Sidransky E. Gaucher disease: mutation and polymorphism spectrum in the glucocerebrosidase gene (GBA). Hum Mutat. 2008;29(5):567-83.

Hughes AJ, Daniel SE, Kilford L, Lees AJ. Accuracy of clinical diagnosis of idiopathic Parkinson's disease: a clinico-pathological study of 100 cases. J Neurol Neurosurg Psychiatry. 1992;55(3):181-4.

Huttenlocher J, Stefansson H, Steinberg S, Helgadottir HT, Sveinbjornsdottir S, Riess O, et al. Heterozygote carriers for CNVs in PARK2 are at increased risk of Parkinson's disease. Hum Mol Genet. 2015;24(19):5637-43.

Hwu WL, Chiou YW, Lai SY, Lee YM. Dopa-responsive dystonia is induced by a dominant-negative mechanism. Ann Neurol. 2000;48(4):609-13.

Ibanez P, Lesage S, Janin S, Lohmann E, Durif F, Destee A, et al. Alpha-synuclein gene rearrangements in dominantly inherited parkinsonism: frequency, phenotype, and mechanisms. Arch Neurol. 2009;66(1):102-8.

Ichinose H, Ohye T, Takahashi E, Seki N, Hori T, Segawa M, et al. Hereditary progressive dystonia with marked diurnal fluctuation caused by mutations in the GTP cyclohydrolase I gene. Nat Genet. 1994;8(3):236-42.

Inzelberg R, Weinberger M, Gak E. Benign hereditary chorea: an update. Parkinsonism Relat Disord. 2011;17(5):301-7.

Iossifov I, O'Roak BJ, Sanders SJ, Ronemus M, Krumm N, Levy D, et al. The contribution of de novo coding mutations to autism spectrum disorder. Nature. 2014;515(7526):216-21.

Irie S, Kanazawa N, Ryoh M, Mochizuki H, Nomura Y, Segawa M. A case of parkinsonism and dopa-induced severe dyskinesia associated with novel mutation in the GTP cyclohydrolase I gene. Parkinsonism Relat Disord. 2011;17(10):769-70.

Irvine AD, McLean WH, Leung DY. Filaggrin mutations associated with skin and allergic diseases. N Engl J Med. 2011;365(14):1315-27.

Ito Y, Fujita M, Shimada S, Watanabe Y, Okada T, Kusuoka H, et al. Comparison between the decrease of dopamine transporter and that of L-DOPA uptake for detection of early to advanced stage of Parkinson's disease in animal models. Synapse. 1999;31(3):178-85.

Iwabuchi S, Kakazu Y, Koh JY, Harata NC. Abnormal cytoplasmic calcium dynamics in central neurons of a dystonia mouse model. Neurosci Lett. 2013;548:61-6.

Iwata N, Kobayashi K, Sasaoka T, Hidaka H, Nagatsu T. Structure of the mouse

tyrosine hydroxylase gene. Biochem Biophys Res Commun. 1992;182(1):348-54.

Iwatani N, Mabe H, Devriendt K, Kodama M, Miike T. Deletion of NKX2.1 gene encoding thyroid transcription factor-1 in two siblings with hypothyroidism and respiratory failure. J Pediatr. 2000;137(2):272-6.

Jäger R, Russwurm C, Schwede F, Genieser HG, Koesling D, Russwurm M. Activation of PDE10 and PDE11 phosphodiesterases. J Biol Chem. 2012;287(2):1210-9.

Jamora RD, Tan EK, Liu CP, Kathirvel P, Burgunder JM, Tan LC. DYT1 mutations amongst adult primary dystonia patients in Singapore with review of literature comparing East and West. J Neurol Sci. 2006;247(1):35-7.

Jankovic J, McDermott M, Carter J, Gauthier S, Goetz C, Golbe L, et al. Variable expression of Parkinson's disease: a base-line analysis of the DATATOP cohort. The Parkinson Study Group. Neurology. 1990;40(10):1529-34.

Jansen IE, Bras JM, Lesage S, Schulte C, Gibbs JR, Nalls MA, et al. CHCHD2 and Parkinson's disease. Lancet Neurol. 2015;14(7):678-9.

Jarman PR, Bandmann O, Marsden CD, Wood NW. GTP cyclohydrolase I mutations in patients with dystonia responsive to anticholinergic drugs. J Neurol Neurosurg Psychiatry. 1997;63(3):304-8.

Jellinger K. Heterogenous mechanisms of mild cognitive impairment in Parkinson's disease. J Neural Transm. 2012;119(3):381-2.

Jen J, Wan J, Graves M, Yu H, Mock AF, Coulin CJ, et al. Loss-of-function EA2 mutations are associated with impaired neuromuscular transmission. Neurology. 2001;57(10):1843-8.

Jeon BS, Jeong JM, Park SS, Kim JM, Chang YS, Song HC, et al. Dopamine transporter density measured by [123I]beta-CIT single-photon emission computed tomography is normal in dopa-responsive dystonia. Ann Neurol. 1998;43(6):792-800.

Johnson MB, Kawasawa YI, Mason CE, Krsnik Z, Coppola G, Bogdanovic D, et al. Functional and evolutionary insights into human brain development through global transcriptome analysis. Neuron. 2009;62(4):494-509.

Jubault T, Gagnon JF, Karama S, Ptito A, Lafontaine AL, Evans AC, et al. Patterns of cortical thickness and surface area in early Parkinson's disease. Neuroimage. 2011;55(2):462-7.

Junn E, Taniguchi H, Jeong BS, Zhao X, Ichijo H, Mouradian MM. Interaction of DJ-1 with Daxx inhibits apoptosis signal-regulating kinase 1 activity and cell death. Proc Natl Acad Sci U S A. 2005;102(27):9691-6.

Kabakci K, Hedrich K, Leung JC, Mitterer M, Vieregge P, Lencer R, et al. Mutations in DYT1: extension of the phenotypic and mutational spectrum. Neurology. 2004;62(3):395-400.

Kaiser FJ, Bassler N, Jakel O. COTS Silicon diodes as radiation detectors in proton and heavy charged particle radiotherapy 1. Radiation and environmental biophysics. 2010;49(3):365-71.

Kambouris M, Bohlega S, Al-Tahan A, Meyer BF. Localization of the gene for a novel autosomal recessive neurodegenerative Huntington-like disorder to 4p15.3. Am J Hum Genet. 2000;66(2):445-52.

Kancheva D, Chamova T, Guergueltcheva V, Mitev V, Azmanov DN, Kalaydjieva L, et al. Mosaic dominant TUBB4A mutation in an inbred family with complicated hereditary spastic paraplegia. Mov Disord. 2015;30(6):854-8.

Kang HJ, Kawasawa YI, Cheng F, Zhu Y, Xu X, Li M, et al. Spatio-temporal transcriptome of the human brain. Nature. 2011;478(7370):483-9.

Kara E, Hardy J, Houlden H. The pallidopyramidal syndromes: nosology, aetiology and pathogenesis. Curr Opin Neurol. 2013;26(4):381-94.

Kara E, Kiely AP, Proukakis C, Giffin N, Love S, Hehir J, et al. A 6.4 Mb Duplication of the alpha-Synuclein Locus Causing Frontotemporal Dementia and Parkinsonism: Phenotype-Genotype Correlations. JAMA Neurol. 2014;71(9):1162-71.

Kasahara K, Kawakami Y, Kiyono T, Yonemura S, Kawamura Y, Era S, et al. Ubiquitin-proteasome system controls ciliogenesis at the initial step of axoneme extension. Nat Commun. 2014;5:5081.

Kay DM, Moran D, Moses L, Poorkaj P, Zabetian CP, Nutt J, et al. Heterozygous parkin point mutations are as common in control subjects as in Parkinson's patients. Ann Neurol. 2007;61(1):47-54.

Kay DM, Stevens CF, Hamza TH, Montimurro JS, Zabetian CP, Factor SA, et al. A comprehensive analysis of deletions, multiplications, and copy number variations in PARK2. Neurology. 2010;75(13):1189-94.

Keckarevic M, Savic D, Svetel M, Kostic V, Vukosavic S, Romac S. Yugoslav HD phenocopies analyzed on the presence of mutations in PrP, ferritin, and Jp-3 genes. Int J Neurosci. 2005;115(2):299-301.

Khan NL, Graham E, Critchley P, Schrag AE, Wood NW, Lees AJ, et al. Parkin disease: a phenotypic study of a large case series. Brain. 2003;126(Pt 6):1279-92.

Kiely AP, Asi YT, Kara E, Limousin P, Ling H, Lewis P, et al. alpha-Synucleinopathy associated with G51D SNCA mutation: a link between Parkinson's disease and multiple system atrophy? Acta Neuropathol. 2013;125(5):753-69.

Kikuchi A, Takeda A, Fujihara K, Kimpara T, Shiga Y, Tanji H, et al. Arg(184)His mutant GTP cyclohydrolase I, causing recessive hyperphenylalaninemia, is responsible for dopa-responsive dystonia with parkinsonism: a case report. Mov Disord. 2004;19(5):590-3.

Kimura S, Hara Y, Pineau T, Fernandez-Salguero P, Fox CH, Ward JM, et al. The T/ebp null mouse: thyroid-specific enhancer-binding protein is essential for the organogenesis of the thyroid, lung, ventral forebrain, and pituitary. Genes Dev. 1996;10(1):60-9.

Kinghorn KJ, Castillo-Quan JI, Bartolome F, Angelova PR, Li L, Pope S, et al. Loss of PLA2G6 leads to elevated mitochondrial lipid peroxidation and mitochondrial dysfunction. Brain. 2015;138(Pt 7):1801-16.

Kinugawa K, Vidailhet M, Clot F, Apartis E, Grabli D, Roze E. Myoclonus-dystonia: an update. Mov Disord. 2009;24(4):479-89.

Kircher M, Witten DM, Jain P, O'Roak BJ, Cooper GM, Shendure J. A general framework for estimating the relative pathogenicity of human genetic variants. Nat Genet. 2014;46(3):310-5.

Kitada T, Asakawa S, Hattori N, Matsumine H, Yamamura Y, Minoshima S, et al. Mutations in the parkin gene cause autosomal recessive juvenile parkinsonism. Nature. 1998;392(6676):605-8.

Klein C. Genetics in dystonia. Parkinsonism Relat Disord. 2014;20 Suppl 1:S137-42.

Klein C, König IR, Lohmann K. Exome sequencing for gene discovery: Time to set standard criteria. Ann Neurol. 2012:n/a-n/a.

Klein C, Liu L, Doheny D, Kock N, Muller B, de Carvalho Aguiar P, et al. Epsilon-sarcoglycan mutations found in combination with other dystonia gene mutations. Ann Neurol. 2002;52(5):675-9.

Klein C, Lohmann-Hedrich K. Impact of recent genetic findings in Parkinson's disease. Curr Opin Neurol. 2007;20(4):453-64.

Klein C, Lohmann-Hedrich K, Rogaeva E, Schlossmacher MG, Lang AE. Deciphering the role of heterozygous mutations in genes associated with parkinsonism. Lancet Neurol. 2007;6(7):652-62.

Klein C, Wenning GK, Quinn NP, Marsden CD. Ataxia without telangiectasia masquerading as benign hereditary chorea. Mov Disord. 1996;11(2):217-20.

Kleiner-Fisman G, Calingasan NY, Putt M, Chen J, Beal MF, Lang AE. Alterations of striatal neurons in benign hereditary chorea. Mov Disord. 2005;20(10):1353-7.

Kleiner-Fisman G, Lang AE. Benign hereditary chorea revisited: a journey to understanding. Mov Disord. 2007;22(16):2297-305; quiz 452.

Kleiner-Fisman G, Rogaeva E, Halliday W, Houle S, Kawarai T, Sato C, et al. Benign hereditary chorea: clinical, genetic, and pathological findings. Ann Neurol. 2003;54(2):244-7.

Koesling D, Bohme E, Schultz G. Guanylyl cyclases, a growing family of signal-transducing enzymes. FASEB J. 1991;5(13):2785-91.

Koroglu C, Baysal L, Cetinkaya M, Karasoy H, Tolun A. DNAJC6 is responsible for juvenile parkinsonism with phenotypic variability. Parkinsonism Relat Disord.

2013;19(3):320-4.

Korvatska O, Strand NS, Berndt JD, Strovas T, Chen DH, Leverenz JB, et al. Altered splicing of ATP6AP2 causes X-linked parkinsonism with spasticity (XPDS). Hum Mol Genet. 2013;22(16):3259-68.

Koschmidder E, Weissbach A, Bruggemann N, Kasten M, Klein C, Lohmann K. A nonsense mutation in CHCHD2 in a patient with Parkinson disease. Neurology. 2016;86(6):577-9.

Kostic VS, Dobricic V, Stankovic I, Ralic V, Stefanova E. C9orf72 expansion as a possible genetic cause of Huntington disease phenocopy syndrome. J Neurol. 2014;261(10):1917-21.

Kousi M, Anttila V, Schulz A, Calafato S, Jakkula E, Riesch E, et al. Novel mutations consolidate KCTD7 as a progressive myoclonus epilepsy gene. J Med Genet. 2012;49(6):391-9.

Koutsis G, Karadima G, Kartanou C, Kladi A, Panas M. C9ORF72 hexanucleotide repeat expansions are a frequent cause of Huntington disease phenocopies in the Greek population. Neurobiol Aging. 2015;36(1):547 e13-6.

Koutsis G, Karadima G, Kladi A, Panas M. The challenge of juvenile Huntington disease: to test or not to test. Neurology. 2013;80(11):990-6.

Koutsis G, Karadima G, Pandraud A, Sweeney MG, Paudel R, Houlden H, et al. Genetic screening of Greek patients with Huntington's disease phenocopies identifies an SCA8 expansion. J Neurol. 2012;259(9):1874-8.

Krabichler B, Rostasy K, Baumann M, Karall D, Scholl-Burgi S, Schwarzer C, et al. Novel mutation in potassium channel related gene KCTD7 and progressive myoclonic epilepsy. Ann Hum Genet. 2012;76(4):326-31.

Krack P, Pollak P, Limousin P, Hoffmann D, Xie J, Benazzouz A, et al. Subthalamic nucleus or internal pallidal stimulation in young onset Parkinson's disease. Brain. 1998;121 (Pt 3):451-7.

Kramer PL, Heiman GA, Gasser T, Ozelius LJ, de Leon D, Brin MF, et al. The DYT1

gene on 9q34 is responsible for most cases of early limb-onset idiopathic torsion dystonia in non-Jews. Am J Hum Genet. 1994;55(3):468-75.

Krause A, Mitchell C, Essop F, Tager S, Temlett J, Stevanin G, et al. Junctophilin 3 (JPH3) expansion mutations causing Huntington disease like 2 (HDL2) are common in South African patients with African ancestry and a Huntington disease phenotype. Am J Med Genet B Neuropsychiatr Genet. 2015.

Krebs CE, Karkheiran S, Powell JC, Cao M, Makarov V, Darvish H, et al. The Sac1 domain of SYNJ1 identified mutated in a family with early-onset progressive Parkinsonism with generalized seizures. Hum Mutat. 2013;34(9):1200-7.

Krude H, Schutz B, Biebermann H, von Moers A, Schnabel D, Neitzel H, et al. Choreoathetosis, hypothyroidism, and pulmonary alterations due to human NKX2-1 haploinsufficiency. J Clin Invest. 2002;109(4):475-80.

Kruger R, Kuhn W, Muller T, Woitalla D, Graeber M, Kosel S, et al. Ala30Pro mutation in the gene encoding alpha-synuclein in Parkinson's disease. Nat Genet. 1998;18(2):106-8.

Kruger R, Vieira-Saecker AM, Kuhn W, Berg D, Muller T, Kuhnl N, et al. Increased susceptibility to sporadic Parkinson's disease by a certain combined alpha-synuclein/apolipoprotein E genotype. Ann Neurol. 1999;45(5):611-7.

Kuhm C, Gallenmuller C, Dork T, Menzel M, Biskup S, Klopstock T. Novel ATM mutation in a German patient presenting as generalized dystonia without classical signs of ataxia-telangiectasia. J Neurol. 2015;262(3):768-70.

Kumar KR, Djarmati-Westenberger A, Grunewald A. Genetics of Parkinson's disease. Semin Neurol. 2011;31(5):433-40.

Kumar KR, Lohmann K, Masuho I, Miyamoto R, Ferbert A, Lohnau T, et al. Mutations in GNAL: a novel cause of craniocervical dystonia. JAMA Neurol. 2014;71(4):490-4.

Kumar P, Henikoff S, Ng PC. Predicting the effects of coding non-synonymous variants on protein function using the SIFT algorithm. Nat Protoc. 2009;4(7):1073-81.

Kurian MA, Gissen P, Smith M, Heales S, Jr., Clayton PT. The monoamine

neurotransmitter disorders: an expanding range of neurological syndromes. Lancet Neurol. 2011;10(8):721-33.

Kurian MA, Morgan NV, MacPherson L, Foster K, Peake D, Gupta R, et al. Phenotypic spectrum of neurodegeneration associated with mutations in the PLA2G6 gene (PLAN). Neurology. 2008;70(18):1623-9.

Lakics V, Karran EH, Boess FG. Quantitative comparison of phosphodiesterase mRNA distribution in human brain and peripheral tissues. Neuropharmacology. 2010;59(6):367-74.

Laman H. Fbxo7 gets proactive with cyclin D/cdk6. Cell Cycle. 2006;5(3):279-82.

Langbehn DR, Brinkman RR, Falush D, Paulsen JS, Hayden MR. A new model for prediction of the age of onset and penetrance for Huntington's disease based on CAG length. Clin Genet. 2004;65(4):267-77.

Langfelder P, Luo R, Oldham MC, Horvath S. Is my network module preserved and reproducible? PLoS Comput Biol. 2011;7(1):e1001057.

Larsen J, Carvill GL, Gardella E, Kluger G, Schmiedel G, Barisic N, et al. The phenotypic spectrum of SCN8A encephalopathy. Neurology. 2015;84(5):480-9.

Lazaroff M, Patankar S, Yoon SO, Chikaraishi DM. The cyclic AMP response element directs tyrosine hydroxylase expression in catecholaminergic central and peripheral nervous system cell lines from transgenic mice. J Biol Chem. 1995;270(37):21579-89.

Ledoux MS, Dauer WT, Warner TT. Emerging common molecular pathways for primary dystonia. Mov Disord. 2013;28(7):968-81.

Lee HY, Huang Y, Bruneau N, Roll P, Roberson ED, Hermann M, et al. Mutations in the novel protein PRRT2 cause paroxysmal kinesigenic dyskinesia with infantile convulsions. Cell reports. 2012;1(1):2-12.

Lee HY, Xu Y, Huang Y, Ahn AH, Auburger GW, Pandolfo M, et al. The gene for paroxysmal non-kinesigenic dyskinesia encodes an enzyme in a stress response pathway. Human Molecular Genetics. 2004;13(24):3161-70.

Lee J-M, Wheeler Vanessa C, Chao Michael J, Vonsattel Jean Paul G, Pinto Ricardo M, Lucente D, et al. Identification of Genetic Factors that Modify Clinical Onset of Huntington's Disease. Cell. 2015;162(3):516-26.

Lee JM, Ramos EM, Lee JH, Gillis T, Mysore JS, Hayden MR, et al. CAG repeat expansion in Huntington disease determines age at onset in a fully dominant fashion. Neurology. 2012;78(10):690-5.

Lee JY, Yang HJ, Kim JM, Jeon BS. Novel GCH-1 mutations and unusual long-lasting dyskinesias in Korean families with dopa-responsive dystonia. Parkinsonism Relat Disord. 2013;19(12):1156-9.

Lee KW, Hong JH, Choi IY, Che Y, Lee JK, Yang SD, et al. Impaired D2 dopamine receptor function in mice lacking type 5 adenylyl cyclase. J Neurosci. 2002;22(18):7931-40.

Lees AJ, Hardy J, Revesz T. Parkinson's disease. Lancet. 2009;373(9680):2055-66.

Lehericy S, Grand S, Pollak P, Poupon F, Le Bas JF, Limousin P, et al. Clinical characteristics and topography of lesions in movement disorders due to thalamic lesions. Neurology. 2001;57(6):1055-66.

Lein ES, Hawrylycz MJ, Ao N, Ayres M, Bensinger A, Bernard A, et al. Genome-wide atlas of gene expression in the adult mouse brain. Nature. 2007;445(7124):168-76.

Lesage S, Anheim M, Condroyer C, Pollak P, Durif F, Dupuits C, et al. Large-scale screening of the Gaucher's disease-related glucocerebrosidase gene in Europeans with Parkinson's disease. Hum Mol Genet. 2011;20(1):202-10.

Lesage S, Bras J, Cormier-Dequaire F, Condroyer C, Nicolas A, Darwent L, et al. Loss-of-function mutations in RAB39B are associated with typical early-onset Parkinson disease. Neurol Genet. 2015;1(1):e9.

Lesage S, Condroyer C, Klebe S, Honore A, Tison F, Brefel-Courbon C, et al. Identification of VPS35 mutations replicated in French families with Parkinson disease. Neurology. 2012;78(18):1449-50.

Lesage S, Drouet V, Majounie E, Deramecourt V, Jacoupy M, Nicolas A, et al. Loss of

VPS13C Function in Autosomal-Recessive Parkinsonism Causes Mitochondrial Dysfunction and Increases PINK1/Parkin-Dependent Mitophagy. Am J Hum Genet. 2016;98(3):500-13.

Lesage S, Durr A, Tazir M, Lohmann E, Leutenegger AL, Janin S, et al. LRRK2 G2019S as a cause of Parkinson's disease in North African Arabs. N Engl J Med. 2006;354(4):422-3.

Leung JC, Klein C, Friedman J, Vieregge P, Jacobs H, Doheny D, et al. Novel mutation in the TOR1A (DYT1) gene in atypical early onset dystonia and polymorphisms in dystonia and early onset parkinsonism. Neurogenetics. 2001;3(3):133-43.

Leuzzi V, Carducci C, Carducci C, Cardona F, Artiola C, Antonozzi I. Autosomal dominant GTP-CH deficiency presenting as a dopa-responsive myoclonus-dystonia syndrome. Neurology. 2002;59(8):1241-3.

Leuzzi V, Carducci C, Chiarotti F, D'Agnano D, Giannini MT, Antonozzi I, et al. Urinary neopterin and phenylalanine loading test as tools for the biochemical diagnosis of segawa disease. JIMD Rep. 2013;7:67-75.

Lewthwaite AJ, Lambert TD, Rolfe EB, Olgiati S, Quadri M, Simons EJ, et al. Novel GCH1 variant in Dopa-responsive dystonia and Parkinson's disease. Parkinsonism Relat Disord. 2015;21(4):394-7.

Liang CC, Tanabe LM, Jou S, Chi F, Dauer WT. TorsinA hypofunction causes abnormal twisting movements and sensorimotor circuit neurodegeneration. J Clin Invest. 2014;124(7):3080-92.

Limousin P, Pollak P, Benazzouz A, Hoffmann D, Le Bas JF, Broussolle E, et al. Effect of parkinsonian signs and symptoms of bilateral subthalamic nucleus stimulation. Lancet. 1995;345(8942):91-5.

Liou B, Grabowski GA. Is E326K glucocerebrosidase a polymorphic or pathological variant? Mol Genet Metab. 2012;105(3):528-9.

Liu Z, Xiang Y, Sun G. The KCTD family of proteins: structure, function, disease relevance. Cell Biosci. 2013;3(1):45.

Lohmann E, Coquel AS, Honore A, Gurvit H, Hanagasi H, Emre M, et al. A new F-box protein 7 gene mutation causing typical Parkinson's disease. Mov Disord. 2015;30(8):1130-3.

Lohmann E, Welter ML, Fraix V, Krack P, Lesage S, Laine S, et al. Are parkin patients particularly suited for deep-brain stimulation? Mov Disord. 2008;23(5):740-3.

Lohmann K, Wilcox RA, Winkler S, Ramirez A, Rakovic A, Park J-S, et al. Whispering dysphonia (DYT4 dystonia) is caused by a mutation in the TUBB4 gene. Ann Neurol. 2012:n/a-n/a.

Lorenzo-Betancor O, Ogaki K, Soto-Ortolaza AI, Labbe C, Walton RL, Strongosky AJ, et al. DNAJC13 p.Asn855Ser mutation screening in Parkinson's disease and pathologically confirmed Lewy body disease patients. Eur J Neurol. 2015;22(9):1323-5.

Luciano MS, Ozelius L, Sims K, Raymond D, Liu L, Saunders-Pullman R. Responsiveness to levodopa in epsilon-sarcoglycan deletions. Mov Disord. 2009;24(3):425-8.

Lucking CB, Durr A, Bonifati V, Vaughan J, De Michele G, Gasser T, et al. Association between early-onset Parkinson's disease and mutations in the parkin gene. N Engl J Med. 2000;342(21):1560-7.

Ludecke B, Knappskog PM, Clayton PT, Surtees RA, Clelland JD, Heales SJ, et al. Recessively inherited L-DOPA-responsive parkinsonism in infancy caused by a point mutation (L205P) in the tyrosine hydroxylase gene. Human Molecular Genetics. 1996;5(7):1023-8.

Ma L, Chen R, Wang L, Yang Y, Wan X. No mutations in CIZ1 in twelve adult-onset primary cervical dystonia families. Mov Disord. 2013;28(13):1899-901.

Ma LY, Wang L, Yang YM, Feng T, Wan XH. Mutations in ANO3 and GNAL gene in thirty-three isolated dystonia families. Mov Disord. 2015;30(5):743-4.

MacArthur DG, Manolio TA, Dimmock DP, Rehm HL, Shendure J, Abecasis GR, et al. Guidelines for investigating causality of sequence variants in human disease. Nature. 2014;508(7497):469-76.

Marder K, Wang Y, Alcalay RN, Mejia-Santana H, Tang MX, Lee A, et al. Age-specific penetrance of LRRK2 G2019S in the Michael J. Fox Ashkenazi Jewish LRRK2 Consortium. Neurology. 2015;85(1):89-95.

Margolin DH, Kousi M, Chan YM, Lim ET, Schmahmann JD, Hadjivassiliou M, et al. Ataxia, dementia, and hypogonadotropism caused by disordered ubiquitination. N Engl J Med. 2013;368(21):1992-2003.

Margolis RL, Holmes SE, Rosenblatt A, Gourley L, O'Hearn E, Ross CA, et al. Huntington's Disease-like 2 (HDL2) in North America and Japan. Ann Neurol. 2004;56(5):670-4.

Margolis RL, O'Hearn E, Rosenblatt A, Willour V, Holmes SE, Franz ML, et al. A disorder similar to Huntington's disease is associated with a novel CAG repeat expansion. Ann Neurol. 2001;50(6):373-80.

Marras C, Schule B, Munhoz RP, Rogaeva E, Langston JW, Kasten M, et al. Phenotype in parkinsonian and nonparkinsonian LRRK2 G2019S mutation carriers. Neurology. 2011;77(4):325-33.

Marsden CD. The pathophysiology of movement disorders. Neurol Clin. 1984;2(3):435-59.

Marston S, Montgiraud C, Munster AB, Copeland O, Choi O, Dos Remedios C, et al. OBSCN Mutations Associated with Dilated Cardiomyopathy and Haploinsufficiency. PLoS One. 2015;10(9):e0138568.

Martino D, Melzi V, Franco G, Kandasamy N, Monfrini E, Di Fonzo A. Juvenile dystonia-parkinsonism syndrome caused by a novel p.S941Tfs1X ATP13A2 (PARK9) mutation. Parkinsonism Relat Disord. 2015;21(11):1378-80.

Marttila RJ, Kaprio J, Koskenvuo M, Rinne UK. Parkinson's disease in a nationwide twin cohort. Neurology. 1988;38(8):1217-9.

Masuho I, Fang M, Geng C, Zhang J, Jiang H, Ozgul RK, et al. Homozygous GNAL mutation associated with familial childhood-onset generalized dystonia. Neurol Genet. 2016;2(3):e78.

Mata IF, Jang Y, Kim CH, Hanna DS, Dorschner MO, Samii A, et al. The RAB39B p.G192R mutation causes X-linked dominant Parkinson's disease. Mol Neurodegener. 2015;10:50.

Mata IF, Leverenz JB, Weintraub D, Trojanowski JQ, Chen-Plotkin A, Van Deerlin VM, et al. GBA Variants are associated with a distinct pattern of cognitive deficits in Parkinson's disease. Mov Disord. 2015.

Matsui A, Tran M, Yoshida AC, Kikuchi SS, U M, Ogawa M, et al. BTBD3 controls dendrite orientation toward active axons in mammalian neocortex. Science. 2013;342(6162):1114-8.

Matsumine H, Saito M, Shimoda-Matsubayashi S, Tanaka H, Ishikawa A, Nakagawa-Hattori Y, et al. Localization of a gene for an autosomal recessive form of juvenile Parkinsonism to chromosome 6q25.2-27. Am J Hum Genet. 1997;60(3):588-96.

Matsumoto H, Zaha K, Nakamura Y, Hayashi S, Inazawa J, Nonoyama S. Chromosome 9q33q34 microdeletion with early infantile epileptic encephalopathy, severe dystonia, abnormal eye movements, and nephroureteral malformations. Pediatr Neurol. 2014;51(1):170-5.

Matthiesen K, Nielsen J. Binding of cyclic nucleotides to phosphodiesterase 10A and 11A GAF domains does not stimulate catalytic activity. Biochem J. 2009;423(3):401-9.

Mayeux R, Marder K, Cote LJ, Denaro J, Hemenegildo N, Mejia H, et al. The frequency of idiopathic Parkinson's disease by age, ethnic group, and sex in northern Manhattan, 1988-1993. Am J Epidemiol. 1995;142(8):820-7.

Mazzulli JR, Xu YH, Sun Y, Knight AL, McLean PJ, Caldwell GA, et al. Gaucher disease glucocerebrosidase and alpha-synuclein form a bidirectional pathogenic loop in synucleinopathies. Cell. 2011;146(1):37-52.

McNeill A, Duran R, Hughes DA, Mehta A, Schapira AH. A clinical and family history study of Parkinson's disease in heterozygous glucocerebrosidase mutation carriers. J Neurol Neurosurg Psychiatry. 2012;83(8):853-4.

Mead S, Poulter M, Beck J, Webb TE, Campbell TA, Linehan JM, et al. Inherited prion disease with six octapeptide repeat insertional mutation--molecular analysis of

phenotypic heterogeneity. Brain. 2006;129(Pt 9):2297-317.

Meneret A, Ahmar-Beaugendre Y, Rieunier G, Mahlaoui N, Gaymard B, Apartis E, et al. The pleiotropic movement disorders phenotype of adult ataxia-telangiectasia. Neurology. 2014;83(12):1087-95.

Metzker ML. Sequencing technologies - the next generation. Nat Rev Genet. 2010;11(1):31-46.

Milstien S, Katusic Z. Oxidation of tetrahydrobiopterin by peroxynitrite: implications for vascular endothelial function. Biochem Biophys Res Commun. 1999;263(3):681-4.

Mitsui J, Mizuta I, Toyoda A, Ashida R, Takahashi Y, Goto J, et al. Mutations for Gaucher disease confer high susceptibility to Parkinson disease. Arch Neurol. 2009;66(5):571-6.

Miyatake S, Koshimizu E, Hayashi YK, Miya K, Shiina M, Nakashima M, et al. Deep sequencing detects very-low-grade somatic mosaicism in the unaffected mother of siblings with nemaline myopathy. Neuromuscul Disord. 2014;24(7):642-7.

Montfort M, Chabas A, Vilageliu L, Grinberg D. Functional analysis of 13 GBA mutant alleles identified in Gaucher disease patients: Pathogenic changes and "modifier" polymorphisms. Hum Mutat. 2004;23(6):567-75.

Moore RC, Xiang F, Monaghan J, Han D, Zhang Z, Edstrom L, et al. Huntington disease phenocopy is a familial prion disease. Am J Hum Genet. 2001;69(6):1385-8.

Morgante F, Espay AJ, Gunraj C, Lang AE, Chen R. Motor cortex plasticity in Parkinson's disease and levodopa-induced dyskinesias. Brain. 2006;129(Pt 4):1059-69.

Moro E, Volkmann J, Konig IR, Winkler S, Hiller A, Hassin-Baer S, et al. Bilateral subthalamic stimulation in Parkin and PINK1 parkinsonism. Neurology. 2008;70(14):1186-91.

Nagafuchi S, Yanagisawa H, Sato K, Shirayama T, Ohsaki E, Bundo M, et al. Dentatorubral and pallidoluysian atrophy expansion of an unstable CAG trinucleotide on chromosome 12p. Nat Genet. 1994;6(1):14-8.

Nagamoto-Combs K, Piech KM, Best JA, Sun B, Tank AW. Tyrosine hydroxylase gene promoter activity is regulated by both cyclic AMP-responsive element and AP1 sites following calcium influx. Evidence for cyclic amp-responsive element binding protein-independent regulation. J Biol Chem. 1997;272(9):6051-8.

Nair VD, Olanow CW, Sealfon SC. Activation of phosphoinositide 3-kinase by D2 receptor prevents apoptosis in dopaminergic cell lines. Biochem J. 2003;373(Pt 1):25-32.

Najim al-Din AS, Wriekat A, Mubaidin A, Dasouki M, Hiari M. Pallido-pyramidal degeneration, supranuclear upgaze paresis and dementia: Kufor-Rakeb syndrome. Acta Neurol Scand. 1994;89(5):347-52.

Nalls MA, Duran R, Lopez G, Kurzawa-Akanbi M, McKeith IG, Chinnery PF, et al. A multicenter study of glucocerebrosidase mutations in dementia with Lewy bodies. JAMA Neurol. 2013;70(6):727-35.

Nalls MA, Pankratz N, Lill CM, Do CB, Hernandez DG, Saad M, et al. Large-scale meta-analysis of genome-wide association data identifies six new risk loci for Parkinson's disease. Nat Genet. 2014;46(9):989-93.

Nalls MA, Plagnol V, Hernandez DG, Sharma M, Sheerin UM, Saad M, et al. Imputation of sequence variants for identification of genetic risks for Parkinson's disease: a meta-analysis of genome-wide association studies. Lancet. 2011;377(9766):641-9.

Nandhagopal R, Kuramoto L, Schulzer M, Mak E, Cragg J, McKenzie J, et al. Longitudinal evolution of compensatory changes in striatal dopamine processing in Parkinson's disease. Brain. 2011;134(Pt 11):3290-8.

Neudorfer O, Giladi N, Elstein D, Abrahamov A, Turezkite T, Aghai E, et al. Occurrence of Parkinson's syndrome in type I Gaucher disease. QJM. 1996;89(9):691-4.

Neumann J, Bras J, Deas E, O'Sullivan SS, Parkkinen L, Lachmann RH, et al. Glucocerebrosidase mutations in clinical and pathologically proven Parkinson's disease. Brain. 2009;132(Pt 7):1783-94.

Neychev VK, Gross RE, Lehericy S, Hess EJ, Jinnah HA. The functional neuroanatomy of dystonia. Neurobiol Dis. 2011;42(2):185-201.

Niccolini F, Foltynie T, Reis Marques T, Muhlert N, Tziortzi AC, Searle GE, et al. Loss of phosphodiesterase 10A expression is associated with progression and severity in Parkinson's disease. Brain. 2015;138(Pt 10):3003-15.

Niccolini F, Haider S, Reis Marques T, Muhlert N, Tziortzi AC, Searle GE, et al. Altered PDE10A expression detectable early before symptomatic onset in Huntington's disease. Brain. 2015;138(Pt 10):3016-29.

Nichols WC, Pankratz N, Marek DK, Pauciulo MW, Elsaesser VE, Halter CA, et al. Mutations in GBA are associated with familial Parkinson disease susceptibility and age at onset. Neurology. 2009;72(4):310-6.

Nobili F, Naseri M, De Carli F, Asenbaum S, Booij J, Darcourt J, et al. Automatic semi-quantification of [123I]FP-CIT SPECT scans in healthy volunteers using BasGan version 2: results from the ENC-DAT database. Eur J Nucl Med Mol Imaging. 2013;40(4):565-73.

Noyce AJ, Bestwick JP, Silveira-Moriyama L, Hawkes CH, Giovannoni G, Lees AJ, et al. Meta-analysis of early nonmotor features and risk factors for Parkinson disease. Ann Neurol. 2012;72(6):893-901.

Noyce AJ, Lees AJ, Schrag AE. The prediagnostic phase of Parkinson's disease. J Neurol Neurosurg Psychiatry. 2016.

Nutting PA, Cole BR, Schimke RN. Benign, recessively inherited choreo-athetosis of early onset. J Med Genet. 1969;6(4):408-10.

Nuytemans K, Bademci G, Inchausti V, Dressen A, Kinnamon DD, Mehta A, et al. Whole exome sequencing of rare variants in EIF4G1 and VPS35 in Parkinson disease. Neurology. 2013;80(11):982-9.

Nuytemans K, Rademakers R, Theuns J, Pals P, Engelborghs S, Pickut B, et al. Founder mutation p.R1441C in the leucine-rich repeat kinase 2 gene in Belgian Parkinson's disease patients. Eur J Hum Genet. 2008;16(4):471-9.

Nygaard T. An analysis of North American families with dopa-responsive dystonia. In: Segawa M, editor. Hereditary progressive dystonia. London: Parthenon Publishing; 1993. p. 97-106.

Nygaard TG. Dopa-responsive dystonia. Delineation of the clinical syndrome and clues to pathogenesis. Adv Neurol. 1993;60:577-85.

Nygaard TG, Raymond D, Chen C, Nishino I, Greene PE, Jennings D, et al. Localization of a gene for myoclonus-dystonia to chromosome 7q21-q31. Ann Neurol. 1999;46(5):794-8.

Nygaard TG, Takahashi H, Heiman GA, Snow BJ, Fahn S, Calne DB. Long-term treatment response and fluorodopa positron emission tomographic scanning of parkinsonism in a family with dopa-responsive dystonia. Ann Neurol. 1992;32(5):603-8.

Nygaard TG, Trugman JM, de Yebenes JG, Fahn S. Dopa-responsive dystonia: the spectrum of clinical manifestations in a large North American family. Neurology. 1990;40(1):66-9.

Nygaard TG, Wooten GF. Dopa-responsive dystonia: some pieces of the puzzle are still missing. Neurology. 1998;50(4):853-5.

Ogaki K, Koga S, Heckman MG, Fiesel FC, Ando M, Labbe C, et al. Mitochondrial targeting sequence variants of the CHCHD2 gene are a risk for Lewy body disorders. Neurology. 2015;85(23):2016-25.

Oldham MC, Horvath S, Geschwind DH. Conservation and evolution of gene coexpression networks in human and chimpanzee brains. Proc Natl Acad Sci U S A. 2006;103(47):17973-8.

Olgiati S, Quadri M, Bonifati V. Genetics of movement disorders in the next-generation sequencing era. Mov Disord. 2016;31(4):458-70.

Olgiati S, Quadri M, Fang M, Rood JP, Saute JA, Chien HF, et al. DNAJC6 Mutations Associated With Early-Onset Parkinson's Disease. Ann Neurol. 2016;79(2):244-56.

Opladen T, Hoffmann G, Horster F, Hinz AB, Neidhardt K, Klein C, et al. Clinical and biochemical characterization of patients with early infantile onset of autosomal recessive GTP cyclohydrolase I deficiency without hyperphenylalaninemia. Mov Disord. 2011;26(1):157-61.

Ozelius LJ, Hewett JW, Page CE, Bressman SB, Kramer PL, Shalish C, et al. The early-

onset torsion dystonia gene (DYT1) encodes an ATP-binding protein. Nat Genet. 1997;17(1):40-8.

Ozelius LJ, Senthil G, Saunders-Pullman R, Ohmann E, Deligtisch A, Tagliati M, et al. LRRK2 G2019S as a cause of Parkinson's disease in Ashkenazi Jews. N Engl J Med. 2006;354(4):424-5.

Paciotti S, Persichetti E, Pagliardini S, Deganuto M, Rosano C, Balducci C, et al. First pilot newborn screening for four lysosomal storage diseases in an Italian region: identification and analysis of a putative causative mutation in the GBA gene. Clin Chim Acta. 2012;413(23-24):1827-31.

Paisan-Ruiz C, Bhatia KP, Li A, Hernandez D, Davis M, Wood NW, et al. Characterization of PLA2G6 as a locus for dystonia-parkinsonism. Ann Neurol. 2009;65(1):19-23.

Paisan-Ruiz C, Jain S, Evans EW, Gilks WP, Simon J, van der Brug M, et al. Cloning of the gene containing mutations that cause PARK8-linked Parkinson's disease. Neuron. 2004;44(4):595-600.

Paisan-Ruiz C, Li A, Schneider SA, Holton JL, Johnson R, Kidd D, et al. Widespread Lewy body and tau accumulation in childhood and adult onset dystonia-parkinsonism cases with PLA2G6 mutations. Neurobiol Aging. 2012;33(4):814-23.

Palmer CL, Lim W, Hastie PG, Toward M, Korolchuk VI, Burbidge SA, et al. Hippocalcin functions as a calcium sensor in hippocampal LTD. Neuron. 2005;47(4):487-94.

Panagiotakaki E, De Grandis E, Stagnaro M, Heinzen EL, Fons C, Sisodiya S, et al. Clinical profile of patients with ATP1A3 mutations in Alternating Hemiplegia of Childhood-a study of 155 patients. Orphanet J Rare Dis. 2015;10:123.

Pandit J, Forman MD, Fennell KF, Dillman KS, Menniti FS. Mechanism for the allosteric regulation of phosphodiesterase 2A deduced from the X-ray structure of a near full-length construct. Proc Natl Acad Sci U S A. 2009;106(43):18225-30.

Pankratz N, Beecham GW, DeStefano AL, Dawson TM, Doheny KF, Factor SA, et al. Meta-analysis of Parkinson's disease: identification of a novel locus, RIT2. Ann Neurol.

2012;71(3):370-84.

Pankratz N, Pauciulo MW, Elsaesser VE, Marek DK, Halter CA, Wojcieszek J, et al. Mutations in DJ-1 are rare in familial Parkinson disease. Neurosci Lett. 2006;408(3):209-13.

Pankratz N, Wilk JB, Latourelle JC, DeStefano AL, Halter C, Pugh EW, et al. Genomewide association study for susceptibility genes contributing to familial Parkinson disease. Hum Genet. 2009;124(6):593-605.

Park JK, Tayebi N, Stubblefield BK, LaMarca ME, MacKenzie JJ, Stone DL, et al. The E326K mutation and Gaucher disease: mutation or polymorphism? Clin Genet. 2002;61(1):32-4.

Parker N. Hereditary whispering dysphonia. J Neurol Neurosurg Psychiatry. 1985;48(3):218-24.

Parkinson MH, Boesch S, Nachbauer W, Mariotti C, Giunti P. Clinical features of Friedreich's ataxia: classical and atypical phenotypes. J Neurochem. 2013;126 Suppl 1:103-17.

Parkkinen L, O'Sullivan SS, Kuoppamaki M, Collins C, Kallis C, Holton JL, et al. Does levodopa accelerate the pathologic process in Parkinson disease brain? Neurology. 2011;77(15):1420-6.

Pasanen P, Myllykangas L, Siitonen M, Raunio A, Kaakkola S, Lyytinen J, et al. A novel alpha-synuclein mutation A53E associated with atypical multiple system atrophy and Parkinson's disease-type pathology. Neurobiol Aging. 2014;35(9):2180 e1-5.

Patel CV, Handy I, Goldsmith T, Patel RC. PACT, a stress-modulated cellular activator of interferon-induced double-stranded RNA-activated protein kinase, PKR. The Journal of biological chemistry. 2000;275(48):37993-8.

Paudel R, Hardy J, Revesz T, Holton JL, Houlden H. Review: Genetics and neuropathology of primary pure dystonia. Neuropathology and Applied Neurobiology. 2012;38(6):520-34.

Peall KJ, Kurian MA. Benign Hereditary Chorea: An Update. Tremor Other Hyperkinet

Mov (N Y). 2015;5:314.

Peall KJ, Kurian MA, Wardle M, Waite AJ, Hedderly T, Lin JP, et al. SGCE and myoclonus dystonia: motor characteristics, diagnostic criteria and clinical predictors of genotype. J Neurol. 2014;261(12):2296-304.

Peall KJ, Lumsden D, Kneen R, Madhu R, Peake D, Gibbon F, et al. Benign hereditary chorea related to NKX2.1: expansion of the genotypic and phenotypic spectrum. Dev Med Child Neurol. 2014;56(7):642-8.

Peall KJ, Smith DJ, Kurian MA, Wardle M, Waite AJ, Hedderly T, et al. SGCE mutations cause psychiatric disorders: clinical and genetic characterization. Brain. 2013;136(Pt 1):294-303.

Pfeiffenberger C, Allada R. Cul3 and the BTB adaptor insomniac are key regulators of sleep homeostasis and a dopamine arousal pathway in Drosophila. PLoS Genet. 2012;8(10):e1003003.

Piccini P, Burn DJ, Ceravolo R, Maraganore D, Brooks DJ. The role of inheritance in sporadic Parkinson's disease: evidence from a longitudinal study of dopaminergic function in twins. Ann Neurol. 1999;45(5):577-82.

Pinto RM, Dragileva E, Kirby A, Lloret A, Lopez E, St Claire J, et al. Mismatch repair genes Mlh1 and Mlh3 modify CAG instability in Huntington's disease mice: genome-wide and candidate approaches. PLoS Genet. 2013;9(10):e1003930.

Pittman A, Hardy J. Genetic analysis in neurology: the next 10 years. JAMA Neurol. 2013;70(6):696-702.

Plagnol V, Curtis J, Epstein M, Mok KY, Stebbings E, Grigoriadou S, et al. A robust model for read count data in exome sequencing experiments and implications for copy number variant calling. Bioinformatics. 2012;28(21):2747-54.

Pollard KS, Hubisz MJ, Rosenbloom KR, Siepel A. Detection of nonneutral substitution rates on mammalian phylogenies. Genome Res. 2010;20(1):110-21.

Polymeropoulos MH, Lavedan C, Leroy E, Ide SE, Dehejia A, Dutra A, et al. Mutation in the alpha-synuclein gene identified in families with Parkinson's disease. Science.

1997;276(5321):2045-7.

Pons R, Serrano M, Ormazabal A, Toma C, Garcia-Cazorla A, Area E, et al. Tyrosine Hydroxylase Deficiency in Three Greek Patients with a Common Ancestral Mutation. Movement Disorders. 2010;25(8):1086-90.

Proukakis C, Dudzik CG, Brier T, MacKay DS, Cooper JM, Millhauser GL, et al. A novel alpha-synuclein missense mutation in Parkinson disease. Neurology. 2013;80(11):1062-4.

Provenzano C, Zamboni M, Veneziano L, Mantuano E, Garavaglia B, Zorzi G, et al. Functional characterization of two novel mutations in TTF-1/NKX2.1 homeodomain in patients with benign hereditary chorea. J Neurol Sci. 2016;360:78-83.

Pruitt KD, Brown GR, Hiatt SM, Thibaud-Nissen F, Astashyn A, Ermolaeva O, et al. RefSeq: an update on mammalian reference sequences. Nucleic Acids Res. 2014;42(Database issue):D756-63.

Pruitt KD, Harrow J, Harte RA, Wallin C, Diekhans M, Maglott DR, et al. The consensus coding sequence (CCDS) project: Identifying a common protein-coding gene set for the human and mouse genomes. Genome Res. 2009;19(7):1316-23.

Quadri M, Fang M, Picillo M, Olgiati S, Breedveld GJ, Graafland J, et al. Mutation in the SYNJ1 gene associated with autosomal recessive, early-onset Parkinsonism. Hum Mutat. 2013;34(9):1208-15.

Quadri M, Olgiati S, Sensi M, Gualandi F, Groppo E, Rispoli V, et al. PRKRA Mutation Causing Early-Onset Generalized Dystonia-Parkinsonism (DYT16) in an Italian Family. Mov Disord. 2016;31(5):765-7.

Quinn N, Schrag A. Huntington's disease and other choreas. J Neurol. 1998;245(11):709-16.

Rainier S, Thomas D, Tokarz D, Ming L, Bui M, Plein E, et al. Myofibrillogenesis regulator 1 gene mutations cause paroxysmal dystonic choreoathetosis. Archives of neurology. 2004;61(7):1025-9.

Ramirez A, Heimbach A, Grundemann J, Stiller B, Hampshire D, Cid LP, et al.

Hereditary parkinsonism with dementia is caused by mutations in ATP13A2, encoding a lysosomal type 5 P-type ATPase. Nat Genet. 2006;38(10):1184-91.

Rampoldi L, Dobson-Stone C, Rubio JP, Danek A, Chalmers RM, Wood NW, et al. A conserved sorting-associated protein is mutant in chorea-acanthocytosis. Nat Genet. 2001;28(2):119-20.

Rana HQ, Balwani M, Bier L, Alcalay RN. Age-specific Parkinson disease risk in GBA mutation carriers: information for genetic counseling. Genet Med. 2013;15(2):146-9.

Raskind WH, Matsushita M, Peter B, Biberston J, Wolff J, Lipe H, et al. Familial dyskinesia and facial myokymia (FDFM): Follow-up of a large family and linkage to chromosome 3p21-3q21. Am J Med Genet B Neuropsychiatr Genet. 2009;150B(4):570-4.

Rauch A, Wieczorek D, Graf E, Wieland T, Endele S, Schwarzmayr T, et al. Range of genetic mutations associated with severe non-syndromic sporadic intellectual disability: an exome sequencing study. Lancet. 2012;380(9854):1674-82.

Reimand J, Arak T, Vilo J. g:Profiler--a web server for functional interpretation of gene lists (2011 update). Nucleic Acids Res. 2011;39(Web Server issue):W307-15.

Renton AE, Majounie E, Waite A, Simon-Sanchez J, Rollinson S, Gibbs JR, et al. A hexanucleotide repeat expansion in C9ORF72 is the cause of chromosome 9p21-linked ALS-FTD. Neuron. 2011;72(2):257-68.

Ribases M, Serrano M, Fernandez-Alvarez E, Pahisa S, Ormazabal A, Garcia-Cazorla A, et al. A homozygous tyrosine hydroxylase gene promoter mutation in a patient with dopa-responsive encephalopathy: Clinical, biochemical and genetic analysis. Molecular Genetics and Metabolism. 2007;92(3):274-7.

Ritz K, van Schaik BD, Jakobs ME, van Kampen AH, Aronica E, Tijssen MA, et al. SGCE isoform characterization and expression in human brain: implications for myoclonus-dystonia pathogenesis? Eur J Hum Genet. 2011;19(4):438-44.

Robinson RO, Thornett CE. Benign hereditary chorea--response to steroids. Dev Med Child Neurol. 1985;27(6):814-6.

Rogaeva E, Johnson J, Lang AE, Gulick C, Gwinn-Hardy K, Kawarai T, et al. Analysis of the PINK1 gene in a large cohort of cases with Parkinson disease. Arch Neurol. 2004;61(12):1898-904.

Romito LM, Contarino MF, Ghezzi D, Franzini A, Garavaglia B, Albanese A. High frequency stimulation of the subthalamic nucleus is efficacious in Parkin disease. J Neurol. 2005;252(2):208-11.

Rosenbloom B, Balwani M, Bronstein JM, Kolodny E, Sathe S, Gwosdow AR, et al. The incidence of Parkinsonism in patients with type 1 Gaucher disease: data from the ICGG Gaucher Registry. Blood Cells Mol Dis. 2011;46(1):95-102.

Rosewich H, Baethmann M, Ohlenbusch A, Gartner J, Brockmann K. A novel ATP1A3 mutation with unique clinical presentation. J Neurol Sci. 2014;341(1-2):133-5.

Rosewich H, Ohlenbusch A, Huppke P, Schlotawa L, Baethmann M, Carrilho I, et al. The expanding clinical and genetic spectrum of ATP1A3-related disorders. Neurology. 2014;82(11):945-55.

Rosewich H, Thiele H, Ohlenbusch A, Maschke U, Altmuller J, Frommolt P, et al. Heterozygous de-novo mutations in ATP1A3 in patients with alternating hemiplegia of childhood: a whole-exome sequencing gene-identification study. Lancet Neurol. 2012;11(9):764-73.

Rosewich H, Weise D, Ohlenbusch A, Gartner J, Brockmann K. Phenotypic overlap of alternating hemiplegia of childhood and CAPOS syndrome. Neurology. 2014;83(9):861-3.

Ross CA, Tabrizi SJ. Huntington's disease: from molecular pathogenesis to clinical treatment. Lancet Neurol. 2011;10(1):83-98.

Roubergue A, Roze E, Vuillaumier-Barrot S, Fontenille MJ, Meneret A, Vidailhet M, et al. The multiple faces of the ATP1A3-related dystonic movement disorder. Mov Disord. 2013;28(10):1457-9.

Roussigne M, Cayrol C, Clouaire T, Amalric F, Girard JP. THAP1 is a nuclear proapoptotic factor that links prostate-apoptosis-response-4 (Par-4) to PML nuclear bodies. Oncogene. 2003;22(16):2432-42.

Roze E, Apartis E, Clot F, Dorison N, Thobois S, Guyant-Marechal L, et al. Myoclonus-dystonia: clinical and electrophysiologic pattern related to SGCE mutations. Neurology. 2008;70(13):1010-6.

Rozenberg R, Fox DC, Sobreira E, Pereira LV. Detection of 12 new mutations in Gaucher disease Brazilian patients. Blood Cells Mol Dis. 2006;37(3):204-9.

Rubio-Agusti I, Parees I, Kojovic M, Stamelou M, Saifee TA, Charlesworth G, et al. Tremulous cervical dystonia is likely to be familial: clinical characteristics of a large cohort. Parkinsonism Relat Disord. 2013;19(6):634-8.

Russwurm C, Koesling D, Russwurm M. Phosphodiesterase 10A Is Tethered to a Synaptic Signaling Complex in Striatum. J Biol Chem. 2015;290(19):11936-47.

Ryan BJ, Crabtree MJ, Channon KM, Wade-Martins R. Parkinson's disease in GTP cyclohydrolase 1 mutation carriers. Brain. 2015;138(Pt 5):e348.

Ryan BJ, Lourenco-Venda LL, Crabtree MJ, Hale AB, Channon KM, Wade-Martins R. alpha-Synuclein and mitochondrial bioenergetics regulate tetrahydrobiopterin levels in a human dopaminergic model of Parkinson disease. Free Radic Biol Med. 2014;67:58-68.

Saad M, Lesage S, Saint-Pierre A, Corvol JC, Zelenika D, Lambert JC, et al. Genome-wide association study confirms BST1 and suggests a locus on 12q24 as the risk loci for Parkinson's disease in the European population. Hum Mol Genet. 2011;20(3):615-27.

Saitsu H, Tohyama J, Kumada T, Egawa K, Hamada K, Okada I, et al. Dominant-negative mutations in alpha-II spectrin cause West syndrome with severe cerebral hypomyelination, spastic quadriplegia, and developmental delay. Am J Hum Genet. 2010;86(6):881-91.

Salvatore E, Varrone A, Criscuolo C, Mancini P, Sansone V, Strisciuglio C, et al. Nigrostriatal involvement in ataxia with oculomotor apraxia type 1. J Neurol. 2008;255(1):45-8.

Samaranch L, Lorenzo-Betancor O, Arbelo JM, Ferrer I, Lorenzo E, Irigoyen J, et al. PINK1-linked parkinsonism is associated with Lewy body pathology. Brain. 2010;133(Pt 4):1128-42.

Samocha KE, Robinson EB, Sanders SJ, Stevens C, Sabo A, McGrath LM, et al. A framework for the interpretation of de novo mutation in human disease. Nat Genet. 2014;46(9):944-50.

Sanger F, Nicklen S, Coulson AR. DNA sequencing with chain-terminating inhibitors. Proc Natl Acad Sci U S A. 1977;74(12):5463-7.

Santens P, Van Damme T, Steyaert W, Willaert A, Sablonniere B, De Paepe A, et al. RNF216 mutations as a novel cause of autosomal recessive Huntington-like disorder. Neurology. 2015;84(17):1760-6.

Sardi SP, Clarke J, Kinnecom C, Tamsett TJ, Li L, Stanek LM, et al. CNS expression of glucocerebrosidase corrects alpha-synuclein pathology and memory in a mouse model of Gaucher-related synucleinopathy. Proc Natl Acad Sci U S A. 2011;108(29):12101-6.

Satake W, Nakabayashi Y, Mizuta I, Hirota Y, Ito C, Kubo M, et al. Genome-wide association study identifies common variants at four loci as genetic risk factors for Parkinson's disease. Nat Genet. 2009;41(12):1303-7.

Saugier-Veber P, Doummar D, Barthez MA, Czernecki V, Drouot N, Apartis E, et al. Myoclonus dystonia plus syndrome due to a novel 7q21 microdeletion. Am J Med Genet A. 2010;152A(5):1244-9.

Saunders-Pullman R, Blau N, Hyland K, Zschocke J, Nygaard T, Raymond D, et al. Phenylalanine loading as a diagnostic test for DRD: interpreting the utility of the test. Mol Genet Metab. 2004;83(3):207-12.

Saunders-Pullman R, Raymond D, Senthil G, Kramer P, Ohmann E, Deligtisch A, et al. Narrowing the DYT6 dystonia region and evidence for locus heterogeneity in the Amish-Mennonites. Am J Med Genet A. 2007;143A(18):2098-105.

Saunders-Pullman R, Raymond D, Stoessl AJ, Hobson D, Nakamura K, Pullman S, et al. Variant ataxia-telangiectasia presenting as primary-appearing dystonia in Canadian Mennonites. Neurology. 2012;78(9):649-57.

Sawle GV, Leenders KL, Brooks DJ, Harwood G, Lees AJ, Frackowiak RS, et al. Dopa-responsive dystonia: [18F]dopa positron emission tomography. Ann Neurol. 1991;30(1):24-30.

Schneider SA, Lang AE, Moro E, Bader B, Danek A, Bhatia KP. Characteristic head drops and axial extension in advanced chorea-acanthocytosis. Mov Disord. 2010;25(10):1487-91.

Schneider SA, Marshall KE, Xiao J, LeDoux MS. JPH3 repeat expansions cause a progressive akinetic-rigid syndrome with severe dementia and putaminal rim in a five-generation African-American family. Neurogenetics. 2012;13(2):133-40.

Schneider SA, Paisan-Ruiz C, Quinn NP, Lees AJ, Houlden H, Hardy J, et al. ATP13A2 mutations (PARK9) cause neurodegeneration with brain iron accumulation. Mov Disord. 2010;25(8):979-84.

Schneider SA, van de Warrenburg BP, Hughes TD, Davis M, Sweeney M, Wood N, et al. Phenotypic homogeneity of the Huntington disease-like presentation in a SCA17 family. Neurology. 2006;67(9):1701-3.

Schneider SA, Walker RH, Bhatia KP. The Huntington's disease-like syndromes: what to consider in patients with a negative Huntington's disease gene test. Nat Clin Pract Neurol. 2007;3(9):517-25.

Schols L, Peters S, Szymanski S, Kruger R, Lange S, Hardt C, et al. Extrapyramidal motor signs in degenerative ataxias. Arch Neurol. 2000;57(10):1495-500.

Schrag A, Ben-Shlomo Y, Brown R, Marsden CD, Quinn N. Young-onset Parkinson's disease revisited--clinical features, natural history, and mortality. Mov Disord. 1998;13(6):885-94.

Schrag A, Quinn NP, Bhatia KP, Marsden CD. Benign hereditary chorea--entity or syndrome? Mov Disord. 2000;15(2):280-8.

Schrag A, Schott JM. Epidemiological, clinical, and genetic characteristics of early-onset parkinsonism. Lancet Neurol. 2006;5(4):355-63.

Schuchman EH. The pathogenesis and treatment of acid sphingomyelinase-deficient Niemann-Pick disease. J Inherit Metab Dis. 2007;30(5):654-63.

Schule B, Kock N, Svetel M, Dragasevic N, Hedrich K, De Carvalho Aguiar P, et al. Genetic heterogeneity in ten families with myoclonus-dystonia. J Neurol Neurosurg

Psychiatry. 2004;75(8):1181-5.

Schupbach M, Lohmann E, Anheim M, Lesage S, Czernecki V, Yaici S, et al. Subthalamic nucleus stimulation is efficacious in patients with Parkinsonism and LRRK2 mutations. Mov Disord. 2007;22(1):119-22.

Schwarz JM, Cooper DN, Schuelke M, Seelow D. MutationTaster2: mutation prediction for the deep-sequencing age. Nat Methods. 2014;11(4):361-2.

Schwenk J, Metz M, Zolles G, Turecek R, Fritzius T, Bildl W, et al. Native GABA(B) receptors are heteromultimers with a family of auxiliary subunits. Nature. 2010;465(7295):231-5.

Seaman MNJ. Recycle your receptors with retromer. Trends Cell Biol. 2005;15(2):68-75.

Seeger TF, Bartlett B, Coskran TM, Culp JS, James LC, Krull DL, et al. Immunohistochemical localization of PDE10A in the rat brain. Brain Res. 2003;985(2):113-26.

Segawa M, Nomura Y, Hayashi M. Dopa-responsive dystonia is caused by particular impairment of nigrostriatal dopamine neurons different from those involved in Parkinson disease: evidence observed in studies on Segawa disease. Neuropediatrics. 2013;44(2):61-6.

Segawa M, Nomura Y, Yukishita S, Nishiyama N, Yokochi M. Is phenotypic variation of hereditary progressive dystonia with marked diurnal fluctuation/dopa-responsive dystonia (HPD/DRD) caused by the difference of the locus of mutation on the GTP cyclohydrolase 1 (GCH-1) gene? Adv Neurol. 2004;94:217-23.

Selikhova M, Williams DR, Kempster PA, Holton JL, Revesz T, Lees AJ. A clinico-pathological study of subtypes in Parkinson's disease. Brain. 2009;132(Pt 11):2947-57.

Sharma M, Ioannidis JP, Aasly JO, Annesi G, Brice A, Bertram L, et al. A multi-centre clinico-genetic analysis of the VPS35 gene in Parkinson disease indicates reduced penetrance for disease-associated variants. J Med Genet. 2012;49(11):721-6.

Sheerin UM, Charlesworth G, Bras J, Guerreiro R, Bhatia K, Foltynie T, et al. Screening

for VPS35 mutations in Parkinson's disease. Neurobiol Aging. 2012;33(4):838 e1-5.

Shi CH, Mao CY, Zhang SY, Yang J, Song B, Wu P, et al. CHCHD2 gene mutations in familial and sporadic Parkinson's disease. Neurobiol Aging. 2016;38:217 e9- e13.

Shimohata T, Hara K, Sanpei K, Nunomura J, Maeda T, Kawachi I, et al. Novel locus for benign hereditary chorea with adult onset maps to chromosome 8q21.3 q23.3. Brain. 2007;130(Pt 9):2302-9.

Sidransky E, Lopez G. The link between the GBA gene and parkinsonism. Lancet Neurol. 2012;11(11):986-98.

Sidransky E, Nalls MA, Aasly JO, Aharon-Peretz J, Annesi G, Barbosa ER, et al. Multicenter analysis of glucocerebrosidase mutations in Parkinson's disease. N Engl J Med. 2009;361(17):1651-61.

Simon-Sanchez J, Marti-Masso JF, Sanchez-Mut JV, Paisan-Ruiz C, Martinez-Gil A, Ruiz-Martinez J, et al. Parkinson's disease due to the R1441G mutation in Dardarin: a founder effect in the Basques. Mov Disord. 2006;21(11):1954-9.

Simon-Sanchez J, Schulte C, Bras JM, Sharma M, Gibbs JR, Berg D, et al. Genome-wide association study reveals genetic risk underlying Parkinson's disease. Nat Genet. 2009;41(12):1308-12.

Simons C, Wolf NI, McNeil N, Caldovic L, Devaney JM, Takanohashi A, et al. A de novo mutation in the beta-tubulin gene TUBB4A results in the leukoencephalopathy hypomyelination with atrophy of the basal ganglia and cerebellum. Am J Hum Genet. 2013;92(5):767-73.

Singleton AB, Farrer M, Johnson J, Singleton A, Hague S, Kachergus J, et al. alpha-Synuclein locus triplication causes Parkinson's disease. Science. 2003;302(5646):841.

Singleton AB, Hardy J, Traynor BJ, Houlden H. Towards a complete resolution of the genetic architecture of disease. Trends Genet. 2010;26(10):438-42.

Siuciak JA, McCarthy SA, Chapin DS, Fujiwara RA, James LC, Williams RD, et al. Genetic deletion of the striatum-enriched phosphodiesterase PDE10A: evidence for altered striatal function. Neuropharmacology. 2006;51(2):374-85.

Siuciak JA, McCarthy SA, Chapin DS, Martin AN, Harms JF, Schmidt CJ. Behavioral characterization of mice deficient in the phosphodiesterase-10A (PDE10A) enzyme on a C57/Bl6N congenic background. Neuropharmacology. 2008;54(2):417-27.

Skoblov M, Marakhonov A, Marakasova E, Guskova A, Chandhoke V, Birerdinc A, et al. Protein partners of KCTD proteins provide insights about their functional roles in cell differentiation and vertebrate development. Bioessays. 2013;35(7):586-96.

Sleigh G, Lindenbaum RH. Benign (non-paroxysmal) familial chorea. Paediatric perspectives. Arch Dis Child. 1981;56(8):616-21.

Smith BN, Ticozzi N, Fallini C, Gkazi AS, Topp S, Kenna KP, et al. Exome-wide rare variant analysis identifies TUBA4A mutations associated with familial ALS. Neuron. 2014;84(2):324-31.

Snow BJ, Nygaard TG, Takahashi H, Calne DB. Positron emission tomographic studies of dopa-responsive dystonia and early-onset idiopathic parkinsonism. Ann Neurol. 1993;34(5):733-8.

Soderling SH, Beavo JA. Regulation of cAMP and cGMP signaling: new phosphodiesterases and new functions. Curr Opin Cell Biol. 2000;12(2):174-9.

Someko H, Hanajima R, Tsutsumi R, Tominaga N, Nomura Y, Hoshino K, et al. Abnormal myocardial scintigraphy in a GTP cyclohydrolase 1 mutation carrier with Parkinson's disease. Mov Disord. 2016;31(3):422-3.

Spatola M, Wider C. Genetics of Parkinson's disease: the yield. Parkinsonism Relat Disord. 2014;20 Suppl 1:S35-8.

Spencer CC, Plagnol V, Strange A, Gardner M, Paisan-Ruiz C, Band G, et al. Dissection of the genetics of Parkinson's disease identifies an additional association 5' of SNCA and multiple associated haplotypes at 17q21. Hum Mol Genet. 2011;20(2):345-53.

Spillantini MG, Schmidt ML, Lee VM, Trojanowski JQ, Jakes R, Goedert M. Alpha-synuclein in Lewy bodies. Nature. 1997;388(6645):839-40.

Stamelou M, Charlesworth G, Cordivari C, Schneider SA, Kagi G, Sheerin UM, et al. The phenotypic spectrum of DYT24 due to ANO3 mutations. Mov Disord.

2014;29(7):928-34.

Stamelou M, Edwards MJ, Bhatia KP. Late onset rest-tremor in DYT1 dystonia. Parkinsonism Relat Disord. 2013;19(1):136-7.

Staropoli JF, Karaa A, Lim ET, Kirby A, Elbalalesy N, Romansky SG, et al. A homozygous mutation in KCTD7 links neuronal ceroid lipofuscinosis to the ubiquitin-proteasome system. Am J Hum Genet. 2012;91(1):202-8.

Stavropoulos N, Young MW. insomniac and Cullin-3 regulate sleep and wakefulness in Drosophila. Neuron. 2011;72(6):964-76.

Steegborn C. Structure, mechanism, and regulation of soluble adenylyl cyclases - similarities and differences to transmembrane adenylyl cyclases. Biochim Biophys Acta. 2014;1842(12 Pt B):2535-47.

Steinlein OK, Villain M, Korenke C. The PRRT2 mutation c.649dupC is the so far most frequent cause of benign familial infantile convulsions. Seizure : the journal of the British Epilepsy Association. 2012;21(9):740-2.

Stepensky P, Keller B, Shamriz O, NaserEddin A, Rumman N, Weintraub M, et al. Deep intronic mis-splicing mutation in JAK3 gene underlies T-B+NK- severe combined immunodeficiency phenotype. Clin Immunol. 2016;163:91-5.

Stevanin G, Brice A. Spinocerebellar ataxia 17 (SCA17) and Huntington's disease-like 4 (HDL4). Cerebellum. 2008;7(2):170-8.

Stevanin G, Fujigasaki H, Lebre AS, Camuzat A, Jeannequin C, Dode C, et al. Huntington's disease-like phenotype due to trinucleotide repeat expansions in the TBP and JPH3 genes. Brain. 2003;126(Pt 7):1599-603.

Stogios PJ, Downs GS, Jauhal JJ, Nandra SK, Prive GG. Sequence and structural analysis of BTB domain proteins. Genome Biol. 2005;6(10):R82.

Suganuma T, Mushegian A, Swanson SK, Abmayr SM, Florens L, Washburn MP, et al. The ATAC acetyltransferase complex coordinates MAP kinases to regulate JNK target genes. Cell. 2010;142(5):726-36.

Tadic V, Kasten M, Bruggemann N, Stiller S, Hagenah J, Klein C. Dopa-responsive dystonia revisited: diagnostic delay, residual signs, and nonmotor signs. Arch Neurol. 2012;69(12):1558-62.

Taipa R, Pereira C, Reis I, Alonso I, Bastos-Lima A, Melo-Pires M, et al. DJ-1 linked parkinsonism (PARK7) is associated with Lewy body pathology. Brain. 2016.

Takahashi H, Levine RA, Galloway MP, Snow BJ, Calne DB, Nygaard TG. Biochemical and fluorodopa positron emission tomographic findings in an asymptomatic carrier of the gene for dopa-responsive dystonia. Ann Neurol. 1994;35(3):354-6.

Takanashi M, Li Y, Hattori N. Absence of Lewy pathology associated with PINK1 homozygous mutation. Neurology. 2016.

Tassin J, Durr A, Bonnet AM, Gil R, Vidailhet M, Lucking CB, et al. Levodopa-responsive dystonia. GTP cyclohydrolase I or parkin mutations? Brain. 2000;123 (Pt 6):1112-21.

Tayebi N, Callahan M, Madike V, Stubblefield BK, Orvisky E, Krasnewich D, et al. Gaucher disease and parkinsonism: a phenotypic and genotypic characterization. Mol Genet Metab. 2001;73(4):313-21.

Tayebi N, Walker J, Stubblefield B, Orvisky E, LaMarca ME, Wong K, et al. Gaucher disease with parkinsonian manifestations: does glucocerebrosidase deficiency contribute to a vulnerability to parkinsonism? Mol Genet Metab. 2003;79(2):104-9.

Terbeek J, Hermans S, Van Laere K, Vandenberghe W. Parkinson's disease in GTP cyclohydrolase 1 mutation carriers. Brain. 2015;138(Pt 5):e350.

Termsarasab P, Yang AC, Frucht SJ. Intermediate Phenotypes of ATP1A3 Mutations: Phenotype-Genotype Correlations. Tremor Other Hyperkinet Mov (N Y). 2015;5:336.

Termsarasab P, Yang AC, Frucht SJ. Myoclonus in ataxia-telangiectasia. Tremor Other Hyperkinet Mov (N Y). 2015;5:298.

Tezenas du Montcel S, Clot F, Vidailhet M, Roze E, Damier P, Jedynak CP, et al. Epsilon sarcoglycan mutations and phenotype in French patients with myoclonic

syndromes. J Med Genet. 2006;43(5):394-400.

Thorwarth A, Schnittert-Hubener S, Schrumpf P, Muller I, Jyrch S, Dame C, et al. Comprehensive genotyping and clinical characterisation reveal 27 novel NKX2-1 mutations and expand the phenotypic spectrum. J Med Genet. 2014;51(6):375-87.

Threlfell S, West AR. Review: Modulation of striatal neuron activity by cyclic nucleotide signaling and phosphodiesterase inhibition. Basal Ganglia. 2013;3(3):137-46.

Tinti C, Yang C, Seo H, Conti B, Kim C, Joh TH, et al. Structure/function relationship of the cAMP response element in tyrosine hydroxylase gene transcription. J Biol Chem. 1997;272(31):19158-64.

Tomiyama H, Li Y, Funayama M, Hasegawa K, Yoshino H, Kubo S, et al. Clinicogenetic study of mutations in LRRK2 exon 41 in Parkinson's disease patients from 18 countries. Mov Disord. 2006;21(8):1102-8.

Tomlinson CL, Stowe R, Patel S, Rick C, Gray R, Clarke CE. Systematic review of levodopa dose equivalency reporting in Parkinson's disease. Mov Disord. 2010;25(15):2649-53.

Trabzuni D, Ryten M, Walker R, Smith C, Imran S, Ramasamy A, et al. Quality control parameters on a large dataset of regionally dissected human control brains for whole genome expression studies. J Neurochem. 2011;119(2):275-82.

Trender-Gerhard I, Sweeney MG, Schwingenschuh P, Mir P, Edwards MJ, Gerhard A, et al. Autosomal-dominant GTPCH1-deficient DRD: clinical characteristics and long-term outcome of 34 patients. J Neurol Neurosurg Psychiatry. 2009;80(8):839-45.

Tsunemi T, Krainc D. Zn(2)(+) dyshomeostasis caused by loss of ATP13A2/PARK9 leads to lysosomal dysfunction and alpha-synuclein accumulation. Hum Mol Genet. 2014;23(11):2791-801.

Turjanski N, Bhatia K, Burn DJ, Sawle GV, Marsden CD, Brooks DJ. Comparison of striatal 18F-dopa uptake in adult-onset dystonia-parkinsonism, Parkinson's disease, and dopa-responsive dystonia. Neurology. 1993;43(8):1563-8.

Vaarmann A, Kovac S, Holmstrom KM, Gandhi S, Abramov AY. Dopamine protects

neurons against glutamate-induced excitotoxicity. Cell Death Dis. 2013;4:e455.

Valente EM, Edwards MJ, Mir P, DiGiorgio A, Salvi S, Davis M, et al. The epsilon-sarcoglycan gene in myoclonic syndromes. Neurology. 2005;64(4):737-9.

Valente EM, Salvi S, Ialongo T, Marongiu R, Elia AE, Caputo V, et al. PINK1 mutations are associated with sporadic early-onset parkinsonism. Ann Neurol. 2004;56(3):336-41.

Valente EM, Warner TT, Jarman PR, Mathen D, Fletcher NA, Marsden CD, et al. The role of DYT1 in primary torsion dystonia in Europe. Brain. 1998;121 (Pt 12):2335-9.

Van Bogaert P, Azizieh R, Desir J, Aeby A, De Meirleir L, Laes JF, et al. Mutation of a potassium channel-related gene in progressive myoclonic epilepsy. Ann Neurol. 2007;61(6):579-86.

van den Heuvel L, Luiten B, Smeitink JAM, Rijk-van Andel JF, Hyland K, Steenbergen-Spanjers GCH, et al. A common point mutation in the tyrosine hydroxylase gene in autosomal recessive L-DOPA-responsive dystonia in the Dutch population. Human Genetics. 1998;102(6):644-6.

van der Knaap MS, Naidu S, Pouwels PJ, Bonavita S, van Coster R, Lagae L, et al. New syndrome characterized by hypomyelination with atrophy of the basal ganglia and cerebellum. AJNR Am J Neuroradiol. 2002;23(9):1466-74.

van Gaalen J, Giunti P, van de Warrenburg BP. Movement disorders in spinocerebellar ataxias. Mov Disord. 2011;26(5):792-800.

Vemula SR, Xiao J, Bastian RW, Momcilovic D, Blitzer A, LeDoux MS. Pathogenic variants in TUBB4A are not found in primary dystonia. Neurology. 2014;82(14):1227-30.

Veneziano L, Parkinson MH, Mantuano E, Frontali M, Bhatia KP, Giunti P. A novel de novo mutation of the TITF1/NKX2-1 gene causing ataxia, benign hereditary chorea, hypothyroidism and a pituitary mass in a UK family and review of the literature. Cerebellum. 2014;13(5):588-95.

Verbeek MM, Steenbergen-Spanjers GC, Willemsen MA, Hol FA, Smeitink J, Seeger J, et al. Mutations in the cyclic adenosine monophosphate response element of the tyrosine

hydroxylase gene. Ann Neurol. 2007;62(4):422-6.

Verstraeten A, Theuns J, Van Broeckhoven C. Progress in unraveling the genetic etiology of Parkinson disease in a genomic era. Trends Genet. 2015;31(3):140-9.

Vilarino-Guell C, Rajput A, Milnerwood AJ, Shah B, Szu-Tu C, Trinh J, et al. DNAJC13 mutations in Parkinson disease. Hum Mol Genet. 2014;23(7):1794-801.

Vilarino-Guell C, Wider C, Ross OA, Dachsel JC, Kachergus JM, Lincoln SJ, et al. VPS35 mutations in Parkinson disease. Am J Hum Genet. 2011;89(1):162-7.

Vulinovic F, Lohmann K, Rakovic A, Capetian P, Alvarez-Fischer D, Schmidt A, et al. Unraveling cellular phenotypes of novel TorsinA/TOR1A mutations. Hum Mutat. 2014;35(9):1114-22.

Walker JM, Lwin A, Tayebi N, LaMarca ME, Orvisky E, Sidransky E. Glucocerebrosidase mutation T369M appears to be another polymorphism. Clin Genet. 2003;63(3):237-8.

Walker RH. The non–Huntington disease choreas: Five new things. Neurology: Clinical Practice. 2016.

Walker RH, Jung HH, Dobson-Stone C, Rampoldi L, Sano A, Tison F, et al. Neurologic phenotypes associated with acanthocytosis. Neurology. 2007;68(2):92-8.

Wang JL, Cao L, Li XH, Hu ZM, Li JD, Zhang JG, et al. Identification of PRRT2 as the causative gene of paroxysmal kinesigenic dyskinesias. Brain. 2011;134(Pt 12):3493-501.

Wang K, Li M, Hakonarson H. ANNOVAR: functional annotation of genetic variants from high-throughput sequencing data. Nucleic Acids Res. 2010;38(16):e164.

Ward CD, Duvoisin RC, Ince SE, Nutt JD, Eldridge R, Calne DB. Parkinson's disease in 65 pairs of twins and in a set of quadruplets. Neurology. 1983;33(7):815-24.

Warner TT, Granata A, Schiavo G. TorsinA and DYT1 dystonia: a synaptopathy? Biochem Soc Trans. 2010;38(2):452-6.

Weiss D, Brockmann K, Srulijes K, Meisner C, Klotz R, Reinbold S, et al. Long-term follow-up of subthalamic nucleus stimulation in glucocerebrosidase-associated

Parkinson's disease. J Neurol. 2012;259(9):1970-2.

Wider C, Melquist S, Hauf M, Solida A, Cobb SA, Kachergus JM, et al. Study of a Swiss dopa-responsive dystonia family with a deletion in GCH1: redefining DYT14 as DYT5. Neurology. 2008;70(16 Pt 2):1377-83.

Wilcox RA, Winkler S, Lohmann K, Klein C. Whispering dysphonia in an Australian family (DYT4): a clinical and genetic reappraisal. Mov Disord. 2011;26(13):2404-8.

Wild EJ, Mudanohwo EE, Sweeney MG, Schneider SA, Beck J, Bhatia KP, et al. Huntington's disease phenocopies are clinically and genetically heterogeneous. Mov Disord. 2008;23(5):716-20.

Wild EJ, Tabrizi SJ. The differential diagnosis of chorea. Pract Neurol. 2007;7(6):360-73.

Wild EJ, Tabrizi SJ. Huntington's disease phenocopy syndromes. Curr Opin Neurol. 2007;20(6):681-7.

Willemsen MA, Verbeek MM, Kamsteeg E-J, de Rijk-van Andel JF, Aeby A, Blau N, et al. Tyrosine hydroxylase deficiency: a treatable disorder of brain catecholamine biosynthesis. Brain. 2010;133:1810-22.

Willemsen MA, Verbeek MM, Kamsteeg EJ, de Rijk-van Andel JF, Aeby A, Blau N, et al. Tyrosine hydroxylase deficiency: a treatable disorder of brain catecholamine biosynthesis. Brain. 2010;133(Pt 6):1810-22.

Wilson GR, Sim JC, McLean C, Giannandrea M, Galea CA, Riseley JR, et al. Mutations in RAB39B cause X-linked intellectual disability and early-onset Parkinson disease with alpha-synuclein pathology. Am J Hum Genet. 2014;95(6):729-35.

Winder-Rhodes SE, Evans JR, Ban M, Mason SL, Williams-Gray CH, Foltynie T, et al. Glucocerebrosidase mutations influence the natural history of Parkinson's disease in a community-based incident cohort. Brain. 2013;136(Pt 2):392-9.

Worth PF, Srinivasan V, Smith A, Last JI, Wootton LL, Biggs PM, et al. Very mild presentation in adult with classical cellular phenotype of ataxia telangiectasia. Mov Disord. 2013;28(4):524-8.

Wu RM, Lin CH, Lin HI. The p.L302P mutation in the lysosomal enzyme gene SMPD1 is a risk factor for Parkinson disease. Neurology. 2014;82(3):283.

Xiao J, Uitti RJ, Zhao Y, Vemula SR, Perlmutter JS, Wszolek ZK, et al. Mutations in CIZ1 cause adult onset primary cervical dystonia. Ann Neurol. 2012;71(4):458-69.

Xiao J, Vemula SR, Xue Y, Khan MM, Kuruvilla KP, Marquez-Lona EM, et al. Motor phenotypes and molecular networks associated with germline deficiency of Ciz1. Exp Neurol. 2016.

Xie F, Cen Z, Ouyang Z, Wu S, Xiao J, Luo W. Homozygous p.D331Y mutation in PLA2G6 in two patients with pure autosomal-recessive early-onset parkinsonism: further evidence of a fourth phenotype of PLA2G6-associated neurodegeneration. Parkinsonism Relat Disord. 2015;21(4):420-2.

Xiromerisiou G, Houlden H, Sailer A, Silveira-Moriyama L, Hardy J, Lees AJ. Identical twins with Leucine rich repeat kinase type 2 mutations discordant for Parkinson's disease. Mov Disord. 2012;27(10):1323.

Xiromerisiou G, Houlden H, Scarmeas N, Stamelou M, Kara E, Hardy J, et al. THAP1 mutations and dystonia phenotypes: Genotype phenotype correlations. Mov Disord. 2012;27(10):1290-4.

Xu B, Ionita-Laza I, Roos JL, Boone B, Woodrick S, Sun Y, et al. De novo gene mutations highlight patterns of genetic and neural complexity in schizophrenia. Nat Genet. 2012;44(12):1365-9.

Yen TJ, Gay DA, Pachter JS, Cleveland DW. Autoregulated changes in stability of polyribosome-bound beta-tubulin mRNAs are specified by the first 13 translated nucleotides. Molecular and cellular biology. 1988;8(3):1224-35.

Yen TJ, Machlin PS, Cleveland DW. Autoregulated instability of beta-tubulin mRNAs by recognition of the nascent amino terminus of beta-tubulin. Nature. 1988;334(6183):580-5.

Yeung W-l, Wong VCN, Chan K-y, Hui J, Fung C-w, Yau E, et al. Expanding Phenotype and Clinical Analysis of Tyrosine Hydroxylase Deficiency. Journal of Child Neurology. 2011;26(2):179-87.

Youle RJ, Narendra DP. Mechanisms of mitophagy. Nat Rev Mol Cell Biol. 2011;12(1):9-14.

Zabetian CP, Hutter CM, Yearout D, Lopez AN, Factor SA, Griffith A, et al. LRRK2 G2019S in families with Parkinson disease who originated from Europe and the Middle East: evidence of two distinct founding events beginning two millennia ago. Am J Hum Genet. 2006;79(4):752-8.

Zabetian CP, Samii A, Mosley AD, Roberts JW, Leis BC, Yearout D, et al. A clinic-based study of the LRRK2 gene in Parkinson disease yields new mutations. Neurology. 2005;65(5):741-4.

Zafeiriou DI, Willemsen MA, Verbeek MM, Vargiami E, Ververi A, Wevers R. Tyrosine hydroxylase deficiency with severe clinical course. Molecular Genetics and Metabolism. 2009;97(1):18-20.

Zarranz JJ, Alegre J, Gomez-Esteban JC, Lezcano E, Ros R, Ampuero I, et al. The new mutation, E46K, of alpha-synuclein causes Parkinson and Lewy body dementia. Ann Neurol. 2004;55(2):164-73.

Zech M, Castrop F, Schormair B, Jochim A, Wieland T, Gross N, et al. DYT16 revisited: exome sequencing identifies PRKRA mutations in a European dystonia family. Mov Disord. 2014;29(12):1504-10.

Zech M, Gross N, Jochim A, Castrop F, Kaffe M, Dresel C, et al. Rare sequence variants in ANO3 and GNAL in a primary torsion dystonia series and controls. Mov Disord. 2014;29(1):143-7.

Zhang M, Xi Z, Fang S, Ghani M, Sato C, Moreno D, et al. Mutation analysis of CHCHD2 in Canadian patients with familial Parkinson's disease. Neurobiol Aging. 2016;38:217 e7-8.

Zhu D, Burke C, Leslie A, Nicholson GA. Friedreich's ataxia with chorea and myoclonus caused by a compound heterozygosity for a novel deletion and the trinucleotide GAA expansion. Mov Disord. 2002;17(3):585-9.

Zhu S, Perez R, Pan M, Lee T. Requirement of Cul3 for axonal arborization and dendritic elaboration in Drosophila mushroom body neurons. J Neurosci.

2005;25(16):4189-97.

Zhuang X, Belluscio L, Hen R. G(olf)alpha mediates dopamine D1 receptor signaling. J Neurosci. 2000;20(16):RC91.

Ziegan J, Wittstock M, Westenberger A, Dobricic V, Wolters A, Benecke R, et al. Novel GNAL mutations in two German patients with sporadic dystonia. Mov Disord. 2014;29(14):1833-4.

Zimprich A, Benet-Pages A, Struhal W, Graf E, Eck SH, Offman MN, et al. A mutation in VPS35, encoding a subunit of the retromer complex, causes late-onset Parkinson disease. Am J Hum Genet. 2011;89(1):168-75.

Zimprich A, Biskup S, Leitner P, Lichtner P, Farrer M, Lincoln S, et al. Mutations in LRRK2 cause autosomal-dominant parkinsonism with pleomorphic pathology. Neuron. 2004;44(4):601-7.

Zimprich A, Grabowski M, Asmus F, Naumann M, Berg D, Bertram M, et al. Mutations in the gene encoding epsilon-sarcoglycan cause myoclonus-dystonia syndrome. Nat Genet. 2001;29(1):66-9.

Zuhlke C, Burk K. Spinocerebellar ataxia type 17 is caused by mutations in the TATA-box binding protein. Cerebellum. 2007;6(4):300-7.

Appendix- Sequences of primers used in this thesis

ADCY5_exon1_1_FOR	GCGGATCCTCAGCTACTTCT
ADCY5_exon1_1_REV	GCTCCTCCAGACCCACCT
ADCY5_exon1_2_FOR	CAGCTTCCGCTCCAAGTC
ADCY5_exon1_2_REV	GATGAGGATCACGCCGAC
ADCY5_exon1_3_FOR	CTACTTCTTCCGCCTGAACC
ADCY5_exon1_3_REV	TCTTTGGAGTCCAGCTGAGG
ADCY5_exon10_FOR	ACGGCTTAGGCTTCTGGTCT
ADCY5_exon10_REV	GGAAGCCTCCCTAGAACTCG
ADCY5_exon11_FOR	CTGTCTCAACTGCCCTCTCC
ADCY5_exon11_REV	AAACTTCTCTCCGTGCCTGA
ADCY5_exon12_FOR	CTGAAGCTGTGAGGATGG
ADCY5_exon12_REV	TGCCAAGCACAATACTCG
ADCY5_exon13_FOR	CTCCTGGTCAGCTGCAGAAT
ADCY5_exon13_REV	ACCCAGGTGCGAAACAAATA
ADCY5_exon14_FOR	TTTTGTCCCCATCAGTGTCA
ADCY5_exon14_REV	GTGAGCTGGTGAGACCCTGT
ADCY5_exon15_FOR	ACCAGGGCCCTTCACTTTAT
ADCY5_exon15_REV	AACAAGGCCGTTTTCCAGAT
ADCY5_exon16_FOR	CCCTGAAAATGTCGTTGGAT
ADCY5_exon16_REV	GGCCTTCTCCTTCACTACCC
ADCY5_exon17_FOR	AGGAAGGCTTTCTGGAGGAG
ADCY5_exon17_REV	CAGAGTGCAGGGAGCAGAC
ADCY5_exon18_FOR	GCGTGACTGGTGCTTTTTCT
ADCY5_exon18_REV	AGCTCCCATCATCACTGCTT
ADCY5_exon19_FOR	TGAAGAGCGGACACATGAAG
ADCY5_exon19_REV	CAGGGAACACACCACATCAG
ADCY5_exon2_FOR	CCAGGTGTGAGTTTGCTGAG
ADCY5_exon2_REV	GGACTCTCTCCAGGGGAAAC
ADCY5_exon20_FOR	AGGCTCCTTGTGTCTTGCAT
ADCY5_exon20_REV	CTTCCAAGACATCAGCGTCA
ADCY5_exon21_FOR	GCTCTACCCCACAGCAGTTC
ADCY5_exon21_REV	CTGCTTCCATGCCTCTGG
ADCY5_exon3_FOR	GGGAGAGCCTGAGAGGTTTT
ADCY5_exon3_REV	TCCATGGGACACCATGATAA
ADCY5_exon4_FOR	CCTTGATCACACCACTGCAC
ADCY5_exon4_REV	CAGTGCTGAAAGCAACTCCA
ADCY5_exon5_FOR	GCACGGGGTGAATCTTTTT
ADCY5_exon5_REV	TGCTGTAGGGAACAGGAACC
ADCY5_exon6_FOR	TTGGACTCTAGGGCTGGATG
ADCY5_exon6_REV	GCACAGGTGATTTGGCAAG
ADCY5_exon7_FOR	TGTGCCAGGATGTTCAGTGT

ADCY5_exon7_REV	AGGAACCGCAACTGCATAAG
ADCY5_exon8_FOR	TGGCATTAGGGAGTTTGGAG
ADCY5_exon8_REV	TAGTCCAAAGTTGGGGCAAA
ADCY5_exon9_FOR	CACGTCCTTTGGGAGACTGT
ADCY5_exon9_REV	GTGCTGAGGCTCTGTCCTTC
CACNA1B_exon28_FOR	TGTGGTGCAGGTCTTGAGTT
CACNA1B_exon28_REV	ATTTGTGTGCAGGAGGGAAG
DDC_exon 10_FOR	GAGGTGGTCCAGTCTAGGGTAC
DDC_exon 10_REV	CAAGACCAGAAACAGTCCACAG
DDC_exon 11_FOR	GCGTGTGATCAACAAACCTG
DDC_exon 11_REV	GGGAGGAGATGTGTGACAGC
DDC_exon 12_FOR	AAATAGGCGAGCCGGTGAG
DDC_exon 12_REV	TCTAAAGTCCCGAAAGACCTCC
DDC_exon 13_FOR	ATTGCCAAGAGCGTCTAAATG
DDC_exon 13_REV	GCATGGAGGTAATGAACAACAC
DDC_exon 14_FOR	GCACTGTCTTTCCTACATGACC
DDC_exon 14_REV	CTCCAGGAGGACACTCTTGC
DDC_exon 2_FOR	ACGGCTTGCTTGGTATCC
DDC_exon 2_REV	AAATTTCTCTCCAACCTGACTG
DDC_exon 3_FOR	CTCTTGAGGCCTGGCTTTC
DDC_exon 3_REV	TGCATAGGTACCGTGTCCC
DDC_exon 4_FOR	CCAAATTCTGCAATGCCTG
DDC_exon 4_REV	GCATGAGTGCCTCTTTCCC
DDC_exon 5_FOR	GGTACCAATGCCTTCGCTATG
DDC_exon 5_REV	CCAAACATTCGGGTCTTGAAG
DDC_exon 6_FOR	GGCCTGGTAATAACTGCATG
DDC_exon 6_REV	GAGACGGAGTTTCACCTTATTG
DDC_exon 7_FOR	GAGGTTACAGCGGTGACTGG
DDC_exon 7_REV	ACGAGGAAGGTTTGCTAAATTC
DDC_exon 8_FOR	AAGAAGGTGCTCAGACAGGG
DDC_exon 8_REV	TGAAGGGAGAGGTCAATAACAG
DDC_exon 9_FOR	ACCACTGTGGATTAGTTGTGCC
DDC_exon 9_REV	TTCTTTCACTGTCACCTCGGAC
GBA_PCR_fragment 1(ex.1-4)_FOR	CCTAAAGTTGTCACCCATAC
GBA_PCR_fragment 1(ex.1-4)_REV	AGCAGACCTACCCTACAGTTT
GBA_PCR_fragment 2(ex.5-7)_FOR	GACCTCAAATGATATACCTG
GBA_PCR_fragment 2(ex.5-7)_REV	AGTTTGGGAGCCAGTCATTT
GBA_PCR_fragment 3 (ex.8-11)_REV	ACCACCTAGAGGGGAAAGTG
GBA_PCR_fragment 3(ex.8-11)_FOR	TGTGTGCAAGGTCCAGGATCAG
GBA_sequencing_exon1_FOR	CTGTGTCATGTGACGCTCCT
GBA_sequencing_exon1_REV	CAGTGCCAGGATTCCAGAAG
GBA_sequencing_exon10-11_FOR	5-GGGTCCGTGGGTGGGT

GBA_sequencing_exon10-11_REV	5-TGCTGTGCCCTCTTTAGTCA
GBA_sequencing_exon2_FOR	5-CCTGCCCAGGAGAGTAGTTG
GBA_sequencing_exon2_REV	5-CTCTGTGCTACCTCCCCACT
GBA_sequencing_exon3_FOR	5-CAAGGGGTGAGGAATTTTGA
GBA_sequencing_exon3_REV	5-TATCAGTACCCAGCGGGAAA
GBA_sequencing_exon4_FOR	
GBA_sequencing_exon4_REV	5-GACAGAATGGGCAGAGTGAGA
GBA_sequencing_exon5_FOR	5-CAGGAGCCCAAGTTCCC
GBA_sequencing_exon5_REV	5-TGTCTGTACAAGCAGACCTACCC
GBA_sequencing_exon6_FOR	5-GCTGAACCGGATGCACTG
GBA_sequencing_exon6_REV	5-GCTAAATGGGAGGCCAGTC
GBA_sequencing_exon7_FOR	5-ACACCCAGCTGGTCTGGTC
GBA_sequencing_exon7_REV	5-TGGATGCTGGATTTGAAGGT
GBA_sequencing_exon8_FOR	
GBA_sequencing_exon8_REV	5-CTTCTGTCAGTCTTTGGTGAAA
GBA_sequencing_exon9_FOR	5-CCCACATGTGACCCTTACCT
GBA_sequencing_exon9_REV	5-TGTAGGAGATGATAGGCCTGGT
GCH1_exon 1_FOR	CCGGGCCATAAAAAGGAG
GCH1_exon 1_REV	CGCCAAAAGTGAGGCAACTC
GCH1_exon 2_FOR	CTTTCCTCCCTCCGTTCTCC
GCH1_exon 2_REV	ACCTGAGATATCAGCAATTGGCAGC
GCH1_exon 3_FOR	AGATGTTTTCAAGGTAATACATTGTCG
GCH1_exon 3_REV	TAGATTCTCAGCAGATGAGGGCAG
GCH1_exon 4_FOR	GTCCTTTTTGTTTTATGAGGAAGGC
GCH1_exon 4_REV	GGTGATGCACTCTTATAATCTCAGC
GCH1_exon 5_FOR	CTCTGTGGCCCAGTCAGC
GCH1_exon 5_REV	AGGCTCAGGGATGGAAATCT
GCH1_exon 6_FOR	CATTTGTGTAAGAAGGGATATTTCG
GCH1_exon 6_REV	AGTGACAAGGAATAAAGTTCACATC
KCTD17_exon 1_FOR	AGGCGCGGACTACAGCTC
KCTD17_exon 1_REV	CCACGGCAATGGGTACATC
KCTD17_exon 2_FOR	TCTCCCTCCACTCTCCTTC
KCTD17_exon 2_REV	TCCTGGTTGTCCAAATGG
KCTD17_exon 3_FOR	GGAGGGAACAAGAGGAGAATG
KCTD17_exon 3_REV	TCCCAACCTCCTCTGCTTC
KCTD17_exon 4_FOR	TCTTCTTTGGGTATGTTGCG
KCTD17_exon 4_REV	TGGTCAGAGGCTAGGAGGTC
KCTD17_exon 5_FOR	GAGGTCTGTCGTATCCTGCC
KCTD17_exon 5_REV	AGAGGTGGAGGGATGGTG
KCTD17_exon 6_FOR	CTTTCACCTTGCCTGAGACC
KCTD17_exon 6_REV	AGGCAAGTGGCTGAGCTAAC
KCTD17_exon 7_FOR	CAGGGTTAGCTCAGCCACTT

KCTD17_exon 7_REV	AGGCAGGGTGCAGATGAGAT
KCTD17_exon 8_FOR	TCTGTGCCCACTAACCCTG
KCTD17_exon 8_REV	TCAAGAGATGAGCACCCTCC
KCTD17_exon 9_FOR	CACCCGTCAATCTCCTCTC
KCTD17_exon 9_REV	AGGCAGGAGTAAGTCACAGC
LRRK2_exon41_FOR	AGGGACAAAGTGAGCACAGAA
LRRK2_exon41_REV	CACATCTGAGGTCAGTGGTTATC
NKX2-1_exon 1_FOR	GGCAGAAGAGAGGCAGACAG
NKX2-1_exon 1_REV	CGGACAGGTCTTTAGGAG
NKX2-1_exon 2_FOR	CGGCGTTAAGGTAACACC
NKX2-1_exon 2_REV	AGTGCCTGTTCTTGGACC
NKX2-1_exon 3_1_FOR	GCTAGGCTGCCTGGGTCA
NKX2-1_exon 3_1_REV	CGCTGTCCTGCTGCAGTT
NKX2-1_exon 3_2_FOR	GTTCCAGAACCACCGCTACA
NKX2-1_exon 3_2_REV	GTTTGCCGTCTTTCACCAG
NKX2-1_exon 3_3_FOR	CAACAGGCTCAGCAGCAGT
NKX2-1_exon 3_3_REV	GGTGGATGGTGGTCTGTGT
PARK2_exon1_FOR	GAGGCCTGGAGGATTTAACC
PARK2_exon1_REV	GCCCCGTCATTGACAGTT
PARK2_exon10_FOR	TGTTATTGCCAAATGCAACC
PARK2_exon10_REV	GGAACTCTCCATGACCTCCAG
PARK2_exon11_FOR	ACAGGGAACATAAACTCTGATCC
PARK2_exon11_REV	CAACACACCAGGCACCTTCAGA
PARK2_exon12_FOR	GTTTGGGAATGCGTGTTTT
PARK2_exon12_REV	AGAATTAGAAAATGAAGGTAGACA
PARK2_exon2_FOR	ATGTTGCTATCACCATTTAAGGG
PARK2_exon2_REV	AGATTGGCAGCGCAGGCGGCATG
PARK2_exon3_FOR	TCTCGCATTTCATGTTTGACA
PARK2_exon3_REV	TAAATATGCACCCGGTGAGG
PARK2_exon4_FOR	ACAAGCTTTTAAAGAGTTTCTTGT
PARK2_exon4_REV	AGGCAATGTGTTAGTACACA
PARK2_exon5_FOR	TGGAAACATGTCTTAAGGAGTACA
PARK2_exon5_REV	TTCCTGGCAAACAGTGAAGA
PARK2_exon6_FOR	AGAGATTGTTTACTGTGGAAACA
PARK2_exon6_REV	GTCCGTGGAGGGAAGTGAC
PARK2_exon7_FOR	TGCCTTTCCACACTGACAGGTACT
PARK2_exon7_REV	TCTGTTCTTCATTAGCATTAGAGA
PARK2_exon8_FOR	CAACACTGGCAGTTGATAGTCAT
PARK2_exon8_REV	GGAGCCCAAACTGTCTCATT
PARK2_exon9_FOR	TGCAGTCAGTTTGAAAGCTC
PARK2_exon9_REV	AATATAATCCCAGCCCATGTGCA
PDE10A_exon1_FOR	GTCCCCACCAGCAGTAGTCA

PDE10A_exon1_REV	CTCCTGCCCCTCCAGAGAA
PDE10A_exon10_FOR	TGCCAAAGCAGAAAAATCAA
PDE10A_exon10_REV	GGTGAATTCCTAAGCCACCA
PDE10A_exon11_FOR	CCAACCAATTAGAGTATAGGACAGC
PDE10A_exon11_REV	TGCAATGTCATTCCCAGAAG
PDE10A_exon12_FOR	CACGCATTTAAGTAAAACAGTGC
PDE10A_exon12_REV	AACTGAATTGGGACGTGGAG
PDE10A_exon13_FOR	TGCAAAGATTGAGGGGAGAT
PDE10A_exon13_REV	CCTTCCAGGGCATTTTATGA
PDE10A_exon14_FOR	TCATGTCTGCACATCCCAGT
PDE10A_exon14_REV	AAGCAGACAATGGCAACACA
PDE10A_exon15_FOR	TGGCTAAGAAGGCAGGAAAA
PDE10A_exon15_REV	CAAACAAAGATCGTGGTGAGG
PDE10A_exon16_FOR	GGATTCAGTCAGGGTGGAAA
PDE10A_exon16_REV	CCATGTCATCAATGTGCTCCT
PDE10A_exon17_FOR	CCAAGATTCCTAAGGGTTTGC
PDE10A_exon17_REV	GCCATAATGATCTTCCTTTTCC
PDE10A_exon18_FOR	CCAAAACGCAGTTTTCGTTA
PDE10A_exon18_REV	TGCCAGCAATCTTGTCAAAC
PDE10A_exon19_FOR	TGTCCTGGCTGTCACTTCTG
PDE10A_exon19_REV	TGACTCACCACAGTTCTCTGAAA
PDE10A_exon2_FOR	AAGCAGTAGCTTCCCCTTCC
PDE10A_exon2_REV	TTAGTCACGGATCTTTCTTTTGT
PDE10A_exon20_FOR	TTGGGTTAACAACCACAAACA
PDE10A_exon20_REV	TCTGCCTGGAATAACCCATT
PDE10A_exon21_FOR	GGCCTCAGAAACAGAACAGTC
PDE10A_exon21_REV	AACCAAAGGGGAGAAGTCGT
PDE10A_exon22_FOR	GTGCCACAGGACTGTTTGGT
PDE10A_exon22_REV	TGGAAAAGTACCCCTTCTGG
PDE10A_exon3_FOR	AAGAGGAAGCATTGCAAAAA
PDE10A_exon3_REV	CCTTCAATTTGCACCCTCTC
PDE10A_exon4_FOR	CATGTGCTATAAAAGCATAATGAATAA
PDE10A_exon4_REV	TTTTAGGTTTGACTCACCTCTGG
PDE10A_exon5_FOR	GACTCACATCTGCCTCTCACC
PDE10A_exon5_REV	ATGCCTAAATGTTGCCATGT
PDE10A_exon6_FOR	ATCATGGCAAAGCACCTTTC
PDE10A_exon6_REV	TGGGTAAAGGGAATTTTCTGA
PDE10A_exon7_FOR	CAAGTATCATGGCAATTTCTGA
PDE10A_exon7_REV	TTTCCTCTCTAAACAGAAACAGGT
PDE10A_exon8_FOR	TCCTTTGTTGAGATGACTACAAGT
PDE10A_exon8_REV	GGCATTGGGTGACTTAACCT
PDE10A_exon9_FOR	CCCAAGTGATTGTGTTAGGC

PDE10A_exon9_REV	TGGTCTATTTCTGCCACAGG
SPR_exon 1_FOR	ATCCCAAGGGAACCAGCAC
SPR_exon 1_REV	TCTAGGCGTCCTATCTGACCC
SPR_exon 2_FOR	GATATCTGGAGGAACTTGGGAG
SPR_exon 2_REV	TGTGGGTTGTTTCCTGGAG
SPR_exon 3_FOR	CAGGGACCTGAAACCTTCTG
SPR_exon 3_REV	TCTATGTGTAAGGCAGGACTGC
TH_exon 1_FOR	TTCCACGGACGAGCCCTTTC
TH_exon 1_REV	TTGCATGGACCCTGAGCCTG
TH_exon 11_12_FOR	CTGCCTCTCCCCATCCTT
TH_exon 11_12_REV	AGGTCCAGGCCTCAGTTTC
TH_exon 13_FOR	TCTACCCAAGGAACCCAC
TH_exon 13_REV	CTCAAGGCCAGAAGGAAG
TH_exon 14_FOR	GAGCTCTGAGCCACTGTGAAG
TH_exon 14_REV	TCACCACAGGCAGCACAAC
TH_exon 2_FOR	CCTTGATTGAAATGTGGTG
TH_exon 2_REV	GCTGAACTCCCAAGAAGG
TH_exon 3_FOR	TGCCTCTGTGTGCCATCAG
TH_exon 3_REV	AGGAACTCAGCCCACACAGC
TH_exon 4_FOR	GAACGGGATCTGTGTGCTG
TH_exon 4_REV	ACGTGGTCACTGTAGGGTCC
TH_exon 5_6_FOR	TCAAGGTGGGTGACACAG
TH_exon 5_6_REV	TGACAAGATGGGTCCTCC
TH_exon 7_FOR	ACCTGTGCCCAGTGAAGCTC
TH_exon 7_REV	TCACACGCCAGGATTCCAG
TH_exon 8_9_10_FOR	AGGCACCCACAGTTCAGGAG
TH_exon 8_9_10_REV	GAGCAGGCAGCACACTTCAC